ENHANCE ENERGY CLIVE MMV PLAN

APPENDICES B:

Geological, Hydrogeological and Mineralogical Characterization of the Sedimentary Succession Overlying the Leduc (D3-A) and Nisku (D-2) Oil Reservoirs in the Clive Oil Field in Alberta

July, 2019

APPENDIX B

Geological, Hydrogeological and Mineralogical Characterization of the Sedimentary Succession Overlying the Leduc (D3-A) and Nisku (D-2) Oil Reservoirs in the Clive Oil Field in Alberta

Confidential Client Report to Enhance Energy Inc.

by

Alberta Innovates – Technology Futures

December 2011

Disclaimer

1. This Report was prepared as an account of work conducted at the ALBERTA INNOVATES - TECHNOLOGY FUTURES ("AITF") on behalf of Enhance Energy Inc. All reasonable efforts were made to ensure that the work conforms to accepted scientific, engineering and environmental practices, but AITF makes no other representation and gives no other warranty with respect to the reliability, accuracy, validity or fitness of the information, analysis and conclusions contained in this Report. Any and all implied or statutory warranties of merchantability or fitness for any purpose are expressly excluded. Enhance Energy Inc. acknowledges that any use or interpretation of the information, analysis or conclusions contained in this Report is at its own risk. Reference herein to any specified commercial product, process or service by trade-name, trademark, manufacturer or otherwise does not constitute or imply an endorsement or recommendation by AITF.

2. The information contained in this Report is confidential and may not be distributed, referenced or quoted without the prior written approval of Enhance Energy Inc.

3. Any authorized copy of this Report distributed to a third party shall include an acknowledgement that the Report was prepared by AITF and shall give appropriate credit to AITF and the authors of the Report.

4.

Authors

This report was prepared by a team of AITF staff comprising:

Stefan Bachu, Ph.D., P.Eng., Project Manager

Tyler Hauck, M.Sc., P.Geol. and Jesse Peterson, P.Geol., Geology

Anatoly Melnik, Geol.I.T., and Stefan Bachu, Ph.D., P.Eng., Deep Hydrogeology

Catherine Main, M.Sc., P. Geol., and Don Jones, B.Sc., Shallow Hydrogeology

Ernest Perkins, Ph.D., P. Geol., Mineralogy

Alberta Innovates Technology Futures

Executive Summary

A major challenge in mitigating climate change effects is the reduction of anthropogenic CO_2 emissions through a broad portfolio of measures, including CO_2 capture, utilization and storage (CCUS). The Alberta and federal governments have provided significant financial support for the implementation of large-scale CCUS demonstration projects in western Canada, among them being Enhance Energy's "Alberta Carbon Trunk Line" Project. Enhance Energy Inc. will construct and operate a 240 km pipeline that will collect CO_2 from industrial emitters in and around Alberta's Industrial Heartland and transport it to aging oil reservoirs in central Alberta, more specifically the Leduc (D3-A) and Nisku (D-2) reservoirs in the Clive oil field, for secure storage in CO_2-EOR projects

All CCUS projects require the study of the fate and effects of the stored CO_2, and the development of an active monitoring program to ensure that there is no CO_2 leakage from the storage unit. In the case of CO_2-EOR operations, CO_2 is stored in the respective oil reservoir(s), and monitoring of the fate and effects of CO_2 in the reservoir(s) is part of the engineering practice. However, monitoring for CO_2 leakage and for effects of CO_2 injection outside the reservoir requires knowledge of the characteristics of the sedimentary succession above the oil reservoir(s) into which CO_2 is injected. The geology, hydrogeology and rock mineralogy in the sedimentary succession from the top of the Leduc (D3-A) and Nisku (D2) oil reservoirs to the ground surface were studied and characterized in the area of the Clive oil field to provide the basis for the evaluation of possible effects of CO_2 injection and for the development of a monitoring program.

A very thick package of Paleozoic, Mesozoic and Cenozoic sediments (around 2000 m thick) overlies the Clive Leduc (D3-A) and Nisku (D2) pools in the study area. The majority of sedimentary units are continuous across the study area, except for those Paleozoic strata in proximity to the sub-Cretaceous unconformity and at the base of the Tertiary and Quaternary deposits, which were truncated as a result of pre-Cretaceous and Cenozoic erosional events, respectively. A detailed hydrogeological characterization of the sedimentary succession overlying the Leduc (D3-A) and Nisku (D-2) reservoirs in the Clive oil field has been completed using analyses of formation waters, drillstem tests and core analyses to identify and evaluate the competence of the main barriers (aquitards) to cross-formational flow, in light of the proposed CO_2 EOR operation and further permanent CO_2 storage in these reservoirs.

All the geological, hydrogeological and mineralogical evidence collected and interpreted in this study indicates that the Leduc (D3-A) and Nisku (D-2) oil reservoirs in the Clive study area are capped by a strong and thick primary seal (caprock), the Calmar-Wabamun Aquitard (which includes in places remnants of the Carboniferous shales of the Exshaw and Lower Banff formations). This primary seal constitutes a barrier to upward migration and leakage of CO_2 from the oil reservoirs targeted for CO_2 enhanced oil recovery in the area. The primary caprock is overlain in turn in by a succession of

aquifers, listed in ascending order: Lower Mannville, Viking, Basal Belly River and Upper Belly River, separated by strong intervening aquitards: Joli Fou, McKay and Bearpaw, which constitute secondary traps and secondary barriers, respectively, for any CO_2 that may leak from the oil reservoirs through wells that penetrate the oil reservoirs. In the case of CO_2 leakage, the formation water will become acidic locally, resulting in reactions with the rock minerals and potentially formation of new minerals. The Leduc, Nisku, Calmar and Wabamun strata are primarily carbonate and/or sulphate mineral containing formations. The overlying strata are all siliciclastics (sandstones and shales) and can only be distinguished apart by the amount of other phases present. Some of the carbonate minerals present in the overlying formations (calcite, dolomite and/or siderite) will likely dissolve. Illite and potassium feldspar would probably react to form kaolinite and change the formation water composition slightly. The presence of plagioclase suggests that, as it dissolves into the more acidic formation water, the increased levels of calcium in the formation will result in calcite precipitation.

The strength of the aquitards in the sedimentary succession indicates that no CO_2 leakage is possible through the natural geological and hydrogeological system in the Clive study area. The only possible leakage pathway for CO_2 injected in the Leduc (D3-A) and Nisku (D2) reservoirs is through one or more of the ~309 wells that penetrate the oil-producing horizons in these reservoirs. The deep aquifers and aquitards in the study area are overlain by a succession of shallow aquifers which are within the depth of protected groundwater in the area: Horseshoe Canyon, Scollard-Paskapoo and Surficial. These aquifers should be monitored for any potential leakage of CO_2. Thus, an evaluation of the potential for CO_2 leakage through wells, the geochemical evaluation of the effects of potential CO_2 leakage, and the development of a monitoring program in the Clive area are recommended as potential subjects of study in a follow-up Phase 2 of the current work.

Alberta Innovates Technology Futures

Table of Contents

List of Figures

List of Tables

1. Introduction

1.1 Background

Interpretation of the temperature record on a scale of centuries to millennia indicates a slight increase in global annual temperatures in the last 150 years, in the order of 0.76ºC (IPCC, 2007). Predictions are that, if continuing in a business-as-usual (BAU) scenario, humankind is facing significant climate change by the end of this century as a result of warming forecast to be in the range of 1.1 to 6.3ºC, depending on greenhouse gas emissions scenario. It is very likely (>90% likelihood) and generally accepted that the main cause of the observed global warming is the increase in atmospheric concentrations of greenhouse gases, such as carbon dioxide (CO_2), methane (CH_4) and nitrous oxide (N_2O) (IPCC. 2007). This increase, noticeable since the beginning of the industrial revolution, is due to human activity in land use (agriculture and deforestation), which is the major factor in CH_4 and N_2O concentrations increases, and increasing consumption of fossil energy resources, which accounts for >80% of the increase in CO_2 concentrations (IPCC, 2007). Of all the greenhouse gases, CO_2, whose atmospheric concentration has risen from pre-industrial levels of 280 ppm to 380 ppm in 2005, is the most important greenhouse gas, being responsible for about two-thirds of the enhanced "greenhouse gas" effect (IPCC, 2007, Bryant, 1997). Although a direct causal link between the carbon cycle, including CO_2 and CH_4, and global warming has not been demonstrated, circumstantial evidence points toward this link, which has generally been accepted by a broad segment of the scientific community, population and policy makers.

A major challenge in mitigating climate change effects is the reduction of anthropogenic CO_2 emissions through a broad portfolio of measures which includes increasing energy efficiency and conservation, and switching from fossil-based energy production to other forms of energy such as nuclear, solar, wind and other renewables. However, it is being recognized that, due to population increase and economic development, scarcity or cost of other forms of energy production, and lack of infrastructure, the consumption of fossil fuels, mainly coal for electricity generation, will continue to increase this century. Besides increasing energy efficiency and conservation, and switching to less carbon-intensive fuels (such as from coal to gas) or to renewables, solar and nuclear energy, artificially increasing the capacity and capture rate of CO_2 sinks is a recognized means for reducing anthropogenic CO_2 emissions into the atmosphere. The latter could be achieved through manipulating biological processes to capture and sequester CO_2 that has already been emitted and dispersed in the atmosphere, and through the capture of CO_2 from large stationary sources prior to potential release into the atmosphere, and utilization or storage in various geological media (this process is known as Carbon Capture, Utilization and Storage, or CCUS). The "utilization" in CCUS consists mainly in using CO_2 captured from large stationary sources for CO_2 enhanced oil recovery (CO_2-EOR). The "storage" in CCUS consists of capturing CO_2 from large stationary sources, transporting it to a storage site, and isolation from the atmosphere by injecting it into

deep saline aquifers or depleted oil and gas reservoirs (IEA, 2004, 2010; IPCC, 2005). Currently there are more than a hundred CO_2-EOR operations in the world, the great majority of them being in the U.S. However, they predate CCUS and, for various reasons, they are not considered as CO_2 storage operations except for the Weyburn-Midale project in southeastern Saskatchewan which uses CO_2 from a coal-gasification plant in North Dakota. Geological storage of CO_2 is actively pursued at several locations around the globe, but all are storing CO_2 captured at gas plants after the separation of CO_2 from produced natural gas (e.g., Sleipner and Snohvit in Norway, and In Salah in Algeria).

CCUS is strongly supported by the G8 and the International Energy Agency (IEA, 2010). In 2008, the International Energy Agency (IEA) and the Carbon Sequestration Leadership Forum (CSLF) recommended to the leaders of G8:

> **"G8 heads of government are urged to recognize the critical role of CCS in tackling global climate change and demonstrate the political leadership necessary to act now to initiate widespread deployment of this technology. CCS can achieve substantial reductions in CO_2 in a world faced with increased demand for fossil fuels. With CCS, fossil fuels will become part of the solution, not part of the problem…"**

The potential of this technology has been recognized by the G8, which consequently recommended the implementation of a series of large-scale demonstration projects to prove its potential[1], and also by individual governments in Australia, Canada, the European Union and USA. Aware of the potential of CCUS to reduce anthropogenic CO_2 emissions, the federal, Alberta and Saskatchewan governments have provided significant financial support for the implementation of large-scale CCUS demonstration projects in western Canada. Among the projects that have been initiated in western Canada is Enhance Energy's "Alberta Carbon Trunk Line" Project, known also as ACTL.

1.2 The ACTL Project

Enhance Energy Inc. will construct and operate the Alberta Carbon Trunk Line, which is a 240 km pipeline that will collect CO_2 from industrial emitters in and around Alberta's Industrial Heartland and transport it to aging oil reservoirs in central Alberta, more specifically the Clive oil field first and beyond as the project progresses, for secure storage in CO_2-EOR projects (Figure 1). The Clive oil field is located east to northeast of Joffre and immediately north of the Red Deer River. At full capacity the ACTL route will provide access to oil reservoirs capable of producing an additional billion barrels of high-quality light-crude oil while storing 14.6 Mt CO_2.

[1] At the Hokkaido Toyako Summit in 2008, the G8 leaders committed to announce 20 large-scale CCS demonstration projects globally by 2010, with a view to beginning broad deployment of CCS by 2020.

All CCUS projects require the study of the fate and effects of the stored CO_2, and the development of an active monitoring program to ensure that there is no CO_2 leakage from the storage unit. In the case of CO_2-EOR operations, CO_2 is stored in the respective oil reservoir(s), and monitoring of the fate and effects of CO_2 in the reservoir(s) is part of the engineering practice. However, monitoring for CO_2 leakage and for effects of CO_2 injection outside the reservoir requires knowledge of the sedimentary succession above the oil reservoir(s) into which CO_2 is injected. Conceptually, the sedimentary succession in a CCUS operation can be divided into:

1) The storage complex comprising the injection unit (reservoir) and primary caprock (seal) above the injection unit;
2) The succession of aquifers and aquitards between the primary seal and the base of protected groundwater; and
3) The sedimentary succession from the base of shallow protected groundwater, defined in Alberta as groundwater with salinity (Total Dissolved Solids, or TDS) less than 4000 mg/L, to the ground surface.

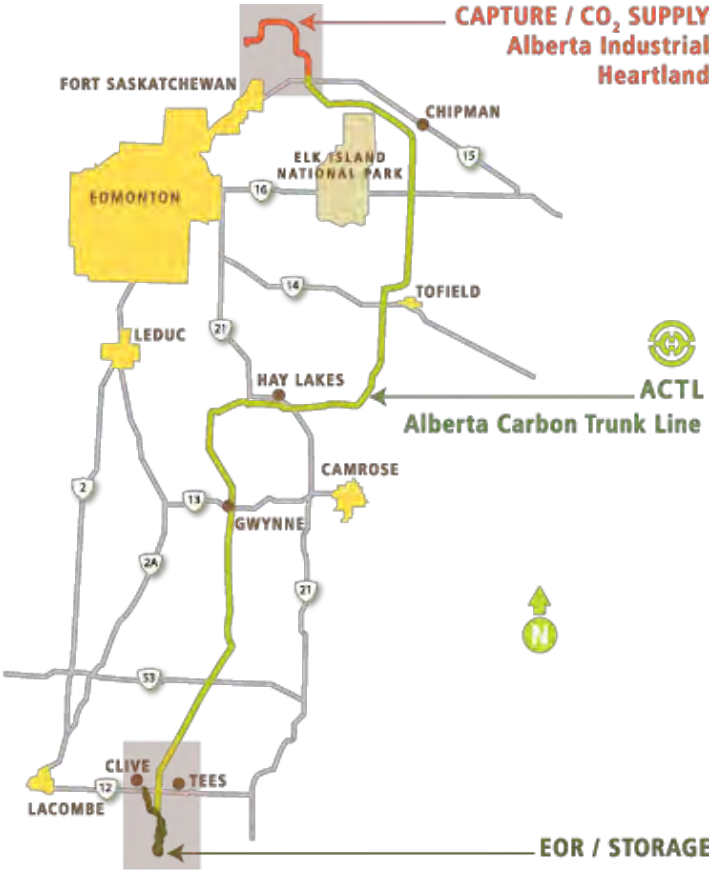

Figure 1: Location of the Alberta Carbon Trunk Line (ACTL). Reproduced from Enhance Energy Inc.'s fact sheet at http://www.enhanceenergy.com.

Effects of CO_2 injection are generally of two types:

- Geomechanical, as a result of pressure increase during CO_2 injection, and
- Geochemical as a result of CO_2 coming in contact with formation water and rocks. These effects are particularly important if CO_2 leaks into protected groundwater that is used for human consumption and for agricultural and industrial purposes (hence the division of the sedimentary succession presented previously).

In the case of the Alberta Carbon Trunk Line project, Enhance Energy is taking care of studying, predicting and monitoring the effects of CO_2 injection into the Leduc (D3-A) and Nisku (D2) oil reservoirs in the Clive oil field, which are the oil reservoirs targeted for CO_2-EOR in the initial phase of the ACTL project. In regard to studying the geomechanical effects of injecting CO_2 on the overlying sedimentary succession, and the geochemical effects in case of CO_2 leakage from the Leduc and Nisku reservoirs, Enhance Energy has retained Alberta Innovates – Technology Futures (AITF) to study these effects in a staged approach that consists of several phases. In Phase 1 of the study, AITF in collaboration with University of Saskatchewan studied the geology, hydrogeology, rock mineralogy and geomechanical properties of the sedimentary succession from the top of the Leduc (D3-A) and Nisku (D2) oil reservoirs, whose primary seal (caprock) is the combined interval of the anhydritic upper portion of the Nisku Formation and the shaley Calmar Formation, to the ground surface. The study area is defined as illustrated in Figure 2, covering 171 sections of land. A total 1715 wells were drilled within the study area, of which 660 wells reach the top of the Nisku Formation; most of those are located within the D-2 pools.

Geological delineation and characterization of the sedimentary succession above the reservoirs targeted for CO_2-EOR has the purpose of identifying and characterizing the succession of aquifers and aquitards (caprocks) in the sedimentary succession, including coal beds known to be present. This is because saline aquifers overlying the target oil reservoirs constitute additional traps for CO_2 in case of upwards leakage, while the intervening aquitards (caprocks) and coal beds constitute secondary barriers to CO_2 upwards leakage (the upper part of the Nisku Formation and the Calmar Formation caprock overlying the oil reservoirs constitutes the primary barrier). The coal beds are a barrier to leaked CO_2 due to coal's adsorbing properties. The hydrogeological characterization comprises an analysis of aquifer hydrodynamics based on pressure, and chemistry of formation waters. In addition, aquifer porosity and permeability, determined based on existing core and drillstem test data, are important for establishing the strength of CO_2 and formation water flow. The mineralogical analysis of the aquifer rocks is essential in assessing the geochemical integrity of the caprock, and the geochemical effects of the injected CO_2 in selected aquifers in case of CO_2 leakage. Finally, a geomechanical Mechanical Earth Model (MEM) of the sedimentary succession above the Leduc (D3-A) and Nisku (D2) oil reservoirs is needed for future modelling of

geomechanical effects of CO_2 injection, particularly if the reservoir pressure during the CO_2 storage phase of the project will increase above the initial reservoir pressure to reverse the effects of water invasion from the underlying aquifers, and if CO_2 will be injected at a lower temperature than that of the reservoirs.

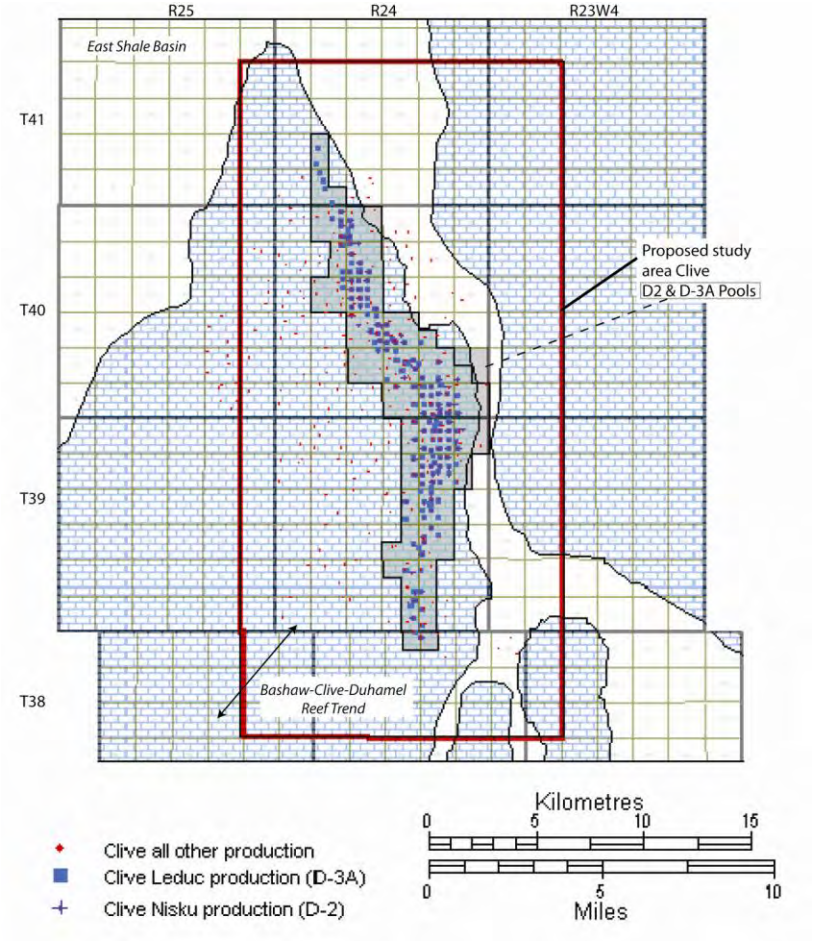

Figure 2: Study area, delineated by the red line, for the assessment of the sedimentary succession above the Leduc (D3-A) and Nisku (D2) oil reservoirs in the Clive oil field.

Two separate reports are provided to Enhance Energy as a result of work executed in Phase 1 of this study:

- This report by Alberta Innovates – Technology Futures, covering the geology, hydrogeology and mineralogy of the sedimentary succession overlying the Leduc (D3-A) and Nisku (D2) oil reservoirs in the Clive oil field, and
- A companion report produced by University of Saskatchewan describing the geomechanical properties and the Mechanical Earth Model of the same sedimentary succession.

This report comprises chapters on the geology, hydrogeology and mineralogy of the sedimentary succession, and appendices with relevant figures and data tables.

2. Geology

2.1 Geological Setting and Study Area

The Enhance Clive study area is located in south-central Alberta, between the cities of Edmonton and Calgary (Figure 3), and is centered on the Clive oil field, where oil is produced from a Devonian Leduc Formation reef called the Bashaw Reef Complex (the Leduc is known informally as D3 for production purposes), and from overlying Devonian Nisku Formation carbonates (known informally as D2). The study area for geology ranges from Townships 38 to 41 and Ranges 23 to 25 west of the 4th Meridian (Figure 3). The study area was expanded beyond the initial Enhance Clive study area (identified by a red border in Figure 1) to provide better data control and avoid artificial edge effects. Sedimentary strata comprising the Nisku to those units defining the bedrock underneath Quaternary deposits were resolved structurally as part of a geological mapping task. For reference, the Nisku Formation, the deepest formation delineated in the study area, ranges in depth from 1881 to 2092 m.

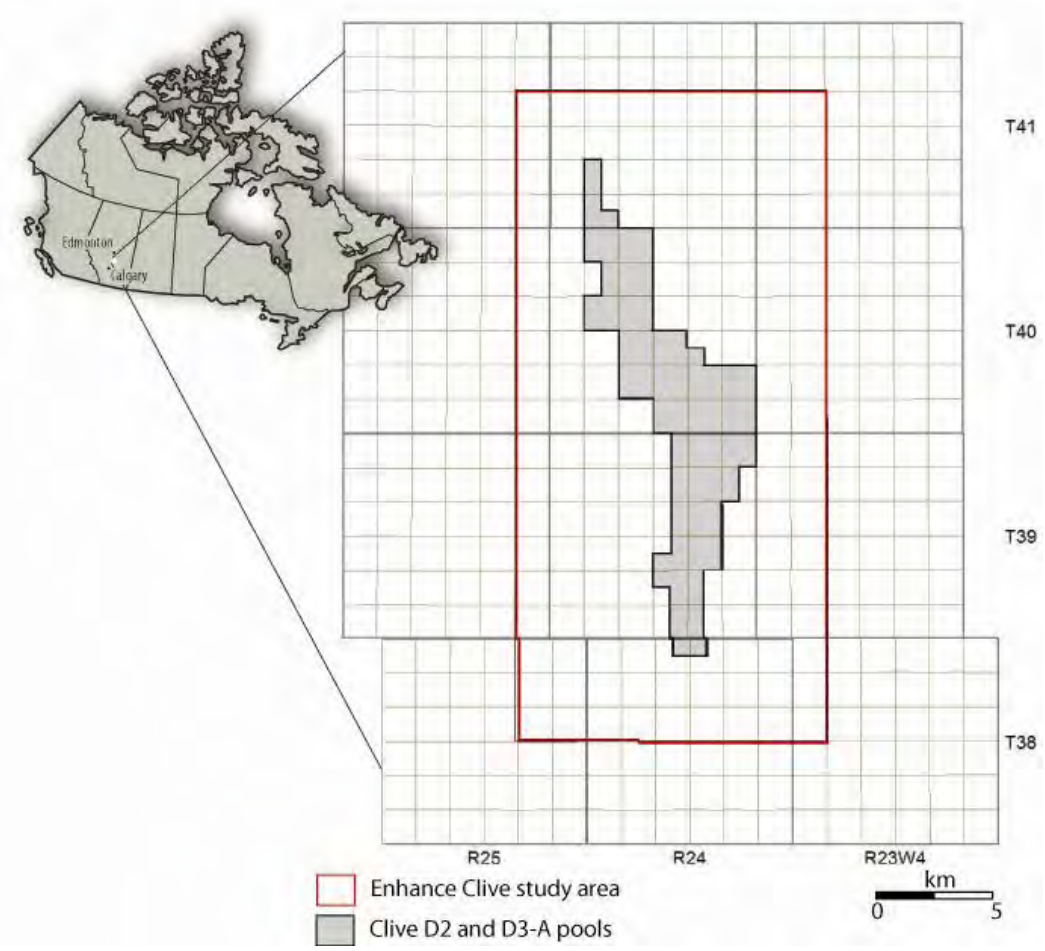

Figure 3: Location of the Enhance Clive study area and of the geological study area in south-central Alberta.

Sedimentary strata in the study area were deposited in the Alberta Basin and are the culmination of deposition predominantly within two distinct stages of tectonic evolution of the Alberta Basin. The first stage involves an early Phanerozoic (Cambrian) to Late Jurassic miogeocline-platform stage (Price, 1994); essentially deposition on what can be considered predominantly a passive cratonic margin. During this stage, deposition of sedimentary strata was dominated by the growth of carbonates (Figure 4), especially during the Devonian, during which time major carbonate reef and platform complexes formed in the Alberta Basin, including the Bashaw Leduc (D3) reef complex and the overlying Nisku Formation (D2) which form the Clive oil field (Figure 3).

The second major phase of basin evolution involves orogenic cycles affecting the western cratonic margin of North America. Two major cycles are represented in the Alberta Basin by the Jurassic-Early Cretaceous Columbian and Late Cretaceous-Tertiary Laramide orogenies. During the second phase of basin evolution the uplift of the Cordillera due to accretion of allochtonous terranes from the west began to take place and marked a major shift in sedimentation style and patterns across the basin. The accretion of terranes on the western cratonic margin caused dislocation of a supracrustal

wedge that was stacked and thickened north-eastward onto the cratonic margin, the weight of which produced the foreland trough east of the Cordillera (Price, 1994). As a result of tectonic loading at the western margin of the basin during the Columbian orogeny, Paleozoic strata were tilted south-westward with a slope in the Enhance Clive study area of approximately 13 m/km (0.74º). Major erosional events prior to Cretaceous deposition resulted in significant removal of Mississippian strata, and complete erosional truncation of Triassic and Jurassic sediments from the study area. Consequently, in the study area the Mississippian Banff and Devonian Wabamun formations are successively exposed west to east beneath Cretaceous strata at the sub-Cretaceous unconformity (Figure 4). Throughout Mesozoic time the foreland basin, created as a result of the Columbian and Laramide orogenies and paralleling the mountain chain, was the locus of much of the sedimentation derived from erosion of the newly formed Cordillera, and as such, the sediments filling the basin during this stage are dominated by siliciclastics (Figure 4).

2.2 Dataset and Methods

A total of 672 wells in GeoLogic's GeoScout were used for picking the stratigraphic tops in the geological study area (Figure 5) for the formations in the sedimentary succession from Devonian Leduc Fm. to the Cretaceous Lea Park Fm. (Figure 4). A total of 542 of these wells are located within the Enhance Clive study area, while the remaining 130 wells are located outside of the main study area to supplement data distribution, and to aid in avoiding edge effects in structure and isopach maps. Of the 672 wells, approximately 150 are shallow wells used for resolving formations in the Upper Cretaceous Belly River and Edmonton groups in the study area. The majority of these wells are shallow coalbed methane wells, in which geophysical logs are of good quality given that they were drilled recently.

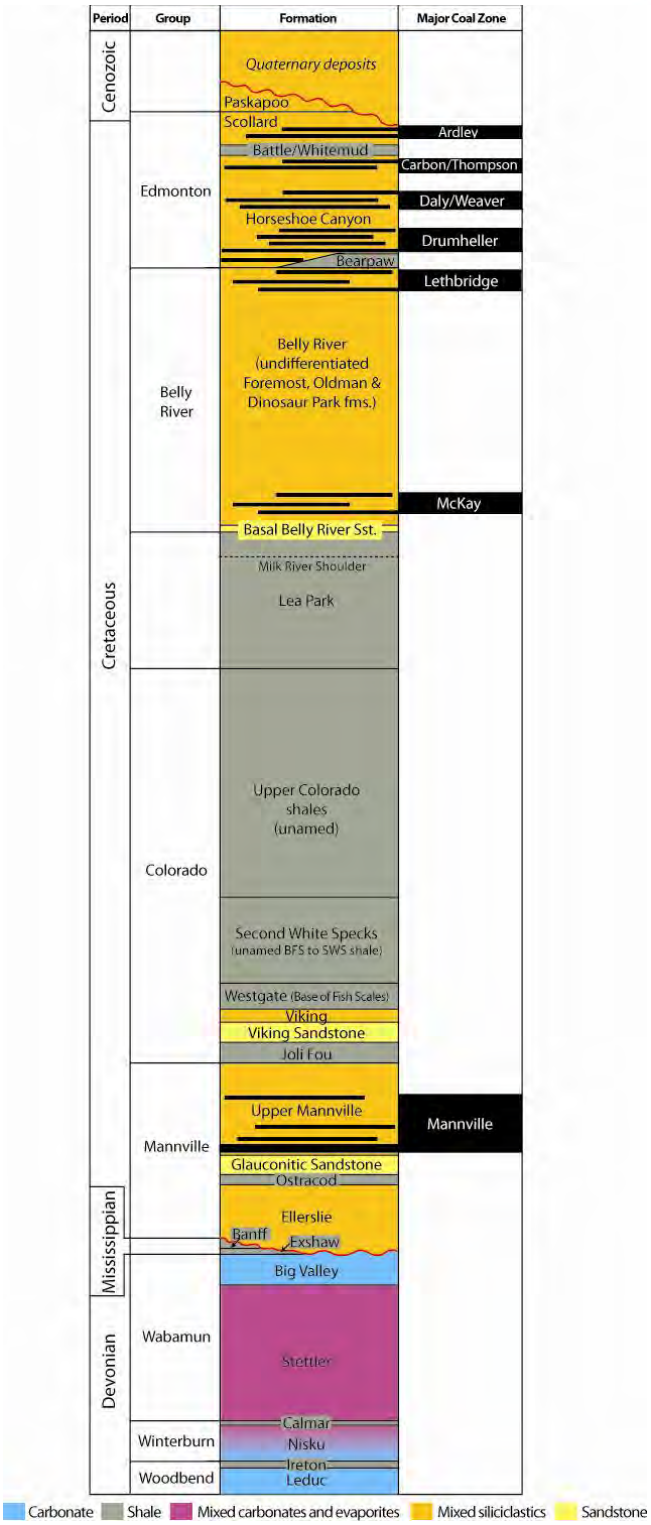

Figure 4: Lithostratigraphic column, including major coal zones, for the Enhance Clive study area.

All tops for the stratigraphic column outlined in Figure 4 were manually picked or verified through the use of cross-sections and, where possible, were cross-referenced with

stratigraphy and correlations from literature. Two strike and one dip cross-section, whose locations are shown in Figure 5 together with the locations of wells used in the study, are presented to illustrate the stratigraphy in the area. Of the strike cross-sections, A-A' resolves deep stratigraphy (Figure 6), and B-B' was constructed to resolve the shallow stratigraphy (Figure 7). A shallow dip section (C-C', Figure 8) is presented to illustrate depositional relationships east-to-west in the Belly River and Edmonton groups.

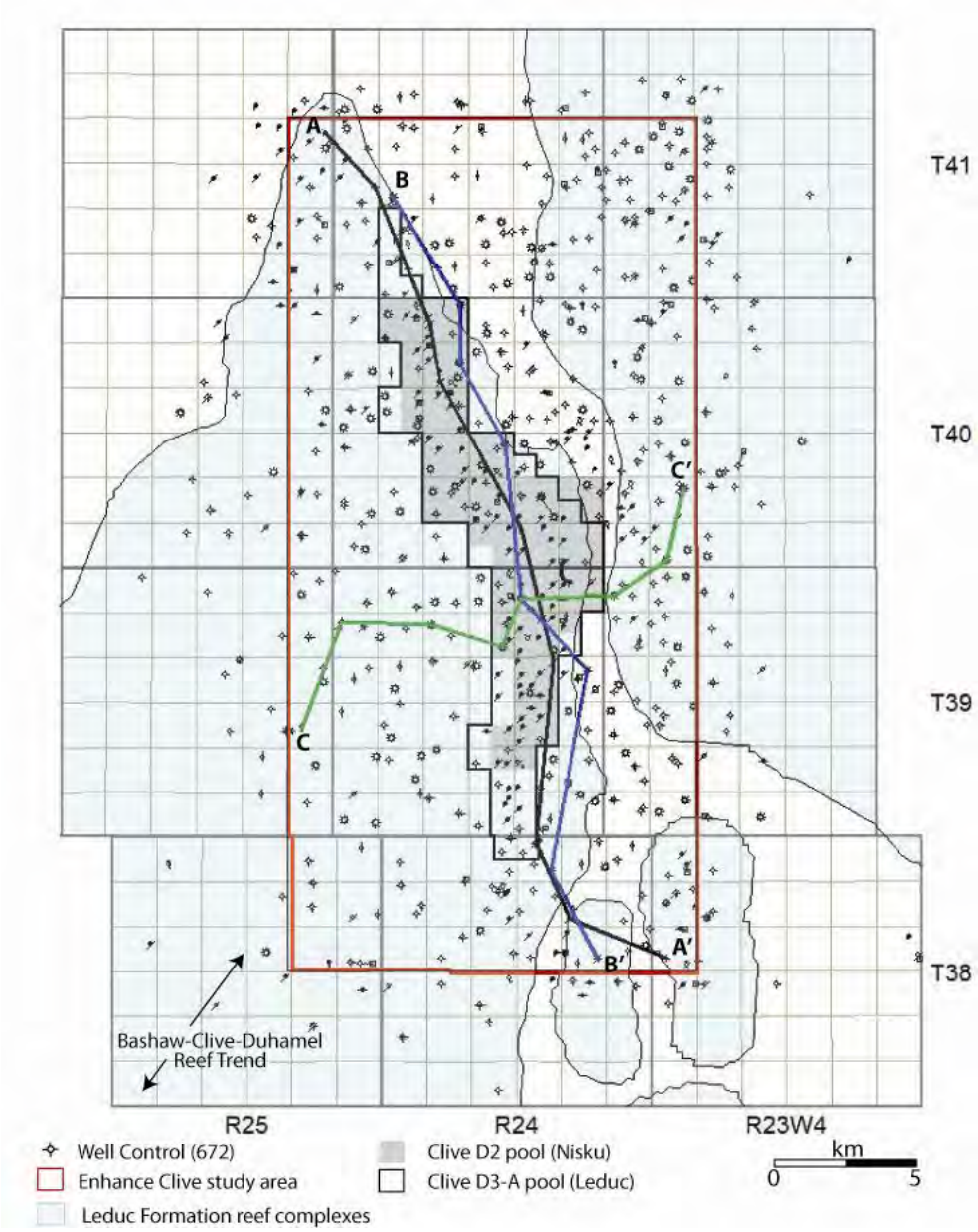

Figure 5: Well control used for mapping and lines of cross-section in the geological study area. The Clive D2 (Nisku) and D3-A (Leduc) field outlines are shown, as well as the approximate edges of the Leduc reef complexes.

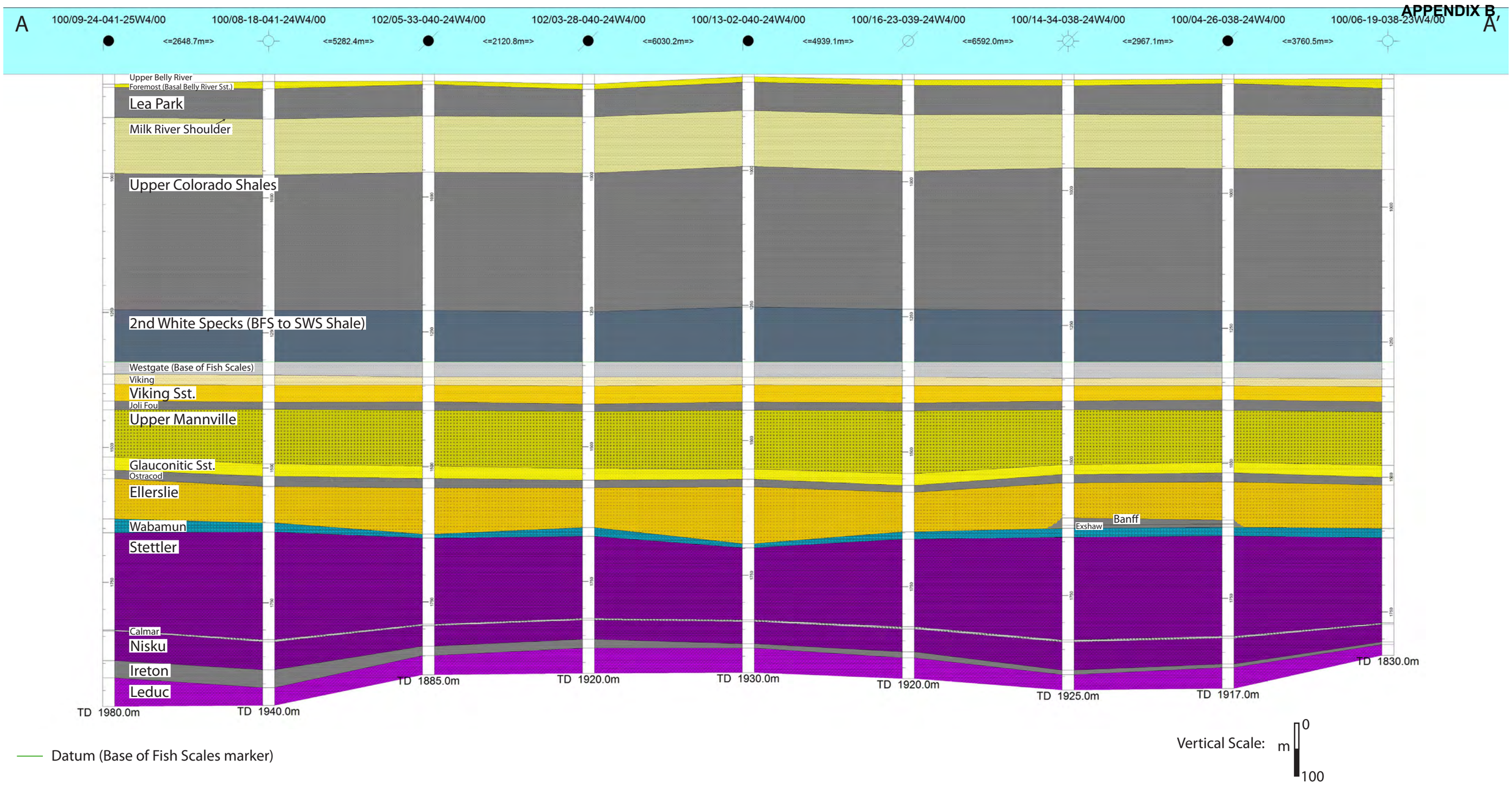

Datum (Base of Fish Scales marker)

Vertical Scale: m 0 100

Horizontal Scale: equal spacing between wells

Figure 6 - Stratigraphic strike (NW - SE) cross-section A - A' dispalying Upper Belly River Group strata to Leduc Formation strata in the Enhance Clive study area.

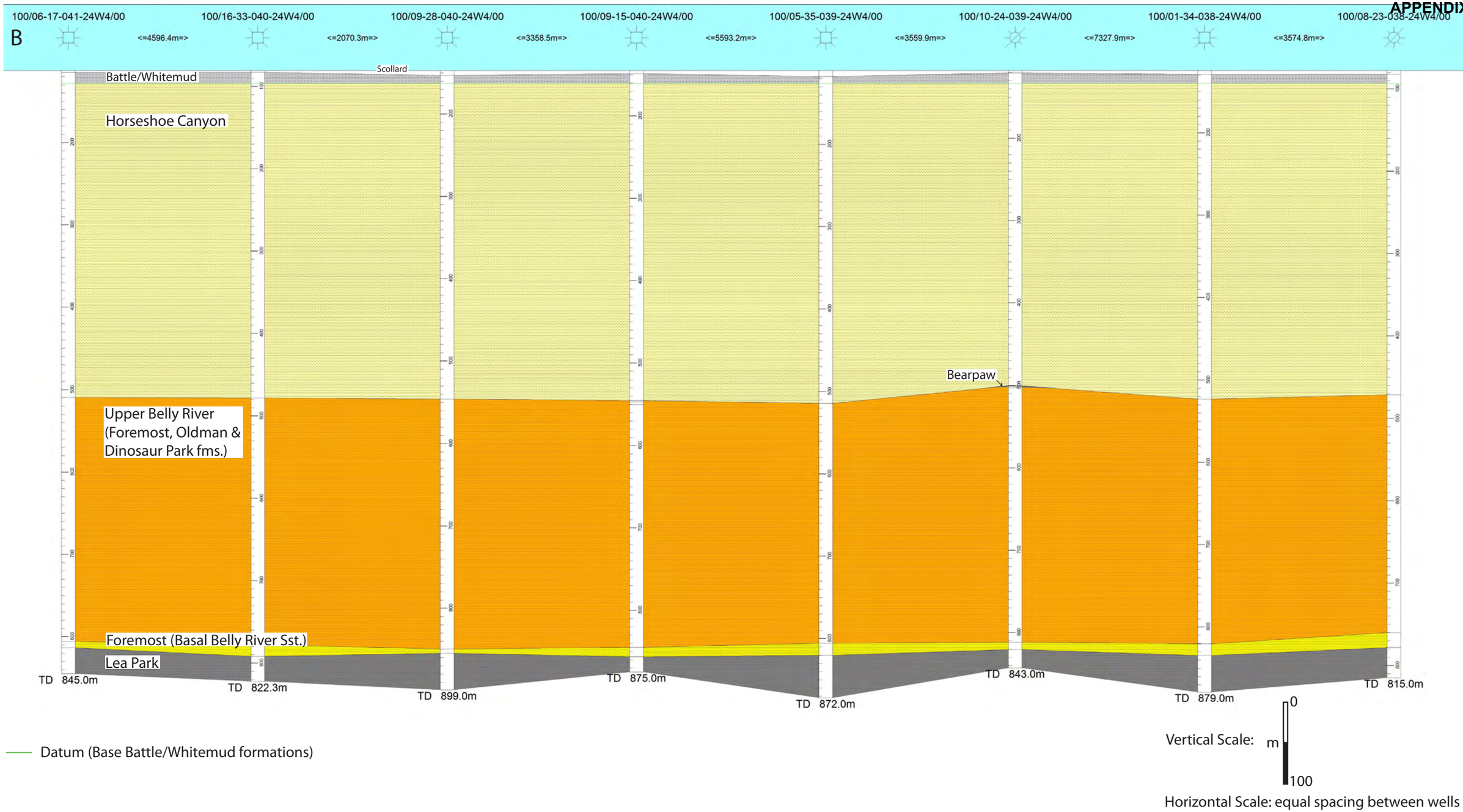

Figure 7 - Stratigraphic strike (NW - SE) cross-section B - B' dispalying Battle/Whitemud Formation strata to Lea Park Formation strata in the Enhance Clive study area. Where the Bearpaw Formation is missing due to non-depostion, the base of the Horseshoe Canyon Formation is approximated by the base of the Drumheller coal zone.

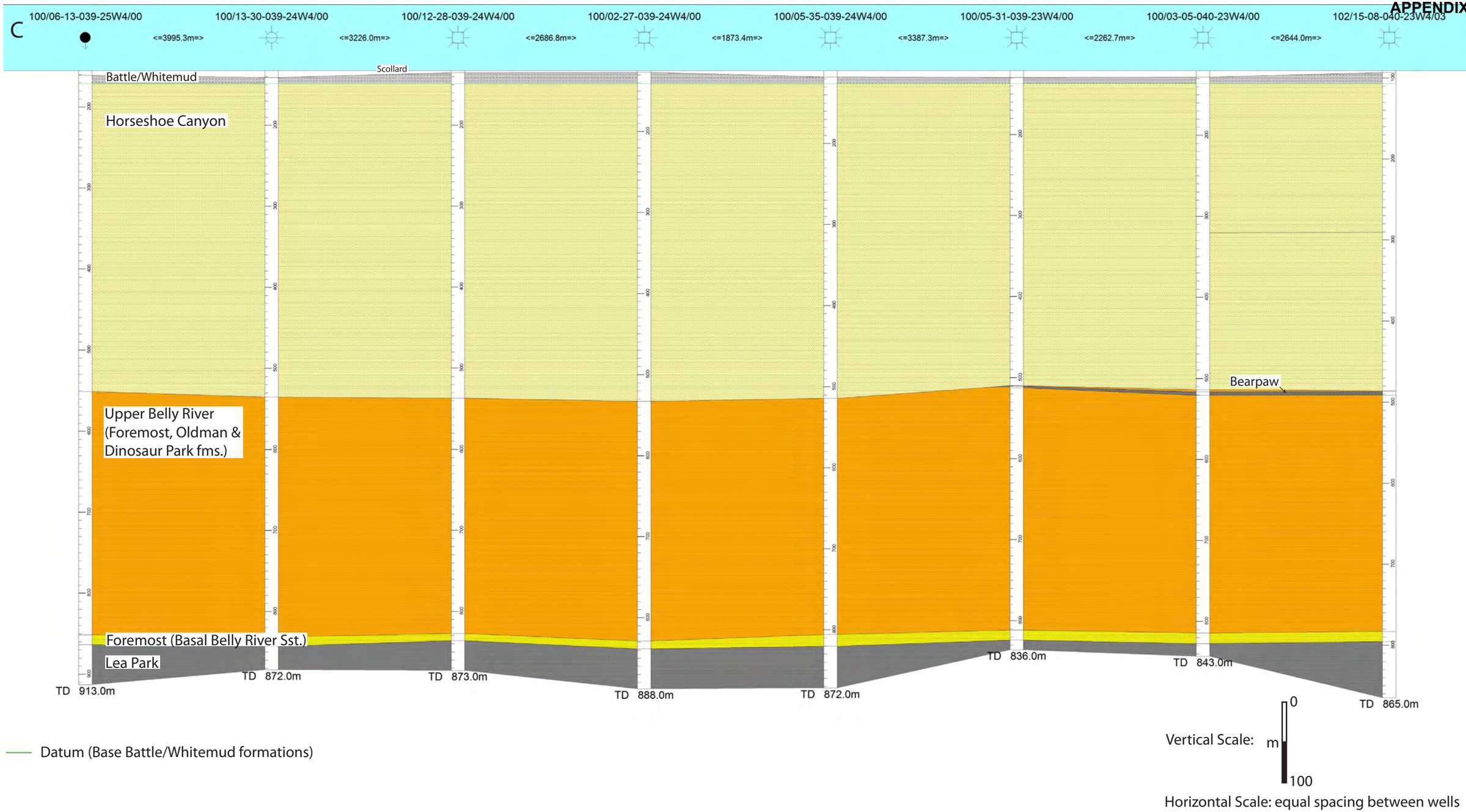

Figure 8 - Stratigraphic dip (SW - NE) cross-section C - C′ dispalying Battle/Whitemud Formation strata to Lea Park Formation strata in the Enhance Clive study area. Where the Bearpaw Formation is missing due to non-depostion, the base of the Horseshoe Canyon Formation is approximated by the base of the Drumheller coal zone.

For Upper Cretaceous strata overlying the Lea Park Formation at the top of the sedimentary column (Figure 4), an additional data set publicly-available from the Alberta Geological Survey (Glombick, 2010) was used for the top of the Belly River Formation pick, which was subsequently used as a reference for correlation for this surface in a great number of wells in the study area. Another Alberta Geological Survey dataset, the coal database (Wynne and Beaton, 2003), was used to aid in picking the Whitemud and Battle formations due to the proximity of these formations to the Carbon-Thompson and Ardley coal zones (Figure 4). Shallow geological data from the Alberta Water Well Information Database, a public database maintained by Alberta Environment's Groundwater Information Centre, were used to define the top of the bedrock. A digital elevation model (DEM) was used to define the ground surface.

For the Mannville, McKay and Lethbridge coal zones (Figure 4), tops and bases were resolved in as many wells as possible, predominantly within wells with a combination of neutron-density, sonic and resistivity logs. Cumulative thicknesses of the individual coal seams therein were compiled and are presented in Section 2.3.8.

Well data in Geographic Latitude and Longitude, with a North American Datum 1983, were imported into Landmark's Geographix software for the construction of maps. Maps are displayed using a Universal Transverse Mercator system centered on Zone 12 (114 to 108 degrees west Longitude). Contour maps were constructed using a minimum curvature algorithm. Isopach maps are volumetrically correct (i.e., no negative thicknesses). All structure and isopach maps are collected in Appendix 1, and are referenced in the text by Figure A.n. Although all the structure top and isopach maps were produced for the expanded geological study area, in Appendix 1 they are presented only for the Enhance Clive study area.

2.3 Depositional History and Architecture of Strata above the Ireton Formation

2.3.1 Winterburn Group

The lowermost unit of the Devonian Winterburn Group is the Nisku Formation (Figure 4). Whereas the Woodbend reefs of the underlying Leduc Formation gain conspicuous topography due to their biohermal/pinnacle nature, the Nisku Formation is a platform carbonate sequence (Stoakes, 1980) displaying a homoclinal ramp morphology in the study area (Watts, 1987). The Nisku Formation directly overlies the Ireton Formation. At the top of the Ireton Formation are the carbonates of the Camrose Member, which are difficult to differentiate on logs from the Nisku Formation due to similar carbonate lithologies.

Elevations for the top of the Nisku Formation range from -1085 to -880 metres above sea level (mASL) (Figure A.1 Figure A.1: Structural elevation of the top of the Nisku Formation in the Enhance Clive study area.). The structure of the top of the Nisku Formation appears to be affected by the presence of the underlying Leduc Formation

reef complexes, where compaction of the Ireton Formation over the reef and late-stage Leduc reef growth may have played a factor in the present day structure of the Nisku Formation.

The deposition of the upper Nisku Fm. was eventually terminated by the progradation of silts and shales of the Calmar Formation after a drop in relative sea level (Stoakes, 1992; Hearn et al., 2011).

Elevations for the Calmar Formation range from -1085 to -875 mASL (Figure A.2). Similar to the underlying Nisku Formation, the Calmar Formation displays unbroken and uniform structural dip to the southwest until around -975 mASL, where the structure appears to be affected by the underlying Leduc Formation Reef complexes. Its thickness ranges from 1 to 8 metres, averaging 3.3 metres across the study area (Figure A.3).

2.3.2 Wabamun Group

Strata of the Wabamun Group conformably overlie the Calmar Formation. In the study area the Wabamun Group consists predominantly of evaporitic deposits of the Stettler Formation (Burrowes and Krause, 1987) (Figure 4), deposited in a semi-restricted carbonate shelf environment (Halbertsman and Meijer-Drees, 1987). Strata of the Big Valley Formation overlie the Stettler Formation, and comprise open marine limestones that were deposited during a second Wabamun Group transgression (the first transgression was responsible for Stettler Fm. and equivalent strata elsewhere in Alberta) (Burrowes and Krause, 1987).

Elevations for the top of Stettler Formation range from -875 to -730 mASL (Figure A.4). The stratum is generally deepest in the southwest of the study area. Its thickness ranges from 80 to 210 metres, averaging 166 metres across the study area (Figure A.5). The Stettler Formation is thickest in the western part of the study area.

Elevations for the top of Big Valley Formation range from -855 to -720 mASL (Figure A.6). Its thickness ranges from 3 to 29 metres, averaging 14.5 metres across the study area (Figure A.7). It appears that the Big Valley Formation is affected by the presence or absence of the overlying Mississippian strata, and therefore affected by pre-Cretaceous erosion - the thinnest parts of the formation correspond to areas where strata of the Carboniferous Exshaw and Banff formations are removed by pre-Cretaceous erosion (compare Figure A.7 and Figure A.8).

2.3.3 Lower Mississippian Strata

Following deposition of the Big Valley Formation, a change in the tectonic setting influenced depositional settings in the Alberta Basin. A suspect change in tectonic regime in the south from passive to convergent settings (Antler Orogeny in the western

U.S.) is considered responsible for the creation of accommodation and the resultant deposition of the deep-water, low-oxygen (anoxic) shales of the Exshaw Formation (Savoy and Mountjoy, 1995; Caplan and Bustin, 1998). The Exshaw Formation is overlain by the Banff Formation, which comprises an overall shallowing-upward sequence of deeper-water siliciclastics to shallow-marine carbonate ramp settings (Savoy and Mountjoy, 1995). Both the Exshaw and Banff formations were erosionally truncated by events that culminated with the Columbian Orogeny (Figure 4). Herein the remnants of Exshaw and Lower Banff formations are dominated by shales and are amalgamated for mapping and analysis purposes.

Where present, elevations for the top of the Exshaw-Banff interval range from -845 to -725 mASL (Figure A.8). The thickness of this interval ranges from 0 m at its erosional boundary, to 85 metres in the southwest (Figure A.9).

2.3.4 Mannville Group

Pre-Cretaceous erosional events linked with the late Jurassic Columbian Orogeny led to removal of most of the Mississippian and the Permian to Jurassic sedimentary succession in the study area. The resulting surface on which Cretaceous sedimentation began had considerable topographic relief in much of the Alberta Basin. In the study area the Paleozoic relief consists of Big Valley to Banff Formation strata. Lower Cretaceous sediments of the Mannville Group, namely the Ellerslie Formation, were deposited on the sub-Cretaceous unconformity (Figure 4), reflecting a series of transgressions and regressions of the Boreal Sea inundating from, and receding to, the north. Elevations for the sub-Cretaceous unconformity range from -855 to -725 mASL (Figure A.10). The resultant sedimentary patterns comprise complex assortments of fluvial, marginal-marine, and marine sediments. Cant (1996) considered Ellerslie deposition to have occurred during an overall transgressive event, with non-marine environments dominating in the location of the Enhance Clive study area. Commonly, the lower part of the Ellerslie Formation comprises relatively thick sandstones that have been informally called the Basal Quartz. Interbedded with and overlying these sandstones are variable amounts of shale and siltstone (Hayes et al., 1994).

Elevations for the top of the Ellerslie Formation range from -760 to -635 mASL (Figure A.11). Its thickness ranges from 40 to 120 metres, averaging 81 metres across the study area (Figure A.12) Thickness trends in the Ellerslie Formation result from topography on the underlying sub-Cretaceous unconformity, where the thickest portions of the Ellerslie are located in areas where pre-Cretaceous incision was focused (e.g., see 100 m contour on Figure A.12 and compare with -800 mASL contour on Figure A.10). Deposition of the Ellerslie Formation began in these topographic lows on the sub-Cretaceous unconformity, and onlapped the adjacent topographic highs as deposition progressed.

A subsequent significant rise in relative sea level resulted in widespread brackish embayment/seaway settings over the local-scale study area (Hubbard et al., 1999; Smith, 1994; McLean and Wall, 1981). During this time the brackish influence is evidenced in deposits of the Ostracod Formation (Figure 4). The Ostracod Formation disconformably overlies the Ellerslie Formation, marked by a trangressive flooding surface due to continued incursion of the Boreal Sea to the south (Karvonen and Pemberton, 1997). In the Jenner-Suffield area of south-east Alberta the Ostracod consists of variable amounts of siltstone, shale, calcareous shale, argillaceous limestone and calcareous sandstone (Karvonen and Pemberton, 1997). Similar lithologies were observed in a core from the Enhance Clive study area, in which coquina beds were also observed.

Elevations for the top of the Ostracod Formation range from-735 to -620 mASL (Figure A.13). Its thickness ranges from 8 to 28 metres, averaging 15 metres across the study area (Figure A.14).

The Ostracod Formation is overlain by the Glauconitic Sandstone Formation (Figure 4), which comprises a series of progradational, mostly shoreface sandbodies resulting from highstand conditions (Cant and Abrahamson, 1996). Commonly, valleys incise the sandbodies as a result of lower order sea level fluctuations, with estuarine deposits dominating the fill of the incised valley (Smith, 1994; Cant, 1996). The Glauconitic Sandstone Formation is dominantly quartz sandstone, with glauconite-rich intervals, interbedded with shale and siltstone. Generally in Alberta, the Glauconitic Sandstone becomes increasingly paralic, or continentally influenced, further to the south (Hayes et al., 1994).

Elevations for the top of the Glauconitic Sandstone Formation range from -725 to -595 mASL (Figure A.15). Thicknesses range from 9 to 36 metres, averaging 24 metres across the study area (Figure A.16). Thicknesses are highest in the southwest and northeast portions of the study area.

Continued highstand conditions and an influx of sediments from the Cordillera led to deposition of the undifferentiated Upper Mannville (Smith, 1994). The Upper Mannville comprises a highly mixed siliciclastic unit that resulted from deposition in predominantly non-marine settings in the study area, consisting of interbedded quartz to valcano-feldspathic sandstones, siltstone and shale. Feldspathic content in the sandstones is derived from exposed igneous and metamorphic rocks in the Cordillera (Hayes, 1994).

Elevations for the top of the undifferentiated Upper Mannville range from -620 to-495 mASL (Figure A.17). Thicknesses range from 80 to 125 metres in the south-central portion of the study area. The unit averages 101 metres across the study area (Figure A.18).

2.3.5 Colorado Group and Lea Park Formation

The Colorado Group in the study area is dominated by a thick succession of fine-grained deposits (Figure 4). The base of the Colorado Group represents a basin-wide unconformity that preceded transgression and the eventual deposition of the Joli Fou Formation. Detailed studies of the mudstones deposited within the group have revealed that deposition occurred in an expansive north-south trending eiperic sea, formed by the connection of the northern Boreal and southern Tethyan oceans (Roca et al., 2008; Schröder-Adams et al., 1996; Leckie et al., 1994). The Joli Fou Formation is overlain by the Viking Formation. In this report three distinct log markers were used to differentiate the shale succession above the Viking Formation, in ascending order: the Base of Fish Scales, top of the Second White Specks, and top of First White Specks (top of Colorado Group) (Figure 4). These markers represent times during which significant amounts of organic matter were concentrated on the sea floor (Roca et al., 2008; Leckie et al., 1994), resulting in high radioactivity and distinct gamma ray responses amenable to regional correlation.

The Joli Fou Formation is a widespread unit across much of the basin. It represents deposits formed after a major transgression across existing Upper Mannville units, thus it disconformably overlies the Mannville Group (Leckie et al., 1994). Lithologically the Joli Fou Formation comprises non-calcareous marine shales with minor interbedded sandstones (Simpson, 1997).

Elevations for the top of the Joli Fou Formation range from-605 to -480 mASL (Figure A.19). Thicknesses range from 12 to -24 metres, averaging 16.4 metres across the study area (Figure A.20).

The Viking Formation was deposited during high rates of sediment supply from the western Cordillera, resulting in progradation of marginal-marine sandstones east and north during an overall transgressive event (Burton and Walker, 1999; MacEachern et al., 1999; Reinson et al., 1994). In central Alberta, the Viking Sandstone unit has been shown to consist of a number of linear coarsening-upward offshore to shoreface successions, some of which are sharp-based, that erosively overlie the Joli Fou Formation (Reinson et al., 1994). In addition to marine sandstones, the unit may consist of conglomeratic intervals. Many of the conglomeratic linear bodies are encased in offshore mudstones and form excellent reservoirs, such as in the Joffre Field just south of the study area. In this study, the Viking Formation has been subdivided into the Viking Sandstone unit and the overlying Viking “shaly” unit, the latter consisting of silty shales and interbedded sandstones.

Elevations for the top of the Viking Sandstone unit range from -575 to -450 mASL (Figure A.21). Thicknesses range from 19 to 35 metres, averaging 30 metres across the study area (Figure A.22).

Elevations for the top of the "shaly" Viking unit range from -560 to-425 mASL (Figure A.23). Thicknesses range from 6 to 21 metres, averaging 15 metres across the study area (Figure A.24).

The Base of Fish Scales (BFS) marker is a distinct gamma ray excursion, present across much of the Alberta Basin. In this report, the interval between the top of the Viking Formation and the Base of Fish Scales marker is termed the Westgate Formation following MacEachern et al. (1999). The Westgate Formation consists of dark mudstone with some interbedded silty shales and bentonites (Leckie et al., 1994). The Westgate marks deposition during a time of continued marine transgression over the Viking Formation (MacEachern et al., 1999).

The top of the Second White Specks (SWS) is another basin-wide marker easily defined in the local-scale study area. Elevated gamma ray counts are related to high uranium content due to an abundance of white spheres consisting of coccoliths and coccospheres (Leckie et al., 1994). In this report the BFS – SWS shale is an interval that includes both the Second White Specks and the Fish Scales Formation (Figure 4). As such, high gamma ray counts are indicative of much of the interval. This thick shale succession was deposited during a lengthy time of elevated relative-sea level in the study area (Roca et al., 2008).

The top of the First White Specks (FWS) is the youngest of three basin-wide markers easily identified on logs in the study area. Similar to the SWS, high radioactivity is the result of high uranium content from microfossils (Leckie et al., 1994). In this report the interval between the FWS and SWS is termed the Upper Colorado shale (Figure 4). Deposition of this interval represents the second peak of marine transgression following deposition of the BFS-SWS shale. Lithologically the unit comprises calcareous mudstones, minor bentonites, fish remains and phosphorite nodules (Simpson, 1997; Leckie et al., 1994).

Overlying the Colorado Group, the Lea Park Formation in the study area is an undifferentiated interval of sediments comprised of marine mudstones and siltstones. In southern Alberta, the interval comprising the Lea Park is coarser-grained and is differentiated into the marginal-marine Milk River and Pakowki formations, which represent regressive and transgressive sedimentation, respectively (Power and Walker, 1996; Leckie et al., 1994). Thus, although not represented by significant sand bodies in the local-scale study area, the marine Lea Park interval encompasses both regressive and transgressive events. The latter transgressive event, recorded as Pakowki Formation mudstone deposition over Milk River sandstones to the south, is recorded in the study area as a distinctive resistivity log marker called the Milk River Shoulder (Power and Walker, 1996), which aided in correlation of the overlying Basal Belly River Sandstone unit (Figure 2).

In this study all of the fine-grained Colorado Group and Lea Park Formation deposits above the Viking Formation are mapped together as a single package of sediments,

since they constitute a significant regional aquitard. Elevations for the top of the Lea Park Formation range from 0 to 85 mASL (Figure A.25). The thickness of the sediments from the top of the Viking Formation to the top of the Lea Park Formation ranges from 510 to 573 metres, averaging 538 metres across the study area (Figure A.26).

2.3.6 Belly River Group

The Belly River Group characterizes the first pulse of sediment from the Cordillera following the Laramide Orogeny (Dawson et al., 1994). Cordillera-derived sediments prograded eastward and eventually capped the Lea Park Formation. The lower contact with the Lea Park Formation is gradational in the study area and represents the transition from open-marine to deltaic and fluvial sedimentation (Power and Walker, 1996). Deltaic and fluvial sedimentation is recorded in the lowermost unit of the Belly River Group, commonly known as the Basal Belly River Sandstone unit (the Basal Belly River Sandstone unit is part of the Foremost Formation; in this report the Belly River Group is subdivided only into the Basal Belly River sandstone and the overlying undifferentiated deposits named Upper Belly River) (Figure 4). The transition from the Lea Park Formation to the Basal Belly River is typically transitional, representing prograding shoreface environments with pulses of coarsening upward sandstones encased in shales (Power and Walker, 1996). In this study an effort was made to pick the base of the Basal Belly River (top of Lea Park) at the first occurrence of a significant sandy pulse across the study area.

Elevations for the top of the Basal Belly River Sandstone unit range from 10 to100 mASL (Figure A.27). Its thickness ranges from 3 to 23 metres, averaging 11 metres across the study area (Figure A.28).

Overlying the Basal Belly River Sandstone unit, the rest of the Belly River Group (Upper Belly River) is undifferentiated in this study, and comprises the rest of the coastal Foremost Formation, and the Oldman and Dinosaur Park formations (Figure 4). The Oldman Formation records predominantly fluvial and associated floodplain sedimentation (Dawson et al., 1994). The Dinosaur Park Formation consists of sandstones and siltstones, with characteristic inclined heterolithic stratification, deposited in fluvial, estuarine and floodplain environments (Hamblin, 1997).

Elevations for the top of the undifferentiated Upper Belly River interval range from 305 to 395 mASL (Figure A.29). Its thickness ranges from 285 to 305 metres, averaging 296 metres across the study area (Figure A.30).

2.3.7 Edmonton Group, Uppermost Cretaceous, Tertiary and Quaternary

The Bearpaw Formation represents a second major Upper Cretaceous transgression within the Alberta Basin, the first occurring during Lea Park time (Dawson et al., 1994).

The lower contact with the top of the Belly River Group reflects the flooding of the Boreal Sea north-westward (Eberth, 1996; Smith, 1994), with maximum transgression and deposition of the Bearpaw Formation shales just northwest of Edmonton (Dawson et al., 1994). The Bearpaw Formation is very thin in the study area, and as such it was difficult to pick. Picking the contact with the overlying Horseshoe Canyon Formation of the Edmonton Group was aided by the use of the Alberta Geological Survey dataset (Glombick, 2010), from which correlations were extended in the study area due to the fact that the top of the Lethbridge Coal Zone is proximal to the base of the Bearpaw Formation (Figure 4). Beyond the depositional edge of the Bearpaw Formation, the Lethbridge and Drumheller coal zones merge, with the base of the resulting coal zone being considered an approximate timeline the base of the Horseshoe Canyon Formation for the purposes of this study.

Elevations for the top of the Bearpaw Formation range from 335 to 400 mASL (Figure A.31). Thicknesses range from 0 m where missing due to non-deposition in the west of the study area, to 8 metres in the northeast (Figure A.32).

The overlying Horseshoe Canyon Formation represents a second pulse of east-southeast prograding (regressive) siliciclastics being deposited into and interfingering with the retreating Bearpaw Sea (Dawson et al., 1994; Smith, 1994). The interfingering nature records minor transgressions of the Bearpaw Sea during retreat to the southeast (Eberth, 1996). The formation comprises sandstone, mudstone and coals deposited in marginal-marine settings (Eberth, 1996).

Elevations for the top of the Horseshoe Canyon Formation range from 690 to 770 mASL (Figure A.33). Thicknesses range from 365 to 400 metres, averaging 382 metres across the study area (Figure A.34).

The Whitemud and Battle formations (Figure 4) record a period of limited sedimentation in the basin, with deposition in lakes and bogs (Dawson et al., 1994). The Whitemud and Battle formations are predominantly fine-grained, with tuffaceous beds in the upper Battle that have a distinctive high gamma ray response that aids in correlation (Dawson et al., 1994). Picking the contact with the underlying Horseshoe Canyon Formation was aided by the use of the Alberta Geological Survey coal database (Wynne and Beaton, 2003), from which correlations were extended in the study area due to the fact that the top of the Carbon-Thompson Coal Zone is proximal to the base of the Battle Formation (Figure 4).

Elevations for the top of the Whitemud-Battle interval range from 700 to 780 mASL (Figure A.35). Its thickness ranges from 5 to 18 metres, averaging 11 metres across the study area (Figure A.36).

The Battle Formation is disconformably overlain by the coarse siliciclastics of the lower part of the Scollard Formation (Dawson et al., 1994). Although locally portions of the Scollard Formation can act as an aquifer, due to the inherent heterogeneity in the

formation, regionally the formation is expected to act as a weak aquitard (Parks and Andriashek, 2009). The Paskapoo Formation consists of interbedded sandstone, siltstone and mudstone with minor coal and bentonite (Parks and Andriashek, 2009). The Scollard and Paskapoo formations, deposited predominantly with fluvial and associated environments, are amalgamated herein for mapping purposes (Figure 4). The combined unit is affected significantly by uplift and Cenozoic erosion following Paskapoo deposition during the Eocene to Miocene, which removed up to 3 km of sediment in the Alberta Basin (Dawson et al., 1994).

Elevations for the top of the Scollard-Paskapoo interval, which defines the top of bedrock, range from 780 to 910 mASL (Figure A.37). The thickness of this interval ranges from 20 to 210 metres, averaging 103 metres across the study area (Figure A.38).

The upper surface of the Scollard-Paskapoo defines the bedrock surface and is a major basin-wide unconformity. Resting on this surface is a complex mixture of unconsolidated Cenozoic sediments, much of which are glacially derived. In this report, unconsolidated sediments of Tertiary and Quaternary age between the top of the bedrock and the ground surface are treated as a single unit. Construction of the base of these deposits and of the ground surface was accomplished through the use of the publicly available Alberta Water Well Information Database.

The Quaternary unconsolidated surficial sediments generally consist of lacustrine deposits underlying glacially derived tills. Incised within these deposits are buried bedrock valleys and meltwater channels filled with fluvially derived sand and gravel. The Buried Buffalo Lake Valley (Agriculture and Agri-Food Canada, 2001) located to the east of the study area, has been eroded into the underlying bedrock. Meltwater channels trending northwest to southeast transect the study area. The thickness of the underlying unconsolidated undifferentiated Tertiary and Quaternary sediments range from 1 to 60 metres, averaging 15 metres across the study area (Figure A.39).

A topographical contour map (Figure A.40) was created using a Digital Elevation Model (DEM). Elevations for the ground surface in the study area range from 790 to 910 mASL (Figure A.40). The land surface elevation is generally higher in the west and lower in the east, with the Red Deer River in the southeast and associated tributaries in the northeast portions of the study area. Topographical highs are found in the southwest and west-central portions of the study area.

2.3.8 Coal Zones

Within the study area coal zones are found within the Upper Mannville, and the Belly River and Edmonton groups (Figure 4). Naming of the major coal zones follows that of Beaton et al. (2006). Coal seams were identified based on geophysical log responses. From the 672 wells selected for the project, wells with a combination of gamma ray,

neutron/density, sonic, sonic/neutron, resistivity, photoelectric, and caliper logs were used to identify the presence of coal seams. There are many coalbed methane wells in the study area, and good quality logs within these wells aided in the delineation of coal seams from the Belly River Group and shallower. Where poor borehole conditions existed — as identified by the caliper log and excessive density correction — sonic, density and neutron log responses that could be otherwise categorized as a coal response were ignored. Calculations of cumulative coal thicknesses (the net thickness of the coal seams from within a given coal zone) were made for the Mannville, McKay and Lethbridge coal zones (Table 1). For the Drumheller, Daly-Weaver, Carbon-Thompson and Ardley coal seams (Figure 4), a small number of Alberta Geological Survey coal database wells (Wynne and Beaton, 2003) were available within the study area, but were too few to generate statistically significant data for structure and thicknesses. For the most part, this small number of shallow coal picks aided in correlation of Belly River and Edmonton Group strata. The Taber Coal Zone (middle undifferentiated Belly River interval) was found to be absent in the study area.

Table 1: Characteristics of the mapped coal zones in the Enhance Clive study area.

		Thickness (m)			Top Coal Zone (mASL)		Base Coal Zone (mASL)	
Coal Zone	# of Wells	Min.	Max.	Avg.	Min.	Max.	Min.	Max.
Lethbridge	93	0.4	3.7	1.7	342.0	392.8	339.2	391.8
McKay	220	0.5	10.9	1.7	11.3	119.6	8.5	109.5
Mannville	433	2.2	15.2	8.4	-684.1	-504.7	-737.1	-559.3

Coals of the Mannville Coal Zone were identified in 433 wells (Figure 9). The base of the zone varies in elevation from -737.1 to 559.3 mASL, and the top from -684.1 to 504.1 mASL. It was not always possible to obtain a net cumulative thickness in all the wells due to poor log quality. Cumulative thicknesses calculated from good logs averages 8.4 metres, and ranges from 2.2 to 15.2 metres.

Coals of the McKay Coal Zone were identified in 220 wells (Figure 10). The base of the zone varies in elevation from 805 to 109.5 mASL, and the top from 11.3 to 119.6 mASL. It was not always possible to obtain a net cumulative thickness in all the wells due to poor log quality. Cumulative thickness calculated from good logs averages 1.7 metres, and ranges from 0.5 to10.9 metres.

Coals of the Lethbridge Coal Zone were identified in 93 wells (Figure 11). The zone was only delineated and cumulative thicknesses calculated where the Bearpaw Formation was recognized, and therefore where it could be differentiated from the coals of the Drumheller coal zone. The base of the zone varies in elevation from 339.2 to 391.8mASL, and the top from 342 to 392.8 mASL. It was not always possible to obtain a net cumulative coal thickness in all the wells due to poor log quality. Cumulative coal thickness calculated from good logs averages 1.7 metres, and ranges from 0.4 to 3.7 metres.

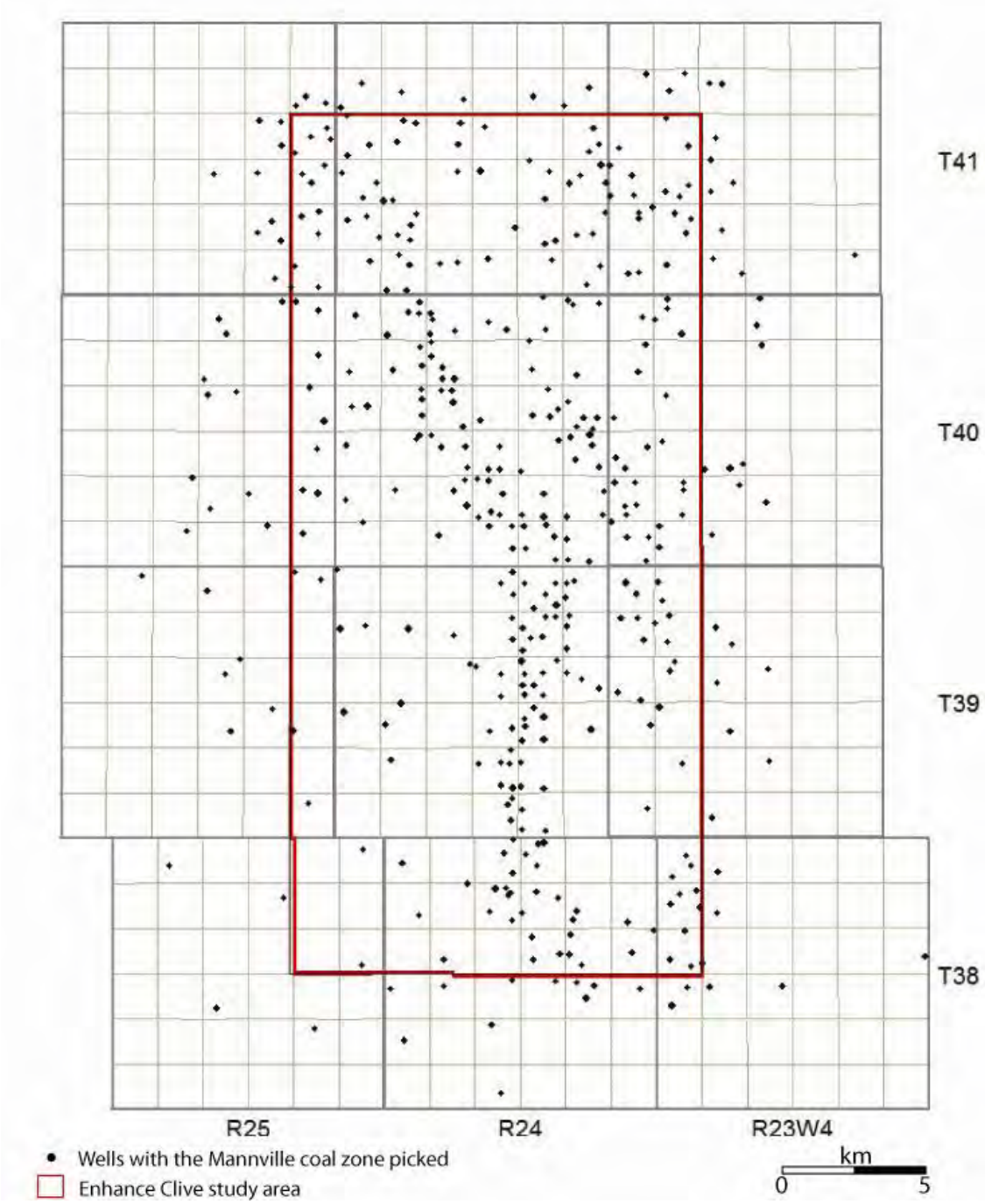

Figure 9: Well control used for mapping the Mannville Coal Zone (433 wells).

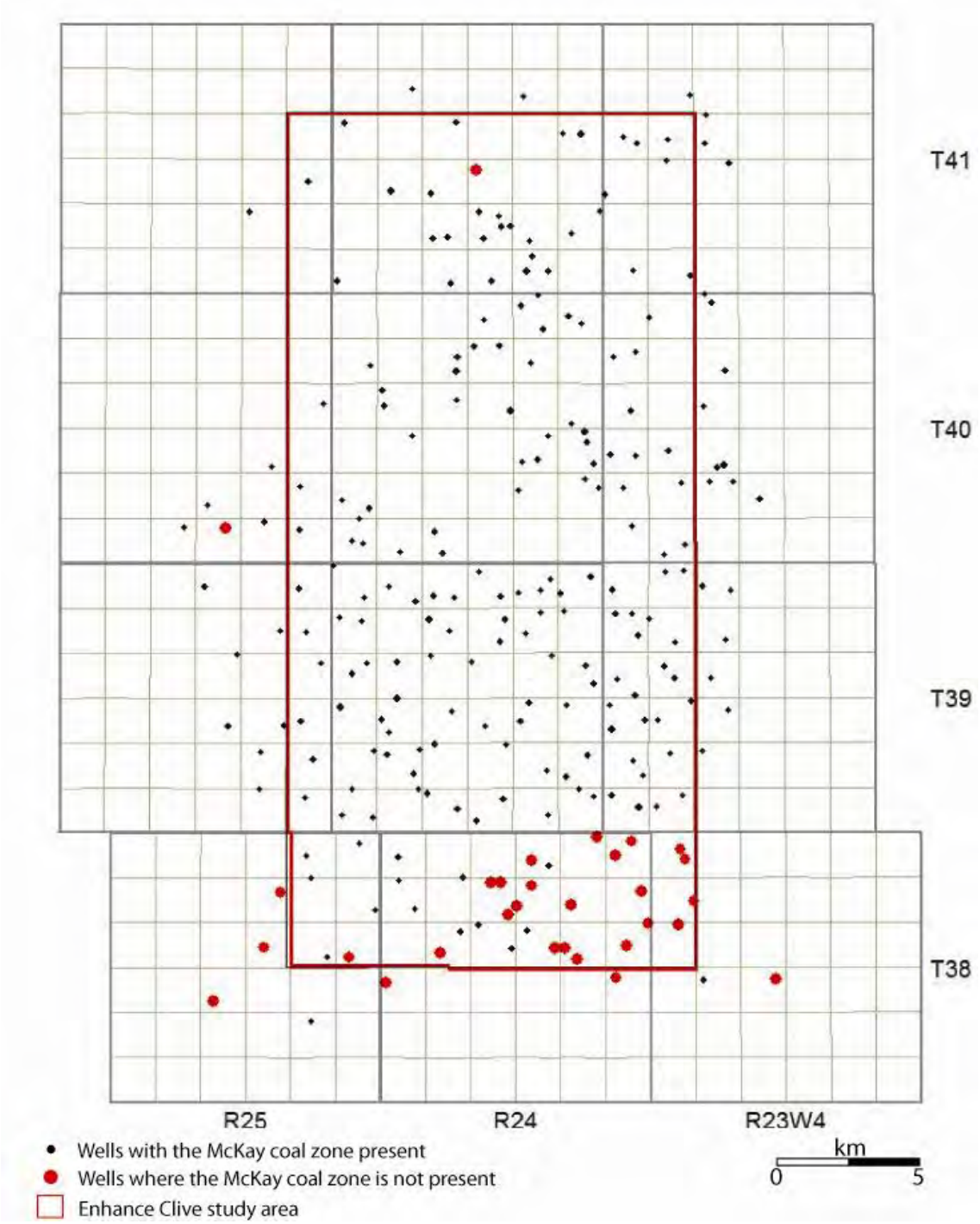

Figure 10: Well control used for mapping the McKay Coal Zone (220 wells).

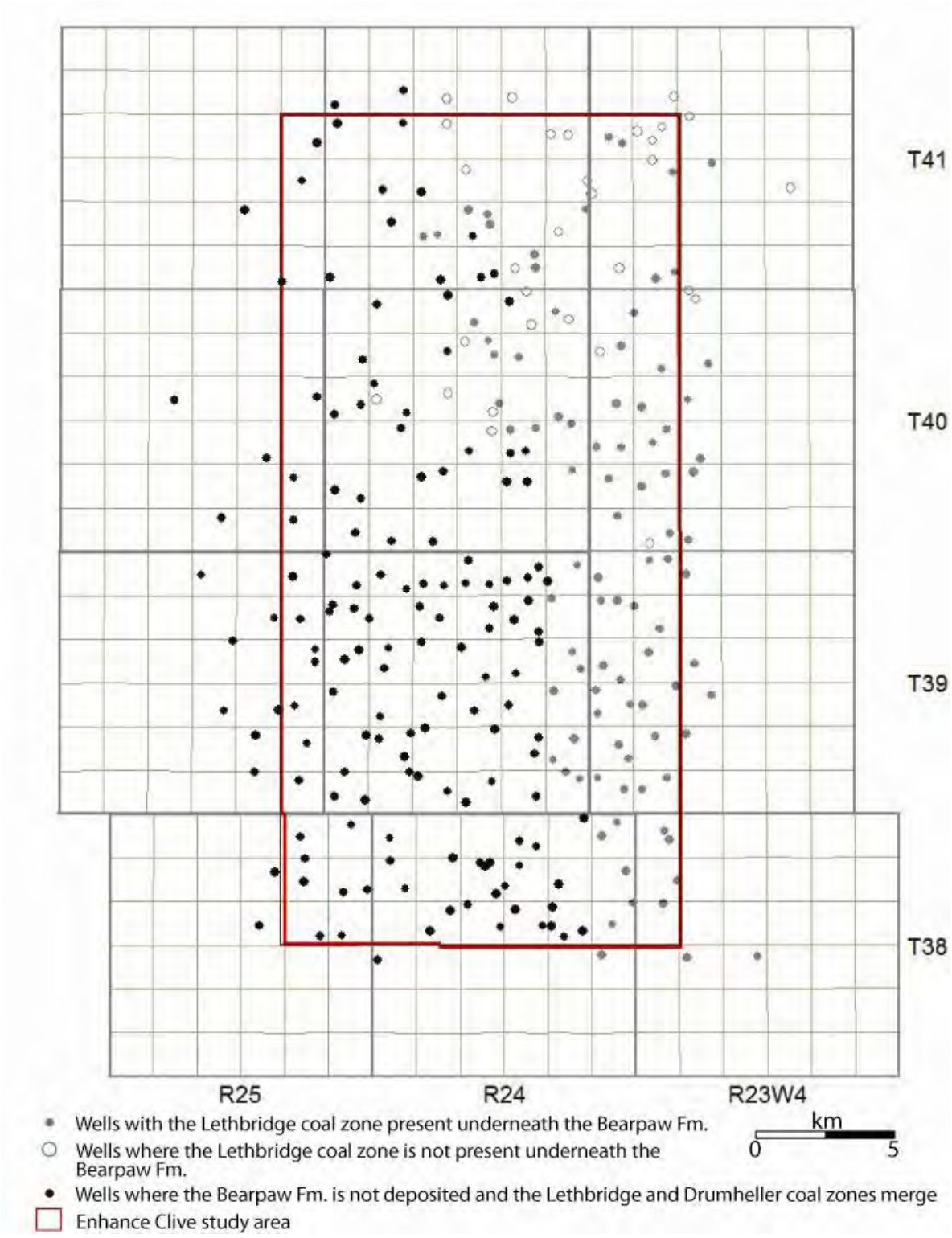

Figure 11: Well control used for mapping the Lethbridge Coal Zone (93 wells).

2.4 Geological Summary

A very thick package of Paleozoic, Mesozoic and Cenozoic sediments overlies the Clive Leduc (D3-A) and Nisku (D2) pools in the Enhance Clive study area. The top of the Paleozoic Nisku Formation to the ground surface, and all differentiable strata therein, were mapped as part of the geological task to define the sedimentary succession overlying the Leduc (D3-A) and Nisku (D2) reservoirs in the Clive oil field. The said stratigraphic interval is defined by strata deposited within two distinct basin evolutionary phases: an early Phanerozoic (Cambrian) to Late Jurassic miogeocline-platform stage with deposition on what can be considered predominantly a passive cratonic margin, and a phase of basin evolution involving orogenic cycles (the Jurassic-Early Cretaceous Columbian and Late Cretaceous-Tertiary Laramide orogenies) that affected the western cratonic margin of North America. The Devonian Nisku Formation to the top of the Mississippian Exshaw-Banff Formation in the study area were deposited within the first stage of basin evolution, and are dominated by carbonates, evaporites and intervening fine siliciclastics. The top of the Devonian Exshaw-Banff and Wabamun formations are affected significantly by erosional events that preceded deposition during the second phase of basin evolution, and form a Paleozoic subcrop that plays a significant role in the hydrogeological characteristics in the study area. Whereas the majority of the Paleozoic sedimentary units are continuous within the study area, the Exshaw-Banff interval is of limited extent due to the described erosional events. As a result of tectonic loading at the western margin of the basin during the Columbian orogeny, Paleozoic strata were tilted south-westward with a slope in the Enhance Clive study area of approximately 13 m/km (0.74º).

The second stage of basin evolution saw a cessation of carbonate growth due to a major influx of siliciclastics. Throughout Mesozoic time the foreland basin, created as a result of the Columbian and Laramide orogenies and paralleling the Rocky Mountain chain, was the locus of much of the sedimentation derived from erosion of the newly formed Cordillera. The majority of sedimentary units filling this foreland trough are continuous across the study area, except for those strata in proximity to the base of the Tertiary and Quaternary deposits, which were truncated as a result of Cenozoic erosional events (Scollard and Paskapoo formations). Only the Bearpaw Formation is limited in extent in the study area due to non-deposition.

A large number of formations considered to act as aquitards overlie the Leduc and Nisku oil reservoirs in the study area, especially within the Mesozoic sedimentary succession (Figure 4). A number of Devonian and Mississippian formations likely constitute aquitards, such as the Calmar, and Exshaw and Banff formations, respectively. Anhydritic intervals within the Nisku and Stettler formations constitute effective barriers, the former of which is evidenced by the nature of Nisku oil accumulation being restricted to the lower Nisku unit. Very thick Colorado Group to Lea Park Formation sediments, consisting of fine-grained siliciclastics, also form a significant barrier to upwards migration of CO_2. In addition, Cretaceous formations contain thick and laterally extensive coal zones, consisting of numerous coal seams of various thicknesses, which act as

additional barriers to upwards migration of CO_2 due to CO_2 affinity to coal onto which surface it adsorbes. The aquitard properties of these strata will be demonstrated in the next chapter.

3. Hydrogeology

3.1 Hydrostratigraphic Framework

3.1.1 Overview

The Hydrogeology Group at the University of Alberta was sub-contracted by AITF to undertake the hydrogeological characterization of deep strata using data from oil and gas wells in order to assess hydraulic communication between aquifers, and to define secondary barriers for CO_2 leakage from the storage unit (Melnik and Rostron, 2011). The study of shallow hydrogeology was conducted by AITF using data from water wells as recorded in Alberta Environment databases. The results of both studies are integrated in this chapter.

The study area for deep hydrogeology was expanded by one additional township on each side of the geology study area, covering TWP 37-42, RG 22-26W4 (Figure 12), to encompass more data and build a better understanding of the regional flow systems present. This expansion of the study area was necessitated by the general scarcity of hydrogeological data (particularly drill-stem tests) compared to geological data. The study of shallow hydrogeology, on the other hand, focused only on the Enhance Clive study area (TWP. 38-41, RG. 23-25) due to the large number of water wells present in the area.

The hydrogeological characterization of the sedimentary succession above the Leduc (D3-A) and Nisku (D-2) oil reservoirs involves an in-depth analysis of the chemistry and flow of formation waters in each aquifer in the succession. The deep hydrogeology of this area has been previously studied in detail as part of broader hydrogeological studies by Rostron (1995); Rostron and Tóth (1997); Rostron et al. (1997); Anfort et al. (2001); and Bachu and Michael (2003). These studies have produced a detailed hydrogeological characterization of the Upper Devonian to Lower Cretaceous sedimentary succession. One of their major conclusions was that hydraulic communication may exist between the Upper Devonian and overlying Cretaceous aquifers. The objective of this study is to update the hydrogeological characterization of the strata above the Nisku Formation, focusing on the assessment of degree of hydraulic communication between various aquifers.

The analyses and steps taken to achieve the study objectives include:

a) Definition and delineation of the hydrostratigraphy (aquifers and aquitards) within the sedimentary succession overlying the Nisku Formation;

b) Analysis of salinity and hydraulic head distributions in each aquifer to describe the patterns of formation water salinity and lateral flow;

c) Detailed analysis of formation water chemistry;

d) Interpretation of hydrochemistry and hydrodynamics in the aquifers using aquifer hydrochemistry and vertical pressure gradients.

e) Summary of hydrogeology and assessment of hydraulic communication between aquifers; and identification of secondary traps and barriers to vertical migration of CO_2.

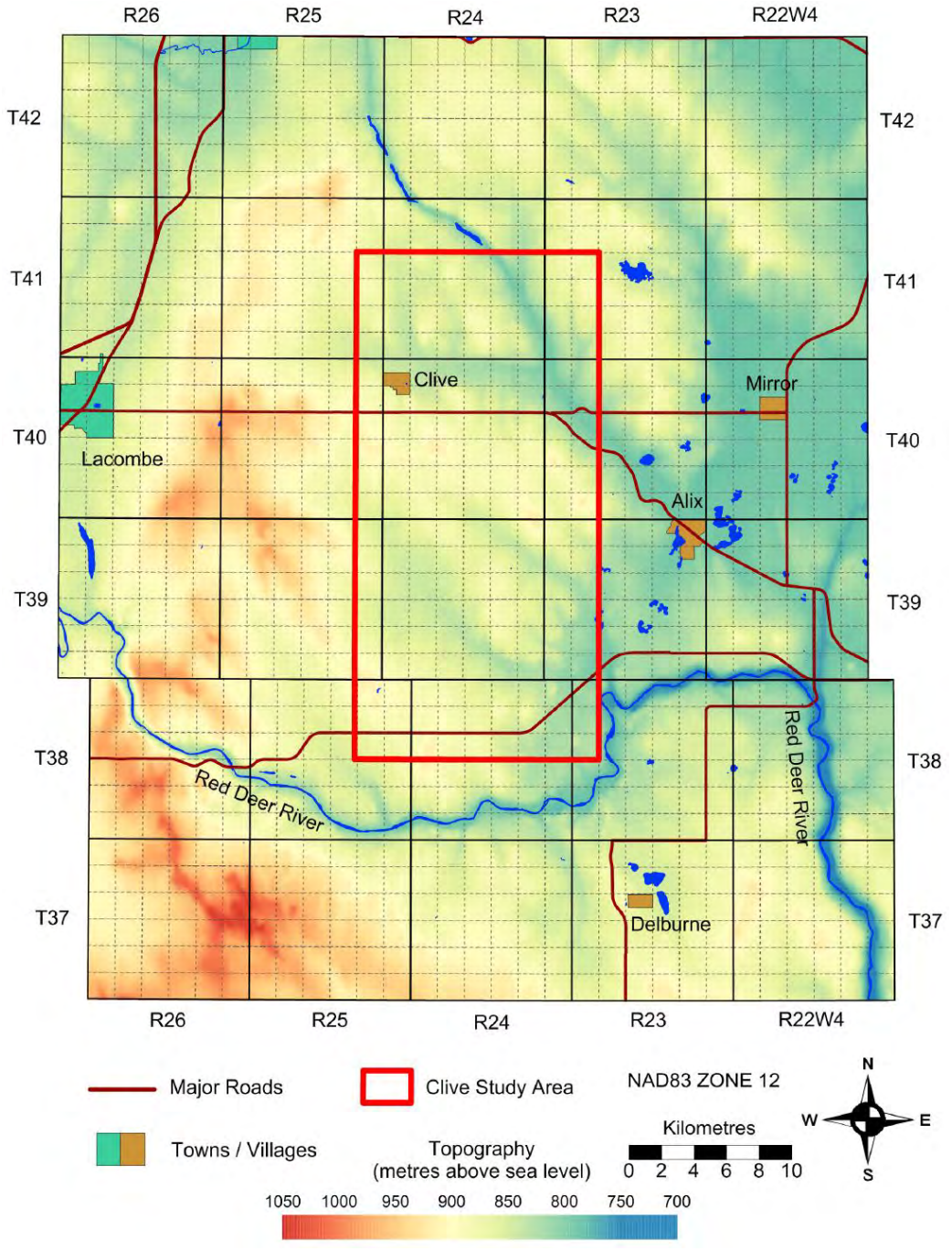

Figure 12: Regional topographic map of the hydrogeological study area. (Topography DEM from GeoBASE; roads and DLS grid from GeoScout).

3.1.2 Major Hydrostratigraphic Units

The sedimentary succession investigated primarily consists of four geologic packages (in ascending stratigraphic order): 1) Upper Devonian carbonates, evaporites and shales; 2) Carboniferous shales present in the west and south; 3) a thick package of Mesozoic mixed siliciclastics and shales; all overlain by 4) Cenozoic till, glacio-fluvial and lacustrine sediments (Figure 4).

Rostron (1995) defined three major aquifer groups in the Upper Devonian and Lower Cretaceous sedimentary succession in the Clive area: 1) Upper Devonian Hydrogeologic Group; 2) Mannville Group Aquifer; and 3) Viking Group Aquifer. The Upper Cretaceous hydrostratigraphy was refined by Bachu and Michael (2003) to include two additional aquifers: 1) Basal Belly River Aquifer; and 2) Upper Belly River Aquifer. This chapter combines the previous results into a single hydrostratigraphic chart for the Enhance Clive and larger hydrogeological study areas (Figure 13).

The Nisku (D-2) oil reservoir is overlain by the Calmar Formation (both are part of the Winterburn Group), which constitutes the primary caprock. The deep hydrostratigraphy of the sedimentary succession overlying the Winterburn Group in the regional study area (Figure 13) consists of four aquifers and five aquitards. This framework has been constructed based the lithology, data quality and availability, and previous hydrogeological studies in the area. Defined aquifers were characterized by using pressures from drill-stem tests and water chemistry data from formations considered to be laterally continuous and permeable.

The base of the hydrostratigraphic section is the Calmar-Wabamun Aquitard. The lower portion of the aquitard consists of anhydritic Upper Nisku Formation (Hearn et al., 2011) overlain by the shales of Calmar Formation. Above that the Wabamun Aquitard in the Enhance Clive study area consists of predominantly evaporitic deposits of the Stettler Formation and marine limestones of the Big Valley Formation (both of the Wabamun Group). In the larger geological and hydrogeological study areas, the Wabamun Group (Calmar-Wabamun Aquitard) is overlain by Lower Mississippian shales of the Exshaw and Lower Banff formations, however, these relatively thin sediments are present only in the southern and western parts of the Enhance Clive study area (Section 2.3.3). For the purpose of the hydrogeological study the Mississippian shales, where present, are included in the Calmar-Wabamun Aquitard.

The Lower Mannville Aquifer is situated immediately above the Calmar-Wabamun Aquitard. The Lower Mannville Aquifer consists of mixed siliciclastics of the Ellerslie Formation, calcareous siltstones and shales of the Ostracod Formation, and coarse clastics of the Glauconitic Formation. However, the majority of the hydrogeological data are from the Ellerslie Formation, which, therefore, is thought to be the main water-bearing unit. The Sub-Cretaceous Unconformity forms the boundary between the underlying Wabamun Aquitard and the overlying Lower Mannville Aquifer.

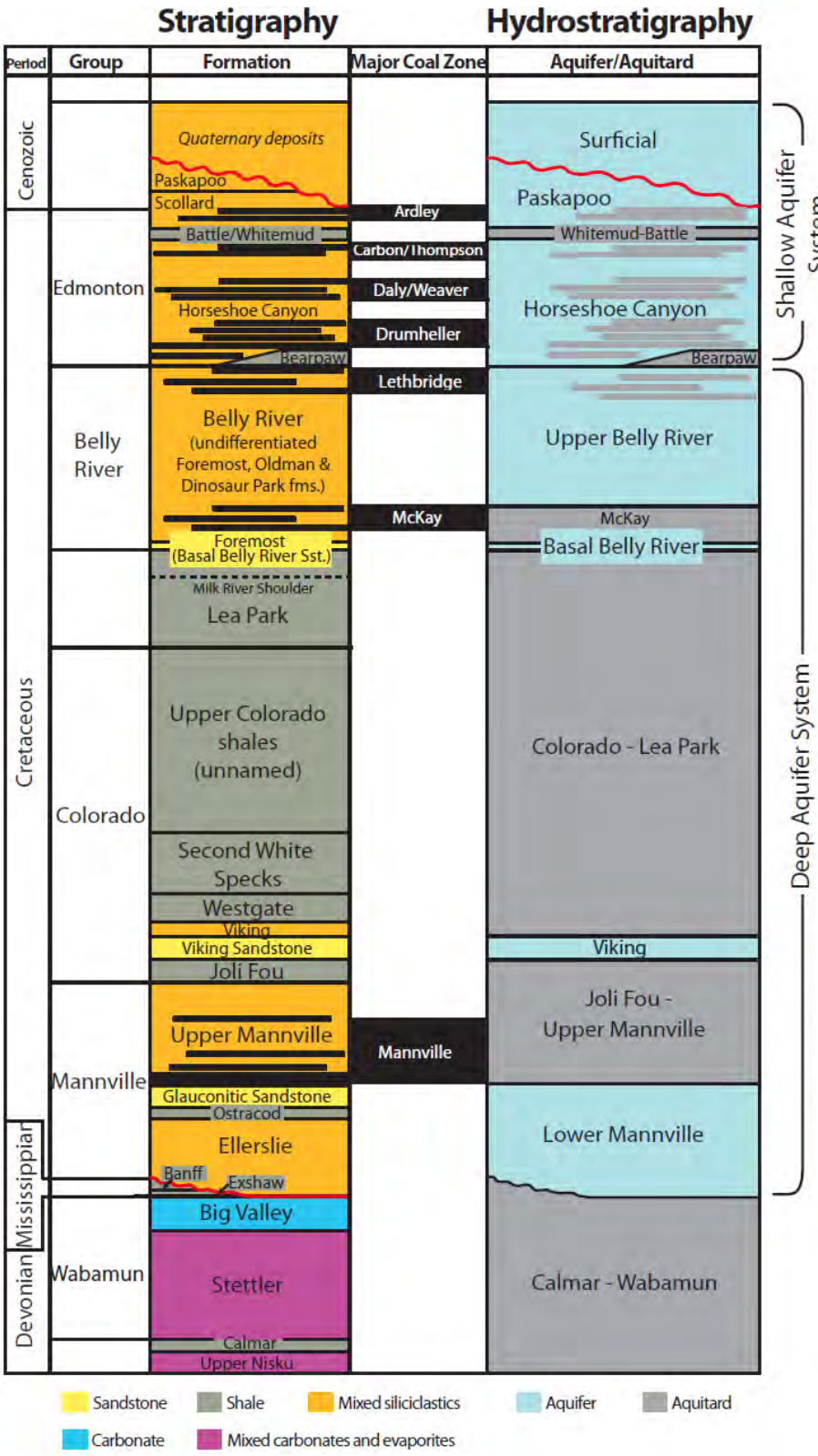

Figure 13: Lithostratigraphic and hydrostratigraphic charts for the Enhance Clive study area.

Overlying the Lower Mannville Aquifer is the Upper Mannville–Joli Fou Aquitard. In the Clive area the Upper Mannville Group consists of thick coals and highly mixed siliciclastics; interbedded quartz to volcano-feldspathic sandstones, siltstone and shale units of non-marine origin (Section 2.3.4), unlike in other parts of Alberta where the Upper Mannville strata are dominantly sandstones or dominantly shales,. The lithology and the lack of any significant water recovered in any of the drill-stem tests from the Upper Mannville in the Clive area indicate that the Upper Mannville Group in this area has very low bulk permeability. Therefore, the Upper Mannville Group has aquitard characteristics and, combined with the overlying shales of the Joli Fou Formation, is interpreted to form the thick Upper Mannville –Joli Fou Aquitard.

The coarse clastics of the Viking “sandstone” Formation constitute the Viking Aquifer. In this area the Viking Formation consists of a lower clean sand unit and an upper “shaly” unit (Section 2.3.5). Fluid recovered from DSTs originated mainly from the sand unit of the Viking, therefore this unit was denoted the aquifer, and the upper shaly unit was incorporated into the overlying aquitard.

Above the Viking Formation is the massive succession of shales and siltstones of the Upper Colorado Group and Lea Park Formation (Section 2.3.5). This thick shale succession, together with the upper shaly unit of the Viking Formation, form the regionally-extensive Colorado-Lea Park Aquitard. This aquitard ranges in thickness from 529.29 m to 586.31 m, with an average of 554 m.

Strata of the Belly River Group overlie the Colorado–Lea Park Aquitard. The Belly River Group has been subdivided into two aquifers: 1) Basal Belly River; and 2) Upper Belly River based on their different geological and hydraulic characteristics. The lower unit, termed the Basal Belly River Aquifer, is composed of coarsening upward sandstones encased in shales (Section 2.3.6). Overlying the Basal Belly River Aquifer is the Upper Belly River Aquifer which consists of undifferentiated fluvial deposits of sandstones and shales. These two aquifers are separated by the “McKay Coal Zone” (Section 2.3.8) and associated fine-grained sediments that act as an aquitard (McKay Aquitard). The Upper Belly River Aquifer is capped by the variably thick shales of the Bearpaw Formation. East of Range 23 the Bearpaw Formation acts as an aquitard (Bachu and Michael, 2003), however west of Range 23 the Bearpaw Formation is absent due to non-deposition.

The shallow hydrostratigraphy consists of three aquifers and one aquitard. The interbedded sandstones, mudstones and coals (Section 2.3.7) of the Horseshoe Canyon Aquifer (Edmonton Group) overlie the Bearpaw Aquitard where present, or the Upper Belly River Aquifer where the Bearpaw Aquitard is absent. According to Alberta Environment, the Horseshoe Canyon Aquifer constitutes the base of groundwater protection in the Clive area (Tokarsky, 1987).

The Whitemud-Battle Aquitard overlies the Horseshoe Canyon Aquifer and consists of the shales of the Whitemud and Battle formations. Above it, the Tertiary sandstones,

mudstones, and coals of Scollard and Paskapoo formations form the Paskapoo Aquifer. The overlying undifferentiated Quaternary sediments form the last aquifer in the succession, named here the Surficial Aquifer.

The hydrogeological analysis presented herein is focused on the Cretaceous and Tertiary aquifers because the Devonian strata overlying the Leduc (D3-A) and Nisku (D-2) oil reservoirs in the Clive area form an aquitard, and the complex lithology, hence hydrostratigraphy and hydrogeology of the Surfical Aquifer is beyond the scope of this report.

3.2 Data Collection and Methodology

3.2.1 Deep Hydrogeology

The regional hydrogeological characterization presented here is based on the chemistry and pressure regime of formation waters. The data for each aquifer were assembled into two separate databases for chemistry and pressures. Chemistry and pressure data for aquitards were not available with exception of three water chemistry analyses from the Stettler Formation (Calmar-Wabamun Aquitard). Interval testing (Khan, 2006; Palombi, 2008) of each data point was used to structurally verify the data points. In this way each data point was placed within the structurally-defined boundaries of its corresponding aquifer based on the geological model described in Chapter 2 and Appendix A. For those data located outside of the geological study area, individual well logs were examined to confirm the sample interval and its formation.

Water Chemistry Data

The water chemistry database for deep aquifers was assembled using the Geofluids software (Rakhit Petroleum Consulting Ltd: now Canadian Discovery Ltd.). In the hydrogeological study area it consists of 1869 water analyses of samples obtained in drill-stem tests (DSTs), production tests and wellhead samples (Table 2). Since the majority of the analyses are from DSTs and wellhead samples, they have a high risk of contamination by (acid) completion fluid, corrosion inhibitor, and various drilling muds (Hitchon and Brulotte, 1994). Removal of these contaminated water analyses was required to ensure that only samples representative of true formation water were used for further analysis. Culling water chemistry is an iterative process due to variability of formation-water chemistry throughout the study area. Culling procedures (detailed in Appendix B) are based on previous studies by Hitchon and Brulotte (1994), Rostron (1994), Hitchon (1996), and Block (2001). More than 85% of initial data were culled as a result of this process (Table 2).

Table 2: Number of chemistry and pressure data collected (initial) and used (final) in the hydrogeological characterization of deep aquifers in the Clive hydrogeological study area.

Aquifer	Chemistry Data		Pressure Data	
	Initial	Final	Initial	Final
Upper Belly River	542	50	1294	73
Basal Belly River		18		48
Viking	482	52	1245	49
Lower Mannville	845	147	2400	136
Total	*1869*	*267*	*4939*	*306*

The values of Total Dissolved Solids (TDS) are calculated through the summation of all ionic constituents dissolved in a groundwater sample. The analysis of TDS distribution is supplemented with the major ion constituents to better understand groundwater evolution and help identify contaminated samples. The chemistry of formation waters in the Cretaceous aquifers was analyzed using maps of TDS and the variation of individual major ions.

Chemistry data were used to produce maps of Total Dissolved Solids (TDS) and ionic cross-plots, which were incorporated in density-dependent flow analysis. The TDS values are calculated through the summation of all ionic constituents dissolved in a groundwater sample. The analysis of TDS distribution is supplemented with the major ion constituents to better understand groundwater evolution and help identify contaminated samples.

Pressure Data

Fluid pressure data (4939 data points) from drill-stem tests (DSTs) were downloaded from GeoScout software (Hydrofax database) into a single excel spreadsheet and supplemented with additional data (Canadian Institute for Formation Evaluation - CIFE). Production data for the study area were also downloaded from GeoScout.

All DSTs were screened using both automated and manual techniques to remove poor-quality and inaccurate fluid pressures. An additional set of culling criteria used to further evaluate the quality of pressure measurements is described in Appendix B.

A “Cumulative Interference Index” (CII) was calculated to determine and quantify the influence of production and injection on the pressures within the respective aquifer-formation. The CII method was initially used by Barson (1993) and Rostron (1994), based on the interference index suggested by Tóth and Corbet (1986). For every DST in a particular aquifer a quantitative index was calculated accounting for radial proximity of a DST to producing or injecting wells and the duration of production or injection. This calculation was implemented in the Visual Basic Code developed by Alkalali (2002). Almost 94% of the initial DST data were culled because of poor quality or production interference (Table 2).

Pressure data were converted to freshwater hydraulic heads using the following equation:

$$h = z + \frac{P}{\rho g} \quad (1)$$

where: h is hydraulic head, p is the extrapolated (true) formation pressure, ρ is the reference water density, g is the gravitational constant, and z is the measurement's (recorder) elevation.

The three main assumptions in construction of fresh-water hydraulic head maps are: (a) the water density is uniform and has a value of 1000 kg/m^3, (b) the aquifer is near horizontal, and 3) there is no vertical flow (i.e. the flow is parallel to the aquifer bedding). However, these assumptions have been shown as incorrect in deep, saline, and sloping aquifers introducing significant errors into the flow interpretation (Davies, 1987; Bachu, 1995a; Bachu and Michael, 2002). Variable water density and aquifers' slope were taken into account by using Water Driving Forces plotted as vectors on the freshwater hydraulic head maps. Davies (1987) defined the "Water Driving Force" (WDF) to correct for the variable density in the sloping aquifers as the vectorial addition of the following terms:

$$WDF = \nabla h + \frac{\Delta\rho}{\rho}\nabla E \quad (2)$$

where: ∇h is the fresh-water hydraulic head gradient, ∇E is the slope of the aquifer or of the corresponding formation top, and $\Delta\rho$ is the density difference between fresh-water and the formation water. The Water Driving "Force" is a fresh-water gradient ∇h corrected by an additional term of aquifer slope ∇E modified by the density contrast $\Delta\rho$ (Alkalali, 2002; Khan, 2006; Palombi, 2008). Structural elevations required to calculate the slope of each aquifer (∇E) in the Clive study area are shown in Appendix A and described in Chapter 2. Additional tops for the greater hydrogeological study area were downloaded from GeoScout and combined with the picks of the Clive area to calculate aquifer slope in the region not covered by the geological study area.

Maps of freshwater hydraulic heads and driving force vectors were produced and combined to show the direction and magnitude of the force driving the flow of formation water. Actual flow strength can be assessed by considering rock permeability and the viscosity of formation water. Vertical flow and hydraulic communication (or lack thereof) can be interpreted by comparing the flow patterns in adjacent aquifers and by using pressure-elevation plots.

Bachu and Michael (2002) have shown that the errors introduced by the use of hydraulic head distributions to analyze the flow of variable-density water in sloping aquifers is minimized if hydraulic heads are calculated using the average water density found in each aquifer, which for the aquifers in the Cretaceous-Tertiary succession in

hydrogeological study area are: Lower Mannville Aquifer - 1060 kg/m^3; Viking Aquifer - 1025 kg/m^3; and Basal and Upper Belly River aquifers - 1000 kg/m^3. The density values are based on the water chemistry analyses. Freshwater hydraulic head maps (potentiometric surfaces) are sufficient for the Basal and Upper Belly River aquifers because the density of formation water in these aquifers is that of freshwater (1000 kg/m^3). For the other two deeper aquifers, Lower Mannville and Viking, maps of hydraulic heads produced with the respective average water density were produced, in addition to the maps of freshwater hydraulic heads and driving force vectors, to illustrate flow direction and strength.

Porosity and Permeability

Porosity and permeability are rock flow properties important in the assessment of the flow of formation water and of other fluids, such as CO_2, in the subsurface. Porosity is an additive (cumulative) volumetric property of the rocks. Permeability is a scale-dependent tensorial property of porous media defining the ability of fluids to flow through the respective medium that is not additive, and scaling-up methods need to be used to estimate permeability at the well and field scales (Dagan, 1989). Permeability is measured in the laboratory on plugs taken from cores (plug-scale permeability), and in drillstem (or hydraulic) tests (well-scale permeability).

Core porosity and permeability were processed for the Cretaceous strata within the Enhance Clive study area. Core analyses for aquitards were not available. Standard measurements from core plugs such as minimum, maximum and median values have been determined for each formation (Section 3.6). In addition, an upscaling procedure has been completed from the core- to well- and regional-scales. Porosity is an additive scalar quantity and as such, it can be scaled up from core- to well-scale according to the following relation:

$$\phi_{well} = \frac{\sum_{1}^{N} l_i \phi_i}{\sum_{1}^{N} l_i} \qquad (3)$$

where: ϕ_i is the porosity measured in plug *i*, l_i is the length of the representative interval for the measured porosity value, and *N* is the number of porosity measurements in the respective well. The geometric average was taken for all well-scale values to arrive at the regional-scale (or field-scale) porosity for each formation (Dagan, 1989).

Due to permeability's tensorial nature, usually three values are measured in core: the maximum horizontal permeability (k_{max}), the permeability in the horizontal direction (k_{90}) orthogonal to k_{max}, and the vertical permeability (k_v). Permeability anisotropy is expressed by the ratios of k_{90} to k_{max} (horizontal anisotropy) and of k_v to k_{max} (vertical anisotropy), and is usually derived by regression analysis of the core measurements. The evaluation of anisotropy is based on core measurements where k_{max}, k_{90} and k_v were

determined in the same core. In many cases only k_{max} is routinely measured, thus data samples for anisotropy determination are usually smaller than the data sample for k_{max}.

Due to permeability being a non-additive quantity, it is scaled up from core- to well-scale according to the power-law averaging as follows:

$$k_{well} = \left[\frac{\sum_{1}^{N} l_i k_i^{\omega}}{\sum_{1}^{N} l_i} \right]^{1/\omega} \quad (4)$$

where: k_i is the maximum permeability measured in plug *i*, and k_{well} is the effective well permeability. In the above expression, ω has values between -1 (harmonic average, for flow in serial systems) and +1 (arithmetic average, for flow in parallel systems). The geometric average is retrieved for ω = 0. Previous work has shown that the value of ω = 0.8 should be used in scaling up from the core- to the well-scale (Desbarats and Bachu, 1994). The geometric average was taken for all well-scale values to arrive at the regional-scale permeability for each formation (Dagan, 1989).

Drill-stem test permeability for the aquifers with data was calculated using the slope of the pressure build-up curve determined from the Horner (1951) extrapolation plot (Earlougher, 1977), according to:

$$kh/\mu = 162.6\mathrm{QB}/\mathrm{m} \quad (5)$$

where: k is permeability (millidarcies), h is reservoir thickness (feet), μ is fluid viscosity (cP), Q is the average flow rate (bbl/day), B is the oil formation volume factor (STB/RB, approximately equal to 1.0), and m is the slope of the pressure build-up curve, in psi per logarithmic cycle.

The collected (initial) pressure data from drill-stem tests were culled according to methods described in Appendix B. The effects of production (Cumulative Interference Index) were not considered because permeability is a rock property and does not depend on pressure conditions. The following additional parameters were required for permeability calculation: (1) the slope of the pressure build-up curve, (2) the total fluid recovery for the DST, and (3) the drill pipe and/or drill collar dimensions. The total fluid recovery and the length of the drill collars are critical parameters when calculating DST permeability because they are needed in the determination of the volumetric flow rate Q.

3.2.2 Shallow Hydrogeology

Water well data for shallow aquifers were obtained from the Alberta Environment Water Well Database through the Groundwater Information Centre (GIC). The data query in the Enhance Clive study area (TWP 38 - 41 and RG 23 – 25W4) produced a list of 1170 wells. A total of 424 water level data and 41 chemistry analyses were extracted from the

database (Table 3). All of the 424 water levels and only 25 chemistry analyses (after culling) were used in the hydrogeological analysis for the shallow aquifers in the Enhance Clive study area.

Wells were separated out based on perforated or screened intervals relative to formation surfaces. When perforation or screened interval details were not available, casing depth and well liner depth were used to determine the completion interval for the purposes of this study. Table 3 indicates that 31 water levels were available for wells within the unconsolidated Quaternary deposits and 383 from wells completed in the Paskapoo Aquifer. Only eight water levels were available for the Horseshoe Canyon Aquifer. Similarly, water chemistry data available for use in this study were limited. Additional water chemistry data (55 water analyses) for the Horseshoe Canyon Aquifer were obtained from GeoScout database. These were production and wellhead samples from Coal Bed Methane (CBM) wells perforated in the Horseshoe Canyon coal seams throughout the larger hydrogeological study area.

Table 3: Data collected from GIC for shallow aquifers and used in the hydrogeological analysis.

Unit/Formation	Water Level Data	Chemistry Data	
		Preliminary	Final
Quaternary Deposits	31	14	5
Paskapoo-Scollard	383	25	18
Horseshoe Canyon	8	1	1
Total	*422*	*40*	*24*

Total Dissolved Solids values were calculated using the following formula for consistency with the GIC database:

$$TDS = 0.6\ Total\ Alkalinity\ \ as CaCO_3\ \ + Na + K + Ca + Mg + SO_4 + Cl + 4.425\ \ NO_3 + NO_2\ \ - N\ \ +\ \ if\ present\ \ 1.285(NH_3 - N) \quad (6)$$

The obtained values were lower than those calculated through simple ionic summation but are still representative of the regional TDS trends.

Hydraulic head values were directly inferred from the static water level measurements. Water Driving Forces were not calculated for these aquifers due to the relatively low TDS in shallow aquifers which has no effect on water density. Consequently, maps of freshwater hydraulic heads can be used to ascertain flow direction and magnitude of the force driving the flow.

No porosity or permeability data were available for the shallow aquifers. Porosity is not measured, and permeability can be derived from hydraulic conductivity calculated from pump tests, but no such tests were available.

3.3 Regional Flow and Salinity of Formation Waters

3.3.1 Lower Mannville Aquifer

The Lower Mannville Aquifer is present across the entire hydrogeological study area and is directly underlain by the Calmar-Wabamun Aquitard.

The distribution of TDS in the Lower Mannville Aquifer is shown in Figure 14. Total Dissolved Solids concentrations in this aquifer are quite variable and increase from south to north in the study area. The TDS ranges from 40 g/L in Twp. 37 to over 130 g/L in the very north. The 100 g/L contour line defines a large saline plume which occupies all of the north-eastern part of the full study area. This plume extends further to the north-east outside of this study area (Rostron et al., 1997; Rostron and Tóth, 1997, Anfort et al., 2001) and its position corresponds with the erosional edge of Banff Formation where the Lower Mannville Aquifer is in direct contact with the underlying Devonian strata. There are several minor isolated points of high and low TDS attributed to local intra-formational variations in chemistry between the Ellerslie and Glauconitic formations (i.e., isolated samples from different formations within the same aquifer may occasionally show slightly different TDS and chemistry).

Hydraulic heads in the Lower Mannville Aquifer calculated with the average water density of 1060 kg/m^3 are shown in Figure 15. Water Driving Force vectors have been calculated and posted on Figure 16. There are no significant areas of density-dependent flow in the study area due to the ambient combination of salinity contrast (Figure 14), hydraulic gradient (Figure 16) and aquifer slope (Figure A.15). The interpreted lateral flow direction is not uniform throughout the entire study area. There are three distinct areas of hydraulic-head highs present, which coincide with hydrocarbon producing fields. The arm of the 450 m contour extends from the west and culminates at 500 m of hydraulic head between Twp. 40 to 41 and Rg. 25. Two other major highs are present in Twp. 38, Rg. 23 and Twp. 39, Rg. 22. Water flows from the above-mentioned highs towards lows in the southeast and northeast, where the head values are below 400 m. The gradients range from 40 m/km near potentiometric highs and decrease towards the potentiometric lows to less than 1 m/km (Figure 16). These results are consistent with the regional flow patterns in the Lower Mannville Aquifer (e.g., Rostron, 1995; Anfort et al., 2001).

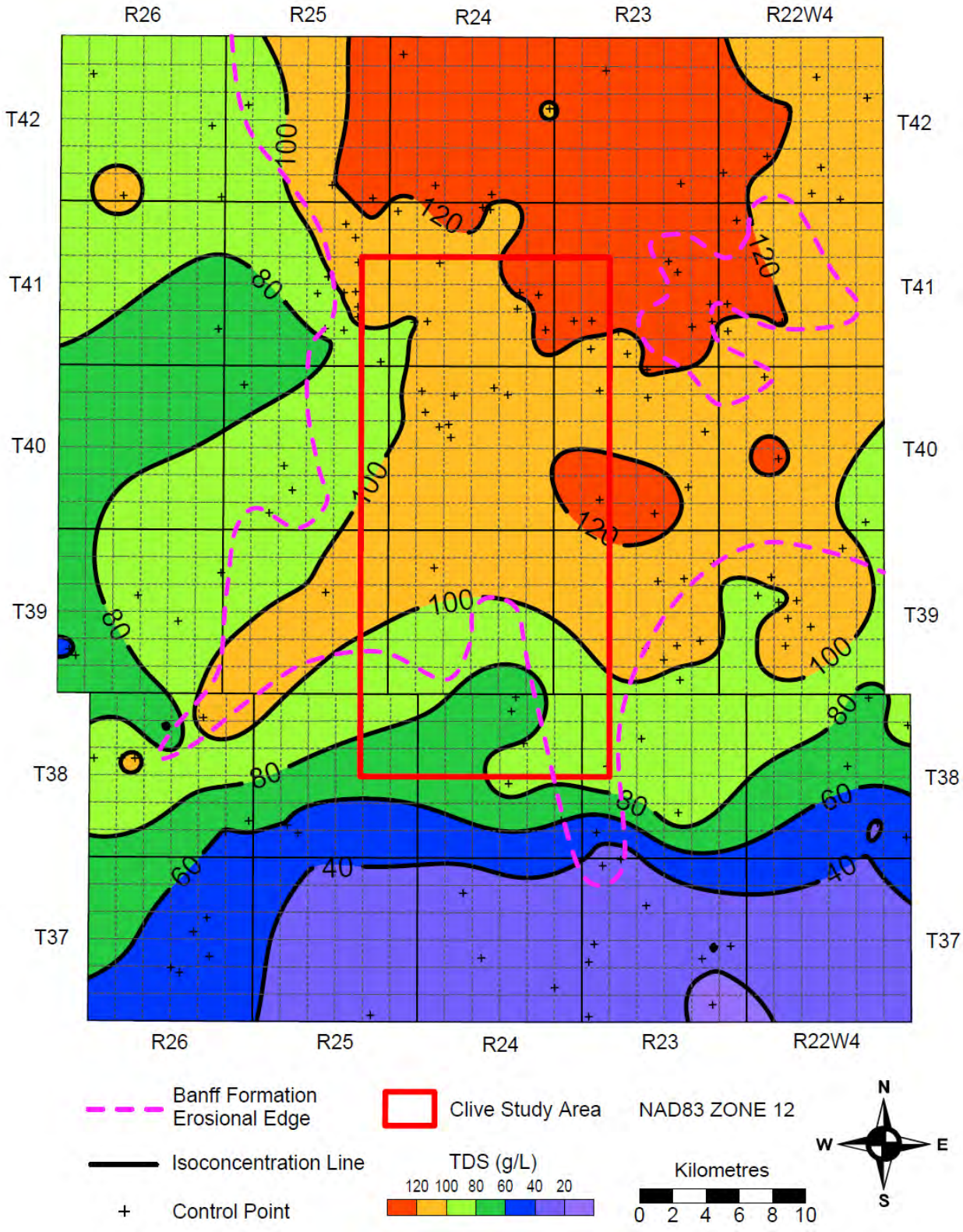

Figure 14: Total dissolved solids distribution (g/L) in the Lower Mannville Aquifer (C.I. = 20 g/L).

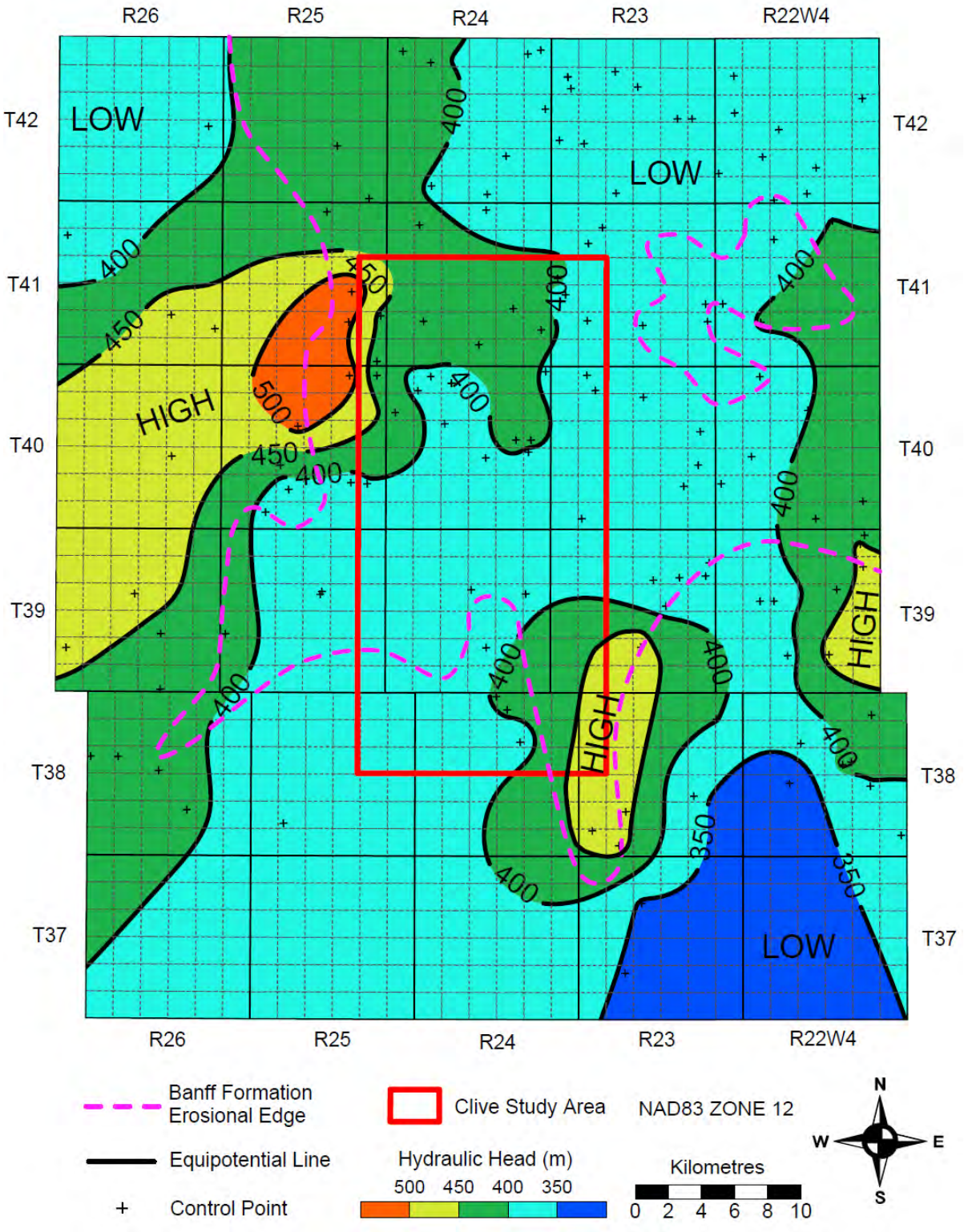

Figure 15: Hydraulic head distribution (m) in the Lower Mannville Aquifer (C.I. = 50 m). Water density (ρ) = 1060 kg/m^3

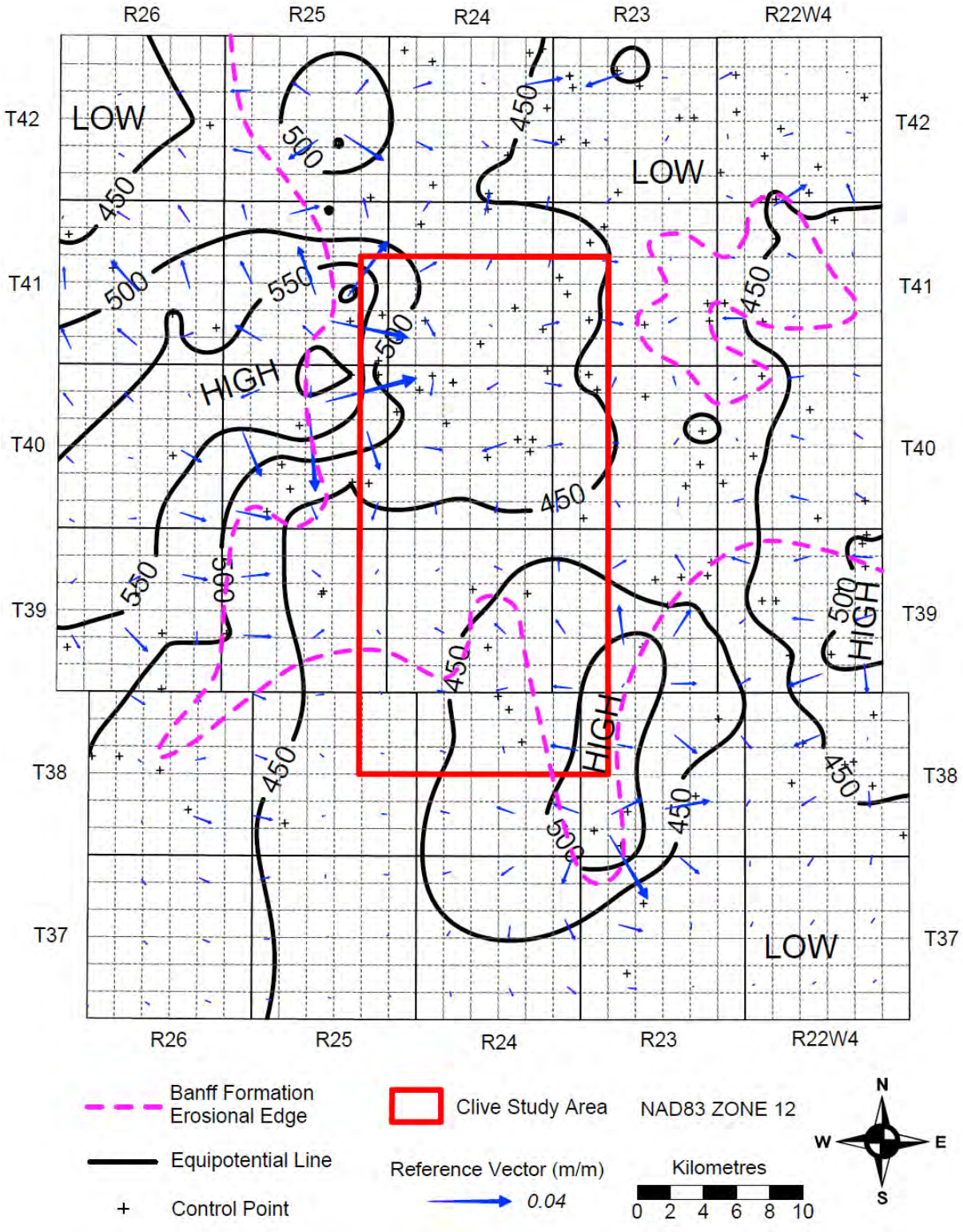

Figure 16: Water Driving Forces (WDF) in the Lower Mannville Aquifer overlain over freshwater hydraulic heads (C.I. = 50 m).

3.3.2 Viking Aquifer

The hydrodynamic regime in the Viking Aquifer is based on data summarized in Table 2. Distributions of TDS and hydraulic heads are shown in Figure 17 and Figure 18, respectively. The most obvious feature is the lack of data (water recovered from DSTs or producing wells) in the south and southwest, which coincides with the boundary of the "Deep Basin" (Masters, 1979; 1984). The Deep Basin is a widespread hydrocarbon-saturated (mainly gas) zone stretching along the Alberta foothills characterized by significant underpressures and lack of formation water (Masters, 1979; 1984; Corbet and Bethke, 1992; Bachu and Underschultz, 1995; Rostron, 1995).

The overall distribution of TDS in the Viking Aquifer (Figure 17) is distinctly different from the underlying Lower Mannville Aquifer (Figure 14). The range of TDS in the Viking Aquifer has been measured between roughly 30 and 60 g/L, with TDS decreasing with depth toward the southwest.

Fluid flow directions in the Viking Aquifer (Figure 18) are more uniform compared to the underlying flow patterns in the Lower Mannville Aquifer. Hydraulic heads in the Viking Aquifer, calculated with an average water density of 1025 kg/m^3, range from 390 m in the northeastern corner of the study area down to 230 m in the central region, much lower than hydraulic heads in any other aquifer and significantly lower than the topographic elevation in the area. The low pressures and corresponding hydraulic heads in the Viking Aquifer are believed to be the result of erosional rebound of the overlying rock framework (Corbet and Bethke, 1992; Parks and Tóth, 1995; Bachu, 1995) or of post-glaciation rebound (Bekele et al., 2003; Lemieux et al., 2008). The hydraulic head distribution the flow of the Viking Aquifer waters downdip, to the southwest. Previous studies in the area (Hitchon, 1969a; 1969b; Bachu and Underschultz, 1995; Rostron, 1995; Rostron and Tóth, 1997; Rostron et al, 1997) have shown similar downdip flow patterns in the Viking Aquifer. Lateral hydraulic gradients range from 20 m/km in the central area along the Deep Basin transition boundary to less than 1 m/km in the northeast (Figure 19).

3.3.3 Basal Belly River Aquifer

The Belly River Group has been separated into two aquifers: 1) the Basal Belly River, and 2) the Upper Belly River. This hydrostratigraphic delineation coincides with the rather significant difference in the values of hydraulic head and change in lithology from the coarse basal sandstone in the Basal Belly River overlain by the continuous MacKay Coal Zone (Figure 13), to the predominantly mixed siliciclastics in the Upper Belly River Group. Using the geological model from Chapter 2 it was possible to distinguish and allocate hydraulic data to either the Basal or Upper Belly River aquifers.

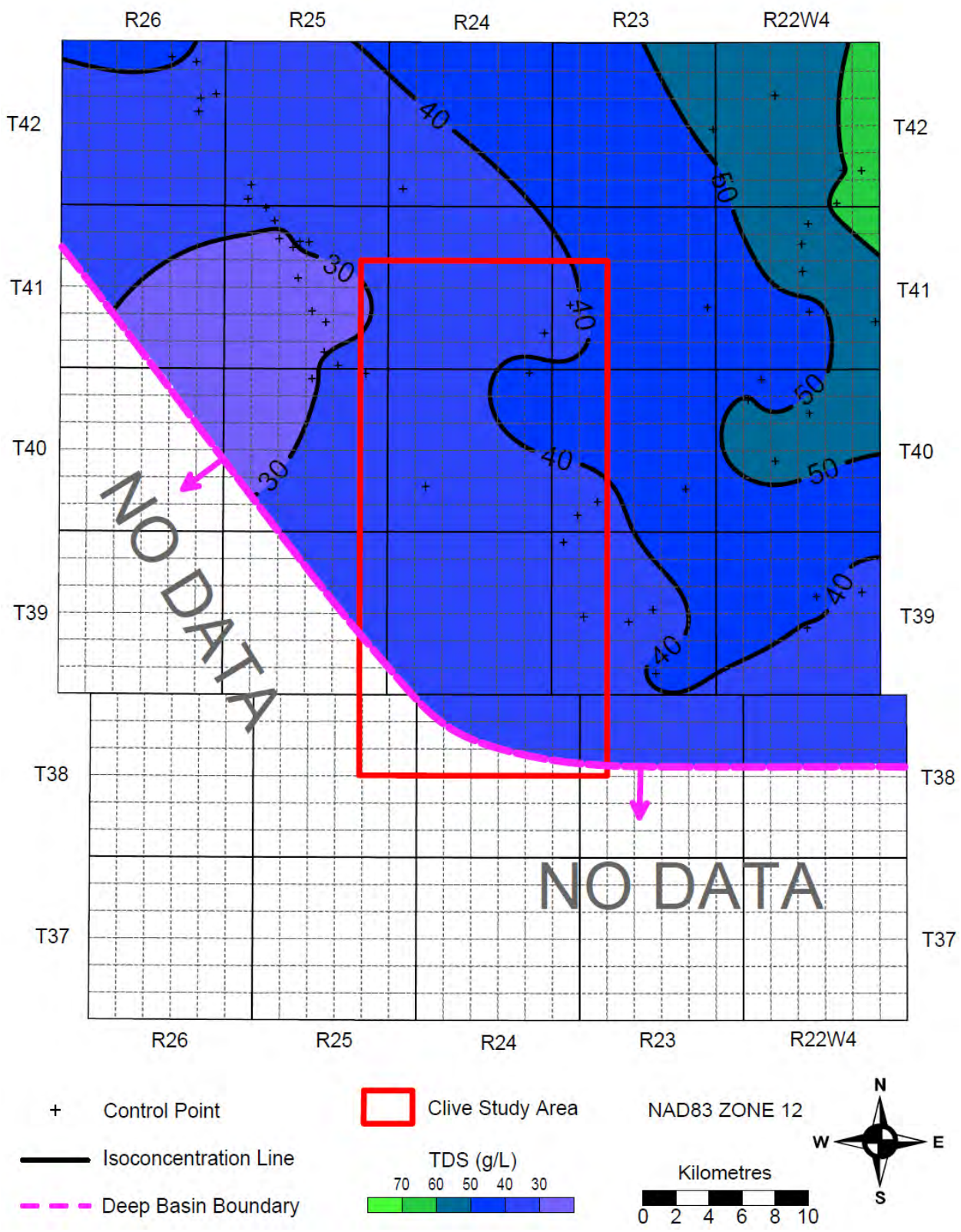

Figure 17: Total dissolved solids distribution (g/L) in the Viking Aquifer (C.I. = 10 g/L).

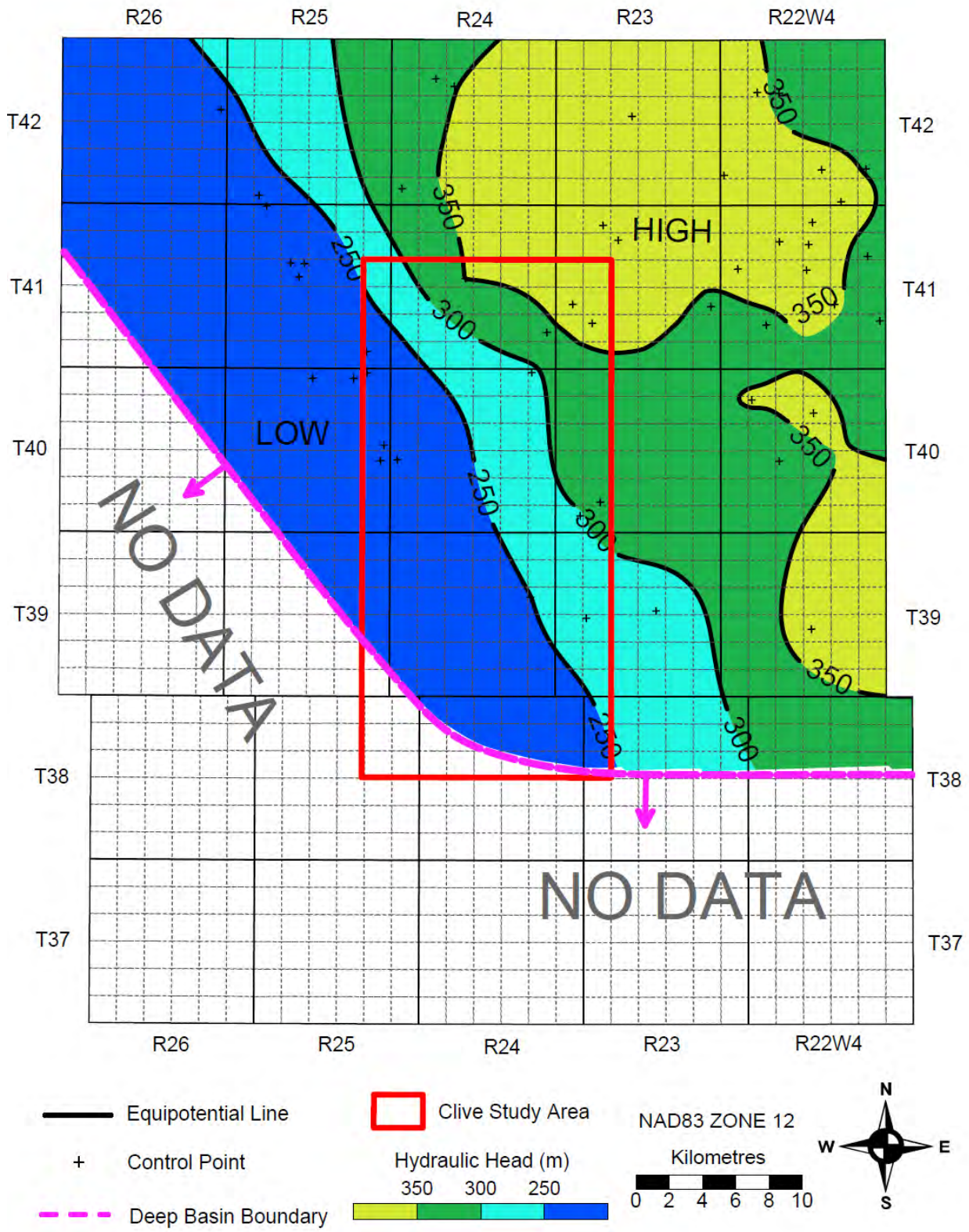

Figure 18: Hydraulic head distribution (m) in the Viking Aquifer (C.I. = 50 m). Water density (ρ) = 1025 kg/m³

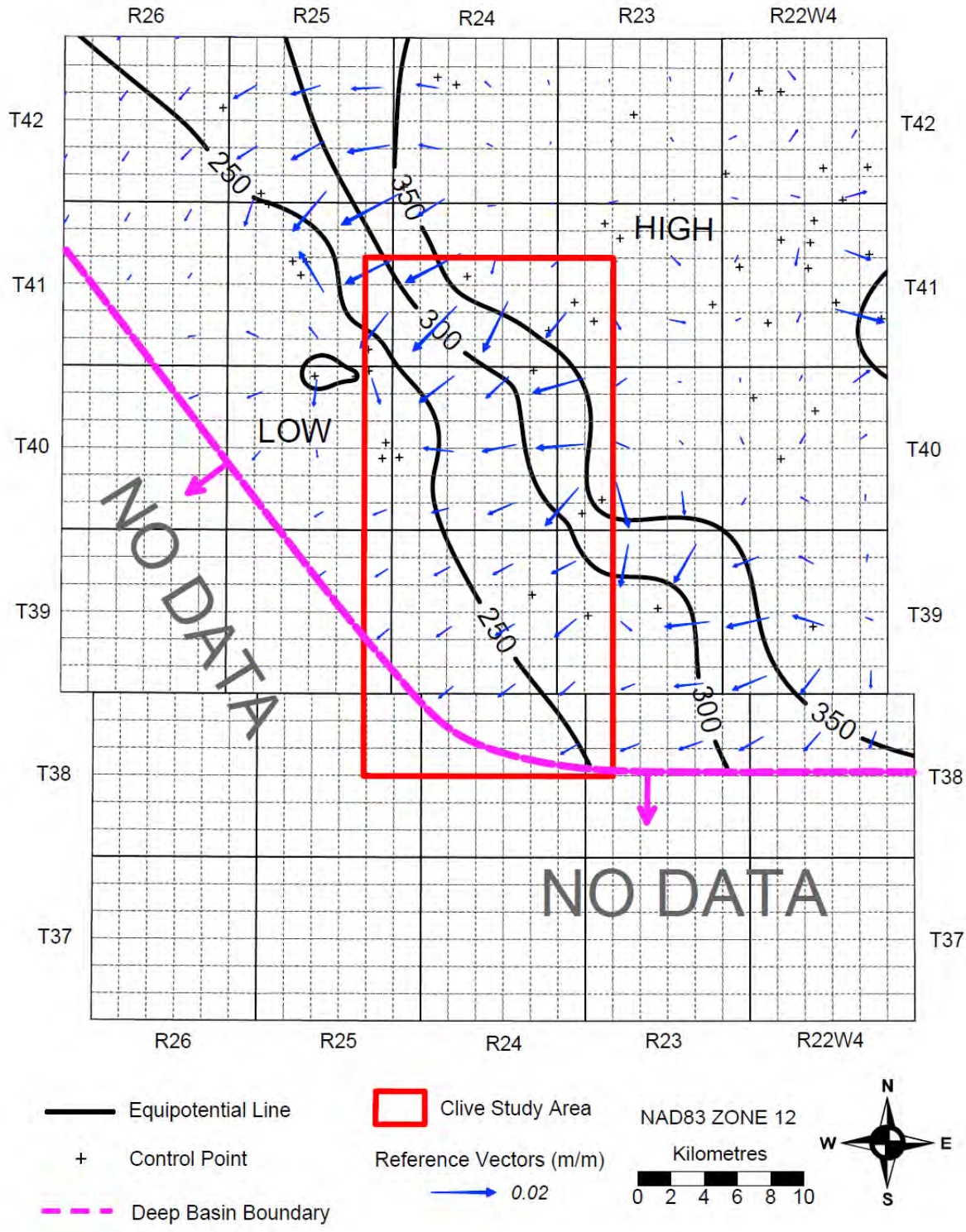

Figure 19: Water Driving Forces (WDF) in the Viking Aquifer overlain over freshwater hydraulic heads (C.I. = 50 m).

The hydrochemistry and flow regime of the Basal Belly River Aquifer are shown in Figure 20 and Figure 21, respectively. Results are based on a fairly limited data control summarized in Table 2. Values of TDS are posted in Figure 20, and show that formation waters are significantly fresher in this aquifer compared to the underlying Cretaceous aquifers. Measured values of TDS range from 10.1 to 15 g/L, much less than in the underlying Viking Aquifer (Figure 17) where the TDS ranged from 30 to 60 g/L. It should be noted that the chemistry data are limited to the northern half of the hydrogeological study area because there are no data points within the Enhance Clive study area itself.

Hydraulic heads in the Basal Belly River Aquifer (Figure 21) are the highest in the northeastern corner of the study area, (almost 600 m), and decrease to the southwest (down to 350 m). Lateral flow directions in this aquifer are generally downdip towards the southwest and are the result of post-glaciation erosional rebound (Bachu and Michael, 2003). Hydraulic gradients range from 1 to 20 m/km. The hydrodynamic regime in the Basal Belly River Aquifer is markedly different from that in the underlying Viking Aquifer (Figure 18), as indicated by the significantly higher hydraulic heads.

3.3.4 Upper Belly River Aquifer

Undifferentiated siliciclastics of the Upper Belly River Group have been combined into a single aquifer, the Upper Belly River Aquifer. This aquifer is separated from the underlying Basal Belly River Aquifer by the MacKay Aquitard.

Distributions of TDS and freshwater hydraulic heads in the Upper Belly River Aquifer are shown in Figure 22 and Figure 23, respectively. Total Dissolved Solids in this aquifer are generally less than 10 g/L across the entire study area (Figure 22). The TDS is highly variable due to the complex nature of the Upper Belly River sands (Chapter 2) and contouring the data reveals no underlying patterns or trend. Thus, the data are only posted to provide bounds on the potential distribution of TDS anywhere in the aquifer.

While the TDS values between the Basal and Upper Belly River aquifers are markedly different, the distributions of freshwater hydraulic heads in the two aquifers are relatively similar. Hydraulic heads in the Upper Belly River Aquifer range between 500 m in the northeast to 400 m the southwest (Figure 23). Water flows downdip from the northeast towards the southwest as the result post-glaciation erosional rebound (Bachu and Michael, 2003). An additional potentiometric high is observed in Twp. 37, Rg. 22 from which water flows to the west and north into a small potentiometric low. Lateral hydraulic gradients vary between 1 to 20 m/km. It should be noted that the potentiometric surface in the Upper Belly River Aquifer is not influenced by surface topography (i.e., the distribution of hydraulic heads (Figure 23) does not correspond to topographic elevations in the study area (Figure 12).

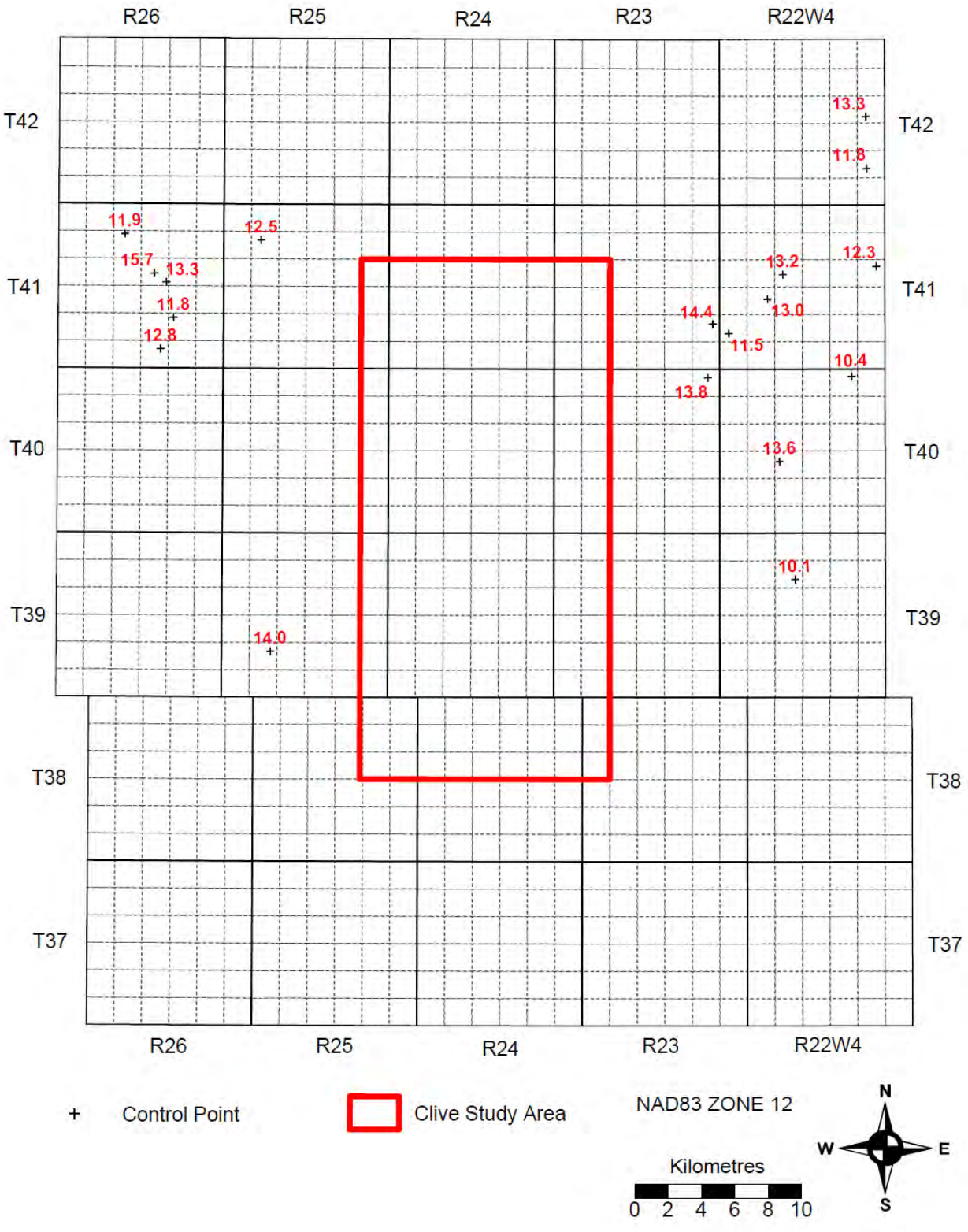

Figure 20: Total dissolved solids distribution (g/L) in the Basal Belly River Aquifer.

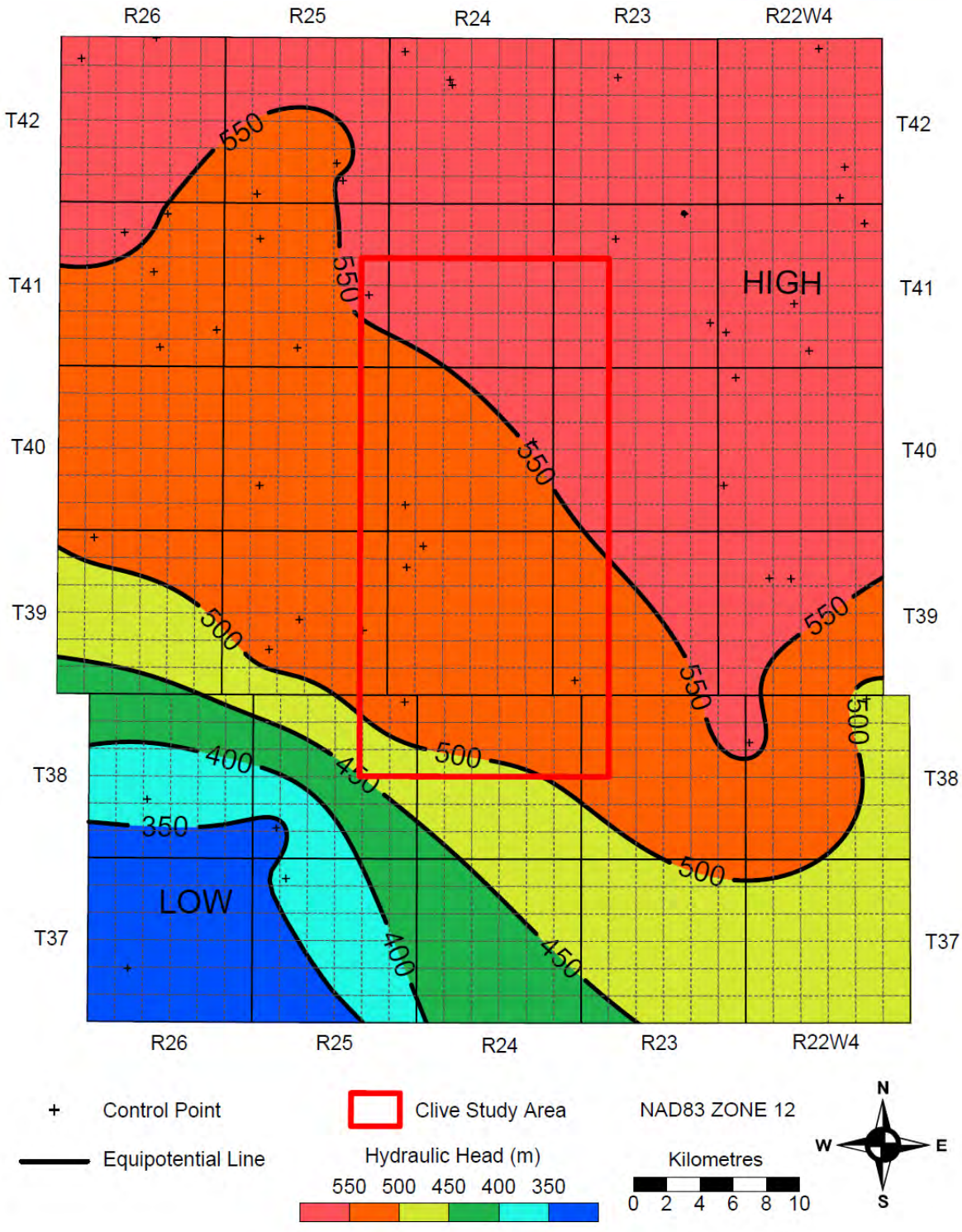

Figure 21: Hydraulic head distribution (m) in the Basal Belly River Aquifer (C.I. = 50 m). Water density (ρ) = 1000 kg/m^3

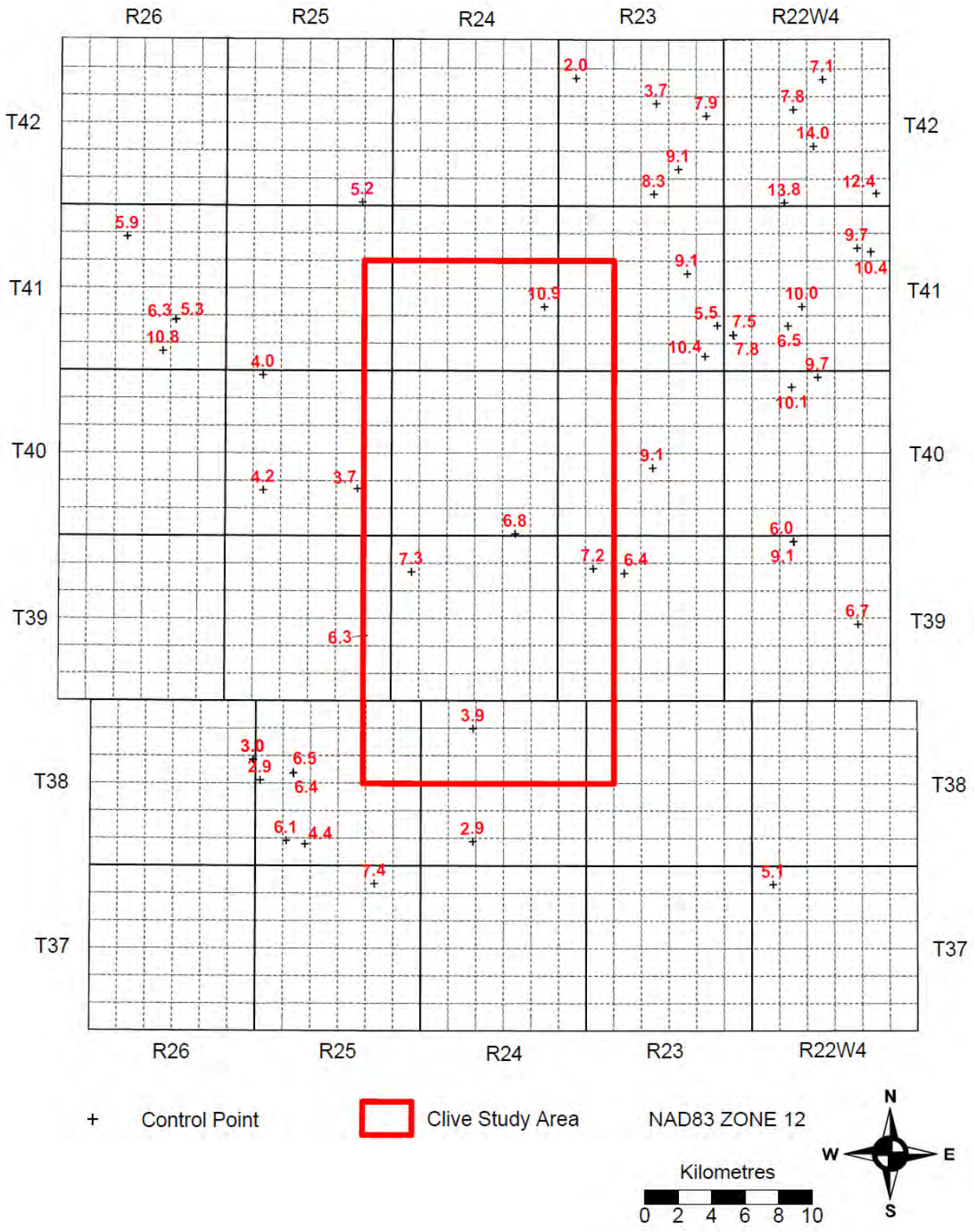

Figure 22: Total dissolved solids distribution (g/L) in the Upper Belly River Aquifer.

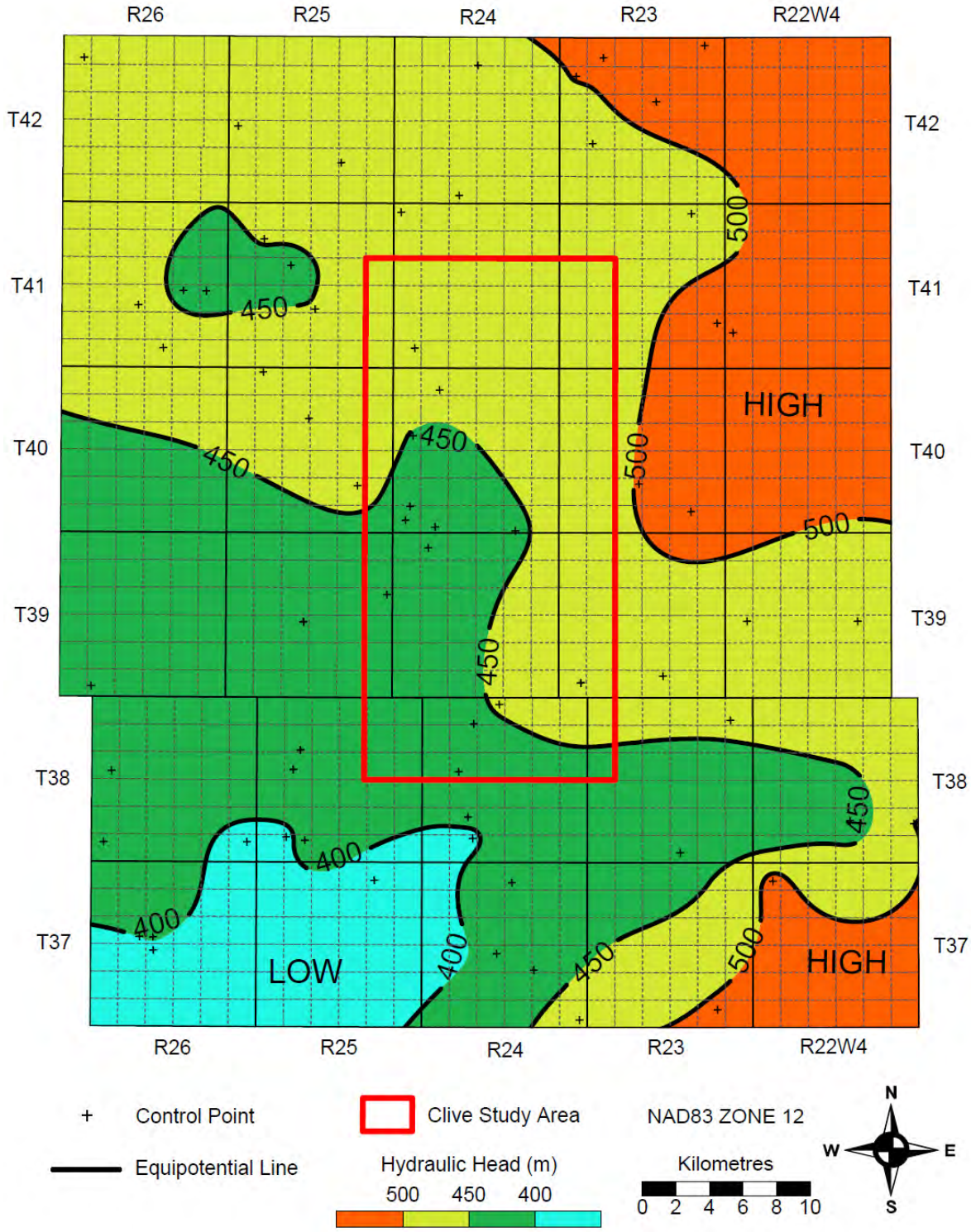

Figure 23: Hydraulic head distribution (m) in the Upper Belly River Aquifer (C.I. = 50 m). Water density (ρ) = 1000 kg/m^3

3.3.5 Horseshoe Canyon Aquifer

The data for the Horseshoe Canyon Aquifer are very limited. The values of TDS and hydraulic heads were posted on Figure 24 and Figure 25, respectively. Total Dissolved Solids are lower than in the underlying Upper Belly River Aquifer, and range between 0.5 and 8.3 g/L (3 g/L on average) (Figure 24). All available chemistry data are located outside of the Enhance Clive study area. Hydraulic head values in the Enhance Clive study area range between 718 m and 798 m (Figure 25). Topography likely controls the flow regime in this aquifer; however, this cannot be confirmed due to the lack of data.

3.3.6 Paskapoo Aquifer

The TDS concentrations in the Paskapoo Aquifer range from 404 mg/L to 1800 mg/L (Table 3). The lowest TDS concentrations appear to be associated with areas of higher elevation, whereas the areas with highest TDS concentrations appear to be associated with areas of lower topographic elevations (Figure 26). It is expected that the topographically high areas represent recharge areas, whereas the lower elevation areas, associated with the ancient buried bedrock river valley and meltwater channel (see Section 2.3.7), may represent areas of discharge.

Although most of the wells screened within the Paskapoo Aquifer have TDS values ranging between 400 mg/L and 1000 mg/L, an area located in the southwestern portion of the study area exhibits higher TDS values ranging from 1325 mg/L to 1800 mg/L. Insufficient information is available at this time to discern the origin of the relatively higher TDS waters.

The Paskapoo Aquifer water levels (Figure 27) appear to generally follow the land surface topography as illustrated in Figure 12. The hydraulic head values range between 800 m and 880 m. The areas of lower elevation represent either the locations of ancient buried bedrock valleys or meltwater channels that are oversized for the present rivers that are found to flow in them. Generally areas of higher water levels are found in wells located in the western portion of the study area.

3.3.7 Surficial (Undifferentiated) Aquifer

Water levels within the surficial, unconsolidated deposits vary based on topography, location and depth. The total dissolved solids (TDS) concentrations ranged from 395 mg/L to 643 mg/L. The flow regime is most likely controlled by the surface topography, however, insufficient water-well levels or well chemistry data were available to produce contoured TDS and groundwater surface maps. The aquifers in the Quaternary unconsolidated sediments will be studied in more detail in future phases of the study, particularly in relation to the development of a monitoring and verification plan.

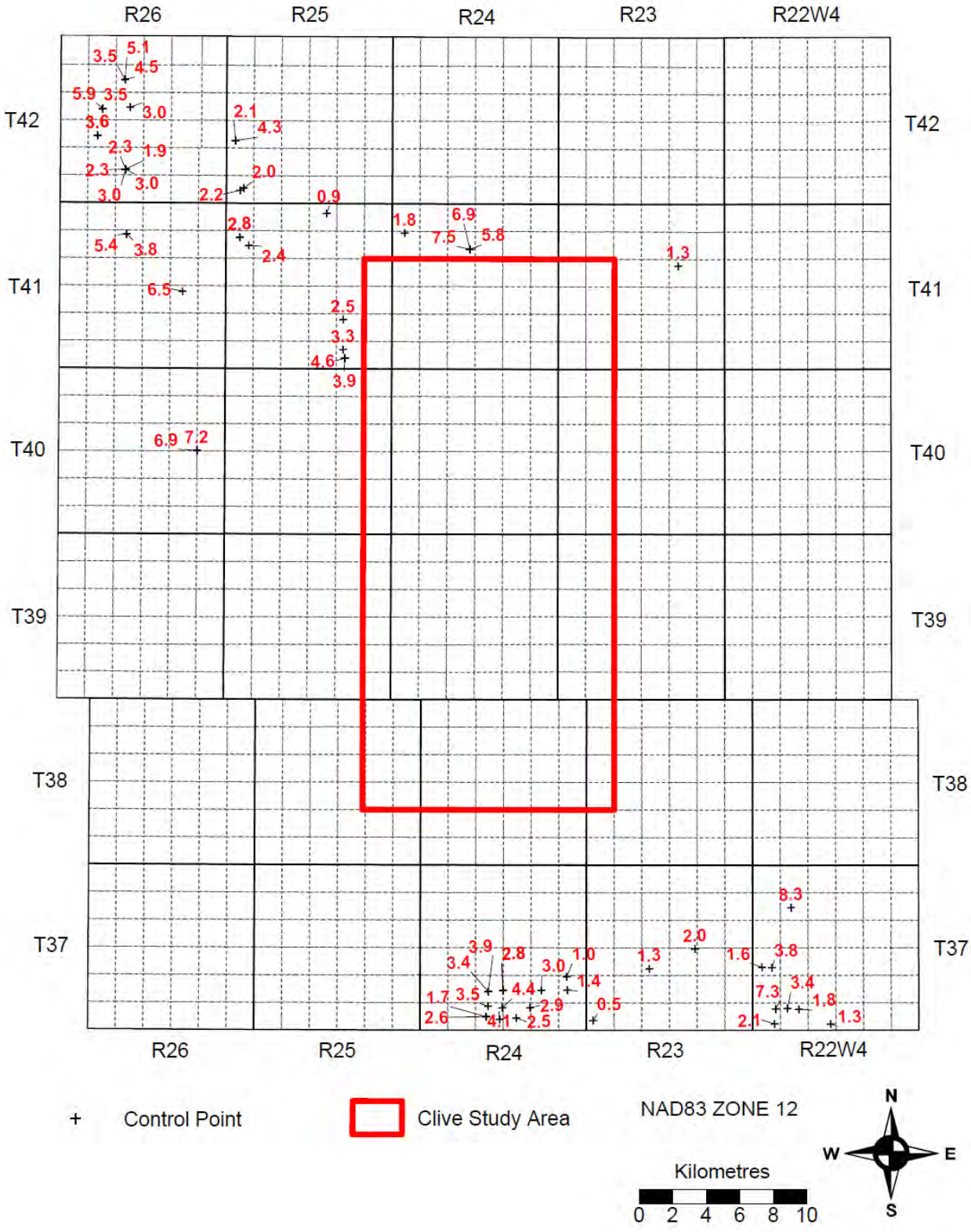

Figure 24: Total dissolved solids distribution (g/L) in the Horseshoe Canyon Aquifer.

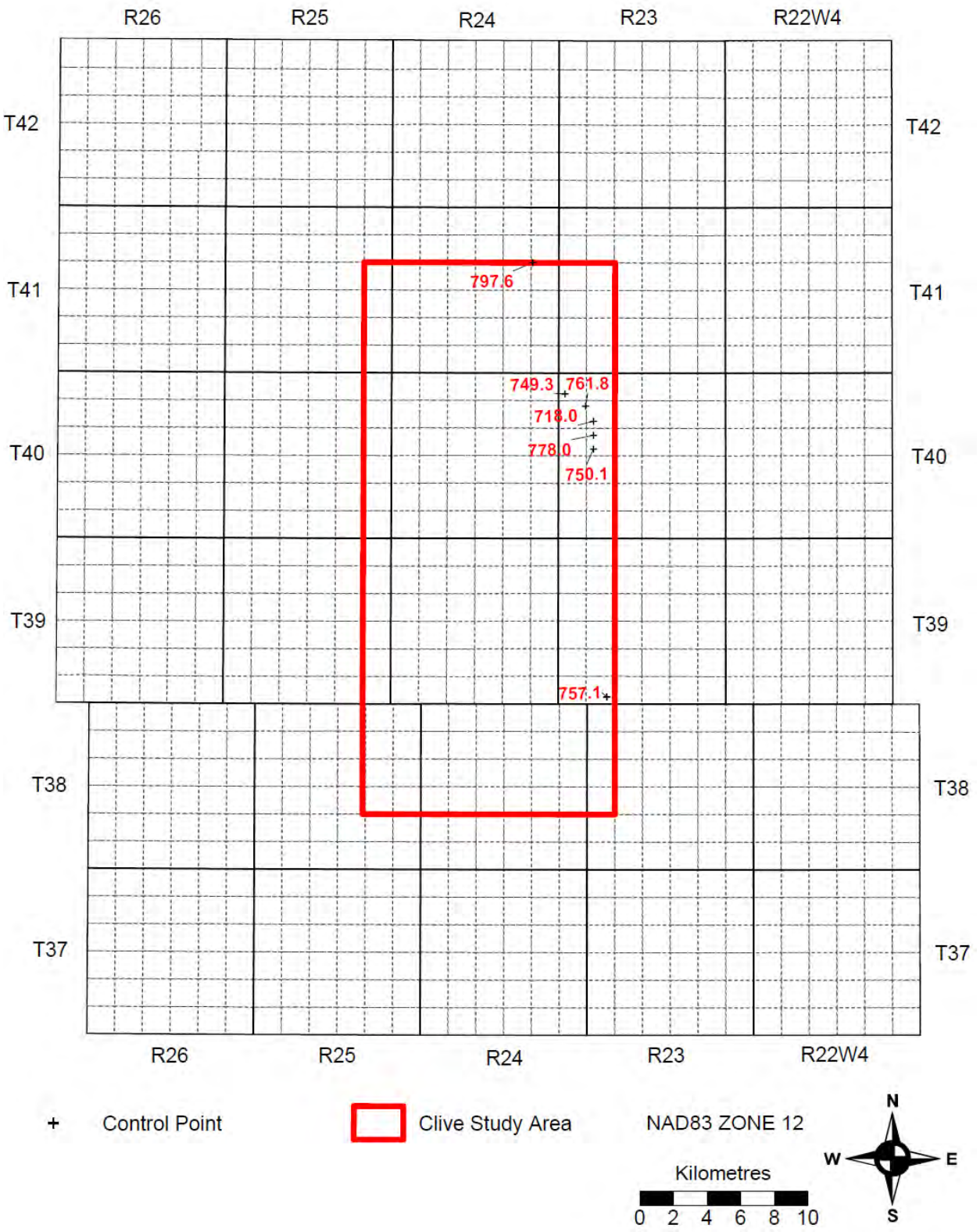

Figure 25: Hydraulic head distribution (m) in the Horseshoe Canyon Aquifer.

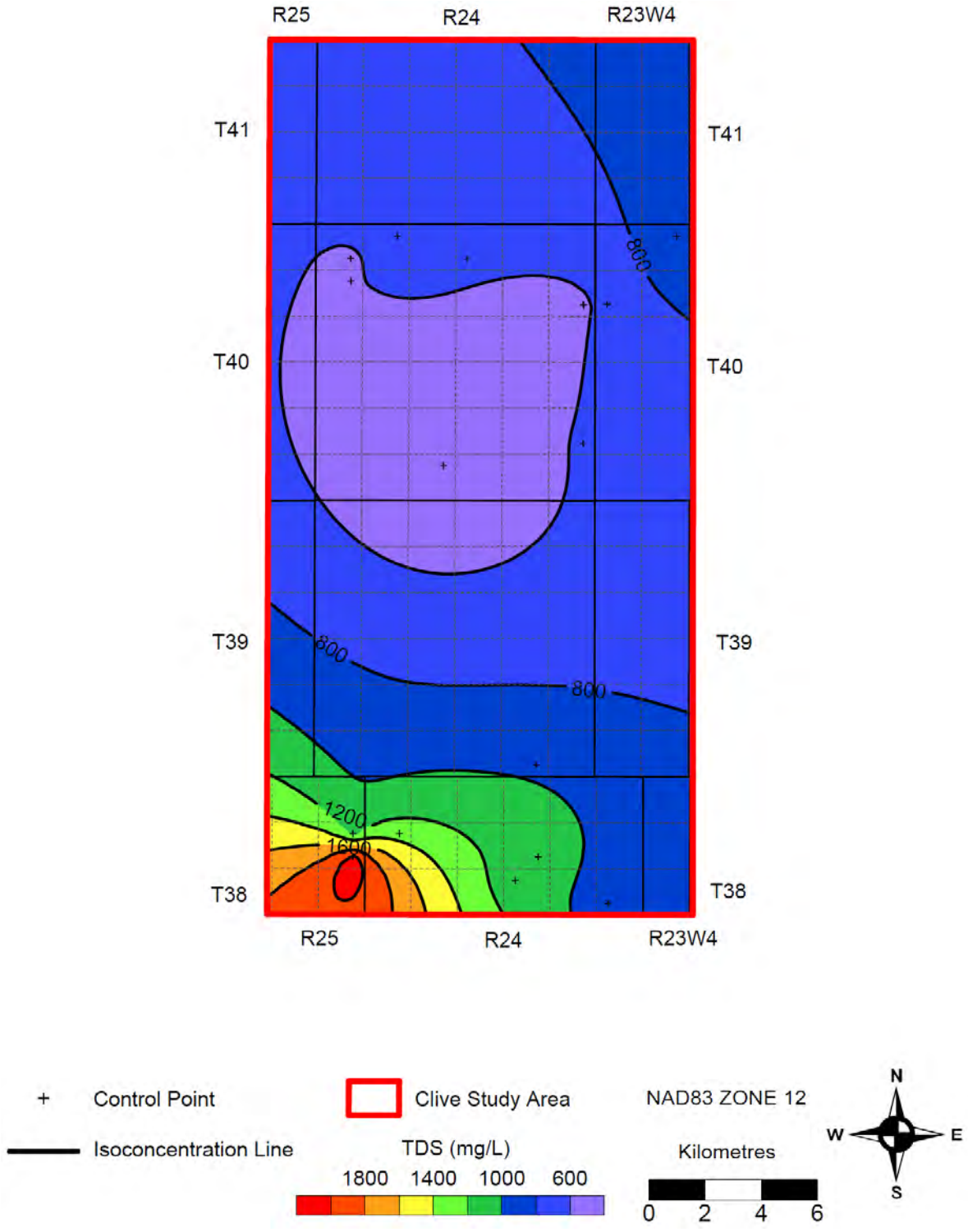

Figure 26: Total dissolved solids distribution (mg/L) in the Paskapoo Aquifer in the Enhance Clive study area.

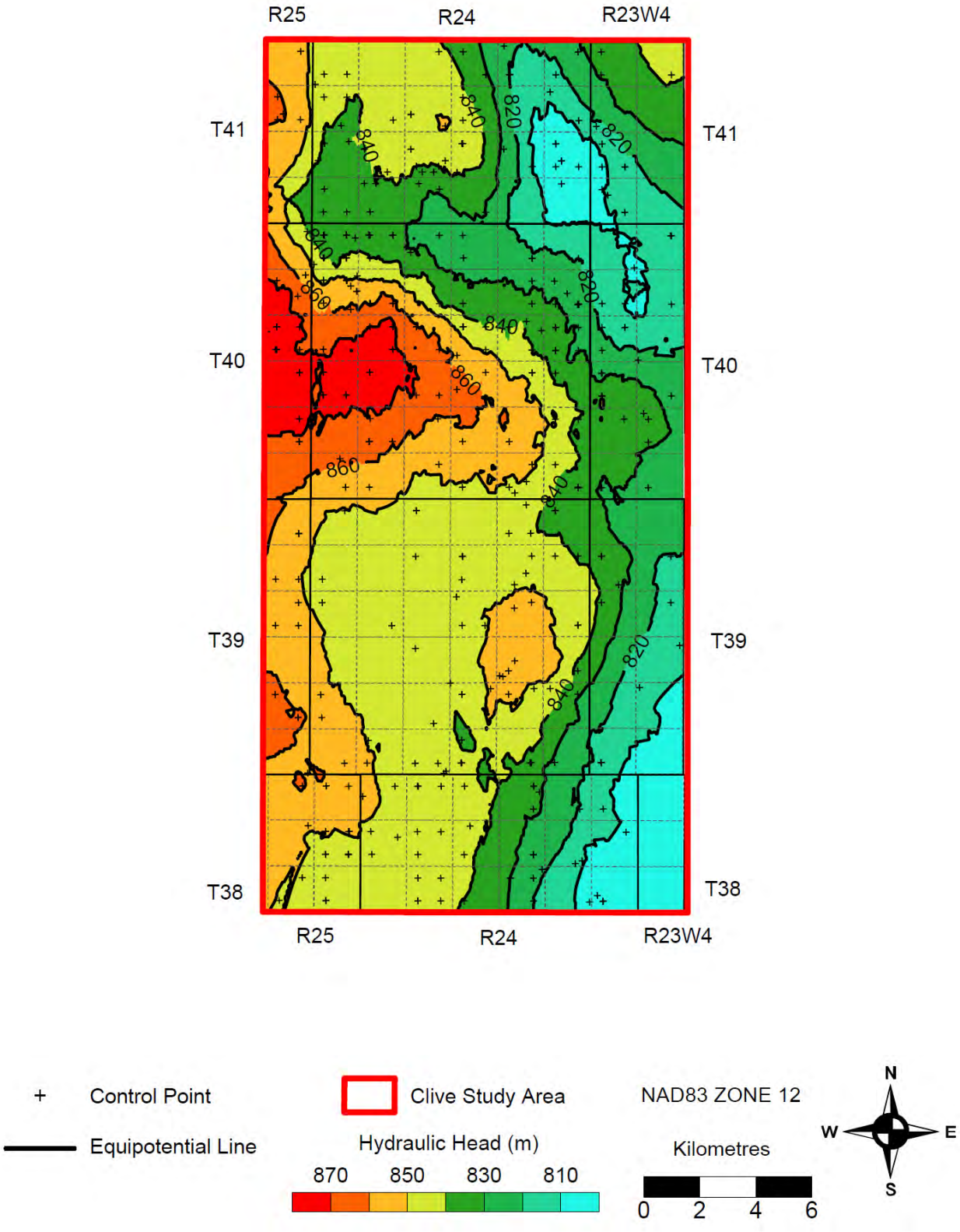

Figure 27: Hydraulic head distribution (m) in the Paskapoo Aquifer (C.I. = 10 m) in the Enhance Clive study area.

3.4 Major Ion Chemistry

Water samples are generally analyzed for the following major ions: sodium (Na^+), potassium (K^+), calcium (Ca^{2+}), magnesium (Mg^{2+}), chloride (Cl^-), sulphate (SO_4^{2-}) and bicarbonate (HCO_3^-). Observed variations and patterns in formation water chemistry and TDS can help in identifying contaminated or anomalous water analyses as well as aid in deciphering the chemical evolution (Chebotarev, 1955; Toth, 1984) and flow path in a regional-scale flow system (Tóth, 1995). Cross-plots of TDS versus major ions were created to evaluate hydrochemical variations within and between aquifers. Potassium was not plotted because it is often not reported or it is combined with sodium (Na+K) due to its low concentrations. Chloride was not plotted because it almost always shows a positive linear relationship with TDS.

Cross-plots of Na, percent cationic Ca and Mg, and the anionic percent of SO_4 and HCO_3 versus TDS for the Lower Mannville, Viking, Basal and Upper Belly River aquifers are shown in Figure 28. There are two distinct clusters in the formation water chemistry data. The Basal and Upper Belly River aquifers have much lower TDS, and therefore, plot separately from the two deeper aquifers (Lower Mannville and Viking) (Figure 28d). Cross-plots for the shallower aquifers (Horseshoe Canyon and Paskapoo) are shown on Figure 29 combined with the underlying Basal and Upper Belly River aquifers for comparison purposes.

The relationship between Na and TDS for all of the aquifers forms a strong positive linear trend throughout the entire range of TDS (Figure 28a and Figure 29a). A slight relative decrease in sodium concentration, hence deviation in the linear trend, is observed in the high salinity range (> 100 g/L) in samples from the Lower Mannville Aquifer (Figure 28a). This is the result of slightly higher calcium concentration in these samples.

Percent cationic calcium versus TDS forms a rather scattered plot with a slight exponential trend, also increasing with TDS (Figure 28b and Figure 29b). Higher calcium percentages (above 5%) and concentrations are observed in the Lower Mannville Aquifer and coincide with the high salinity plume in the central and northeastern parts of the full study area (Figure 14). This is similar to what was observed previously in the area on a regional scale (Rostron et al., 1997; Rostron and Tóth, 1997), where higher calcium was used as a tracer of Devonian brines migrating upward into the Lower Mannville Aquifer. In contrast, the Basal and Upper Belly River aquifers have similar but low percentages of calcium. The Paskapoo Aquifer contains relatively high proportions of calcium (up to 10%) (Figure 29b), which is much higher than the deep aquifers.

Magnesium concentrations are relatively low for all the aquifers, generally below 2% Mg, with a slight increase in concentration with increasing TDS (Figure 28c). The Paskapoo Aquifer has the highest proportions of magnesium of up to 5% (Figure 29c).

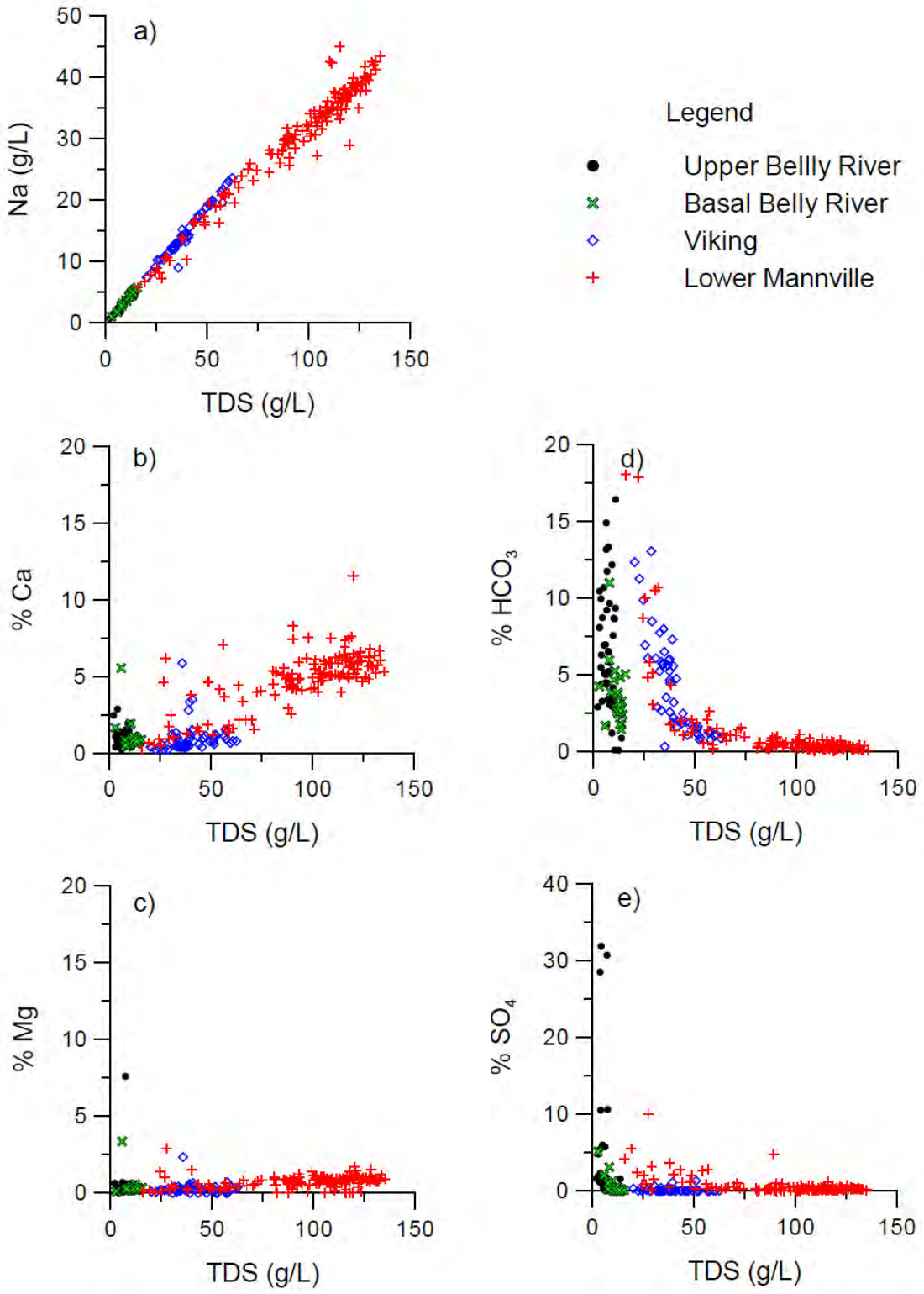

Figure 28: Cross-plots of (a) sodium (Na), (b) percent calcium (%Ca), (c) percent magnesium (%Mg), (d) percent bicarbonate (%HCO_3), and (e) percent sulphate (%SO_4) versus Total Dissolved Solids (TDS) in the Lower Mannville, Viking, Basal and Upper Belly River aquifers.

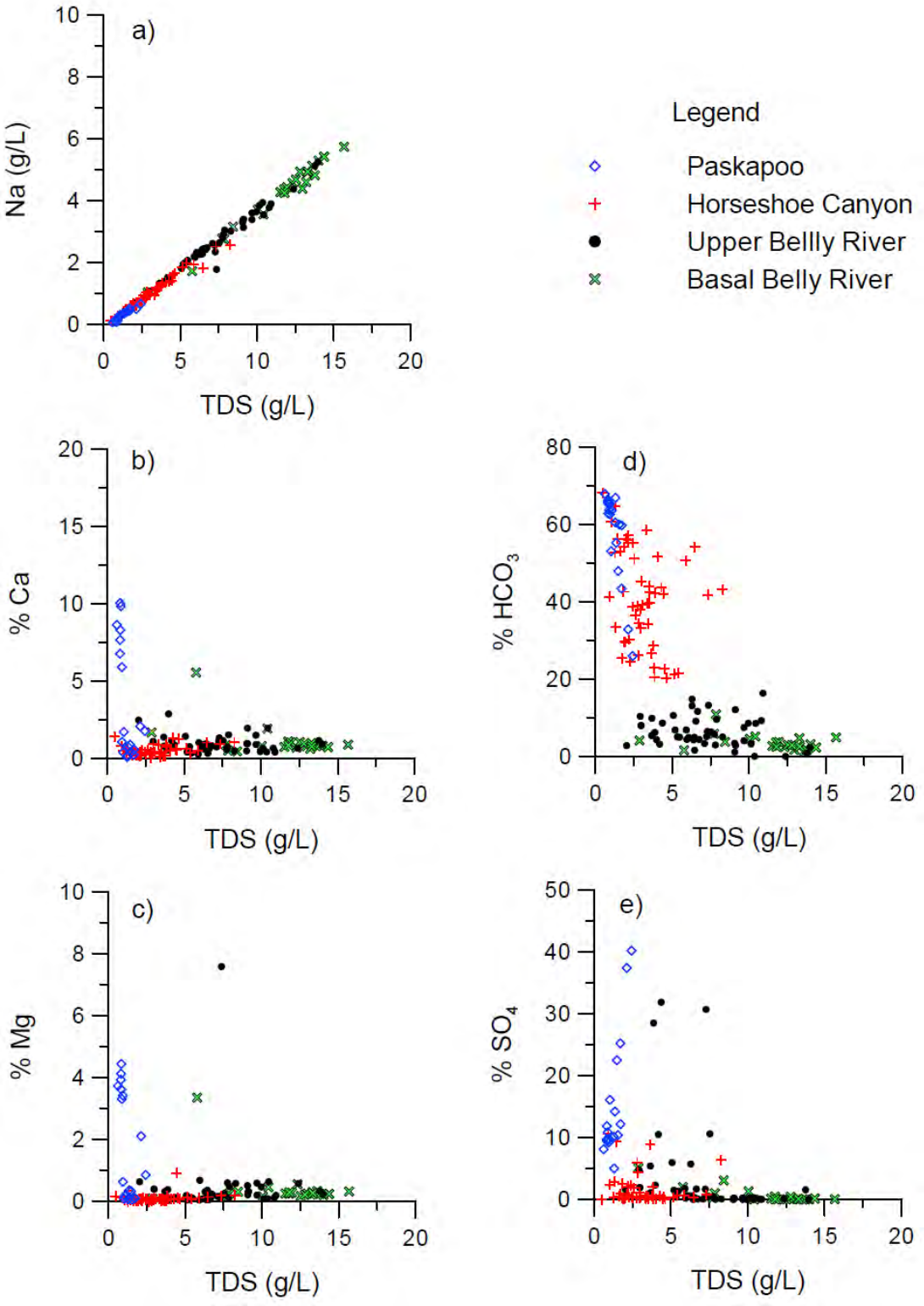

Figure 29: Cross-plots of (a) sodium (Na), (b) percent calcium (%Ca), (c) percent magnesium (%Mg), (d) percent bicarbonate (%HCO_3), and (e) percent sulphate (%SO_4) versus Total Dissolved Solids (TDS) in the Basal and Upper Belly River, Horseshoe Canyon and Paskapoo aquifers.

Bicarbonate concentrations (Figure 28d) for the Lower Mannville and Viking aquifers decrease with increasing TDS. Bicarbonate ranges from almost 3% to 20% for TDS below 40 g/L. For higher salinity waters (> 40 g/L), bicarbonate drops to less than 2%. A plot of bicarbonate versus TDS can also be used to distinguish the Basal Belly River Sandstone Aquifer from the overlying Upper Belly River Aquifer in the study area. Groundwater in the Upper Belly River Aquifer has bicarbonate up to 15%. In contrast, the Basal Belly River Sandstone Aquifer has generally less than 6% bicarbonate. Higher bicarbonate concentrations in the Upper Belly River Aquifer indicate the presence of fresh meteoric recharge waters, whereas low bicarbonate concentrations in the Basal Belly River Aquifer are indicative of more evolved waters, still of a meteoric origin but more saline and of a slightly different composition (e.g., Chebotarev, 1955; Hanor, 1994). The bicarbonate fraction in the Horseshoe Canyon and Paskapoo aquifers (Figure 29d) is much higher than in deep aquifers and ranges from 20% to 70%, indicating the presence of fresh meteoric waters.

Sulphate concentrations generally tend to decrease with increasing TDS. Sulphate concentrations in the Lower Mannville and Viking aquifers are negligible. Percent sulphate in the Basal and Upper Belly River aquifers are highly variable, ranging from less than 1 to over 30% (Figure 28e). The Upper Belly River Aquifer generally has more dissolved sulphate than does the Basal Belly River Aquifer. The Paskapoo aquifer has the highest fraction of sulphate, ranging between 10% and 40% (Figure 29e). Higher SO_4 concentrations are associated with formation waters of meteoric origin that have somewhat evolved in a local-scale flow system (Chebotarev, 1955). With increasing residence time and water-rock interaction, sulphate concentrations decrease and chloride concentrations increase until chloride becomes the dominant ion (Hanor, 1994).

There is only one dominant water type observed in all the deep aquifers: Na-Cl (Khan, 2006). That is, more than 50% of all cations and anions in all waters in all of the aquifers are represented by sodium (Na^+) and chloride (Cl^-), respectively.

Groundwater in the shallow aquifers, on the other hand, consists of several different water types. A series of piper plots were created to determine the water type and chemistry of water samples from wells screened within the Paskapoo Aquifer. Other shallow aquifers did not have sufficient data for this type of hydrochemical analysis. The piper plots for wells belonging to each groundwater type identified in the study area are found in Appendix C. The results of the water chemistry analysis indicate that four groundwater types are found within wells screened in the Paskapoo Aquifer. Generally wells in the study area have Na-HCO_3 based groundwater with varying amounts of calcium and magnesium. Those wells associated with the expected recharge area are dominated by Na-Ca-Mg-HCO_3 based groundwater. It appears that wells located adjacent to the ancient buried river valley and meltwater channel have a Na-HCO_3 based groundwater with hardness ranging from approximately 10 to 53 mg/L.

An area of higher concentrations of sulphate (i.e. approximately 192 mg/L to 976 mg/L), TDS (i.e. approximately 960 mg/L to 2102 mg/L) and sodium (i.e. approximately

335 mg/L to 511 mg/L) is found in an area in the southwest (Figure 26). The reason for the higher values of these specific parameters in the groundwater of this area is not known based on the data examined in this study.

3.5 Vertical Pressure Gradients

An analysis of the pressure variation versus elevation (p-z profiles) has been completed to identify vertical variations in hydraulic gradients, and evaluate the potential for cross-formational flow and hydraulic communication between adjacent aquifers (Tóth, 1978). Pressure-elevation profiles have been created for the aquifers ranging from the Lower Mannville to Paskapoo for the entire hydrogeological study area. Data for the Surficial Aquifer were not plotted due to the lack of information about perforation depths. Pressure-depth (p-d) analysis was not used due to the large variation in topography in the study area (Figure 12).

Pressure data from the hydrogeological study area were plotted versus elevation on Figure 30 and colour-coded to represent the different aquifers. The measured gradient lines (Table 4) were fitted through the observed data trends using linear interpolation. The nominal reference-density gradients for each aquifer are shown for reference. Additional pressure data points from the Nisku Formation in the Clive oil reservoirs were added to the p-z plot for comparison and interpretation purposes.

Table 4: Summary of vertical hydraulic gradients.

Aquifer	Reference Density (kg/m^3)	Reference Hydrostatic Gradient (kPa/m)	Measured (fitted) Gradient (kPa/m)
Paskapoo (Shallow)	1000	9.8	2.8
Upper Belly River	1000	9.8	8.8
Basal Belly River	1000	9.8	8.4
Viking	1025	10.1	10.4
Lower Mannville	1060	10.4	12.7

The p-z profile (Figure 30) immediately highlights the clear separations between the flow systems in the Cretaceous-Tertiary aquifers. A fitted vertical hydraulic gradient of 12.7 kPa/m was calculated in the Lower Mannville Aquifer. This is higher than the hydrostatic reference gradient (10.4 kPa/m), indicating an upward component of flow. It should be noted that several data points have higher pressures which do not fit on the determined gradient; they are associated with the hydrocarbon column(s) of producing oil fields. However, the fact that the majority of data points fall on the gradient indicates

good lateral hydraulic continuity within the aquifer. Pressure data points from the Nisku Formation do not fall on the p-z gradient for pressures in the Lower Mannville Aquifer.

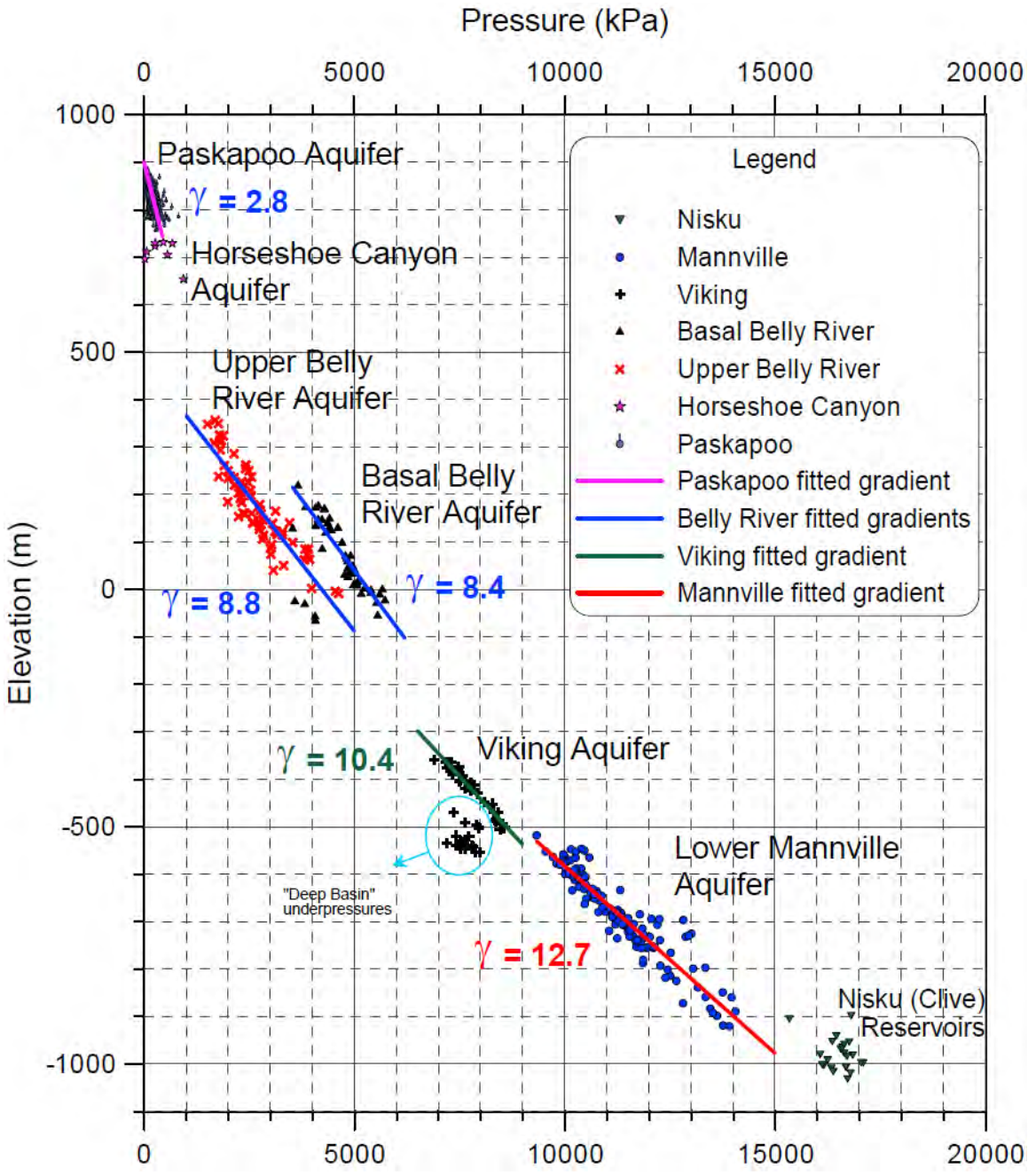

Figure 30: Pressure-elevation (p-z) plot for the entire hydrogeological study area.

Pressure data from the Viking Aquifer fall on a significantly different gradient from the underlying Lower Mannville Aquifer. There are two groups of data: the main group falls with the fitted gradient and a secondary underpressured group. The fitted line through the main group was determined to have a slope of 10.4 kPa/m, which is slightly less than the hydrostatic gradient (10.1 kPa/m). This means that flow in the Viking Aquifer is

mainly lateral with no indication of a vertical flow component, and is different from the flow in the underlying Lower Mannville aquifer. This is consistent with the flow directions shown in the hydraulic head distribution for the Viking Aquifer (Figure 18). The second group of Viking data plot below the main gradient and are associated with large-scale, Deep Basin underpressures observed here and in other Cretaceous formations of west-central Alberta (Bachu and Underschultz, 1993; 1995; Parks and Tóth, 1995; Rostron et al., 1997; Rostron and Tóth, 1997). The origin of these underpressured values remains controversial, however, it should be noted that their presence on a geological time scale implies distinct hydraulic isolation from the overlying and underlying units, as well as from the east-northeastern part of the Viking aquifer. This is strong evidence of excellent sealing capacity for CO_2 in the hydrostratigraphic section of this study area.

Vertical hydraulic gradients in the Basal and Upper Belly River aquifers are significantly different from those in the underlying Viking Aquifer. Thick Colorado and Lea Park shales of the Colorado-Lea Park Aquitard overlie the Viking Aquifer and separate it from the Belly River Group aquifers, with significant pressure difference between the two. A fitted gradient for the Basal Belly River Aquifer was estimated to be 8.4 kPa/m. This value compared to the reference hydrostatic gradient of 9.8 kPa/m indicates a downward, downdip component of flow (Parks and Tóth, 1995; Bachu and Michael, 2003). The fitted gradient for the Upper Belly River Aquifer (8.8 kPa/m) is similar to that of Basal Belly River albeit with a smaller magnitude downward component of flow. Fluid pressures in the Upper Belly River Aquifer are lower than in Basal Belly River Aquifer indicating good hydraulic separation of the two aquifers by the intervening Mckay Aquitard.

Shallow aquifers (Horseshoe Canyon and Paskapoo) have a subhydrostatic vertical gradient of 2.8 kPa/m. This gradient is significantly different from the deeper aquifers and indicates the presence of strong downward flow component.

3.6 Rock Properties

Core data for the Cretaceous aquifers have been assembled and analysed (Table 5 and Table 6). Cored wells within the Lower Mannville Aquifer appear to be evenly distributed throughout the Enhance Clive study area (Figure 31). The majority of the wells containing cores from the Viking Aquifer are located in the western half of the Enhance Clive study area. Only one well with core analyses from the Basal Belly River Aquifer was found in the study area. There were no core analyses reported in the Upper Belly River Aquifer despite the record of two cored wells.

Permeability values calculated from DSTs are summarized in Table 7. Wells with DSTs within the Lower Mannville and Viking aquifers appear to be evenly distributed thoruhgout the Enhance Clive study area (Figure 32). Basal and Upper Belly River aquifers have very low data density.

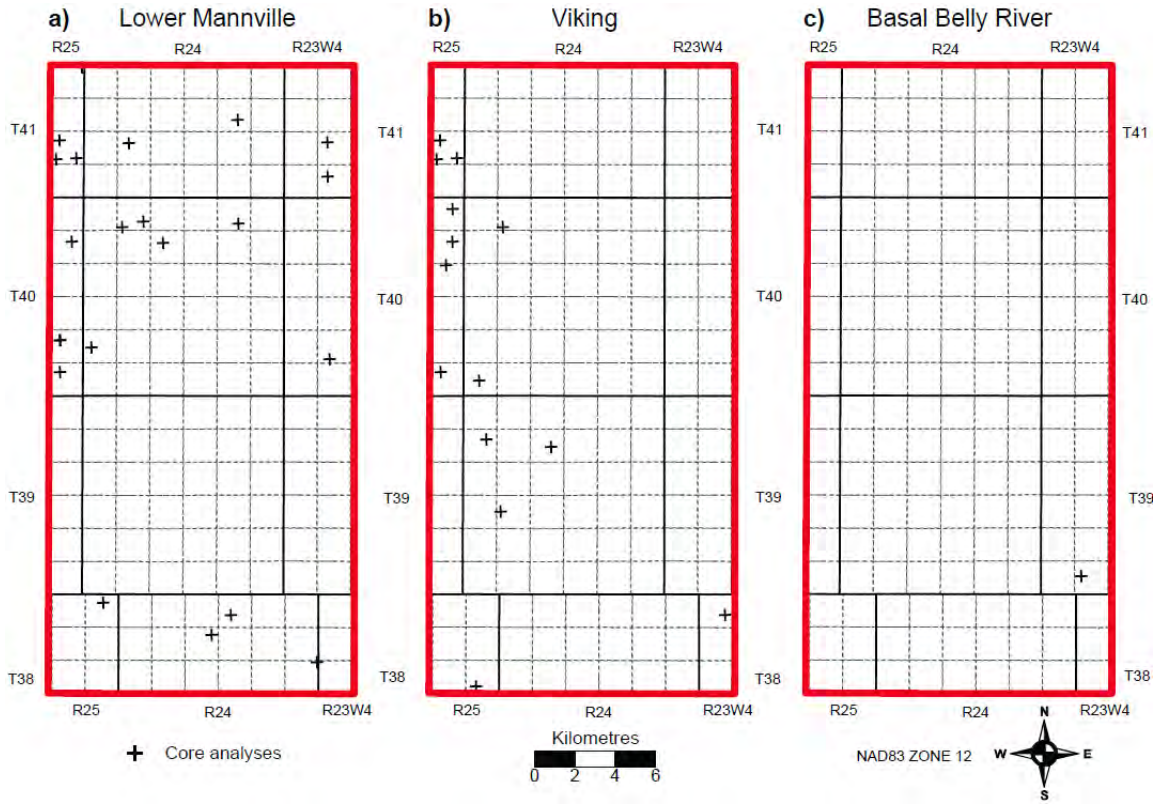

Figure 31: Distribution of wells containing porosity and permeability data from core analyses: a) in the Lower Mannville Aquifer, b) in the Viking Aquifer, and c) in the Basal Belly River Aquifer.

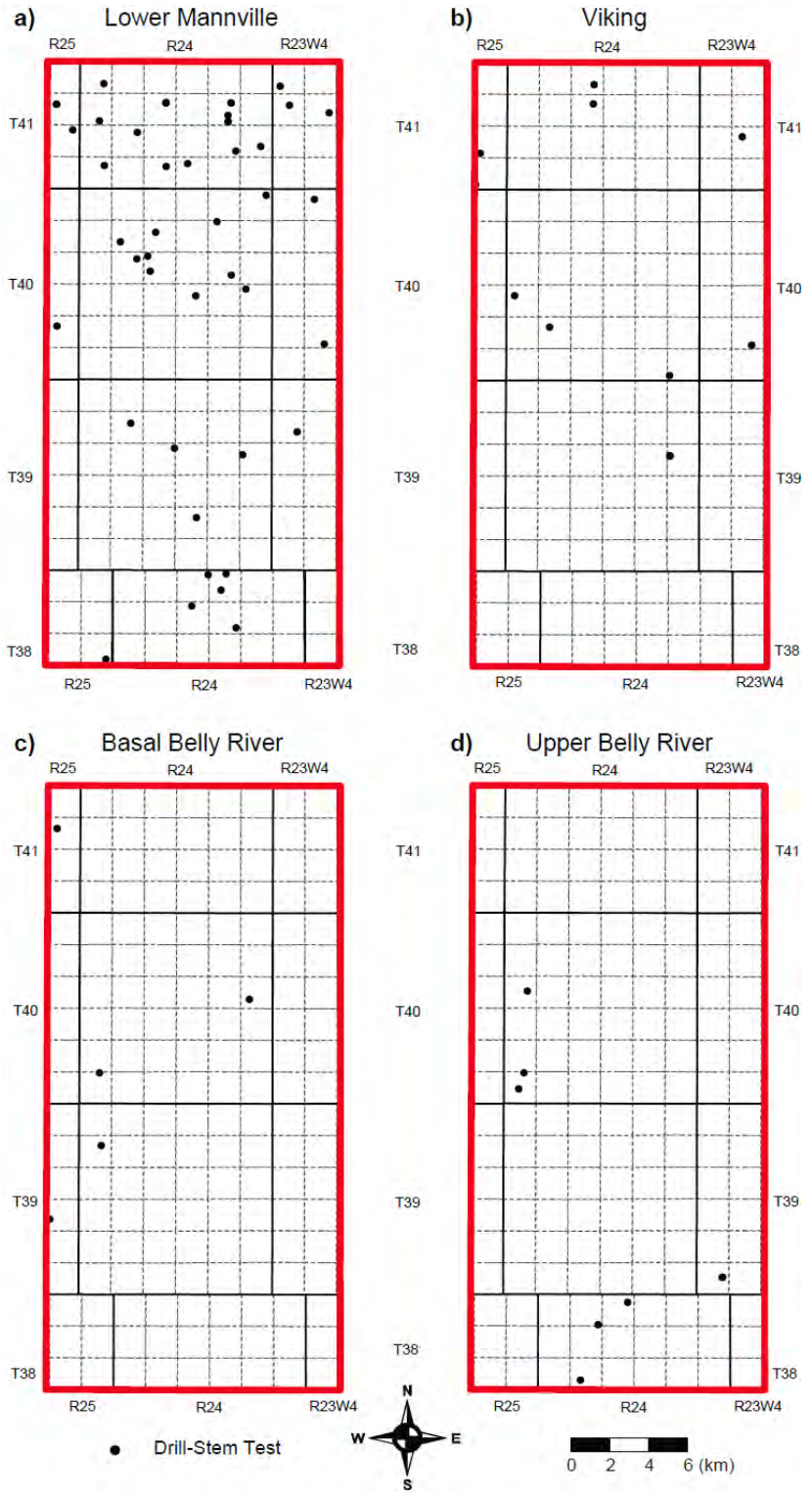

Figure 32: Distribution of wells containing permeability data calculated from drill-stem tests: a) in the Lower Mannville Aquifer, b) in the Viking Aquifer, c) in the Basal Belly River Aquifer, and d) in the Upper Belly River Aquifer.

3.6.1 Porosity

Plug-scale porosity values vary between 1% and 27%, with median values varying between 10.0% and 10.8% (Table 5). Well-scale porosity values vary between 5.3% and 26.5%, with median values ranging between 9.4% and 12.2%. Field-scale porosity values are around 10% (Table 5). As a general observation, it appears that, overall, porosity decreases with increasing depth, which is expected for siliciclastic sediments. The lowest average porosity at both core- and well-scales is observed in the Lower Mannville Aquifer, the deepest aquifer described. The Viking Aquifer has higher average porosity than the Lower Mannville Aquifer, with core-scale median of 10.0% and well-scale median of 10.2%. The Basal Belly River Aquifer is the shallowest has the highest median core- and well-scale porosity at 10.8% and 12.2%, respectively. The field-scale values, calculated as geometric averages of well-scale porosity, show similar trends for the Lower Mannville and Viking aquifers.

Table 5: Core porosity processed in Cretaceous aquifers within the Enhance Clive study area.

Aquifer	No. Wells	No. Plugs	Porosity (%)						
			Core Scale			Well Scale			Field Scale
			Min	Median	Max	Min	Median	Max	
Upper Belly River	2	0	-	-	-	-			-
Basal Belly River	1	12	1.6	10.8	22.5	12.2			-
Viking	14	263	1.0	10.0	27.0	5.3	10.2	26.5	10.6
Lower Mannville	22	853	1.0	10.1	25.9	5.7	9.4	15.2	9.7

3.6.2 Core Permeability

Permeability values at the plug scale vary between 0.01 mD (the lower measurable limit) and several darcies (Table 6). The low median values (<1 mD) indicate that most core permeability values are quite low (Table 6). Well-scale and field-scale permeability values show a decrease of permeability with depth; however the Belly River Aquifer permeability is based on only 12 core plugs taken in a single well and most likely the resulting value is not representative for the aquifer as a whole.

Table 6: Core permeability processed in Cretaceous aquifers within the Enhance Clive study area.

Aquifer	No. Wells	No. Plugs	Permeability (mD)							Anisotropy	
			Core Scale			Well Scale			Field Scale	Hor.	Vert.
			Min	Median	Max	Min	Median	Max			
Upper Belly River	2	0	-	-	-	-			-	-	-
Basal Belly River	1	12	0.06	0.95	86	14.1			-	0.77	0.29
Viking	14	260	0.01	0.52	8770	0.20	12.0	291	7.1	0.82	0.21
Lower Mannville	22	786	0.01	0.51	2425	0.03	2.33	217	2.8	0.84	0.41

The relationship between porosity and permeability in the Lower Mannville, Viking, and Basal Belly River aquifers at the core- and well-scales has been investigated and is shown in Figure 33. An empirical relationship in the form of $k_{MAX} = Ae^{B\emptyset}$ (where k is permeability, $\emptyset$ is porosity, and A and B are numerical coefficients/constants) is apparent for all the aquifers. However, the individual relationships are not provided due to a wide data spread and poor correlation (R^2 of 0.3 – 0.5).

The analyses of permeability anisotropy for Lower Mannville, Viking, and Basal Belly River aquifers are shown in Figure 34 above. The values of horizontal anisotropy (Figure 34a, b and c) range between 0.90 and 0.96 (low anisotropy) with high correlation coefficients (R^2) of 0.985 – 0.995 in all the aquifers. The values of vertical anisotropy (Figure 34d, e and f) range from 0.086 (very high anisotropy) in the Viking aquifer to 0.53 and 0.33 (high anisotropy) in the Lower Mannville and Basal Belly River aquifers, respectively; however the correlations for vertical anisotropy are poorer than for horizontal anisotropy (R^2 in the 0.664 and 0.856 range). No further relationships of permeability anisotropy to facies or lithologies were investigated in this report.

3.6.3 DST Permeability

Permeability values from drill-stem tests vary between 0.05 mD and several darcies (Table 7). Highest median permeability is observed in the Basal Belly River Aquifer (684 mD at the well-scale and 501 mD at the field-scale). However, it should be noted that these values are subject to strong bias towards high permeability due to the very low number of good data points (only five DSTs). Permeability values in the Lower Mannville Aquifer are the second largest in the study area, ranging from the well-scale median of 12.2 mD to the field-scale geometric average of 13.3 mD. The Viking and Upper Belly River aquifers have the lowest permeability values in the study area. It should be noted that field-scale permeability values derived from core measurements and from drill-stem tests are within the same order of magnitude for the Lower Mannville and Viking aquifers, and comparable with that in the Upper Belly River Aquifer. Only for the Basal Belly River Aquifer the field-scale permeability values derived from core and from drill-stem tests differ by a factor of ~40, but this may be statistically explained by the fact that only one well has core analyses and there are only five drill-stem tests in this aquifer, hence the results are not necessarily representative.

Table 7: Permeability values calculated from drill-stem tests for Cretaceous aquifers within the Enhance Clive study area.

Aquifer	No. DSTs	Permeability (mD)			
		Well Scale			Field Scale
		Min	Median	Max	
Upper Belly River	8	0.67	4.35	12.4	3.85
Basal Belly River	5	29.3	684	2,893	501
Viking	11	0.38	5.24	41.7	3.90
Lower Mannville	46	0.05	12.2	1,085	13.3

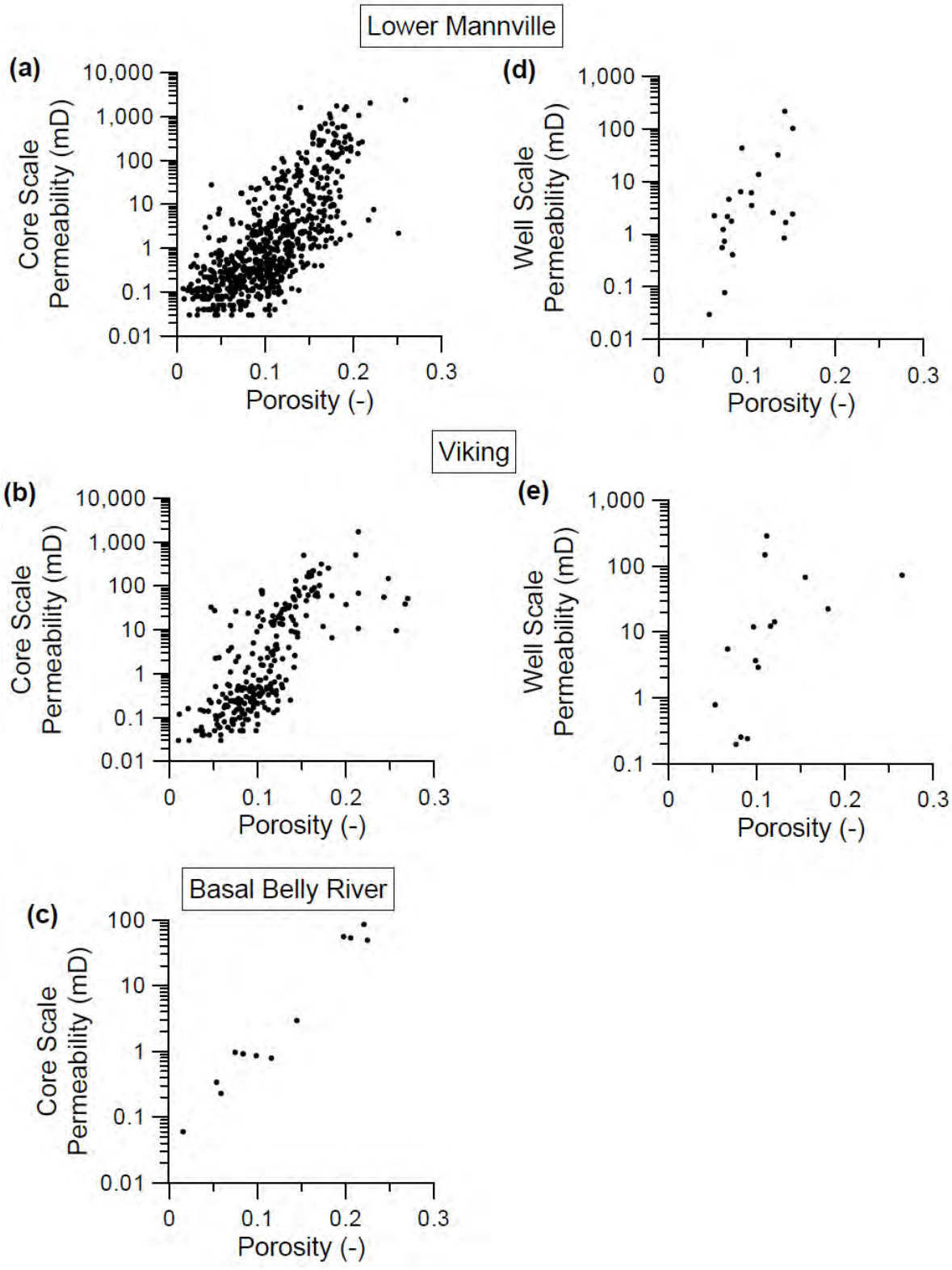

Figure 33: Relationships between: core-scale permeability and porosity for Lower Mannville (a), Viking (b), Basal Belly River (c) aquifers, and well-scale permeability and porosity and for Lower Mannville (d) and Viking (e) aquifers.

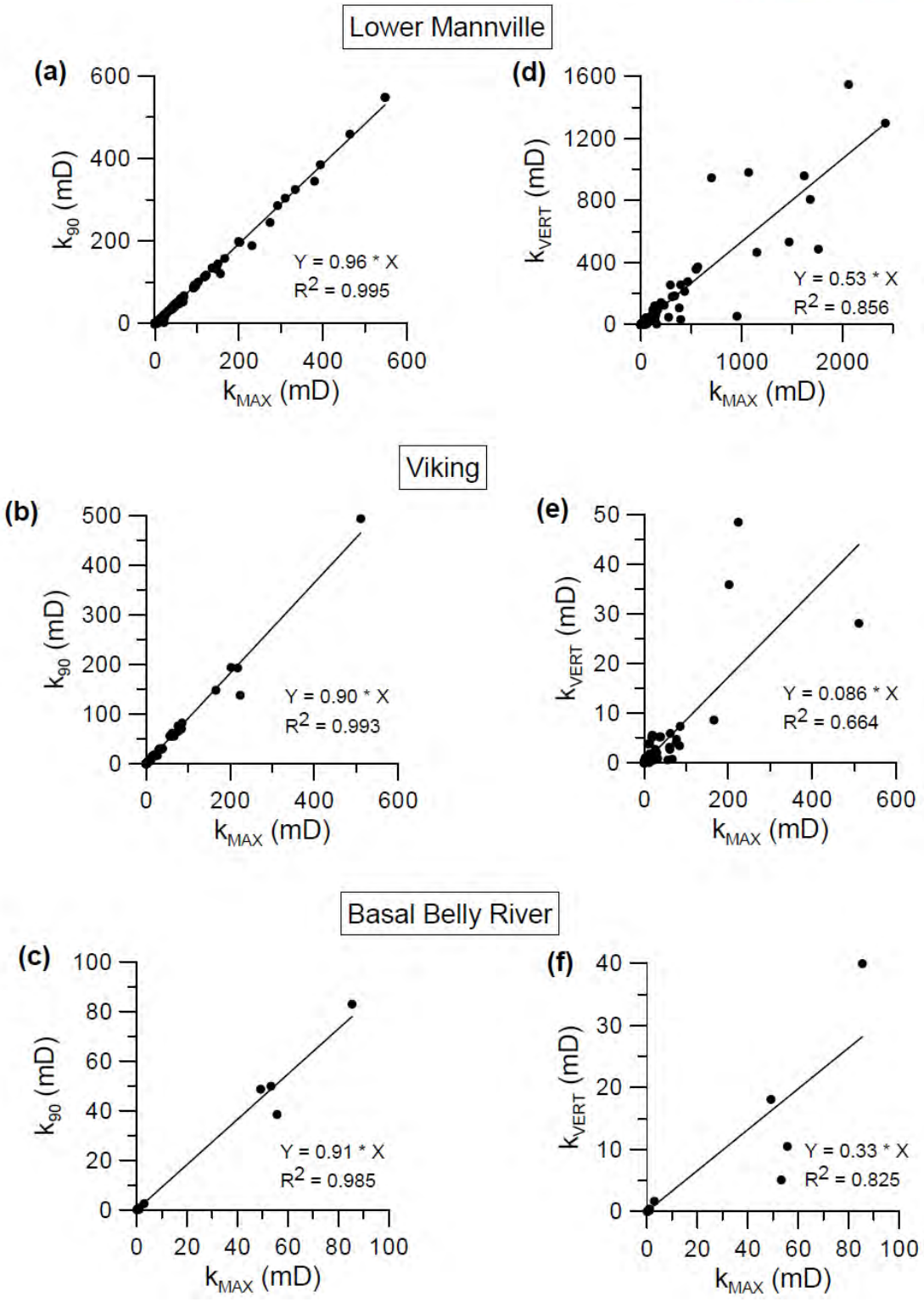

Figure 34: Relationships between: (a,b,c) horizontal permeabilities (k_{90} vs. k_{MAX}), and (d,e,f) vertical and maximum horizontal permeabilities (k_{VERT} vs. k_{MAX}) for Lower Mannville, Viking, and Basal Belly River aquifers.

3.7 Interpretation

Results presented above provide a comprehensive characterization of the hydrostratigraphy and hydrogeology within the Cretaceous sedimentary succession in the Clive area in central Alberta. The main focus is on hydraulic features in aquifers of the Clive field study area, which is the intended target of a large-scale CO_2-EOR operation. This section integrates the chemistry and hydrodynamic regime of all the aquifers to establish the degree of hydraulic communication between the various aquifers in the sedimentary succession overlying the Leduc (D3-A) and Nisku (D-2) reservoirs and discusses the barriers to the upward migration or leakage of CO_2.

3.7.1 Hydrochemistry of Formation Waters

Water chemistry can be useful to differentiate the aquifers in the section and establish their degree of hydraulic communication. Maps of TDS distribution and chemistry cross-plots reveal significant differences in salinity between the four main aquifers in the Clive study area. Total Dissolved Solids in the Lower Mannville Aquifer range from less than 40 g/L in the south to over 120 g/L in the northeast. A large saline plume (defined by the 100 g/L contour) exists in this aquifer in the northeast in the region that corresponds to the absence of the Carboniferous Exshaw and Banff formations and where the Lower Mannville Aquifer and underlying Devonian strata are in direct contact. This plume is most likely the result of past density-driven, downdip, back-flow of heavy brines sourced from the Devonian aquifers to the northeast and outside of the present study area, as noted also on a larger scale by Anfort et al. (2001). It should be noted that the present hydraulic system is dynamic and the lack of evidence in the Enhance Clive study area for density-related flow effects (flow reversals or back-flow) at this time does not mean that they did not exist in the past or that they are not present outside this area.

Rostron (1995) and Rostron et al. (1997) hypothesized, based on elevated calcium concentrations, that high TDS waters in the Lower Mannville Aquifer are sourced from the underlying Nisku Formation to the northeast of the present hydrogeological study area. However, Nisku waters in the Enhance Clive study area appear to have much higher TDS and calcium concentrations than in the overlying Lower Mannville Aquifer (Rostron, 1995; Rostron et al, 1997), showing that the two formations are not in hydraulic communication. In addition to that, three water analyses obtained from DSTs in isolated high-permeability zones of the Stettler Formation (Calmar Wabamun Aquitard) have much higher concentrations of sulphate (likely due to anhydrite dissolution and oversaturation) than in both underlying Nisku Aquifer and overlying Lower Mannville Aquifer. This is further indication that the Calmar-Wabamun Aquitard is a strong barrier to cross-formational flow in the Enhance Clive study area.

Total dissolved solids in the Viking Aquifer range from 30 g/L in the central parts of the hydrogeological study area to 60 g/L in the northeast. No elevated concentrations of calcium have been found within the study area in contrast to the underlying Lower

Mannville Aquifer, interpreted to indicate the lack of any further vertical migration of Devonian formation waters. Viking formation water appears to be connate and represents ancient sea water modified through water-rock interaction and mixing of higher salinity water from the northeast (Connolly et al., 1990; Rostron, 1995). The significant difference in water chemistry between Lower Mannville and Viking aquifers suggests that the Upper Mannville–Joli Fou Aquitard acts as a very effective barrier to the upward migration of water and, consequently, for any leaked CO_2.

Total dissolved solids values in the Basal Belly River Aquifer range between 10 g/L and 15 g/L, significantly lower than in the underlying Viking Aquifer. Total dissolved solids in the Upper Belly River Aquifer are even lower, generally less than 10 g/L. The high proportions of bicarbonate and sulphate ions in Belly River aquifers suggest their meteoric origin, as proposed by others (e.g., Connolly, 1990). Significantly different salinity values in the Belly River and Viking aquifers suggest that the Colorado-Lea Park aquitard is a very strong barrier to the upward migration of formation water. Furthermore, the difference in chemistry between the Basal and Upper Belly River aquifers indicates that the MacKay Aquitard also acts as a competent barrier to cross-formational flow, restricting hydraulic communication between the two aquifers.

Shallow aquifers have freshwater with TDS generally less than 5 g/L, significantly lower than in the deep aquifers. These waters are interpreted to be of meteoric origin (rain and melt water) as indicated by the high bicarbonate (20% - 70%) and sulphate concentrations (10% - 40%). Differences in hydrochemistry indicate the presence of a barrier or multiple barriers (mudstones and coal beds), between the shallow Horseshoe Canyon, Paskapoo and Surficial aquifers themselves, and also between the shallow and deep aquifers.

3.7.2 Regional Fluid Flow

The natural regional-scale flow of formation waters was assessed using maps of hydraulic head distributions and pressure-elevation plots. Hydraulic heads in the Lower Mannville aquifer range from 500 m to 350m. Fluid flow in the Lower Mannville Aquifer is highly complex and is attributed to the presence of geologic heterogeneities (permeability distribution), variable aquifer thickness (transmissivity), and vertical flow (Rostron, 1995; Rostron and Tóth, 1997). The vertical gradient (Figure 30) is 12.7 kPa/m, which is much higher than the hydrostatic gradient (10.4 kPa/m), indicating a vertical upward flow component. The fact that pressure data from the Nisku Formation do not fall on the same vertical gradient as the Lower Mannville Aquifer indicates again that the Calmar-Wabamun Aquitard is a strong barrier to cross-formational flow in the Enhance Clive study area between the Nisku and Lower Mannville strata.

In contrast, hydraulic heads in the Viking Aquifer are much lower than in the Lower Mannville Aquifer, ranging between 390 m and 230 m. Tightly spaced contours, which also correspond to the Deep Basin boundary-transition, represent a major lateral barrier attributed to lower permeability in the sediments therein. Generally there is little or no water found west of this boundary. Flow towards the southwest in the Cretaceous

aquifers has been attributed to the erosional rebound in low diffusivity rocks (Corbet and Bethke, 1992; Parks and Tóth, 1995; Bachu, 1995; Bachu and Underschultz, 1995; Rostron and Tóth, 1997). Given the completely different flow regime identified in the hydraulic head distribution, and lateral flow in the p-z plot, it is evident that the intervening Upper Mannville–Joli Fou Aquitard acts as a strong barrier to cross-formational flow in the study area.

Fluid flow in the Basal Belly River Aquifer is directed towards the southwest. Hydraulic heads range from almost 600 m in the northeast down to 350 m in the southwest. The pattern of hydraulic heads is similar to that in the underling Viking Aquifer implying a similar erosion-rebound driving force on fluid flow in the Basal Belly River Aquifer (e.g., Bachu and Underschultz, 1995; Parks and Tóth, 1995; Bachu and Michael, 2003). However, the hydraulic head values in the Basal Belly River Aquifer are much higher (almost double) than in the Viking Aquifer. Vertical pressure gradients in the Basal Belly River Aquifer of 8.4 kPa/m are also significantly different from that in the Viking Aquifer (10.4 kPa/m). The distinctly different vertical pressure gradients, and magnitude of hydraulic heads, indicate that the Colorado-Lea Park Aquitard acts as a very effective barrier to cross-formational flow between Basal Belly River and Viking aquifers.

Differences in hydraulic heads are also observed between Upper and Lower Belly River aquifers (compare Figure 21 and Figure 23). Hydraulic head values in the Upper Belly River Aquifer differ from those in the Basal Belly River Aquifer by approximately 50 m throughout the study area. This difference is more evident from the pressure-elevation plot (Figure 30): the Upper Belly River Aquifer is significantly underpressured relative to the Basal Belly River Aquifer, despite having similar hydraulic gradients. This indicates that the MacKay Coal Zone, or MacKay Aquitard as defined here, is an effective barrier to cross-formational flow in this sedimentary succession.

The Bearpaw shale overlies the Upper Belly River Aquifer and thus acts as an additional aquitard over part of the study area separating the deep aquifers from the shallow ones. Fluid flow in the shallow Horseshoe Canyon, Paskapoo and Surficial aquifers is topographically controlled and is different from the underlying aquifers. The separation between the two systems is reinforced by the significantly different subhydrostatic vertical gradient (2.8 kPa/m) and much lower TDS in these shallow aquifers than those in the deeper aquifers. Therefore, numerous mudstones and coal beds act as the last major barriers to cross-formational flow.

3.8 Hydrogeological Summary

A detailed hydrogeological characterization of the sedimentary succession overlying the Leduc (D3-A) and Nisku (D-2) reservoirs in the Clive oil field has been completed to identify and evaluate the competence of the main barriers to cross-formation flow in light of the proposed CO_2 EOR operation and further permanent CO_2 storage in these reservoirs.

The hydrostratigraphic column has been constructed based on the geological framework, data quality and availability, and previous larger-scale hydrogeological studies the Clive and adjacent areas. A total of four deep aquifers and five aquitards have been identified in the sedimentary succession overlying the reservoirs targeted for CO_2-EOR, listed in ascending order: Calmar-Wabamun Aquitard, Lower Mannville Aquifer, Upper Mannville–Joli Fou Aquitard, Viking Aquifer, Colorado–Lea Park Aquitard, Basal Belly River Aquifer, McKay Aquitard, Upper Belly River Aquifer, and Bearpaw Aquitard. Shallower strata contain three aquifers and one aquitard: Horseshoe Canyon Aquifer, Whitemud-Battle Aquitard, Paskapoo Aquifer, and Surficial Aquifer, the last two being in contact at the top of the bedrock.

The deepest aquifers, Lower Mannville and Viking, in which water salinity is high and highly variable - hence water density is variable - were examined for density-related flow effects using Water-Driving-Force analysis. Total Dissolved Solids, aquifer slope, and lateral hydraulic gradients were calculated for each aquifer. There are no significant density-related flow effects present in these two aquifers in the Enhance Clive study area.

Fluid flow in the Lower Mannville Aquifer is complex and directed primarily towards the east and north east. Hydraulic heads range from 500 to 350 m, with horizontal hydraulic gradients ranging from 1 to 40 m/km. A composite pressure-elevation plot indicates a vertical component of fluid flow based on a measured super-hydrostatic gradient of 12.4 kPa/m. The distribution of Total Dissolved Solids in the Lower Mannville Aquifer is highly variable, ranging from 40 g/L in the south to over 120 g/L in the north. A large high-TDS (> 100 g/L) plume sourced from the Devonian aquifers has been identified in the northeast. The hydrochemical evidence from the Nisku and Lower Mannville aquifers and the Calmar-Wabamun Aquitard, as well as pressure data from the Nisku reservoirs and the Lower Mannville Aquifer indicates that there is no hydraulic communication between the Nisku Formation and the Lower Mannville Aquifer in the Enhance Clive study area. Therefore, the Calmar-Wabamun Aquitard is a strong barrier to cross-formational flow in this study area.

Fluid flow in the Viking Aquifer is directed towards the southwest. Hydraulic heads range from 390 to 230 m, with lateral hydraulic gradients in the 1 to 20 m/km range. Vertical gradients of 10.4 kPa/m indicate that flow in the Viking Aquifer is mainly lateral, with no indication of a vertical flow component. Hydraulic heads in the Viking Aquifer are much

lower than those in the Lower Mannville Aquifer. Both flow patterns and hydraulic gradients in these two aquifers indicate that they are not in hydraulic communication and that the intervening Upper Mannville-Joli Fou Aquitard is strong. Water chemistry further supports the separation of the Viking Aquifer from the Lower Mannville Aquifer, with TDS in the Viking Aquifer ranging from 30 g/L in the central area to 60 g/L in the northeast, compared to >120 g/L in the Lower Mannville Aquifer.

Fluid flow in the Basal and Upper Belly River aquifers is directed towards the southwest. Vertical pressure analysis shows that the Basal and Upper Belly River aquifers have a downward, downdip component of flow, based on vertical gradients of 8.4 and 8.8 kPa/m, respectively. These gradients are significantly lower than in the underlying Viking Aquifer. Hydraulic heads range between 600 to 350 m in the Basal Belly River Aquifer, and 500 to 400 m in the Upper Belly River Aquifer. These hydraulic head values are much higher than in the Viking Aquifer. Both Basal and Upper Belly River aquifers have TDS values below 15 g/L throughout the entire study area. The Upper Belly River Aquifer appears to be underpressured relative to the Basal Belly River Aquifer. All of these lines of evidence point towards the competence of the Colorado–Lea Park Aquitard as a major barrier to the vertical migration of formation fluids in the Clive study area. Also, the McKay Coal Zone separating the Basal and Upper Belly River Aquifers seems to be a strong aquitard.

The flow in the shallow Horseshoe Canyon, Paskapoo, and Surficial aquifers is controlled by surface topography and is different from that in the deep aquifers. The hydraulic heads are much higher than in the Upper and Basal Belly River aquifer and range between 718 – 798 m in the Horseshoe Canyon and 800 – 880 m in the Paskapoo aquifers. The TDS values are in the Horseshoe Canyon Aquifer are < 5 g/L and in the Paskapoo and Surficial aquifers <1 g/L. The differences in the flow pattern, hydraulic heads, and formation water chemistry indicate the presence of a barrier or multiple barriers (mudstones and coal beds), between the shallow Horseshoe Canyon, Paskapoo and Surficial aquifers themselves, and also between the shallow and deep aquifers in the Enhance Clive study area.

Porosity and permeability of aquifer rocks were analyzed for the Lower Mannville, Viking, Basal Belly River and Upper belly River aquifers based on core analyses and drill-stem tests. No data are available for shallower aquifers. Plug-scale porosity values vary between 1% and 27%, with median values varying between 10.0% and 10.8%. Well-scale porosity values vary between 5.3% and 26.5%, with median values ranging from 9.4% to 12.2%. Field-scale porosity values are around 10%. As a general observation, it appears that, overall, porosity decreases with increasing depth, which is expected for siliciclastic sediments. Permeability values at the plug scale vary between 0.01 mD (the lower measurable limit) and several darcies. However, the low median values (<1 mD) indicate that most core permeability values are quite low. Well-scale and field-scale permeability values show a decrease of permeability with depth. Horizontal permeability anisotropy as determined from core analyses for the three aquifers ranges between 0.90

and 0.96 (low anisotropy). Vertical permeability anisotropy ranges from 0.086 (very high anisotropy) in the Viking aquifer to 0.53 and 0.33 (high anisotropy) in the Lower Mannville and Basal Belly River aquifers, respectively. Permeability values from drill-stem tests vary between 0.05 mD and several darcies. Field-scale values range between 3.85 mD for the Upper Belly River Aquifer and 501 mD for the Basal Belly River Aquifer. Field-scale permeability values derived from core measurements and from drill-stem tests are within the same order of magnitude for the Lower Mannville and Viking aquifers, and comparable with that in the Upper Belly River Aquifer. Only for the Basal Belly River Aquifer the field-scale permeability values derived from core and from drill-stem tests differ by a factor of ~40, but this may be statistically explained by the fact that only one well has core analyses and there are only five drill-stem tests in this aquifer, hence the results are not necessarily representative.

4. Mineralogy

Mineralogical samples have been selected from the aquifers in preparation for the numerical geochemical simulations that will be undertaken as part of the next phase of this project. The sample identification, well location, sample depth and formation name are given in Table 8. The first nine rock samples are listed in ascending stratigraphic order, from above the potential storage complex. Then two samples (EN-10 and EN-11) represent the storage unit. Then samples EN-30 through EN-34 represent additional samples from formations above the storage complex that were not analyzed earlier on, and these are also listed in ascending stratigraphic order.

Table 8: Sample identification, well location and formation

Sample #	Well Location	Depth (m)	Formation
EN-1	6-13-41-25W4	~ 1864.00	Calmar
EN-2	6-13-41-25W4	~ 1860.50	Calmar
EN-3	6-13-41-25W4	~1855.00	Wabamun
EN-4	11-5-41-23W4	~ 1492.00	Ellerslie
EN-5	11-5-41-23W4	~ 1478.00	Ostracod
EN-6	11-5-41-23W4	~1474.00	Ostracod
EN-7	11-5-41-23W4	~ 1463.30	Glauconitic Sandstone
EN-8	11-12-41-25W4	~ 1388.00	Viking
EN-9	9-35-41-23W4	~695.25	Basal Belly River Sandstone
EN-10	9-35-39-24W4	~1847.00	Nisku
EN-11	9-35-39-24W4	~1876.50	Leduc
EN-30	6-7-40-24W4	~1570.50	lowermost Upper Mannville
EN-31	8-6-40-25W4	~1448.00	Colorado shales
EN-32	12-17-39-24W4	~1401.90	Viking Fm. Shale
EN-33	7-14-41-23W4	~548.00	Upper Belly River Sst.
EN-34	12-5-39-23W4	~748.50	lowermost Upper Belly River

As can be seen from Table 8, multiple samples were taken from the Calmar, Ostracod and Belly River formations. At the time of sampling, significant differences in lithology were recognized. Thus two samples were taken from each to represent the observed heterogeneous formation mineralogy.

4.1 Analytical Methodology

A number of different analytical techniques were used to evaluate the mineralogy of each of the samples. These included XRD (X-Ray Diffraction), XRF (X-Ray Fluorescence), LECO[2] (Carbon and Sulphur loss by ignition), ICP-MS (Inductively Coupled Plasma Mass Spectrometry analysis), SEM (Scanning Electron Microscopy) and EDX (Energy Dispersive X-Ray analysis, on the SEM). With the exception of the SEM and XRD, these methods give a direct measurement of the elemental composition of the entire sample. SEM provides an image of a section of the core sample and allows

[2] The term LECO is the name of the original manufacturer for this specific type of instrument, and it is commonly used to indicate the apparatus from all manufacturers.

portions to be analysed by EDX. The user selects the area to be examined and analysed, thus there can be significant sample bias – each phase is usually looked at and analysed. Common phases, like quartz, may only be examined once even though it may be 90% of the sample. However, the SEM does allow identification of phases which are present in trace (or less amounts), a means to evaluate the dimensions of a mineral and the relative relationship of the minerals. XRD provides the identity of the major minerals and gives an estimate of the relative percentage of each. It does not give the composition of the phase. If the phase is non-stoichiometric, it may not be easy to identify via XRD. X-Ray Diffraction ratios should be considered approximate. Although the peak areas are primarily dependent on the relative amount of each phase, they are also strongly dependent on sample preparation, mineral crystallinity and the mineral "reflectivity to X-rays".

A number of different analytical techniques were used to evaluate the geochemical nature of each of the collected rock samples. These include XRD, XRF, LECO, ICP-MS and SEM (with EDX). Each of these techniques is presented below and the results are presented sample by sample in the following pages. The SEM microphotographs were made at selected points in the prepared thick section. EDX analyses were made at selected points on the thick section. The images and analysis were made in order to identify the salient features that were observed. They do not represent the mineral proportions in any way.

X-Ray Diffraction Analysis: The purpose of the X-Ray Diffraction (XRD) analysis was to identify the major crystalline minerals in the core sample. XRD is based on the scattering of X-rays from the crystalline mineral structure, which is characteristic of that phase. The intensity of the X-rays is measured as a function of angle and plotted. This pattern is then compared with the patterns to the standards database maintained by the International Centre for Diffraction Data and used to identify the various phases. XRD analysis is considered to be semi-quantitative as the mineral is identified by the diffraction peak positions, and the fraction of the phase by the relative areas under the major peak(s) for each mineral. This must be considered semi-quantitative as the peak location, height and width for any given mineral is also a function of mineral composition, crystallinity and sample orientation. In addition, unless the mineral has an exceptionally clean diffraction pattern compared to the background, it is often difficult to accurately estimate the peak areas. Complex mixtures of minerals may be difficult to identify because of overlapping characteristic peaks. XRD cannot identify amorphous or poorly crystalline material and difficulties may arise if the samples are poorly prepared (orientated crystal grains). Thus, for most minerals, calculated fractions below 1% are just given as present, and values below 5% should not be considered accurate. To quantify low percentage minerals, either the minerals in the sample must be separated and concentrated before measurement, or other analytical methods must be used in addition to XRD.

One gram of material from each sample was prepared for XRD analysis by crushing and then homogenizing with a SPEX 800D Mixer/Mill or a McCrone Vibrating Micronizing Mill until thoroughly mixed. The sample was then passed through a 45 micron sieve and a spatula was used to assist in the gathering of the fine-grained solid. A top loaded sub sample of the very fine powder was then prepared. A Siemens D5000 X-Ray Diffractometer equipped with a monochrometer was used to collect data. The diffraction pattern was recorded with copper radiation generated at 45 kV and 30 mA and any crystalline compounds in the sample were then matched to compounds in the International Centre for Diffraction Database.

X-Ray Fluorescence and LECO Analysis: The samples were analyzed using X-Ray Fluorescence (XRF) for the major cations and using LECO for carbon and sulphur. XRF measures the concentrations of elements within a sample by measuring the energy of the secondary X-rays generated when the sample is bombarded with high-energy gamma rays. It is useful in measurement of the major elemental composition of a sample when, for practical purposes, the sample is comprised of elements with mass at or above sodium. To do this, a sample of the core material was crushed, ground, pressed into a disc and fused with a flux. The components, SiO_2, TiO_2, Al_2O_3, Fe_2O_3, MnO, MgO, CaO, K_2O, Na_2O, P_2O_5 and L.O.I. (loss on ignition) were measured. The L.O.I measurement is a sum of the volatiles lost during fusion and must be analyzed separately to determine what the volatiles are.

For the samples selected for this project, the LECO analyzer was used to simultaneously determine carbon and sulphur through combustion. A sample was loaded into a tared ceramic boat and combusted at 1350^{o}C. A combustion catalyst is added to each sample to ensure complete combustion in the furnace. The combustion gases are collected and flowed through infra-red absorption detectors. The acronym LECO is based on the principal manufacturer of this analytical apparatus.

The XRF and LECO analyses are given for all samples in Appendix D, along with the ICP-MS analyses. They are all in the same tables of analytical results, as provided by Acme Labs of Vancouver. The first line of the title of the results sheets is "**Method**". If the listed method is "**4X**", then the results refer to XRF analyses. If the listed method is "**2A Leco**", then the results are the carbon and sulphur analytical results using LECO. If the listed method is "**1T**" or "**1E**", then the results are the ICP-MS analysis. For each set of tables, the first results presented are the XRF analyses, then the LECO analyses, and finally the ICP-MS results. After these results, the analytical data for the various laboratory standards are presented.

Inductively Coupled Plasma Mass Spectrometry Analysis: Inductively coupled plasma mass spectrometry (ICP-MS) can be used to determine a range of metals and non-metals at low concentrations, thus it is ideal for evaluating the trace metal concentrations present in a rock sample. ICP-MS is based on injecting a liquid sample as an aerosol into plasma in order to create ionic forms of the elements in the sample. The resulting plasma/ion mixture is injected into a mass spectrometer which separates and measures

the mass of the constituents. The method is extremely accurate in the measurement of small and trace amounts of components, with concentrations of one part in 1012 potentially be measured. It is less appropriate when the component concentrations are high.

For the analyzed samples, the solid sample was acid digested by microwave heating. The digested solutions were then diluted with distilled deionized water (DDW) and analyzed by inductively coupled plasma-mass spectrometry (ICP-MS). Trace metals including Al, An, As, Ba, Be, Bi, B, Cd, Ca, Cl, Cr, Co, Cu, Fe, Pb, Li, Mn, Mo, Ni, Se, Ag, Sr, Tl, Th, Sn, Ti, U, V and Zn in the digested solutions were determined using an external calibration method with Indium used as the internal standard. Digestion of the solid samples was accomplished using a MULTIWAVE-3000 microwave sample preparation system (Anton Paar GmbH, Graz, Austria), equipped with temperature and pressure regulation (through a sensor vessel) and controlled by a personal computer. The ICP-MS system used for analysis was the Perkin-Elmer Elan DRC-II ICP quadrupole mass spectrometer (Thornhill, ON, Canada), equipped with a GemTip cross-flow nebulizer, Ryton spray chamber, plasma torch with a quartz injector, a build-in peristaltic sample pump and CETAC ASX-510/ADX-500 auto-sampler/auto-diluter equipped with a CEASX500\as500B tray and controlled by ICP-MS software.

The solid samples were prepared and digested in a clean-laboratory environment. Approximately 0.22 to 0.25 gram portions of each solid was weighed into a digestion liner, and 5 ml of nitric acid and 0.5 ml of hydrofluoric acid were added. The microwave digestion was carried out in a closed vessel at controlled temperature (175°C) and controlled pressure (200 psi, or ~1379 kPa). The digested solutions were then diluted to 100 ml using distilled deionized water (DDW) before ICP-MS analysis.

In the ICP-MS analysis, all background concentrations of samples and standards were reagent blank subtracted. The external standard calibration curves (0, 10 and 100 µg/L of Al, An, As, Ba, Be, Bi, B, Cd, Ca, Cl, Cr, Co, Cu, Fe, Pb, Li, Mn, Mo, Ni, Se, Ag, Sr, Tl, Th, Sn, Ti, U, V and Zn, and 0, 1, 10 mg/L of Ca) were plotted linearly through zero for each isotope. Correction equations were applied to As, Se, Cr and V for corrections of interferences from chloride (ArCl and ClO) and also applied to Fe, Co and Ni for correction of interferences from calcium oxide and hydroxide. Analytical results were calculated and reported in µg/g. All results reported are corrected for mass of sample and dilution. The final reported analytical results are either ppm or weight %, based upon dry solid sample mass.

The ICP-MS XRF and LECO analyses are given for all samples at the end of this appendix, along with the XRF and LECO analyses. For details on the organization of the results, please refer to the last paragraph in the XRF and LECO section, the section immediately preceding this one.

Scanning Electron Microscopy and Energy Dispersive X-Ray analysis: A scanning electron microscope (SEM) is an electron microscope that images a sample by scanning

it with a high-energy beam of elections. The signals produced include the generation of secondary electrons, backscatter electrons and characteristic X-rays. The secondary electrons are the primary source to create the morphological map of the sample, while the backscatter electrons can be used to provide information about the distribution of different elements in the sample. It was not necessary to use backscatter electrons in the generation of this images and analyses.

Some of these sections were examined on a SEM model JEOL 6301FE, using an accelerating voltage of 5.0 kV. The remainder were examined using a Zeiss EVO MA 15 scanning electron microscope with a LaB6 filament. On both, backscattered images are taken using a Si diode detector. The Energy Dispersive X-ray analyses were taken using a peltier-cooled 10 mm^2 Bruker Quantax 200 Silicon drift detector with 123 eV resolution. Secondary electron images are obtained using an Everhart-Thornley detector. For the range of images and EDX analyses used in this report, the only difference between the JEOL and the Zeiss SEM is that the Zeiss instrument allowed direct annotation of the images.

Magnification for each image ranged from 20 times to 20,000 times.

A small fragment of rock was cut from each sample and a “thick” section was prepared by cementing a layer of rock on a glass slide and polishing it. No cover glass was used. (Note that one sample, EN-34, was water sensitive and only fragments could be mounted on the glass slide).The sample was then gold coated to provide an electrically conductive layer using a Nanotech SEMPrep 2 DC sputter coater.

The mineralogy of the components is based on the morphology of the crystals and elemental analysis as determined by Energy Dispersive X-ray (EDX) of selected spots (~ 1 µm diameter). Note that gold is always present in the EDX measurement as the sample was gold coated.

Within the section for each sample, the images are presented first and then are followed by the EDX analysis. After these, the X-ray diffraction results for the sample are given.

The ICP-ms, LECO and XRD analyses for all samples are given in Appendix D.

The ICP-ms and XRF analyses were performed at ACME laboratories in Vancouver, the SEM and associated EDX analyses were undertaken by AITF using University of Alberta facilities.

All of the data will be numerically combined using LPNorm (Linear Programming Normative analyses) to give the appropriate starting mineralogical conditions for the geochemical modelling. This will be undertaken in the second phase of this program.

4.2 Results

Based on XRD, the mineralogy of each of the samples is summarized in Table 9 (the complete scans are provided in Appendix D).

Table 9: Mineralogical composition of analyzed samples based on XRD.

Mineral	Sample							
	EN 1	EN 2	EN 3	EN 4	EN 5	EN 6	EN 7	EN 8
Anatase						< 1	< 1	
Anhydrite			65					
Calcite		5				20	< 1	
Dolomite	70	50	35			5		
Halite								
Illite		5		< 1	5	5	5	< 1
Kaolinite		< 1		5	5	5	5	< 1
K-Feldspar		5		5			< 1	
Plagioclase				< 1	< 1	< 1	< 1	5
Pyrite	5	5		< 1				< 1
Quartz	20	30	< 1	90	75	65	90	95
Siderite					15			

Mineral	Sample							
	EN 9	EN-10	EN-11	EN-30	EN-31	EN-32	EN-33	EN-34
Anatase						<1	<1	5
Anhydrite		70						
Calcite					20			
Dolomite		30	100		5		15	
Halite						5	<1	<1
Illite	5			5	5		5	5
Kaolinite	10			5	<1	5	5	5
K-Feldspar				5			5	5
Muscovite						5		
Plagioclase	20			10		5	5	10
Pyrite	65			<1	5			<1
Quartz			<1	75	65	70	65	70
Siderite				<1		10		

A quick look at this table indicates that the Calmar, Wabamun, Nisku and Leduc formations are primarily carbonate and/or sulphate mineral containing formations. The remaining are all siliceous and can only be distinguished apart by the amount of other phases present. The XRD results indicate that the Calmar formation is dolomitic with 20

to 30% quartz and significant amounts of pyrite present. They also indicate the Wabamun formation in the study area is predominately composed of anhydrite (calcium sulphate) and dolomite. The Nisku Fm. is predominately composed of anhydrite (calcium sulphate) and dolomite. However, as shown in Appendix D, the high amount of anhydrite observed is most likely due to the presence of an anhydrite vein. The Leduc Formation was found to be 100% dolomite. The Ellerslie Formation is predominately quartz with small amounts (approximately 5%) of kaolinite and potassium feldspar. The Ostracod Formation is predominately quartz for both samples. The deeper Ostracod sample contains in addition siderite, kaolinite and illite, whereas the shallower sample contains calcite, dolomite, kaolinite and illite in addition to the quartz. The Glauconitic Sandstone is predominately quartz with 5% each of illite and kaolinite. The Viking Sandstone sample has a higher proportion of quartz, and 5% calcium plagioclase. The Basal Belly River Sandstone has 65% quartz, 20% plagioclase, 10% kaolinite and 5% illite. The lowermost Upper Mannville has about 75% quartz, 10% plagioclase and 5% of each of illite, kaolinite and potassium feldspar. The Colorado shale has about 65% quartz, 20% calcite and 5% of each dolomite, illite and pyrite. The Viking Formation shale has about 70% quartz and 5% of each kaolinite, muscovite, plagioclase and siderite. Halite was identified (5%) but is probably due to drilling fluid contamination. The Upper Belly River Fm. has about 65% quartz, 15% dolomite and 5% each of illite, kaolinite, potassium feldspar and plagioclase. The lowermost Upper Belly River has about 70% quartz, 10% plagioclase and 5% each of illite, kaolinite and potassium feldspar.The significance of the mineralogy is in the potential reactions that may occur when either carbon dioxide or CO_2-containing fluids encounter them. Calcite and siderite will be expected to dissolve in the short term. Plagioclase is expected to be quite reactive. Illite is also reactive but is expected to react and form more kaolinite. Kaolinite is expected to be relative stable, and quartz will be essentially inert.

A number of minerals were identified in the SEM evaluations that were not identified in the XRD scans. It is expected that these will be present in trace amounts. Some, like rutile, are expected to be inert.

The relationships of the minerals and the matrix can be seen in the SEM evaluation. A number of the SEM images are shown below for illustration purposes, with the complete set presented in the appendices.

Figure 35 shows a large grain of anhydrite present at the center of the Calmar Formation sample, about 1 millimeter in length. No other anhydrite grains were identified in the sample. It is quite large compared to the other minerals, which are up to 20X smaller.

Figure 36 presents a SEM image of the Wabamun formation. It is re-crystallized and formed from anhydrite and dolomite. Very little porosity is visible.

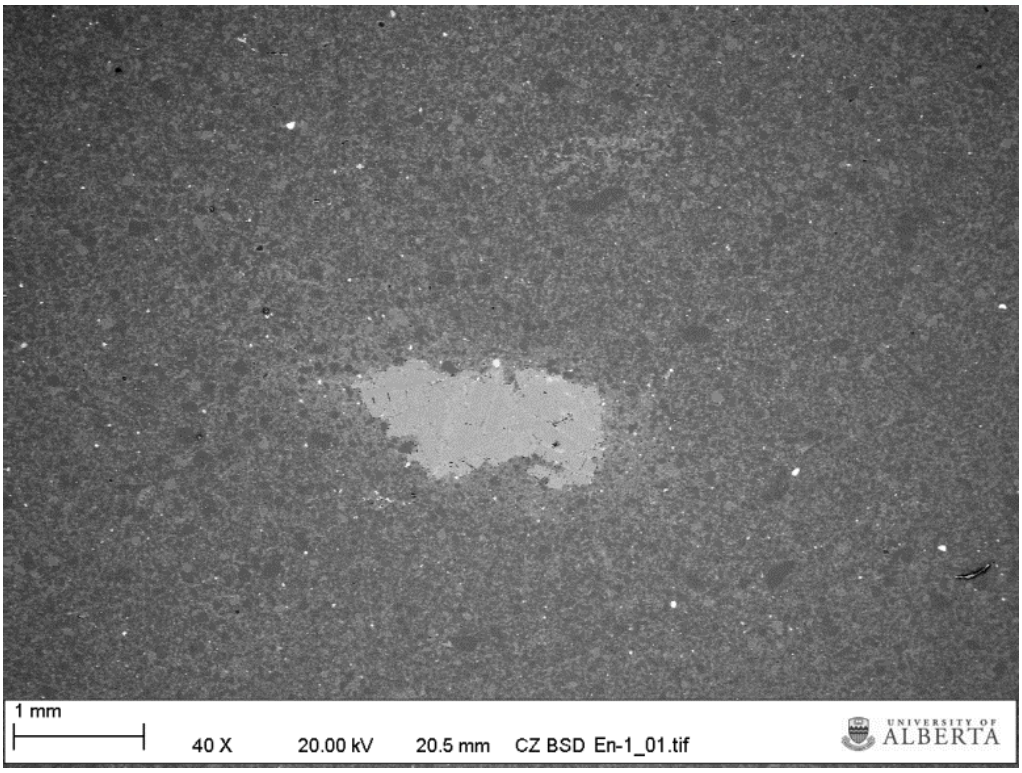

Figure 35: A 40X magnification from sample EN-1, the Calmar Formation.

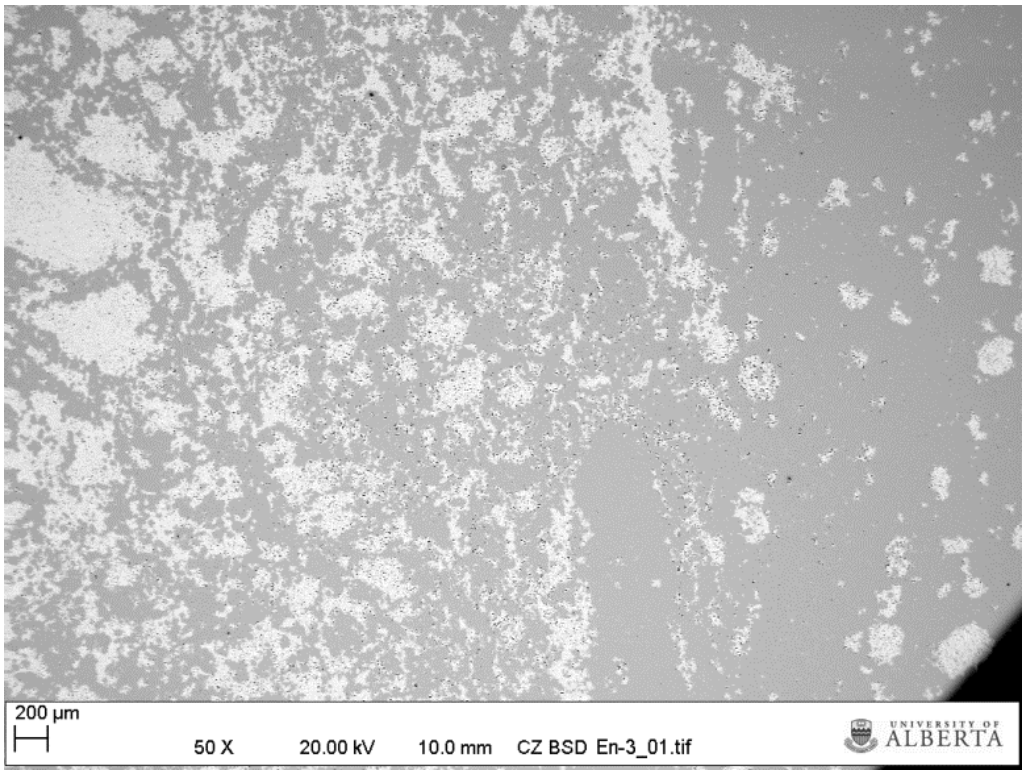

Figure 36: 50X magnification of sample EN-3, the Wabamun Formation.

Figure 37 presents a SEM image of the Ellerslie Formation. The main mineral is quartz, which is present in sub-rounded to slightly angular grains. A number of other minerals can be seen – these were examined by EDX. The data are presented in detail Appendix D. Significant porosity can be seen.

Figure 38 presents a SEM image of the Ostracod Formation. It is quite fine grained, and in addition to the abundance of quartz grains, a number of other minerals are present. The “bright” points in this image are mostly pyrite but some are other heavy minerals.

Figure 39 presents a SEM image of the Glauconitic Sandstone Formation. The sample is predominantly quartz surrounded by clay. The clay is most likely a kaolinite-illite mixture.

Figure 40 presents a SEM image of the sandstones of the Viking Formation. Most of the grains are angular quartz and are approximately 100 to 300 microns in length along the apparent long axis. Porosity is evident from the image. A number of bright grains can be seen, the majority of which are pyrite.

In Figure 41, the Basal Belly River Sandstone has good porosity. More than one half of the grains are quartz, with a number of other minerals present. Based on its appearance, the Basal Belly River Sandstone should be considered to be a reactive formation due to the abundance of minerals other than quartz.

Figure 42 shows an image of the Leduc Formation. In this sample, the formation is comprised entirely of dolomite. Sharp crystal edges can be seen in the pores.

Figure 43 is an SEM image from the Upper Mannville Group. A range of clays and plagioclase are present, suggesting that this is a chemically reactive unit.

Figure 44 is an SEM image from the Colorado shales. The bedding layers can be easily seen. At this particular point, considerable pyrite is present.

Figure 45 is an SEM image from the Viking Formation shale. The bedding plans can be clearly seen.

Figure 46 is an SEM image from sample the Upper Belly River sandstone. This particular sample has a large amount of clay. The sample was slightly water sensitive and partially separated during mounting on the SEM slide.

Appendix D contains the full set of analytical data and SEM images for all of these samples. As mentioned above, they range in composition from carbonates to almost pure quartz sandstone. The range in composition indicates that if they are exposed to carbon dioxide-containing water solutions, there will be very different types of reactions occurring in each. Some of these reactions may be extensive, while others, particularly in the high percentage quartz formations, will be very limited. This will be evaluated in the next phase of the project.

4.3 Mineralogical Summary

Samples were selected from drill core in order to characterize the mineralogy of the Calmar, Wabamun, Ellerslie, Ostracod, Glauconitic Sandstone, Viking and the Basal Belly River Sandstone formations. Multiple samples were taken from the Calmar and Ostracod formations due to the observation that there were significant differences in lithology within these formations. It should be recognized that more variations could exists, but within the scope of this program, this sample set will be used as input for the geochemical modeling portion of the next phase of the study.

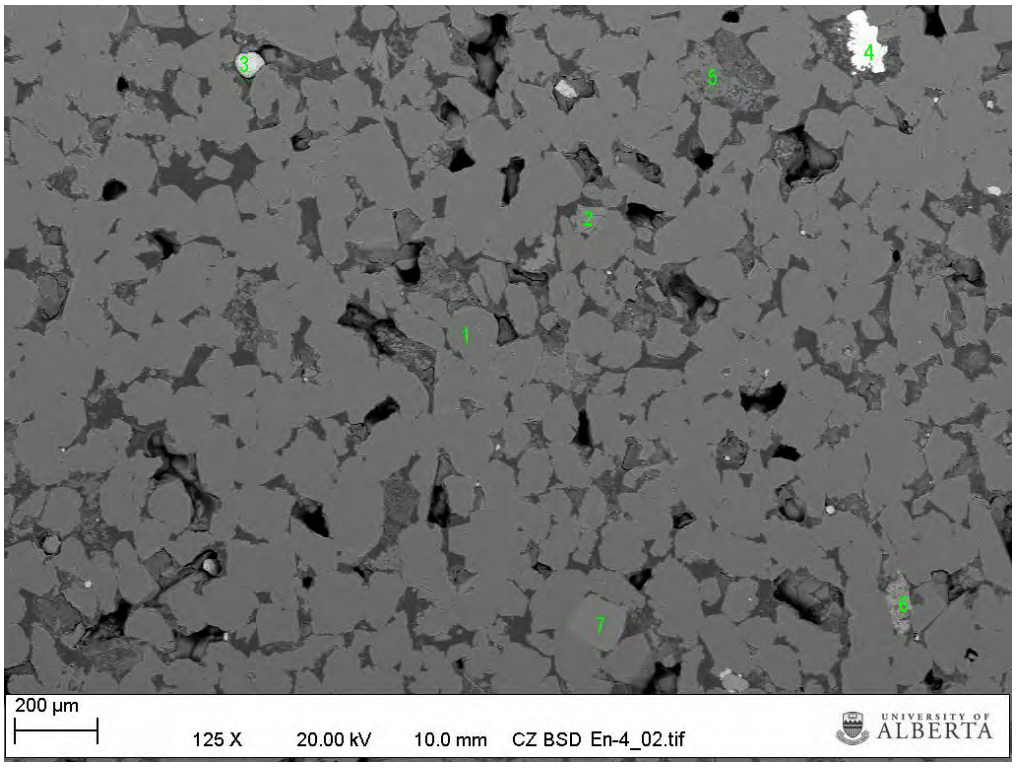

Figure 37: A 125X magnification of sample EN-4, the Ellerslie Formation. The green numbers refer to EDX analysis in Appendix D.

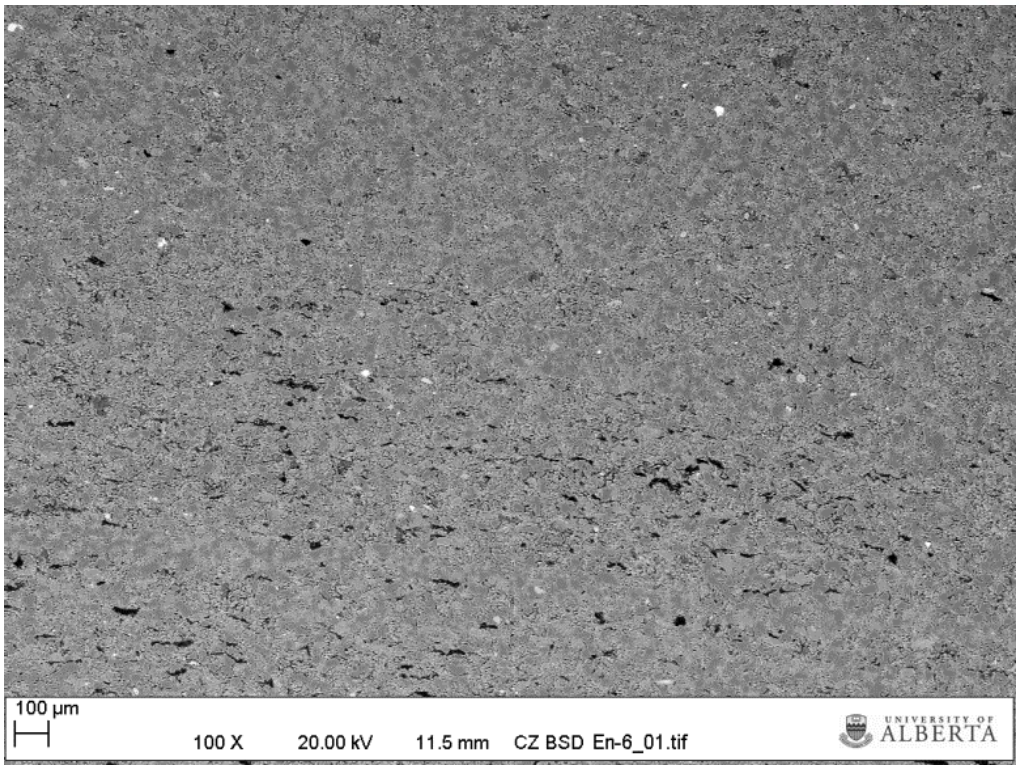

Figure 38: A 100X magnification of sample EN-6, the Ostracod Formation.

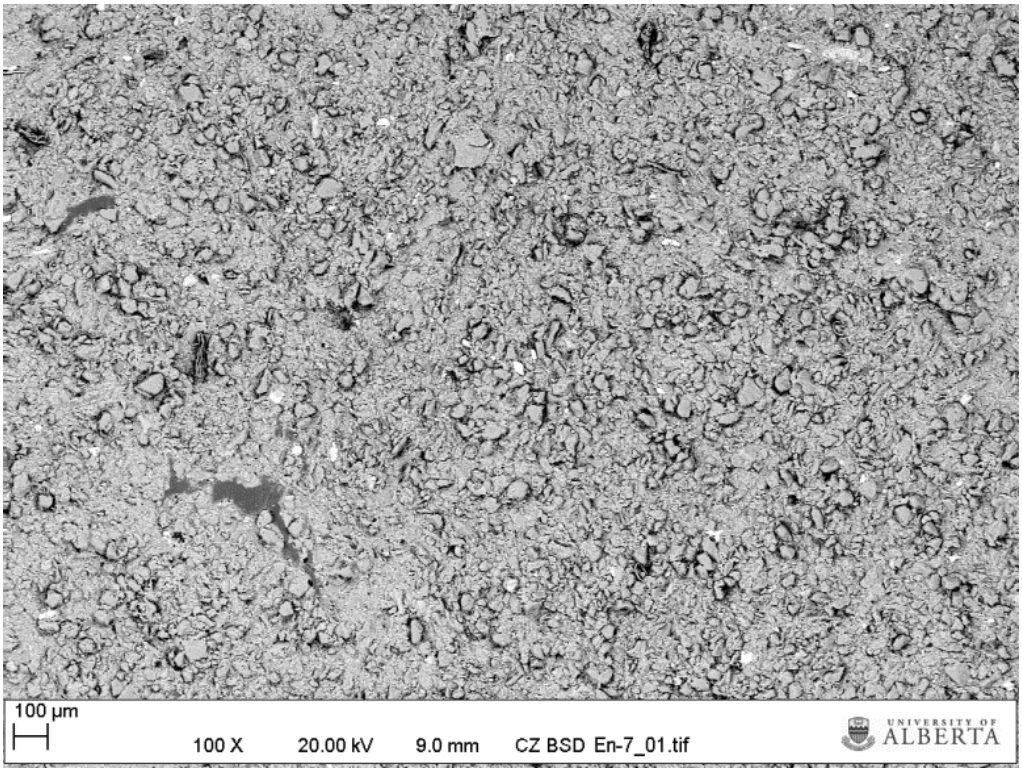

Figure 39: A 100X magnification of sample EN-7, the Glauconitic Sandstone Formation.

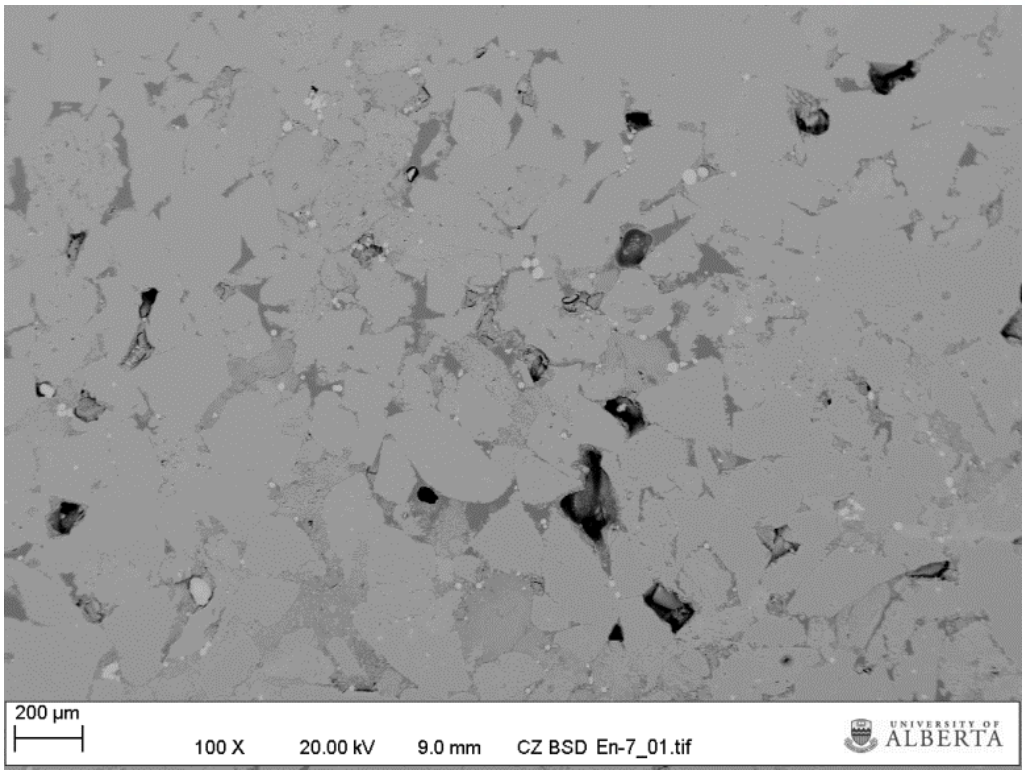

Figure 40: A 100X magnification of sample EN-8, the sandstones of the Viking Formation.

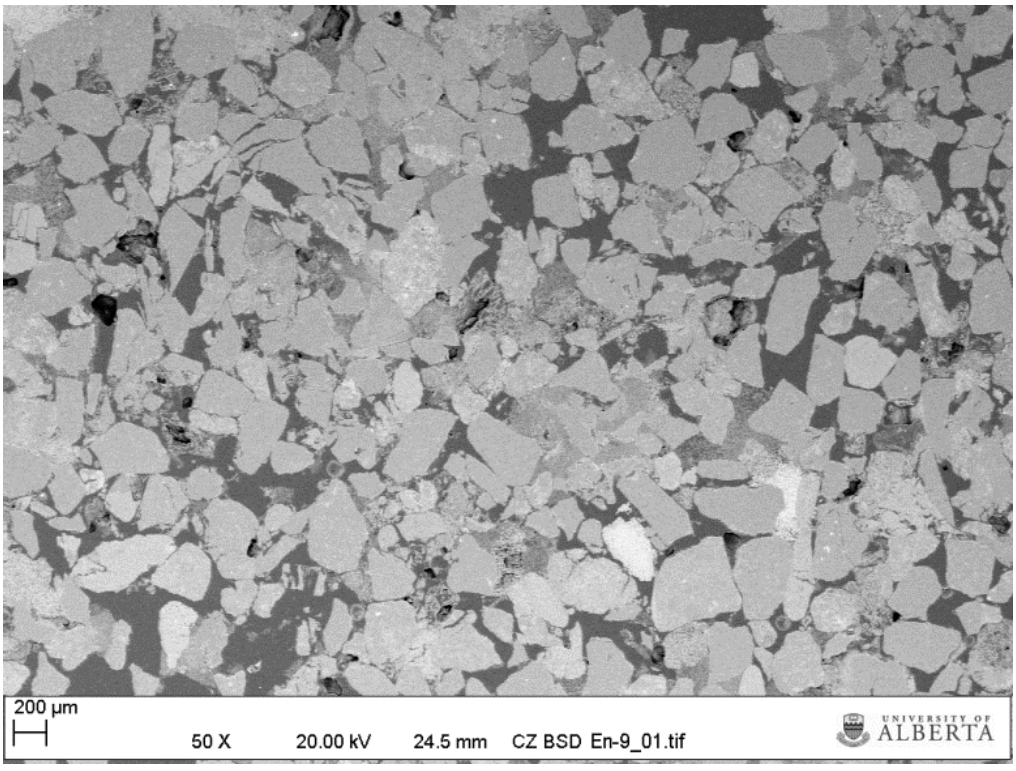

Figure 41: A 50X magnification of sample EN-9, the Basal Belly River Sandstone.

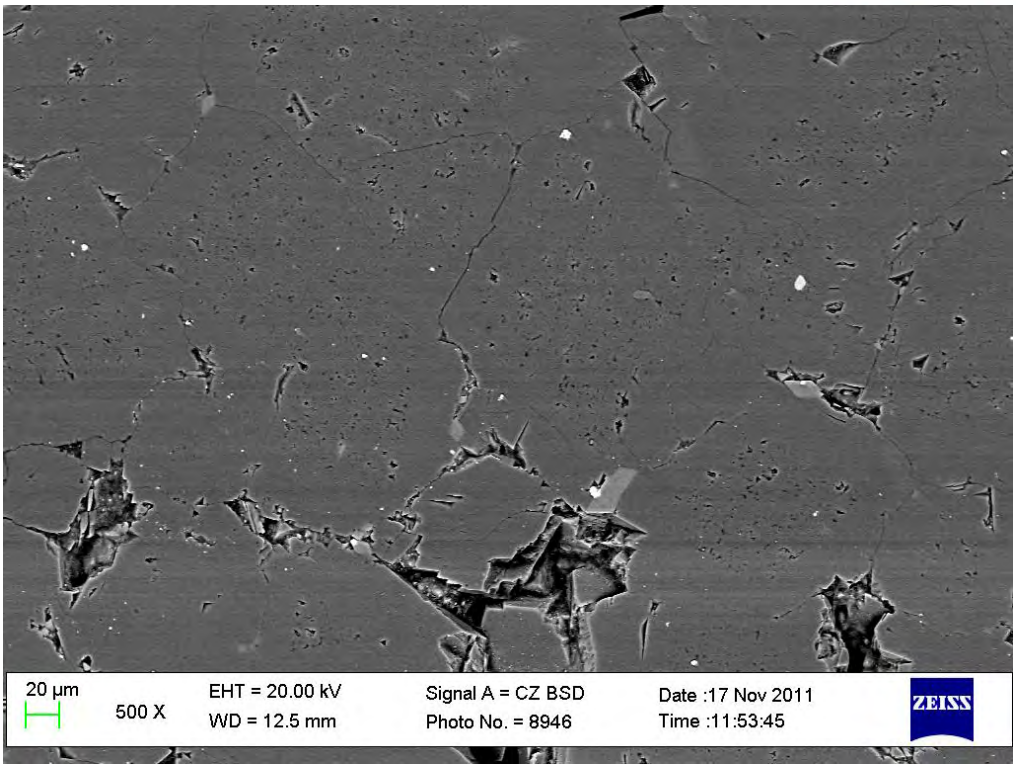

Figure 42: A 500X magnification of sample EN-11, the Leduc formation.

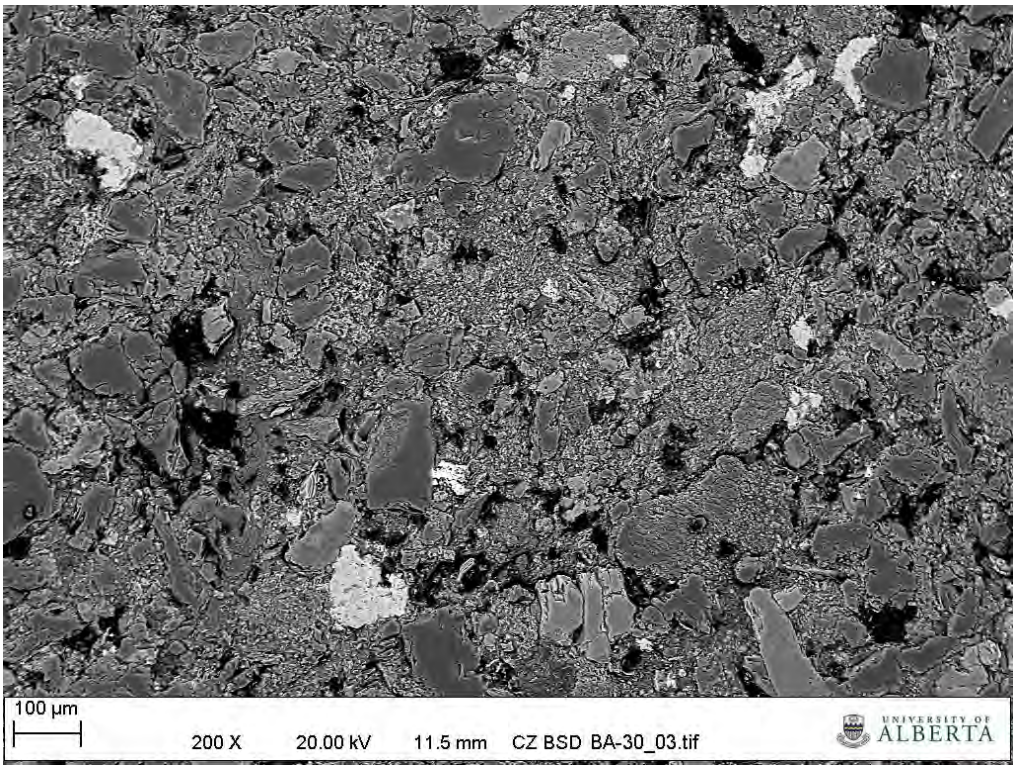

Figure 43: A 200X magnification of sample EN-30, from the lowermost portion of the upper Mannville.

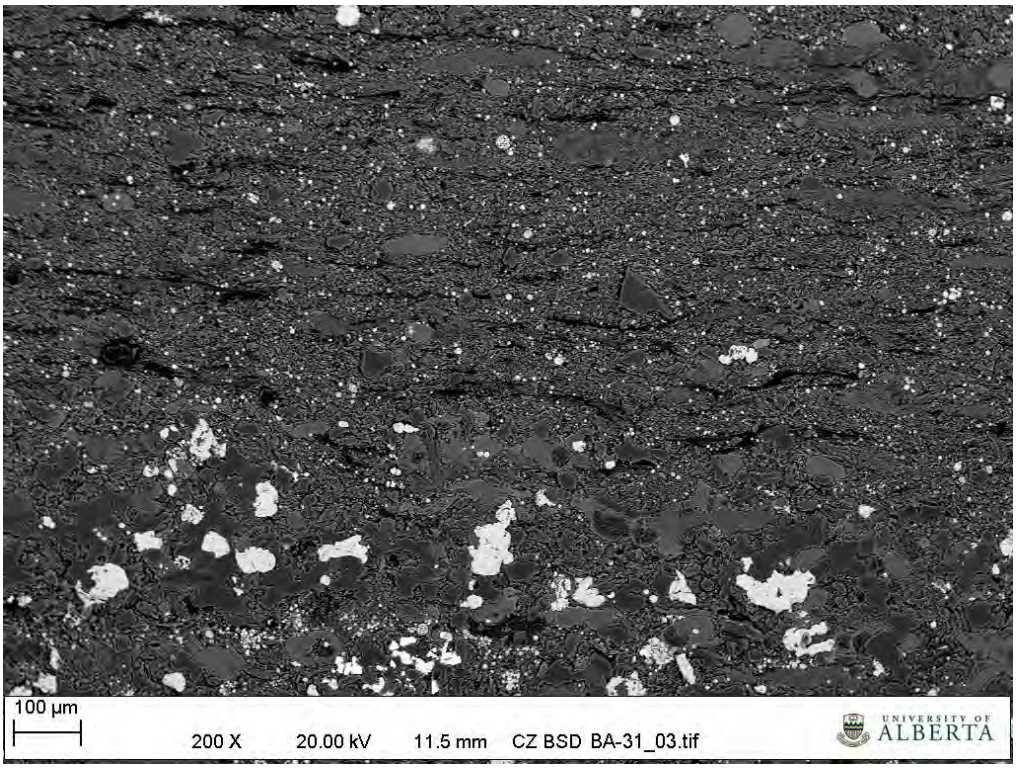

Figure 44: A 200X magnification of the Colorado shale, Sample EN-31.

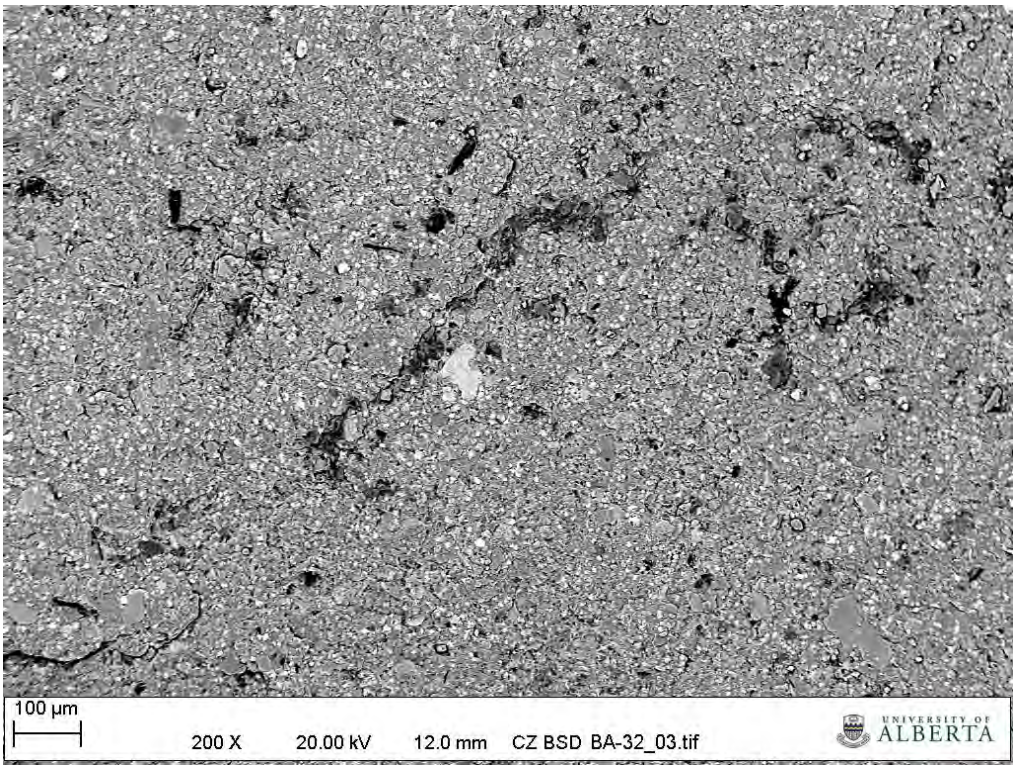

Figure 45: A 200X magnification of the Viking Formation shale, sample EN-32.

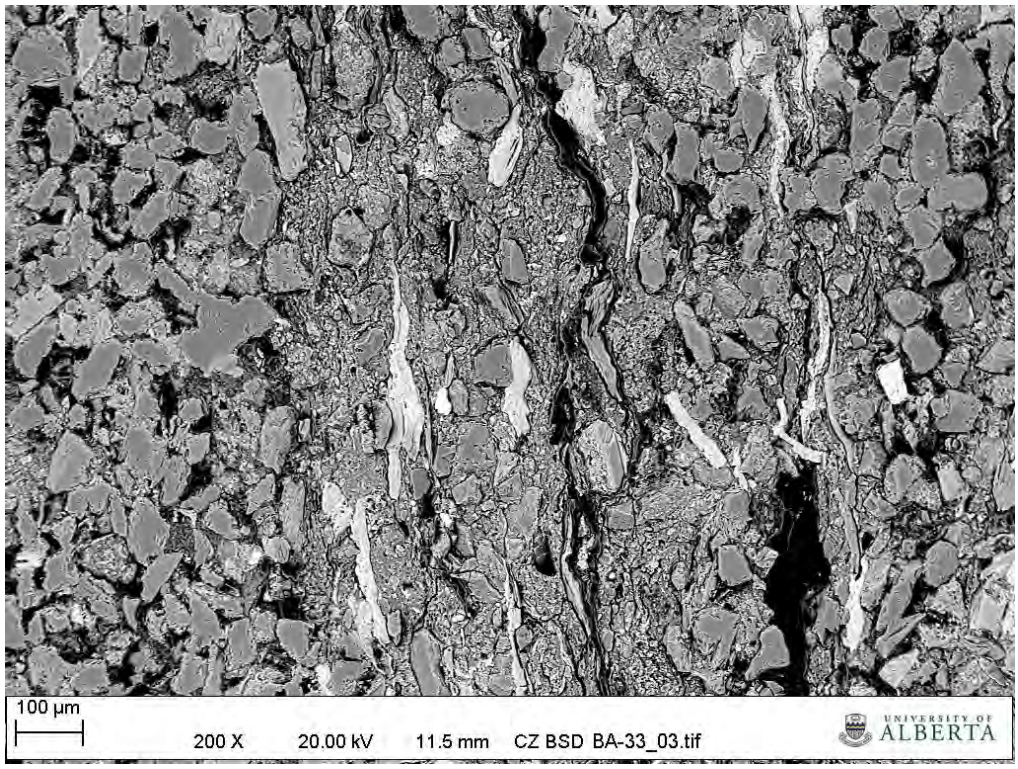

Figure 46: A 200X magnification of sample EN-33, the upper Belly River Sandstone.

A wide range of analytical techniques were used for the mineralogical, including XRD (X-Ray Diffraction), XRF (X-Ray Fluorescence), LECO (Carbon and Sulphur loss by ignition), ICP-MS (Inductively Coupled Plasma Mass Spectrometry analysis), SEM (Scanning Electron Microscopy) and EDX (Energy Dispersive X-Ray analysis, on the SEM).

Given the wide range of formations, the observed mineralogy is relatively limited. The Calmar formation is primarily a dolomite with varying amounts of quartz. Pyrite is present in both samples at 5%. Variable amounts of calcite, illite, potassium feldspar with traces of kaolinite were found in the samples. The Wabamun formation is primarily composed of anhydrite and calcite, with a trace of quartz. The Nisku Formation is predominantly composed of anhydrite (calcium sulphate) and dolomite. However the large amount of anhydrite is most likely due to the presence of an anhydrite vein. The Leduc formation was found to be 100% dolomite. The remaining formations are sandstones or shales, and comprise more than 65% quartz. The Ellerslie and Glauconitic Sandstone formations have 90% quartz, with illite, kaolinite and potassium feldspar present in varying amounts in both. Although the modal amounts of the minerals vary, the two samples from the Ostracod formation are similar. They have 65 to 75% quartz, 5% each of illite and kaolinite and 20% of calcite or siderite (calcium carbonate or iron carbonate). The Viking formation has 95% quartz and 5% plagioclase, while the Basal Belly River Sandstone has 65% quartz, 20% plagioclase, 10% kaolinite and 5% illite. The lowermost Upper Mannville has about 75% quartz, 10% plagioclase and 5% of each of illite,

kaolinite and potassium feldspar. The Colorado shale has about 65% quartz, 20% calcite and 5% of each dolomite, illite and pyrite. The Viking Formation shale has about 70% quartz and 5% of each kaolinite, muscovite, plagioclase and siderite. The Upper Belly River has about 65% quartz, 15% dolomite and 5% each of illite, kaolinite, potassium feldspar and plagioclase. The lowermost Upper Belly River has about 70% quartz, 10% plagioclase and 5% each of illite, kaolinite and potassium feldspar.

From a geochemical perspective, quartz is, for all practical purposes, inert when in contact with CO_2 or CO_2-saturated formation water. However, leakage of CO_2 in these siliciclastic formations is expected to result in more acidic formation waters in the formations reached by CO_2. This will likely result in (some) carbonate mineral dissolution and conversion of illite and potentially potassium feldspar to kaolinite, partially buffering the pH shift and resulting in high potassium concentrations in the formation fluids. The presence of plagioclase in the Viking and Basal Belly River Sandstone formation could be significant for mineralogical precipitation of the leaked CO_2. If the plagioclase reacts to the acidification of the formation water, it will dissolve. This will partially buffer the pH and, more interesting, increase the calcium ion concentration. Thus, there is potential for the later stage precipitation of calcite, resulting in mineralogical precipitation. The shale samples are chemically more complex than the sandstones, as they contain plagioclase as well as a number of different sheet silicates / clays. Thus, they also have potential for geochemical reactions to occur. These reactions will be limited by the low permeability of these formations, which restricts the amount, if any, of penetrating CO_2 or CO_2-saturated water. Both of these possibilities will be evaluated in future phases of the project.

5. Summary

A major challenge in mitigating climate change effects is the reduction of anthropogenic CO_2 emissions through a broad portfolio of measures which includes increasing energy efficiency and conservation, switching from fossil-based energy production to other forms of energy such as nuclear, solar, wind and other renewables, and CO_2 capture, utilization and storage (CCUS). Aware of the potential of CCUS to reduce anthropogenic CO_2 emissions, the Alberta and federal governments have provided significant financial support for the implementation of large-scale CCUS demonstration projects in western Canada, among them being Enhance Energy's "Alberta Carbon Trunk Line" Project, known also as ACTL. Enhance Energy Inc. will construct and operate the Alberta Carbon Trunk Line, which is a 240 km pipeline that will collect CO_2 from industrial emitters in and around Alberta's Industrial Heartland and transport it to aging oil reservoirs in central Alberta, more specifically the Leduc (D3-A) and Nisku (D-2) reservoirs in the Clive oil field first and then other oil reservoirs as the project progresses, for secure storage in CO_2-EOR projects

All CCUS projects require the study of the fate and effects of the stored CO_2, and the development of an active monitoring program to ensure that there is no CO_2 leakage from the storage unit. In the case of CO_2-EOR operations, CO_2 is stored in the respective oil reservoir(s), and monitoring of the fate and effects of CO_2 in the reservoir(s) is part of the engineering practice. However, monitoring for CO_2 leakage and for effects of CO_2 injection outside the reservoir requires knowledge of the characteristics of the sedimentary succession above the oil reservoir(s) into which CO_2 is injected. Enhance Energy has retained Alberta Innovates – Technology Futures (AITF) to study the geology, hydrogeology and rock mineralogy in the sedimentary succession from the top of the Leduc (D3-A) and Nisku (D2) oil reservoirs, whose primary seal (caprock) is the Calmar Formation, to the ground surface. The Enhance Clive study area covers 171 sections of land. A total 1715 wells were drilled within this study area, of which 660 wells reach the top of the Nisku Formation. For the purpose of a study, a geological study area expanded to a Township on each side of the Enhance Clive study area was defined. Because of data scarcity, an even larger hydrogeological study area was defined, comprising an additional Township on each side of the geological study area.

A very thick package of Paleozoic, Mesozoic and Cenozoic sediments (around 2000 m thick) overlies the Clive Leduc (D3-A) and Nisku (D2) pools in the Enhance Clive study area. The majority of sedimentary units are continuous across the study area, except for those Paleozoic strata in proximity to the sub-Cretaceous unconformity and at the base of the Tertiary and Quaternary deposits, which were truncated as a result of pre-Cretaceous and Cenozoic erosional events, respectively. Only the Bearpaw Formation is limited in the study area due to non-deposition. The sedimentary succession comprises in ascending order the Devonian shales of the Calmar Formation and anhydritic carbonates of the Wabamun Group, the thick Cretaceous succession which consists dominantly of sandstones of the Lower Mannville group, mixed siliciclastics of the Upper

Mannville Group, shales of the Joli Fou Formation, sandstones of the Viking Formation, very thick shales of the Colorado Group and Lea Park Formation, sandstones of the Basal Belly River Group, mixed siliciclastics of the Upper Belly River Group, shales of the Bearpaw Formation, sandstones of the Horseshoe Canyon Formation, shales of the Whitemud and Battle formations, and sandstones of the Scollard Formation. The mixed siliciclastics of the Tertiary Paskapoo Formation overlies the Cretaceous succession at the top of the bedrock. Quaternary unconsolidated surficial sediments overlying the bedrock generally consist of lacustrine deposits underlying glacially-derived tills. Incised within these deposits are buried bedrock valleys and meltwater channels filled with sand and gravel of fluvial origin. Coal zones are present in the Upper Mannville and Belly River groups, and in the Horseshoe Canyon, Scollard and Paskapoo formations.

A detailed hydrogeological characterization of the sedimentary succession overlying the Leduc (D3-A) and Nisku (D-2) reservoirs in the Clive oil field has been completed using analyses of formation waters, drillstem tests and core analyses to identify and evaluate the competence of the main barriers (aquitards) to cross-formational flow, in light of the proposed CO_2 EOR operation and further permanent CO_2 storage in these reservoirs.

The hydrostratigraphic column has been constructed based on the geological framework, data quality and availability, and previous larger-scale hydrogeological studies of the Clive and adjacent areas. A total of four deep aquifers and five aquitards have been identified in the deeper sedimentary succession overlying the reservoirs targeted for CO_2-EOR, listed in ascending order: Calmar-Wabamun Aquitard, Lower Mannville Aquifer, Upper Mannville-Joli Fou Aquitard, Viking Aquifer, Colorado-Lea Park Aquitard, Basal Belly River Aquifer, McKay Aquitard, Upper Belly River Aquifer, and Bearpaw Aquitard. Shallower strata contain three aquifers and one aquitard: Horseshoe Canyon Aquifer, Whitemud-Battle Aquitard, Paskapoo Aquifer, and Surficial Aquifer (the package of unconsolidated sediments), the last two being in contact across the bedrock subcrop.

Fluid flow in the Lower Mannville Aquifer is complex and directed primarily towards the east and north east. Hydraulic heads range from 500 to 350 m, with horizontal hydraulic gradients ranging from 1 to 40 m/km. A composite pressure-elevation plot indicates a vertical component of fluid flow based on a measured super-hydrostatic gradient of 12.4 kPa/m. The distribution of Total Dissolved Solids (TDS) in the Lower Mannville Aquifer is highly variable, ranging from 40 g/L in the south to over 120 g/L in the north. A large high-TDS (>100 g/L) plume has been identified in the northeast. This is most likely the result of back-flow of heavy Devonian brines from subcrop regions outside of the study area. The hydrochemical evidence from the Nisku and Lower Mannville aquifers and the Calmar-Wabamun Aquitard, and the pressure data from the Nisku reservoirs and the Lower Mannville Aquifer indicate that there is no hydraulic communication between the Nisku Formation and the Lower Mannville Aquifer in the Enhance Clive study area and that the Calmar-Wabamun Aquitard is a strong barrier to cross-formational flow.

Fluid flow in the Viking Aquifer is directed towards the southwest. Hydraulic heads range from 390 to 230 m, with lateral hydraulic gradients in the 1 to 20 m/km range. Vertical gradients of 10.4 kPa/m indicate that flow in the Viking Aquifer is mainly lateral, with no indication of a vertical flow component. Hydraulic heads in the Viking Aquifer are much lower than those in the Lower Mannville Aquifer. The differences in hydraulic heads, hydraulic gradients and flow patterns between these two aquifers indicate that they are not in hydraulic communication and that the intervening Upper Mannville-Joli Fou Aquitard is strong. Water chemistry further supports the separation of the Viking Aquifer from the Lower Mannville Aquifer, with TDS in the Viking Aquifer ranging from 30 g/L in the central area to 60 g/L in the northeast, compared to >120 g/L in the Lower Mannville Aquifer.

Fluid flow in the Basal and Upper Belly River aquifers is directed towards the southwest. Vertical pressure analysis shows that the Basal and Upper Belly River aquifers have a downward, downdip component of flow, based on vertical gradients of 8.4 and 8.8 kPa/m, respectively. These gradients are significantly lower than in the underlying Viking Aquifer. Hydraulic heads range between 600 to 350 m in the Basal Belly River Aquifer, and 500 to 400 m in the Upper Belly River Aquifer. These hydraulic head values are much higher than in the Viking Aquifer. Both Basal and Upper Belly River aquifers have TDS values below 15 g/L throughout the entire study area. The Upper Belly River Aquifer appears to be underpressured relative to the Basal Belly River Aquifer. All of these lines of evidence point towards the competence (strength) of the Colorado–Lea Park Aquitard as a major barrier to the vertical migration of formation fluids in the Clive study area. Also, the McKay Coal Zone separating the Basal and Upper Belly River Aquifers seems to be a strong aquitard.

The flow in the shallow Horseshoe Canyon, Paskapoo, and Surficial aquifers is controlled by surface topography and is different from that in the deep aquifers. The hydraulic heads are much higher than in the Upper and Basal Belly River aquifer and range between 718 – 798 m in the Horseshoe Canyon and 800 – 880 m in the Paskapoo aquifers. The TDS values are in the Horseshoe Canyon Aquifer are <5 g/L and in the Paskapoo and Surficial aquifers <1 g/L. The differences in the flow pattern, hydraulic heads, and formation water chemistry indicate the presence of a barrier or multiple barriers (mudstones and coal beds), between the shallow Horseshoe Canyon, Paskapoo and Surficial aquifers themselves, and also between the shallow and deep aquifers in the Enhance Clive study area.

Porosity and permeability of aquifer rocks were analyzed for the Lower Mannville, Viking and Basal and Upper Belly River aquifers based on core analyses and drillstem tests. No data are available for shallower aquifers. Plug-scale porosity values vary between 1% and 27%, with median values varying between 10.0% and 10.8%. Well-scale porosity values vary between 5.3% and 26.5%, with median values ranging between 9.4% and 12.2%. Field-scale porosity values are around 10%. As a general observation, it appears that, overall, porosity decreases with increasing depth, which is expected for

siliciclastic sediments. Permeability values at the plug scale vary between 0.01 mD (the lower measurable limit) and several darcies. However, the low median values (<1 mD) indicate that most core permeability values are quite low. Well-scale and field-scale permeability values show a decrease of permeability with depth. The horizontal permeability anisotropy is low (greater than 0.90). Vertical permeability anisotropy ranges from 0.086 (very high anisotropy) in the Viking aquifer to 0.33 and 0.53 (high anisotropy) in the Basal Belly River and Lower Mannville aquifers, respectively. Permeability values from drill-stem tests vary between 0.05 mD and several darcies. Field-scale values range between 3.85 mD for the Upper Belly River Aquifer and 501 mD for the Basal Belly River Aquifer. Field-scale permeability values derived from core measurements and from drill-stem tests are within the same order of magnitude for the Lower Mannville and Viking aquifers, and comparable with that in the Upper Belly River Aquifer. Only for the Basal Belly River Aquifer the field-scale permeability values derived from core and from drill-stem tests differ by a factor of ~40, but this may be statistically explained by the fact that only one well has core analyses and there are only five drill-stem tests in this aquifer, hence the results are not necessarily representative.

The mineralogy of the Calmar, Wabamun, Ellerslie, Ostracod, Glauconitic Sandstone, Viking and the Basal Belly River Sandstone formations was characterised in preparation for geochemical simulations in the next phase of this study. Samples were taken from drill core and evaluated using a range of analytical techniques. In summary, the Calmar and Leduc formations is primarily composed of dolomite. The Wabamun and Nisku formations are almost entirely comprised of anhydrite and dolomite. The remaining formations all have quartz as the dominate mineral, ranging from 65 to 95%. Illite, kaolinite and potassium feldspar are present in most of the remaining samples. Some of the carbonate minerals are observed in about half of these samples. Plagioclase is present in the Viking, Manville and Basal Belly River Sandstone.

In the case of CO_2 leakage into a formation, the formation water will become acidic, resulting in reactions with the rock minerals and potentially formation of new minerals. Some of the carbonate minerals (calcite, dolomite and/or siderite) are expected to dissolve. Illite, and potassium feldspar would probably react to form kaolinite and change the formation water composition slightly. The presence of plagioclase suggests that, as it dissolves into the more acidic formation water, the increased levels of calcium in the formation will result in calcite precipitation. This mechanism for potential mineralogical sequestration of leaked CO_2 is very significant and will be examined in detail in the next phase of the study through geochemical simulations.

In conclusion, all the geological, hydrogeological and mineralogical evidence collected and interpreted in this study indicates that the Leduc (D3-A) and Nisku (D-2) oil reservoirs in the Enhance Clive study area are capped by a strong and thick primary seal (caprock), the Calmar-Wabamun Aquitard (which includes in places remnants of the Carboniferous shales of the Exshaw and Lower Banff formations). This primary seal constitutes a barrier to upward migration and leakage of CO_2 from the oil reservoirs

targeted for CO_2 enhanced oil recovery in the area. The primary caprock is overlain in turn in by a succession of aquifers, listed in ascending order: Lower Mannville, Viking, Basal Belly River and Upper Belly River, separated by strong intervening aquitards: Joli Fou, McKay and Bearpaw, which constitute secondary traps and secondary barriers, respectively, for any CO_2 that may leak from the oil reservoirs through wells that penetrate the oil reservoirs. The strength of the aquitards in the sedimentary succession indicates that no CO_2 leakage is possible through the natural geological and hydrogeological system in the Enhance Clive study area. The only possible leakage pathway for CO_2 injected in the Leduc (D3-A) and Nisku (D2) reservoirs is through one or more of the ~309 wells that penetrate the oil-producing horizons in these reservoirs. The deep aquifers and aquitards in the study area are overlain by a succession of shallow aquifers which are within the depth of protected groundwater in the area: Horseshoe Canyon, Scollard-Paskapoo and Surficial. These aquifers constitute a source of groundwater used for human consumption and agricultural and industrial purposes and they should be monitored for any potential leakage of CO_2. Thus, an evaluation of the potential for CO_2 leakage through wells and the development of a monitoring program in the Enhance Clive area are recommended as potential subjects of study in a follow-up Phase 2 of the current work.

7. References

Agriculture and Agri-Food Canada. 2001. Lacombe County Regional Groundwater Assessment. Prepared by Hydrogeological Consultants Ltd. for Agriculture and Agri-Food Canada.

Alkalali, A., 2002. Petroleum hydrogeology of the Nisku Aquifer in the Western Canada Sedimentary Basin. Unpublished M.Sc. Thesis, Department of Earth and Atmospheric Sciences, University of Alberta, Alberta, Canada, 152 p.

Anfort, S.J., Bachu, S., and Bentley, L.R., 2001. Regional-scale hydrogeology of the Upper Devonian-Lower Cretaceous sedimentary succession, south-central Alberta basin, Canada. American Association of Petroleum Geologists Bulletin, v. 85, p. 637-660.

Bachu, S., 1995a. Flow of variable-density formation water in deep sloping aquifers: review of methods of representation with case studies. Journal of Hydrology. v. 164, p. 19-38.

Bachu, S., 1995. Synthesis and model of formation-water flow, Alberta Basin, Canada. American Association of Petroleum Geologists Bulletin, v. 79, p. 1159-1178.

Bachu S., 1999. Flow systems in the Alberta Basin: Patterns, types and driving mechanisms. Bulletin of Canadian Petroleum Geology, v. 47, p. 455-474.

Bachu, S., and Michael, K., 2002. Flow of variable-density formation water in deep sloping aquifers: minimizing the error in representation and analysis when using hydraulic-head distributions. Journal of Hydrology, v. 259, p. 49-65.

Bachu, S., and Michael, K., 2003. Possible controls of hydrogeological and stress regimes on the producibility of coalbed methane in Upper Cretaceous-Tertiary strata of the Alberta Basin, Canada: American Association of Petroleum Geologists Bulletin, v. 87, p. 1729-1754.

Bachu, S., and Underschultz, J.R., 1993. Hydrogeology of formation waters, northeastern Alberta basin. American Association of Petroleum Geologists Bulletin, v. 77, p. 1745-1768.

Bachu, S., and Underschultz, J.R., 1995. Large-scale erosional underpressuring in the Mississippian–Cretaceous succession, southwestern Alberta basin: American Association of Petroleum Geologists Bulletin, v. 79, p. 989–1004.

Barson, D.B., 1993. The hydrogeological characterization of oil fields in north-central Alberta for exploration purposes. Unpublished Ph.D. thesis, Department of Geology, University of Alberta, Edmonton, Alberta, Canada, 301 p.

Beaton, A., Langenberg, W. and Pană, C., 2006. Coalbed methane resources and reservoir characteristics from the Alberta Plains, Canada. International Journal of Coal Geology, v. 65, p. 93-113.

Bekele, E.B., Rostron, B.J., and Person, M.A., 2003. Fluid pressure implications of erosional unloading, basin hydrodynamics and glaciation in the Alberta Basin, Western Canada. Journal of Geochemical Exploration, v. 78-79, p. 143-147.

Benn, A.A., and B.J. Rostron, 1998. Regional hydrochemistry of Cambrian to Devonian aquifers in the Williston basin, Canada - U.S.A. *in* J. E. Christopher, C. F. Gilboy, D. F. Paterson, and S. L. Bend, eds., Eighth International Williston Basin Symposium: Special Publication, Saskatchewan Geological Society Special Publication No. 13, p. 238-246.

Block, D., 2001. Water resistivity atlas of western Canada CSPG (abs.): Rock the Foundation, abstracts of technical talks, posters, and core displays. Canadian Society of Petroleum Geologists Annual Convention, p. 359-369.

Bryant, E., 1997. *Climate Process and Change*. Cambridge University Press, Cambridge, UK.

Burrowes, O.G. and Krause, F.F., 1987. Overview of the Devonian System: subsurface of Western Canada Basin *In* Devonian Lithofacies and Reservoir Styles in Alberta. F.F. Krause and O.G. Burrowes (eds.). Second International Symposium on the Devonian System, Calgary, Alberta, Canada, p. 1-20.

Burton, J. and Walker, R.G., 1999. Linear transgressive shoreface sandbodies controlled by fluctuations of relative sea level: Lower Cretaceous Viking Formation in the Joffre-Mikawan-Fenn area, Alberta, Canada. SEPM Special Publication 64, p. 255-272.

Cant, D.J., 1996. Sedimentological and sequence stratigraphic organization of a foreland clastic wedge, Mannville Group, Western Canada Basin. Journal of Sedimentary Research, v. 66, p. 1137-1147.

Cant, D.J. and Abrahamson, B., 1996. Regional distribution and internal stratigraphy of the Lower Mannville. Bulletin of Canadian Petroleum Geology, v. 44, p. 508-529

Caplan, M.L. and Bustin, M.R., 1998. Sedimentology and sequence stratigraphy of Devonian-Carboniferous strata, southern Alberta. Bulletin of Canadian Petroleum Geology, v. 46, p. 487-514.

Chebotarev, I.I., 1955. Metamorphism of natural waters in the crust of weathering, 1. Geochemica et Cosmochimica Acta, v. 8, p. 22-48.

Connolly, C.A., Walter, L.M., Baadsgaard, H., and Longstaffe, F.J., 1990. Origin and evolution of formation waters, Alberta Basin, Western Canada Sedimentary Basin, I. Chemistry. Applied Geochemistry, v. 5, p. 375-395.

Corbet, T.F., and Bethke, C.M., 1992. Disequilibrium fluid pressures and groundwater flow in the Western Canada sedimentary basin. Journal of Geophysical Research, v. 19, p. 319-358.

Dagan, G., 1989. Flow and Transport in Porous Formations. Springer Verlag, New York, NY., 465 p.

Davies, P. B., 1987. Modeling areal, variable density, groundwater flow using equivalent freshwater head – analysis of potentially significant errors, in solving groundwater problems with models. Proceedings of the National Water Well Association, International Groundwater Modeling Center Conference, p. 888-903.

Davis, S.N., 1988. Where are the rest of the analyses? Groundwater, v. 26, p. 2-5.

Dawson, F.M., Evans, C.G., Marsh, R. and Hills, L.V., 1994. Uppermost Cretaceous and Tertiary strata of the Western Canada Sedimentary Basin. *In* Geological Atlas of the Western Canada Sedimentary Basin. G.D. Mossop and I. Shetsen (comps.). Calgary, Canadian Society of Petroleum Geologists and Alberta Research Council, p. 387-406.

Desbarats, A.J. and Bachu, S., 1994. Geostatistical analysis of aquifer heterogeneity from the core scale to the basin scale. Water Resources Research, v. 30, p. 673-684.

Earlougher, R.C., 1977. Advances in well test analysis. Society of Petroleum Engineers Monograph, v. 5, 264 p.

Eberth, D.A., 1996. Origin and significance of mud-filled incised valleys (Upper Cretaceous) in southern Alberta, Canada. Sedimentology, v. 43, p. 459-477.

Freeze, R.A., and Cherry, J.A., 1979. Groundwater. New Jersey, Prentice-Hall, 604 p.

Glombick, P., 2010. Subsurface stratigraphic picks of the top of the Belly River Group, Alberta Plains.Energy Resources Conservation Board, ERCB/AGS DIG 2010-0022, URL <http://www.ags.gov.ab.ca/publications/abstracts/DIG_2010_0022.html> [accessed May 2011].

Halbertsman, H.L. and Meijer-Drees, N.C., 1987. Wabamun limestone sequence in north-central Alberta. *In* Devonian Lithofacies and Reservoir Styles in Alberta. F.F. Krause and O.G. Burrowes (eds.). Second International Symposium on the Devonian System, Calgary, Alberta, Canada, p. 21-38.

Hamblin, A.P., 1997. Regional distribution and dispersal of the Dinosaur Park Formation, Belly River Group, surface and subsurface of southern Alberta. Bulletin of Canadian Petroleum Geology, v. 45, p. 377-399.

Hanor, J.S., 1994. Origin of saline fluids in sedimentary basins. *in*: J. Parnell, ed., Geofluids: Origin, Migration and Evolution of Fluids in Sedimentary Basins, p. 151-174.

Hayes, B.J.R., Christopher, J.E., Rosenthal, L., Los, G., McKercher, B., Minken, D., Tremblay, Y.M. and Fennel, J., 1994. Cretaceous Mannville Group of the Western Canada Sedimentary Basin. *In* Geological Atlas of the Western Canada Sedimentary Basin. G.D. Mossop and I. Shetsen (comps.). Calgary, Canadian Society of Petroleum Geologists and Alberta Research Council, p. 317-334.

Hearn, M.R., Machel, H.G. and Rostron, B.J., 2011. Hydrocarbon breaching of a regional aquitard: The Devonian Ireton Formation, Bashaw area, Alberta, Canada. Bulletin of the American Association of Petroleum Geologists, v. 95, p. 1009-1037.

Hitchon, B., 1969a. Fluid flow in the Western Canada Sedimentary Basin, Effect of topography. Water Resources Research, v. 5, p. 186-195.

Hitchon, B., 1969b. Fluid flow in the Western Canada Sedimentary Basin, Effect of geology. Water Resources Research, v. 5, p. 460-469.

Hitchon, B., 1996. Rapid evaluation of the hydrochemistry of a sedimentary basin using only 'standard' formation water analyses: Example from the Canadian portion of the Williston Basin. Applied Geochemistry, v. 11, p. 789-795.

Hitchon, B., and Brulotte, M., 1994. Culling criteria for "standard" formation water analyses. Applied Geochemistry, v. 9, p. 637-645.

Horner, D.R., 1951. Pressure build-up in wells. Proceeding Third World Petroleum Congress, Section 2, p.503-521.

Hubbard, S.M., Pemberton, S.G. and Howard, E.A., 1999. Regional geology and sedimentology of the basal Cretaceous Peace River Oil Sands deposit, north-central Alberta. Bulletin of Canadian Petroleum Geology, v.47, p.270-297.

IEA (International Energy Agency), 2004. *Prospects for CO_2 Capture and Storage*. IEA/OECD, Paris, France.

IEA (International Energy Agency), 2010.*Energy Technology Perspectives: Scenarios and Strategies to 2050*. IEA/OECD, Paris, France.

IPCC (Intergovernmental Panel on Climate Change), 2005. *Special Report on Carbon Dioxide Capture and Storage*. Cambridge University Press, Cambridge, UK, and New York, NY, USA.

IPCC (Intergovernmental Panel on Climate Change), 2007. *Climate Change 2007: The Physical Science Basis. Fourth Assessment Report*, IPCC Secretariat, Geneva, Switzerland.

Karvonen, R.L. and Pemberton, S.G., 1997. Sedimentology, ichnology and stratigraphy of the Ostracode Member (Lower Cretaceous) in the Jenner-Suffield area, southeast Alberta. *In* Petroleum Geology of the Cretaceous Mannville Group, Western Canada. S.G. Pemberton and D.P. James (eds.). Canadian Society of Petroleum Geologists, Memoir 18, p. 103-123.

Khan, D.K., 2006. Hydrogeological characterization of the Weyburn CO_2 project area and Gradient-free inverse conditioning of heterogeneous aquifer models to hydraulic head data. Unpublished Ph.D. Dissertation, Department of Earth and Atmospheric Sciences, University of Alberta, Alberta, Canada, 238 p.

Langmuir, D., 1997. Aqueous Environmental Geochemistry. New Jersey, Prentice-Hall, 600 p.

Leckie, D.A., Battacharya, J.P., Bloch, J., Gilboy, C.F. and Norris, B., 1994. Cretaceous Colorado/Alberta Group of the Western Canada Sedimentary Basin. *In* Geological Atlas of the Western Canada Sedimentary Basin. G.D. Mossop and I. Shetsen (comps.). Calgary, Canadian Society of Petroleum Geologists and Alberta Research Council, p. 335-352

Lemieux, J.-M., Sudicky, E.A., Peltier, W.R., and Tarasov, L., 2008. Simulating the impact of glaciations on continental groundwater flow systems: 2. Model application to the Wisconsinian glaciation over the Canadian landscape. Journal of Geophysical Research, v. 113, F03018, doi:10.1029/2007JF000929.

MacEachern, J.A., Zaitlin, B.A. and Pemberton, S.G., 1999. A sharp-based sandstone of the Viking Formation, Joffre Field, Alberta, Canada: criteria for recognition of transgressively incised shoreface complexes. Journal of Sedimentary Research, v. 69, p. 876-892.

Masters, J.A., 1979. Deep basin gas trap, western Canada. American Association of Petroleum Geologists Bulletin, v. 63, p.152-181

Masters, J.A., 1984. Elmworth - Case study of a deep basin gas field. American Association of Petroleum Geologists Memoir 38, 316 p.

McLean, J.R. and Wall, J.H., 1981. The Early Cretaceous Moosebar Sea in Alberta. Bulletin of Canadian Petroleum Geology, v. 29, p.334-377.

Melnik, A., and Rostron, B.J., 2011. Hydrogeology of the Cretaceous Sedimentary Succession in the Clive Field in Central Alberta. Confidential client report to AITF, University of Alberta, Edmonton, 49 p.

Palombi, D.D., 2008. Hydrogeological characterization of the Williston Basin in Eastern Saskatchewan and Western Manitoba. Unpublished M.Sc. Dissertation, Department of Earth and Atmospheric Sciences, University of Alberta, Alberta, Canada, 196 p.

Parks, K.P., and Tóth, J., 1995. Field evidence for erosion-induced underpressuring in Upper Cretaceous and Tertiary strata, west central Alberta, Canada. Bulletin of Canadian Petroleum Geology, v. 43. p. 281-292.

Parks, K. and Andriashek, L. 2009. Preliminary investigation of potential, natural hydraulic pathways between the Scollard and Paskapoo formations in Alberta: Implications for coalbed methane production. Energy Resources Conservation Board and the Alberta Geological Survey. ERCB/AGS Open File Report 2009 – 16.

Power, B.A. and Walker, R.G., 1996. Allostratigraphy of the Upper Cretaceous Lea Park – Belly River transition in central Alberta, Canada. Bulletin of Canadian Petroleum Geology, v. 44, p. 14-38.

Price, R.A., 1994. Cordilleran tectonics and the evolution of the Western Canada Sedimentary Basin. In Geological Atlas of the Western Canada Sedimentary Basin. G.D. Mossop and I. Shetsen (comps.). Calgary, Canadian Society of Petroleum Geologists and Alberta Research Council, p. 13-24.

Reinson, G.E., Warters, W.J., Cox, J. and Price, P.R., 1994. Cretaceous Viking Formation of the Western Canada Sedimentary Basin. *In* Geological Atlas of the Western Canada Sedimentary Basin. G.D. Mossop and I. Shetsen (comps.). Calgary, Canadian Society of Petroleum Geologists and Alberta Research Council, p. 353-364.

Roca, X., Rylaarsdam, J.R., Zhang, H., Varban, B.L., Sisulak, C.F., Bastedo, K. and Plint, A.G., 2008. An allostratigraphic correlation of Lower Colorado Group (Albian) and equivalent strata in Alberta and British Columbia, and Cenomanian rocks of the Upper Colorado Group in southern Alberta. Bulletin of Canadian Petroleum Geology, v. 56, p. 259-299.

Rostron, B.J., 1994. A new method for culling pressure data used in hydrodynamic studies. American Association of Petroleum Geologists Annual Meeting Abstracts - American Association of Petroleum Geologists and Society of Economic Palaeontologists and Mineralogists, p. 247.

Rostron, B.J., 1995. Cross-formation fluid flow in the Upper Devonian to Lower Cretaceous strata, west-central Alberta, Canada, Unpublished Ph.D. Dissertation, Department of Earth and Atmospheric Sciences, University of Alberta, Alberta, Canada, 226 p.

Rostron, B.J., and Tóth, J., 1997. Cross-formational fluid flow and the generation of a saline plume of formation waters in the Mannville Group, central Alberta. *in:* S.G. Pemberton and D.P. James, eds., Petroleum Geology of the Cretaceous Mannville Group, Western Canada, Canadian Society of Petroleum Geologists Memoir 18, p. 169-190.

Rostron, B.J., Tóth, J., and Machel, H.G., 1997. Fluid flow, hydrochemistry, and petroleum entrapment in Devonian reef complexes, south-central Alberta, Canada. *in:* I.P. Montanez, J.M. Gregg and K.L. Shelton, eds., Basin-Wide Diagenetic Patterns: Integrated Petrologic, Geochemical, and Hydrologic Considerations, SEPM Special Publication 57**,** p. 139-155.

Savoy, L.E. and Mountjoy, E.W., 1995. Cratonic-margin and Antler-age foreland basin strata (Middle Devonian to Lower Carboniferous) of the southern Canadian Rocky Mountains and adjacent plains. *In* Stratigraphic Evolution of Foreland Basins. S.L. Dorobek and G.M. Ross (eds.). SEPM Special Publication 52, p. 213-231.

Schröder-Adams, C.J., Leckie, D.A., Bloch, J., Craig, J., McIntyre, D.J. and Adams, P.J., 1996. Paleoenvironmental changes in the Cretaceous (Albian to Turonian) Colorado Group of Western Canada: microfossil, sedimentological and geochemical evidence. Cretaceous Research, v. 17, p. 311-365.

Simpson, F., 1997. Colorado Group. *In* Lexicon of Canadian Stratigraphy Volume 4: Western Canada, Including Eastern British Columbia, Alberta, Saskatchewan and Southern Manitoba. D. Glass (ed.). Canadian Society of Petroleum Geologists, Calgary, Alberta, Canada

Smith, D.G., 1994. Paleogeographic evolution of the Western Canada Foreland Basin. *In* Geological Atlas of the Western Canada Sedimentary Basin. G.D. Mossop and I. Shetsen (comps.). Calgary, Canadian Society of Petroleum Geologists and Alberta Research Council, p. 277-296.

Stoakes, F.A., 1980. Nature and control of shale basin fill and its effect on reef growth and termination: Upper Devonian Duvernay and Ireton formations of Alberta, Canada. Bulletin of Canadian Petroleum Geology, v. 28, p. 345-410.

Stoakes, F.A., 1992. Woodbend Megasequence. *In* Devonian-Early Mississippian Carbonates of the Western Canada Sedimentary Basin: A Sequence Stratigraphic Framework. J. Wendte, F.A. Stoakes and C.V. Campbell (authors). SEPM Short Course No. 28, Calgary, Alberta, Canada.

Tokarsky, O., 1987. Hydrogeologic cross-section O-O', Red Deer 83A. Alberta Environment.

Tóth, J., 1978. Gravity-induced cross-formational flow of formation fluids, Red Earth region, Alberta, Canada: Analysis, patterns, evolution. Water Resources Research, v. 14, p. 805-843.

Tóth, J., 1984. The role of gravity flow in the chemical and thermal evolution of ground water. *in:* B. Hitchon and E.I. Wallick, (eds.), First Canadian/American Conference on Hydrogeology; Practical Applications of Groundwater Geochemistry, National Water Well Association, Banff, Alberta, Canada, p. 3-39.

Tóth, J. and Corbet, T.F., 1986. Post-Paleocene evolution of regional groundwater flow-systems and their relation to petroleum accumulations, Taber area, southern Alberta, Canada. Bulletin of Canadian Petroleum Geology, v. 34, p. 339-363.

Tóth, J., 1995. Hydraulic continuity in large sedimentary basins. Hydrogeology Journal, v. 3, p. 4-16.

Watts, N.R., 1987. Carbonate sedimentology and depositional history of the Nisku Formation (within the Western Canada Sedimentary Basin) in South Central Alberta. *In* Devonian Lithofacies and Reservoir Styles in Alberta. F.F. Krause and O.G. Burrowes (eds.). Second International Symposium on the Devonian System, Calgary, Alberta, Canada, p. 87-152.

Wynne, D.A. and Beaton, A.P., 2003. Coal Database for the Alberta Plains Area. Energy Resources Conservation Board, ERCB/AGS DIG 2003-0001, URL <http://www.ags.gov.ab.ca/publications/abstracts/DIG_2003_0001.html> [accessed May 2011]

8. APPENDIX A – Geological Structure and Isopach Maps

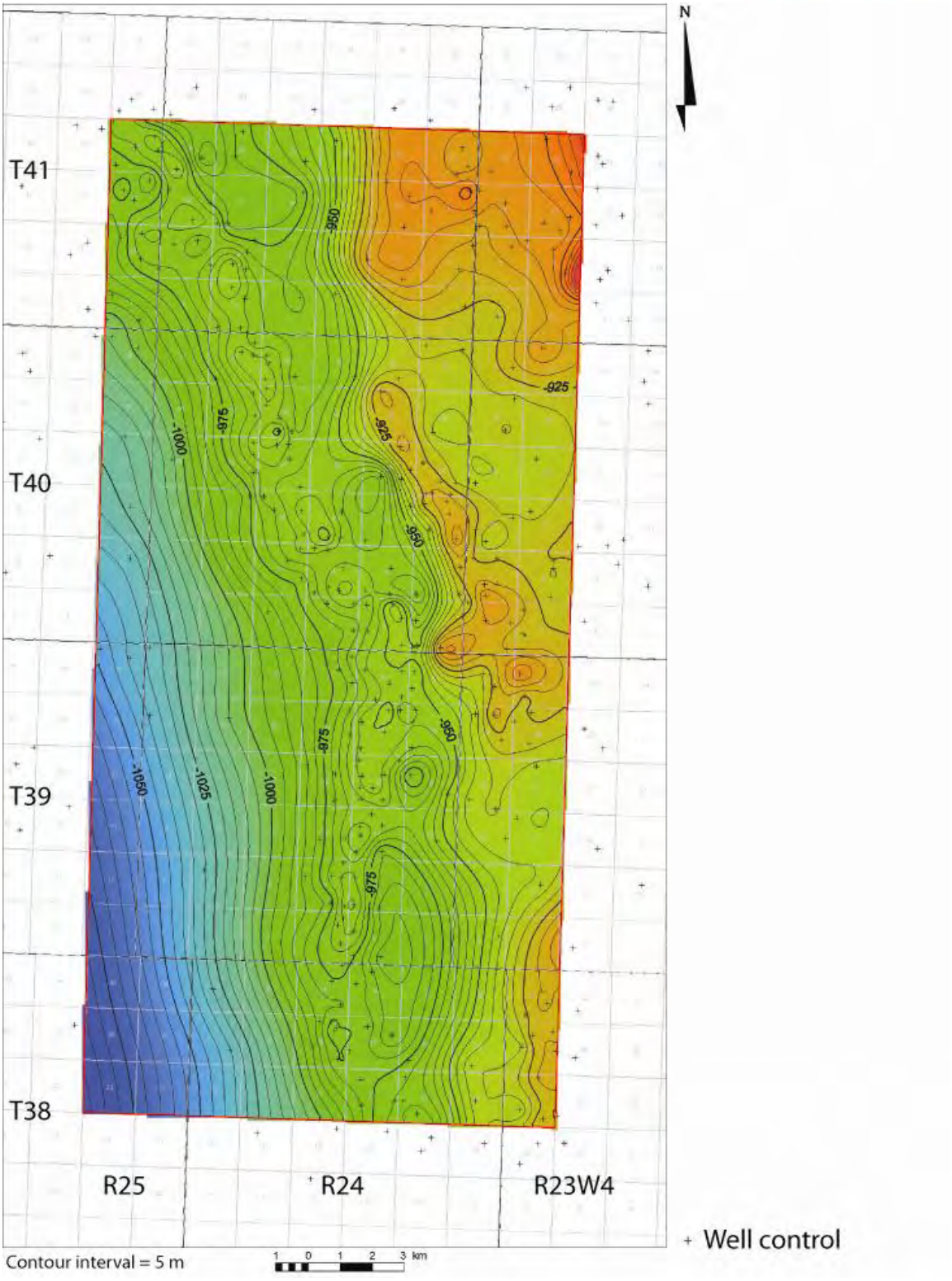

Figure A.1: Structural elevation of the top of the Nisku Formation in the Enhance Clive study area.

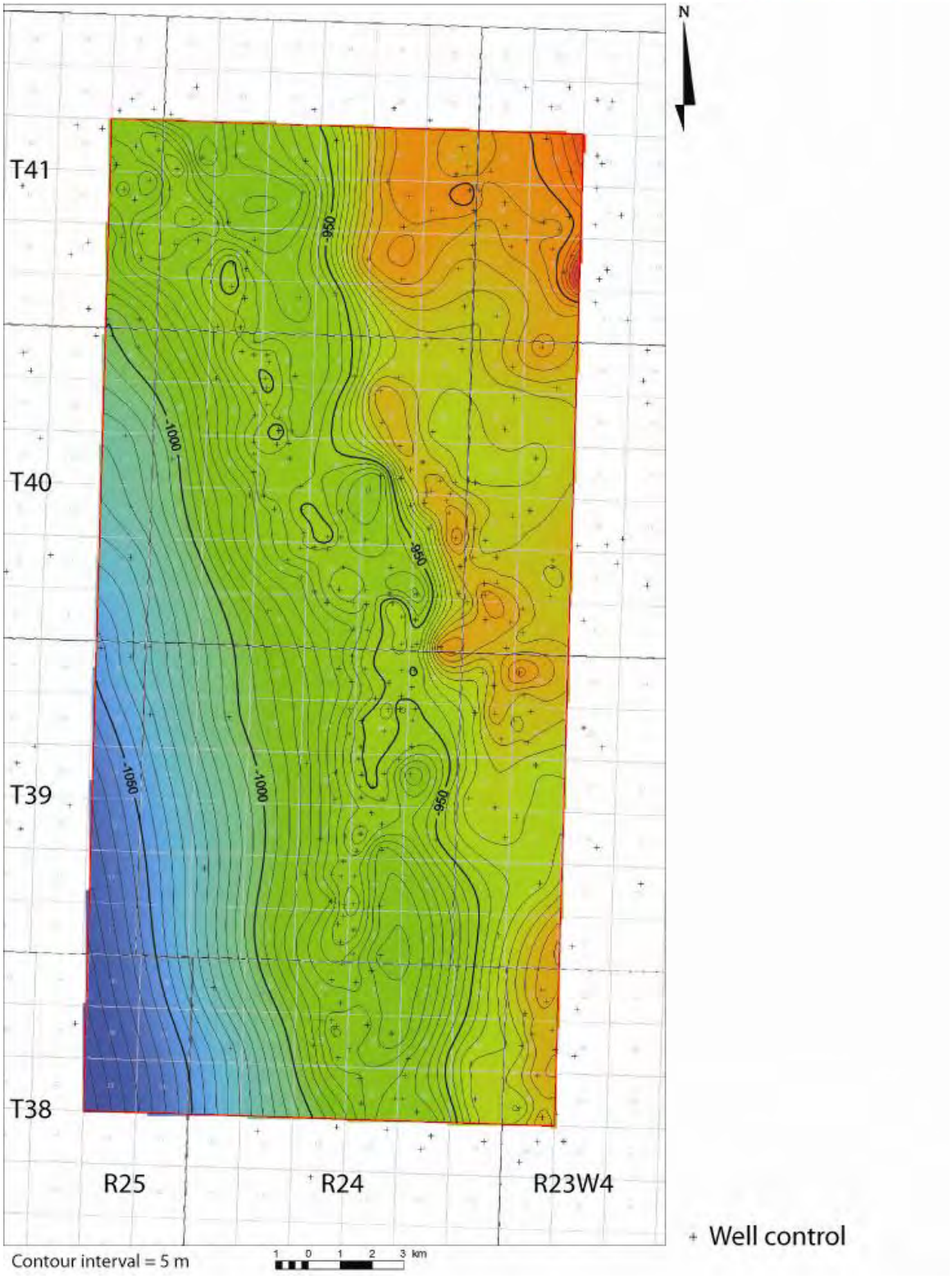

Figure A.2: Structural elevation of the top of the Calmar Formation in the Enhance Clive study area.

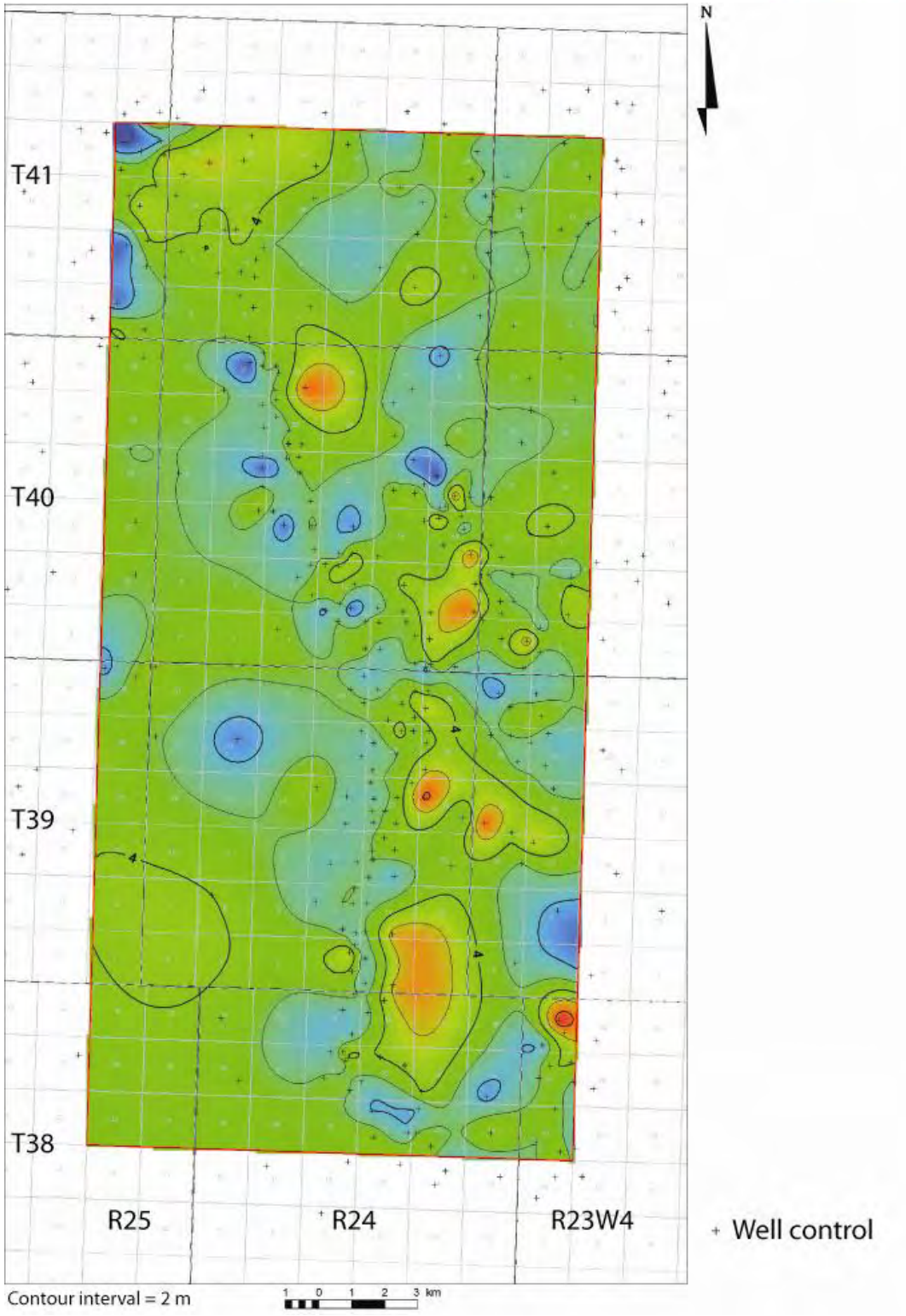

Figure A.3: Isopach of the Calmar Formation in the Enhance Clive study area.

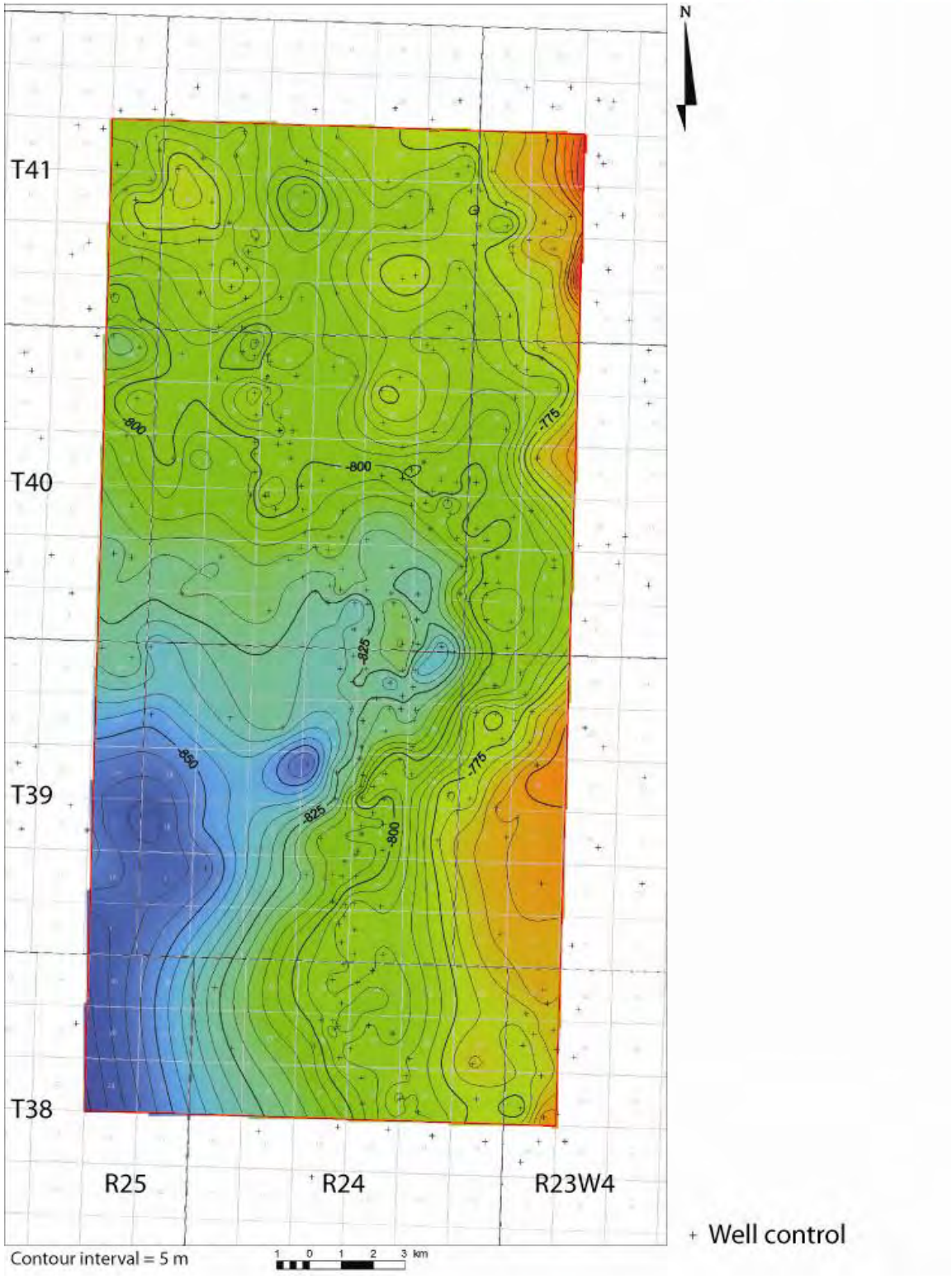

Figure A.4: Structural elevation of the top of the Stettler Formation in the Enhance Clive study area.

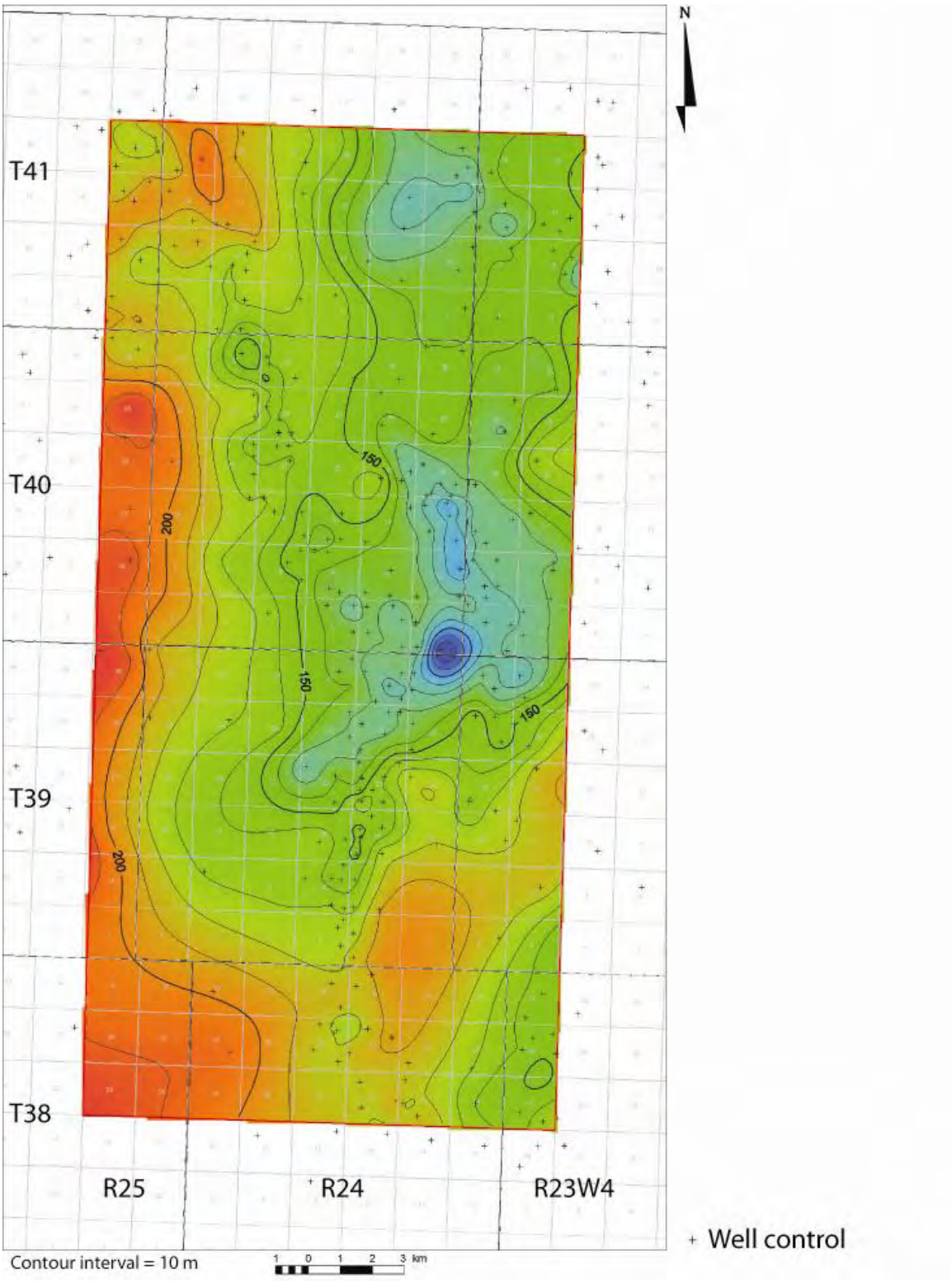

Figure A.5: Isopach of the Stettler Formation in the Enhance Clive study area.

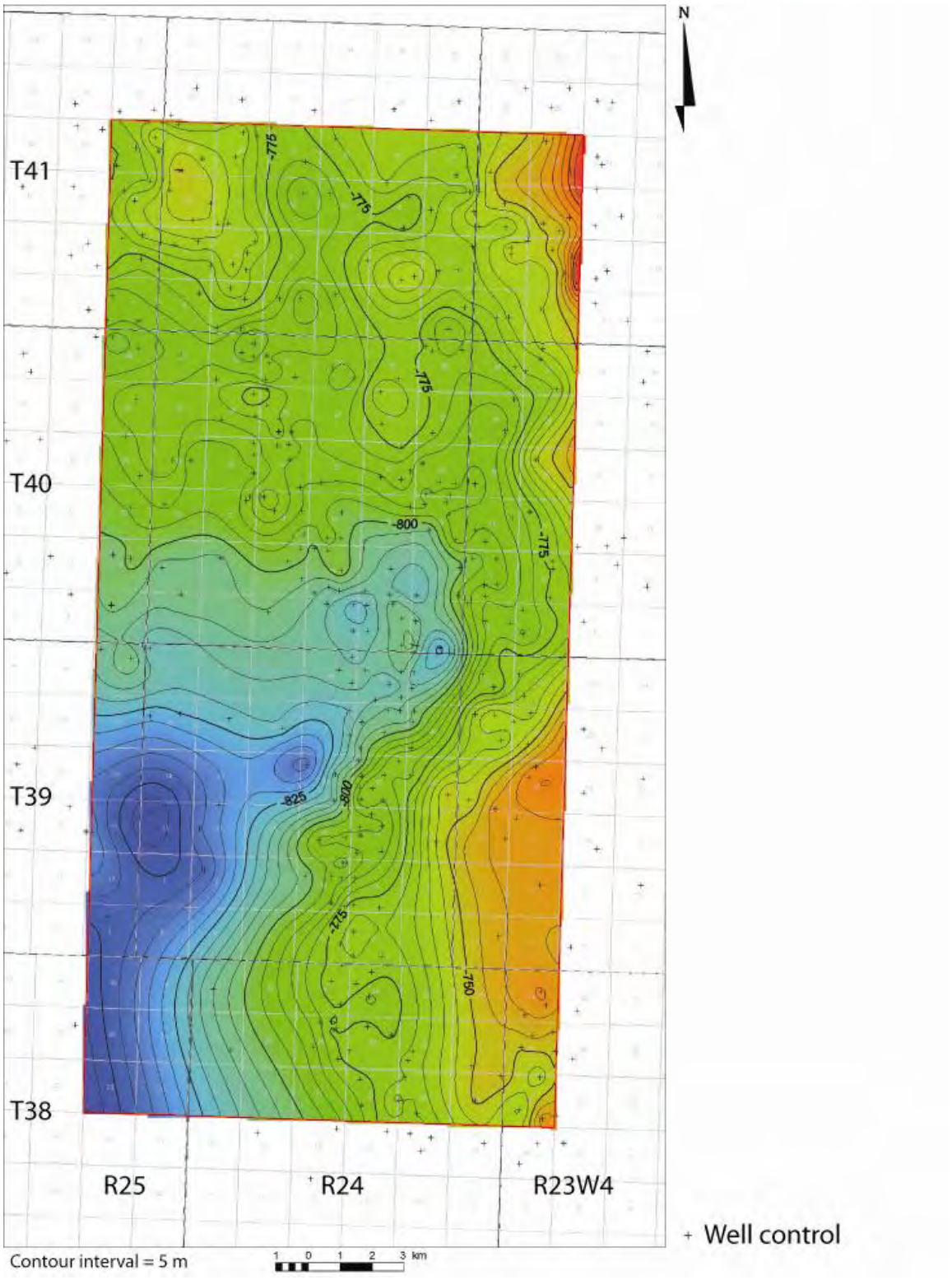

Figure A.6: Structural Elevation of the top of the Big Valley Formation in the Enhance Clive study area.

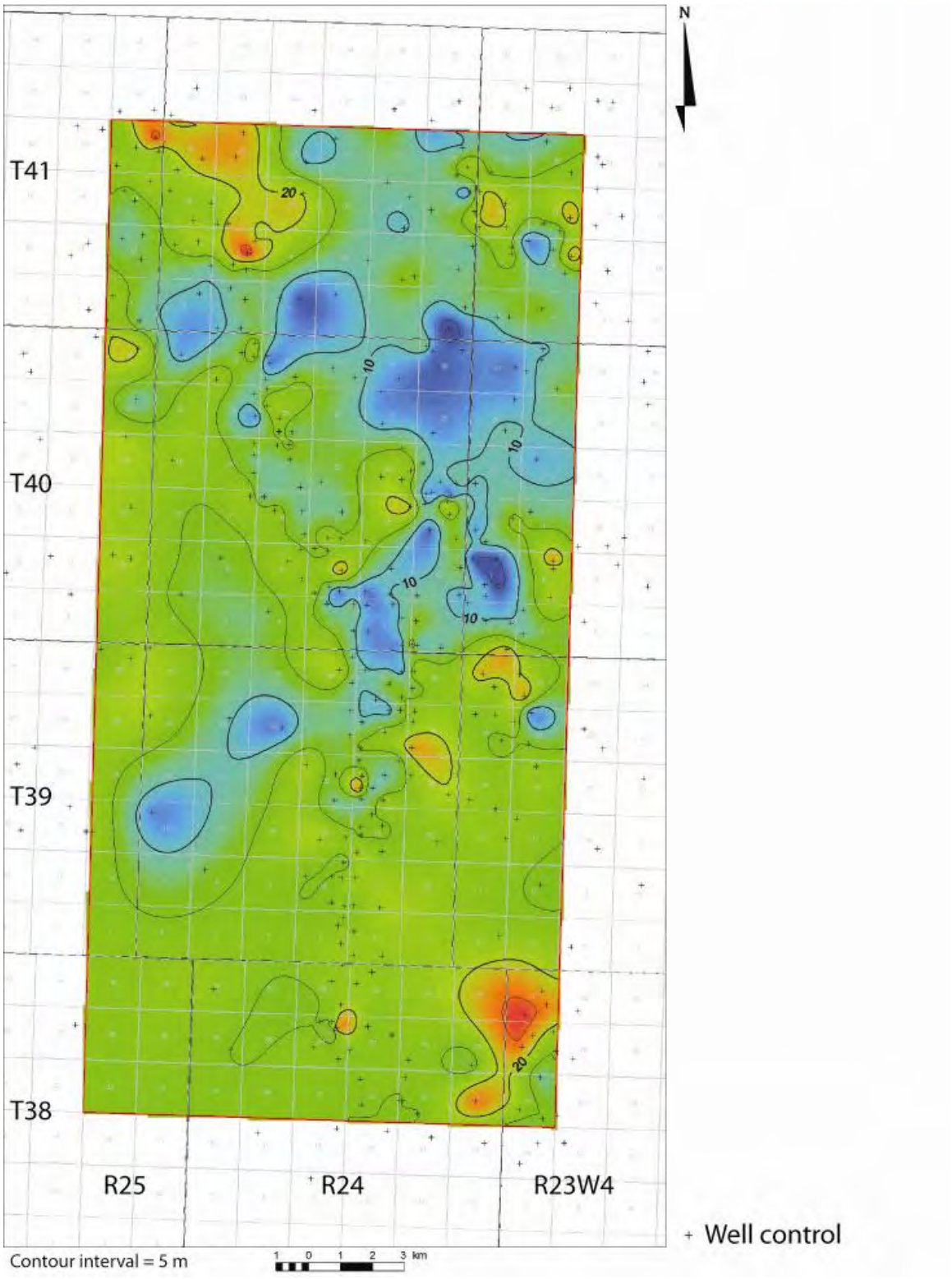

Figure A.7: Isopach of the Big Valley Formation in the Enhance Clive study area.

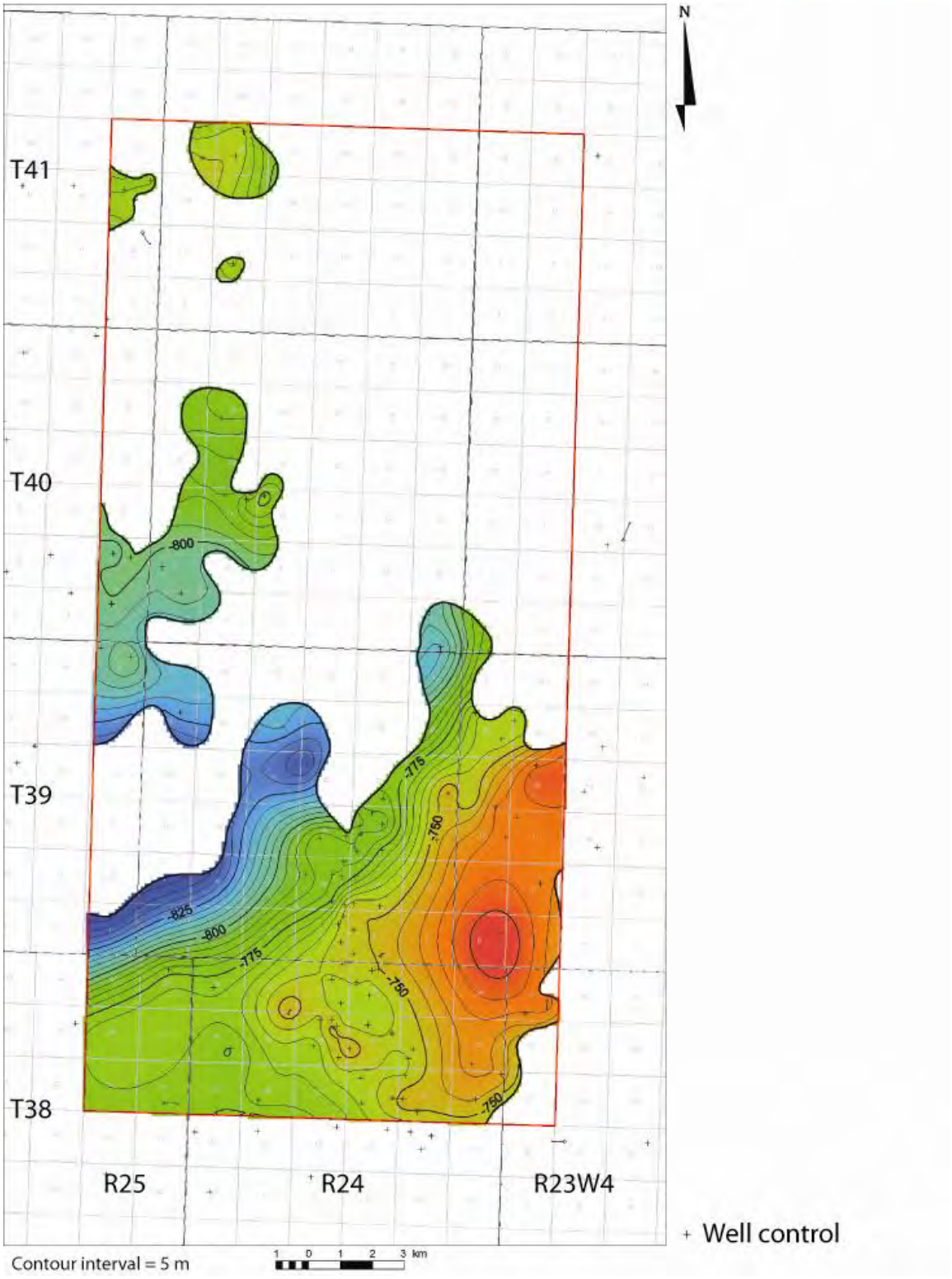

Figure A.8: Structural elevation of the Mississippian Exshaw and Banff formations in the Enhance Clive study area.

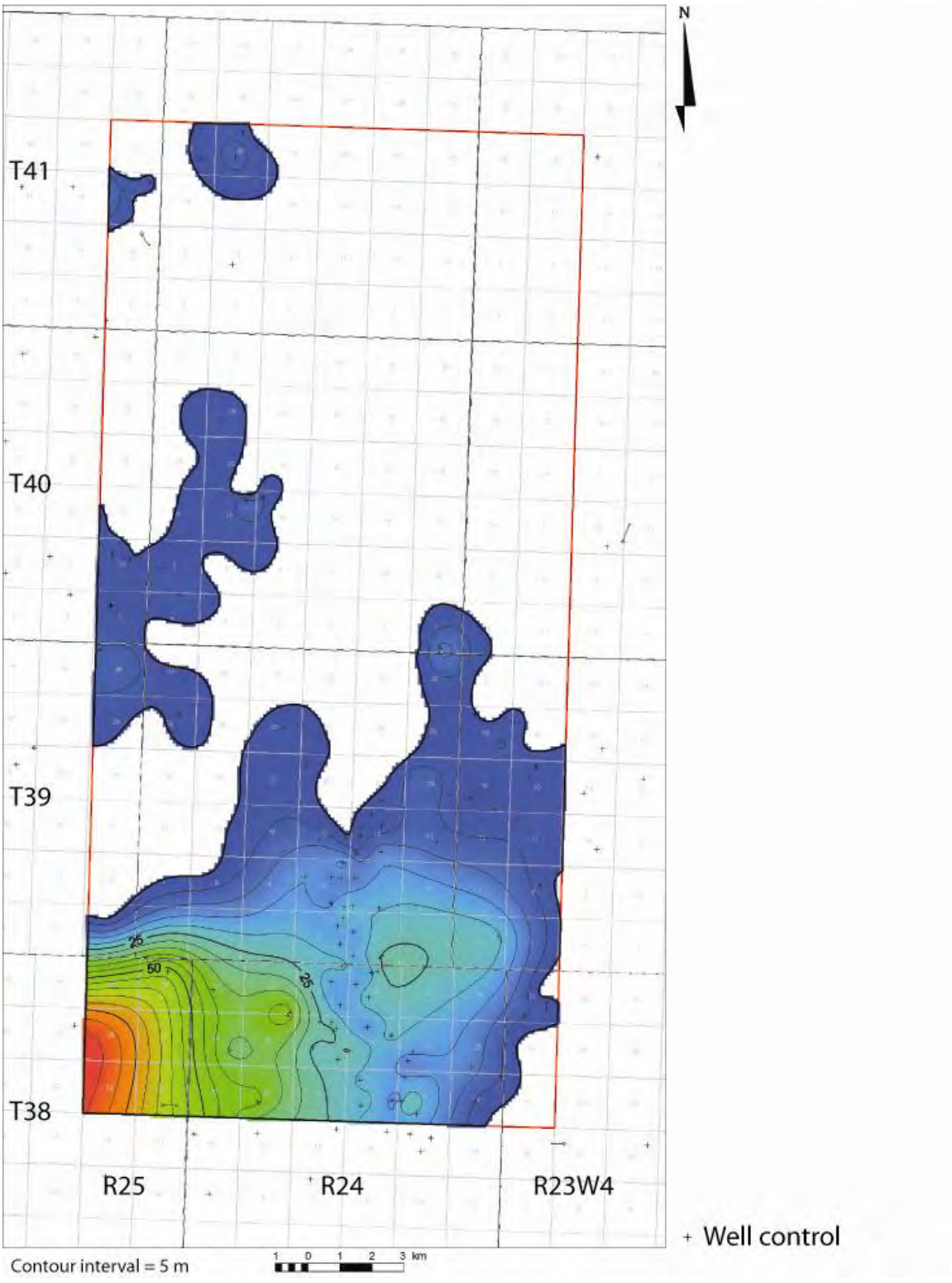

Figure A.9: Isopach of the Mississippian Exshaw and Banff formations in the Enhance Clive study area.

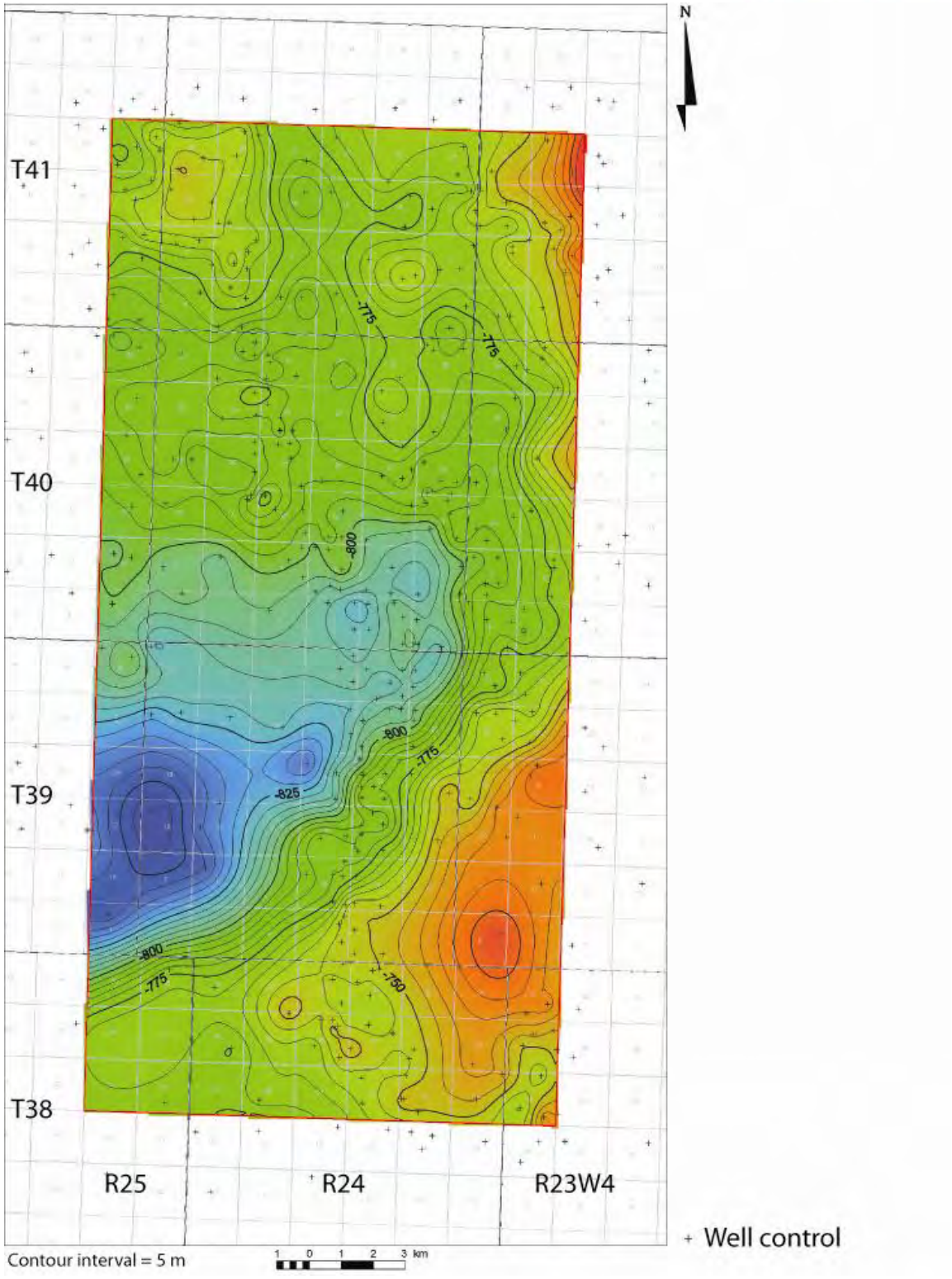

Figure A.10: Structural elevation at the sub-Cretaceous unconformity in the Enhance Clive study area.

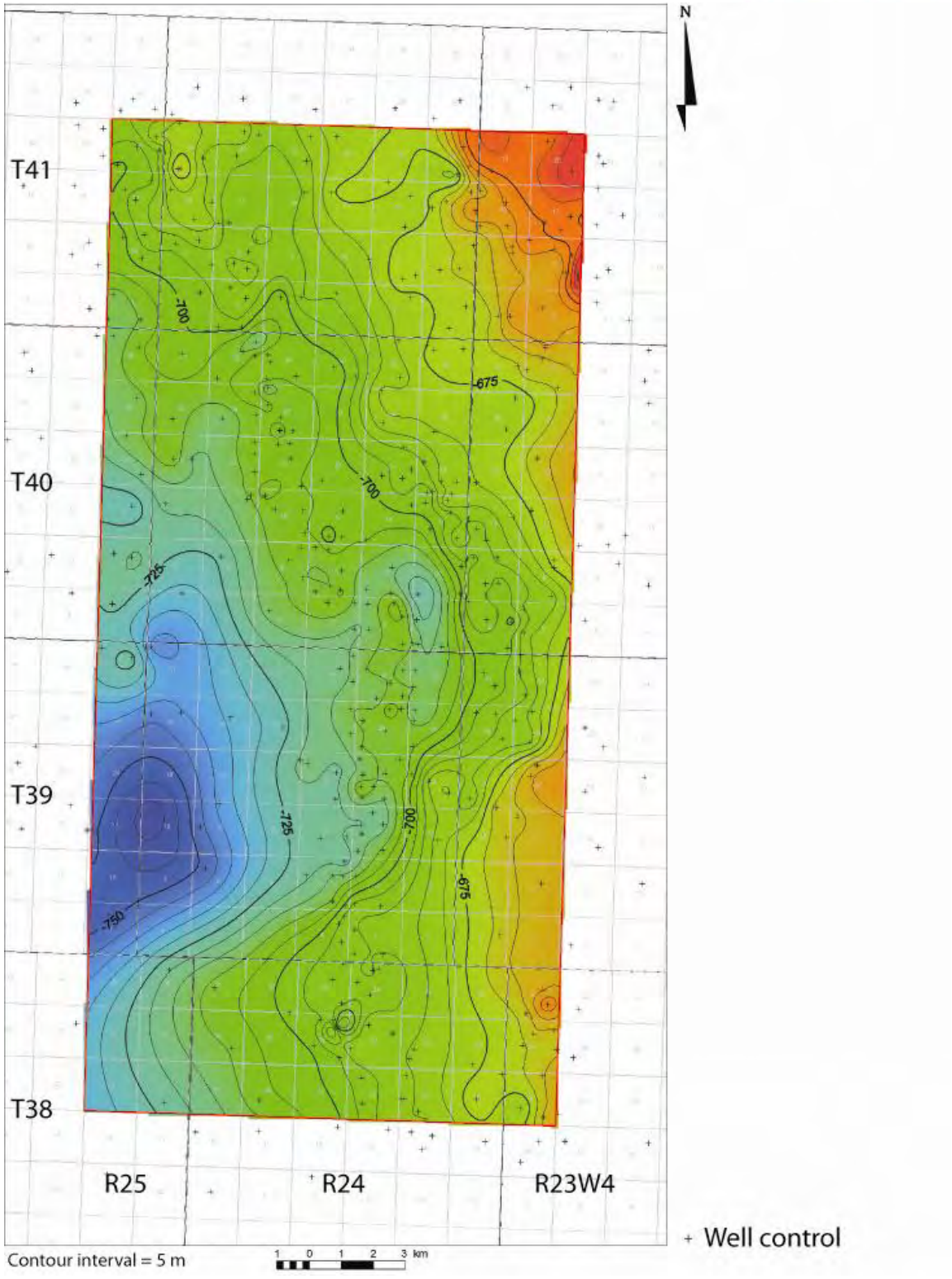

Figure A.11: Structural elevation of the top of the Ellerslie Formation in the Enhance Clive study area.

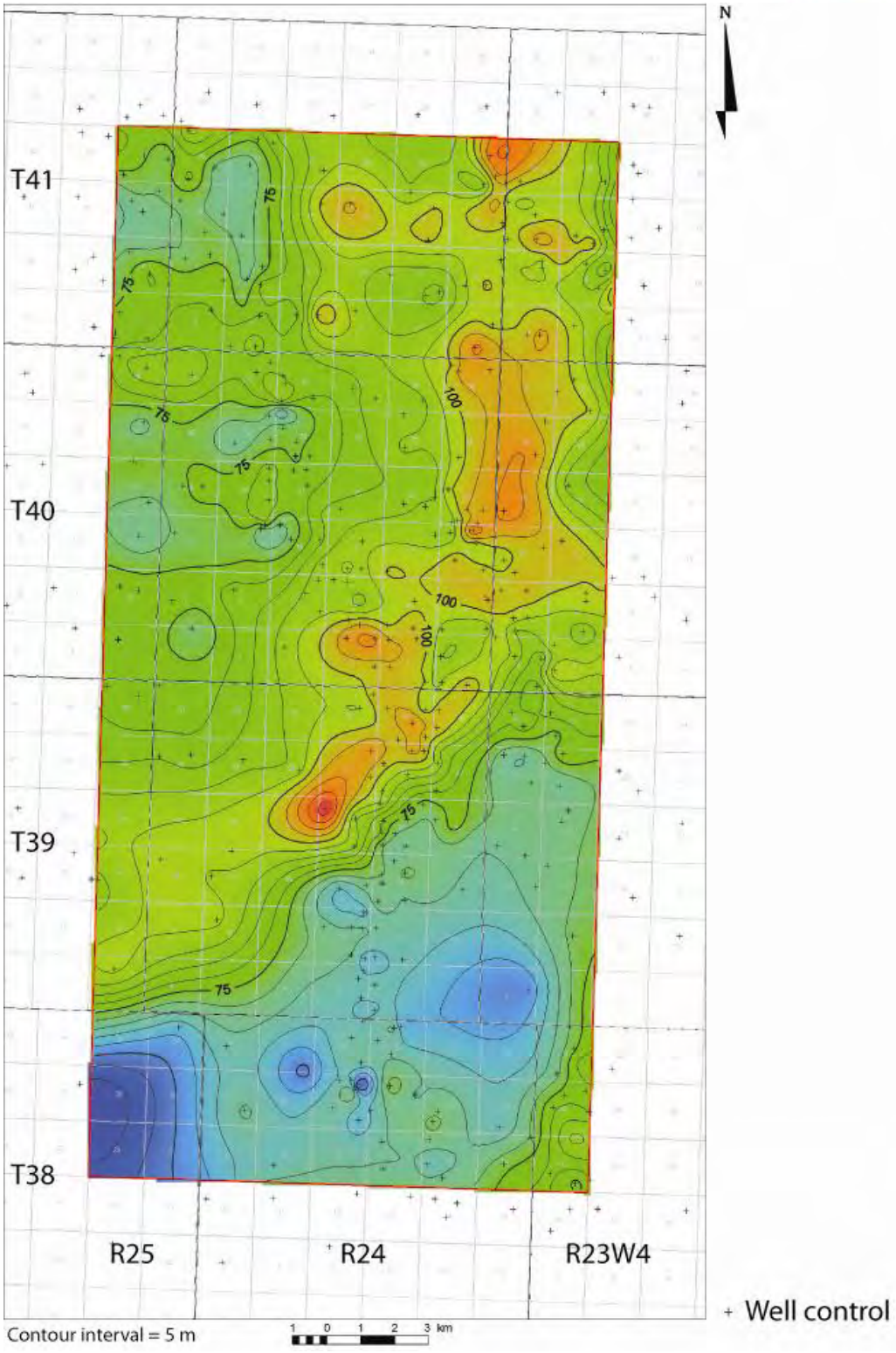

Figure A.12: Isopach of the Ellerslie Formation in the Enhance Clive study area.

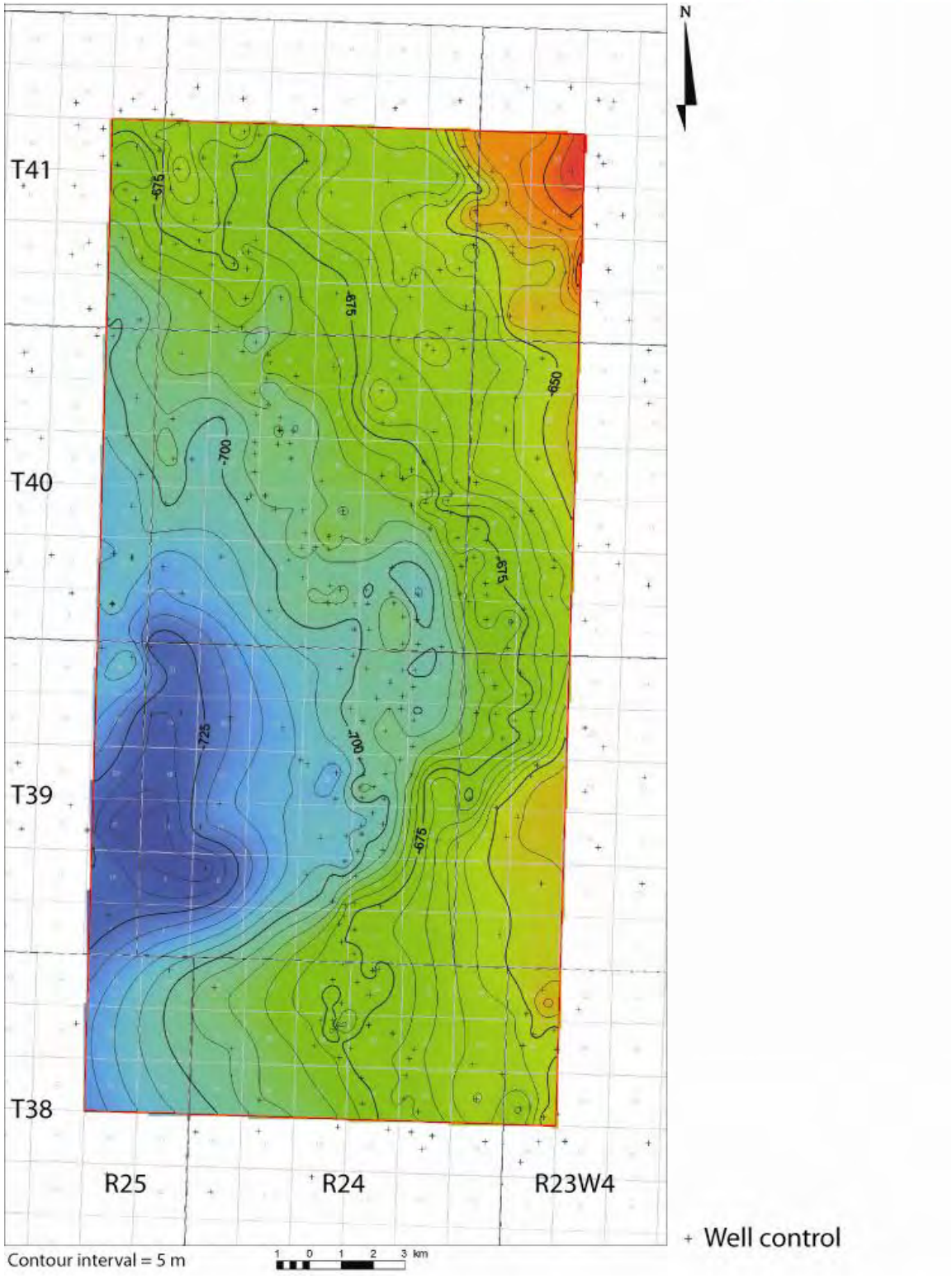

Figure A.13: Structural elevation of the top of Ostracod Formation in the Enhance Clive study area.

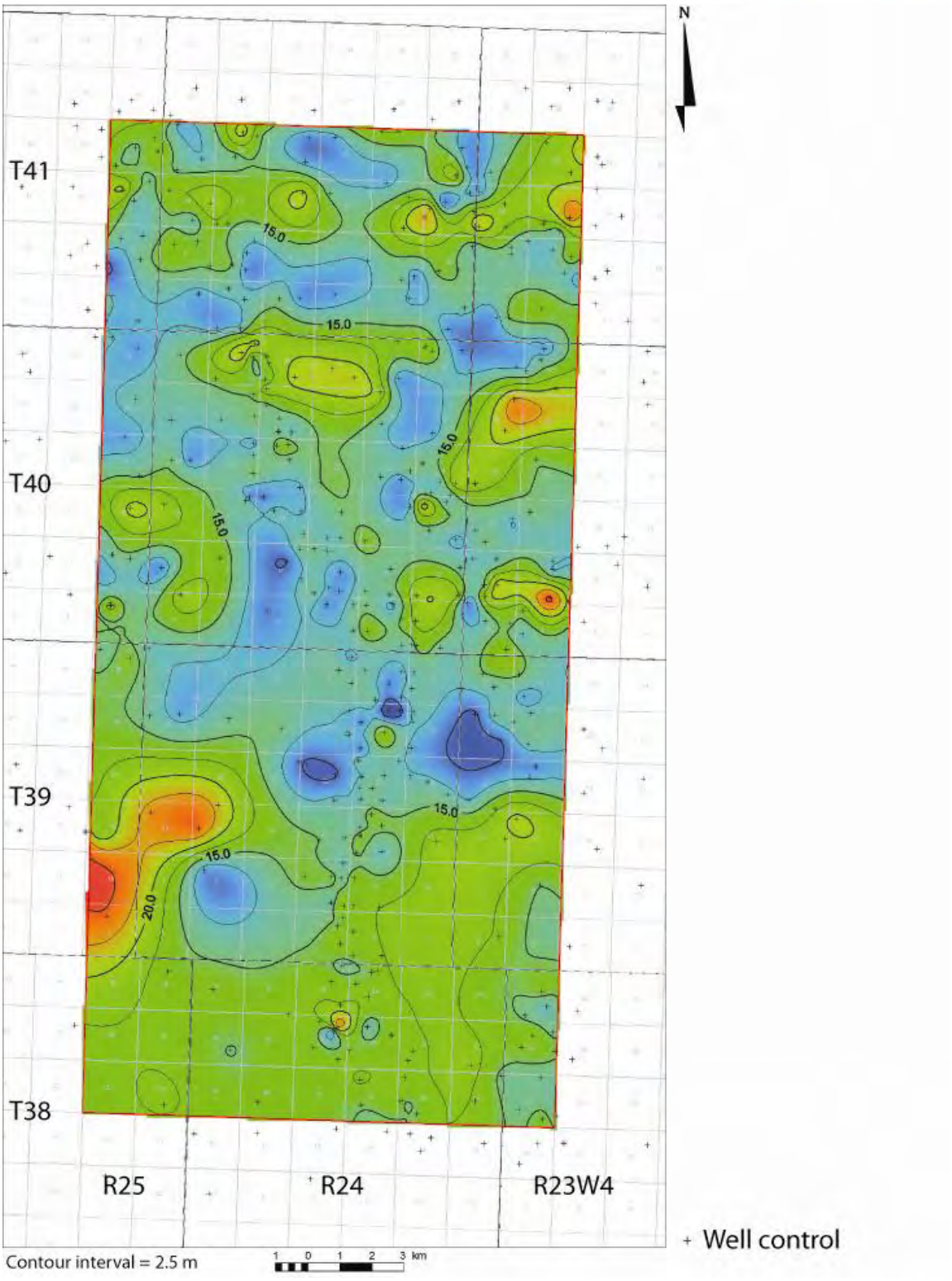

Figure A.14: Isopach of the Ostracod Formation in the Enhance Clive study area.

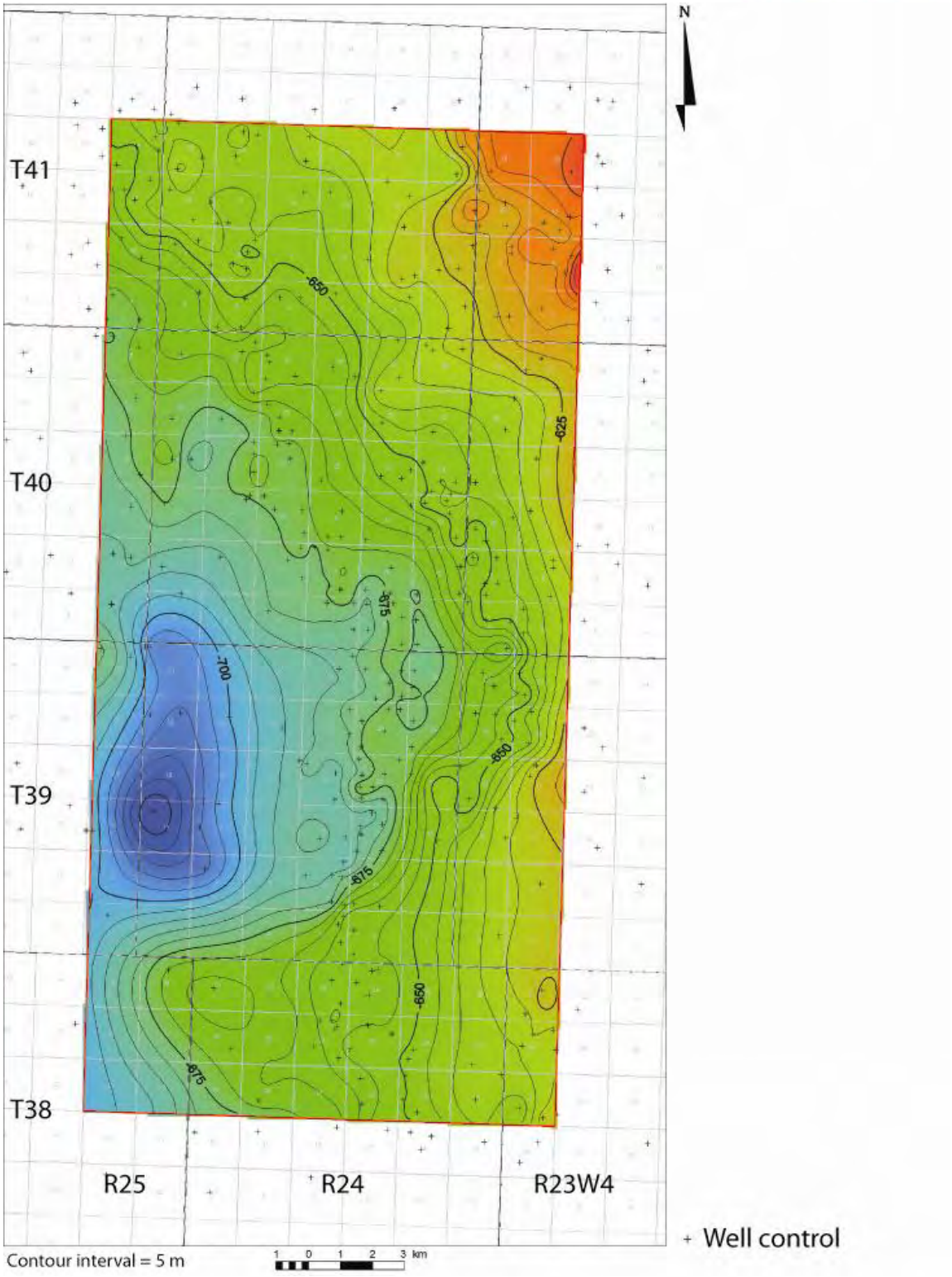

Figure A.15: Structural elevation of the top of the Glauconitic Sandstone Formation in the Enhance Clive study area.

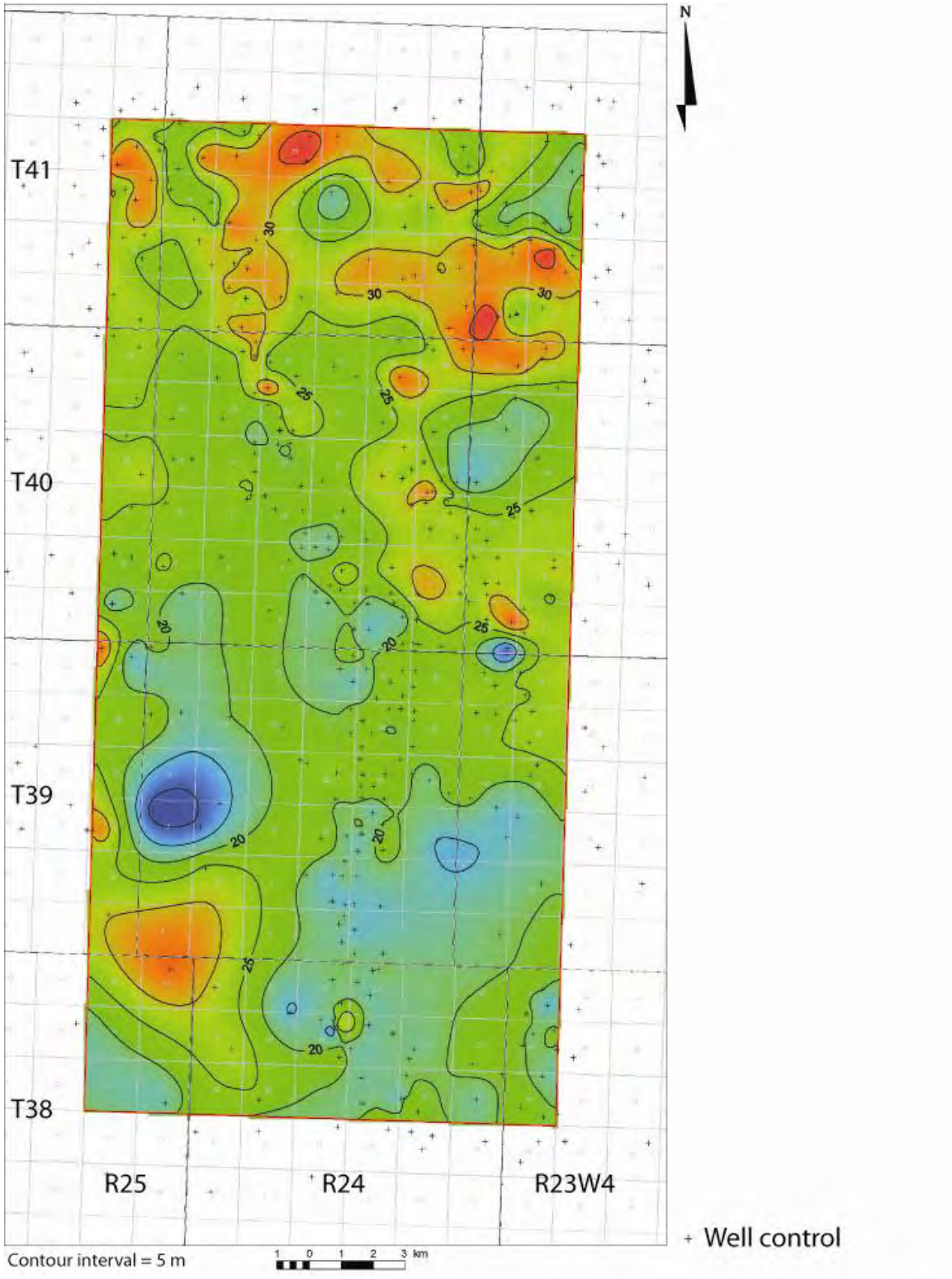

Figure A.16: Isopach of the Glauconitic Sandstone Formation in the Enhance Clive study area.

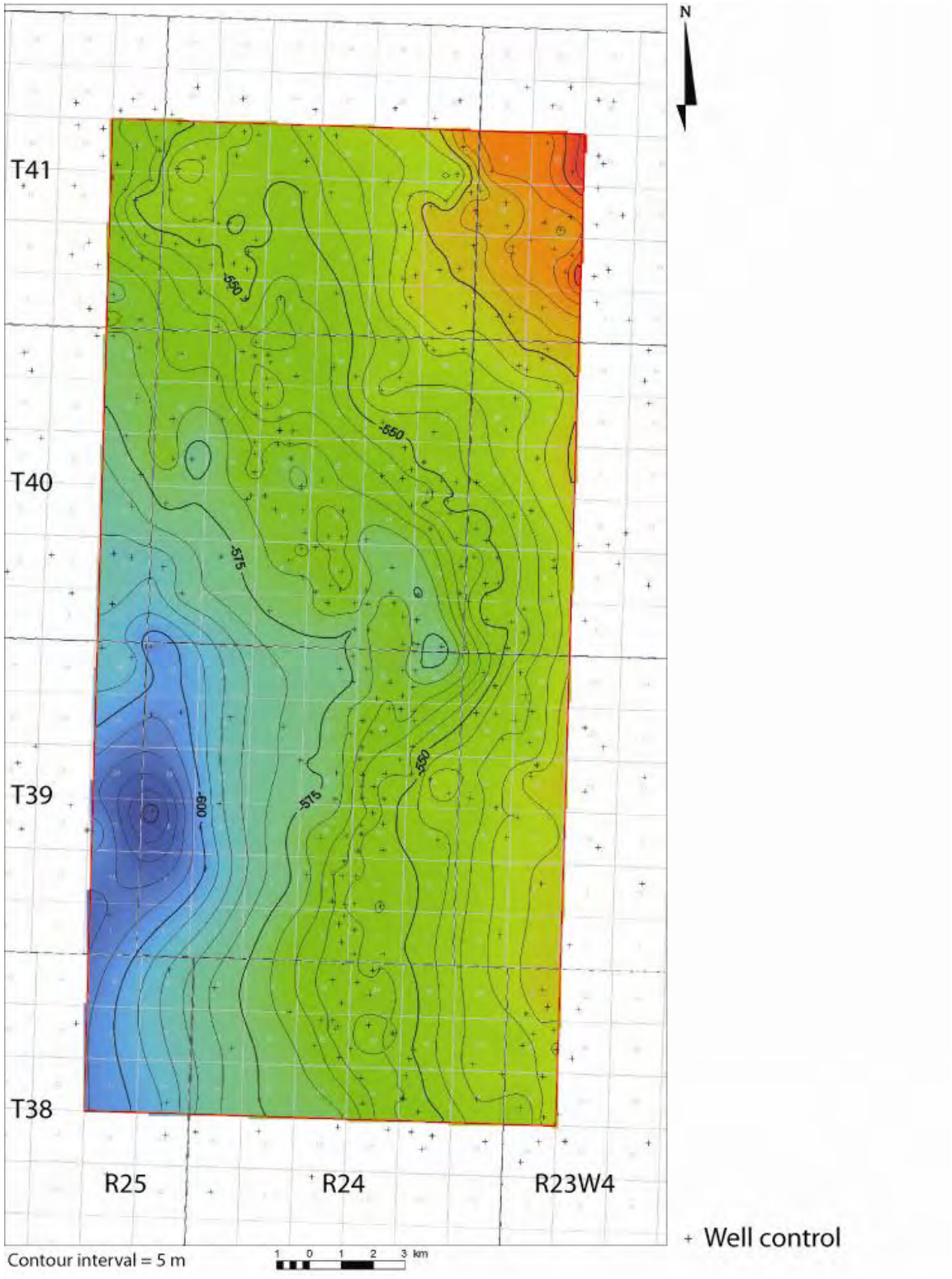

Figure A.17: Structural elevation of the top of the Upper Mannville unit in the Enhance Clive study area.

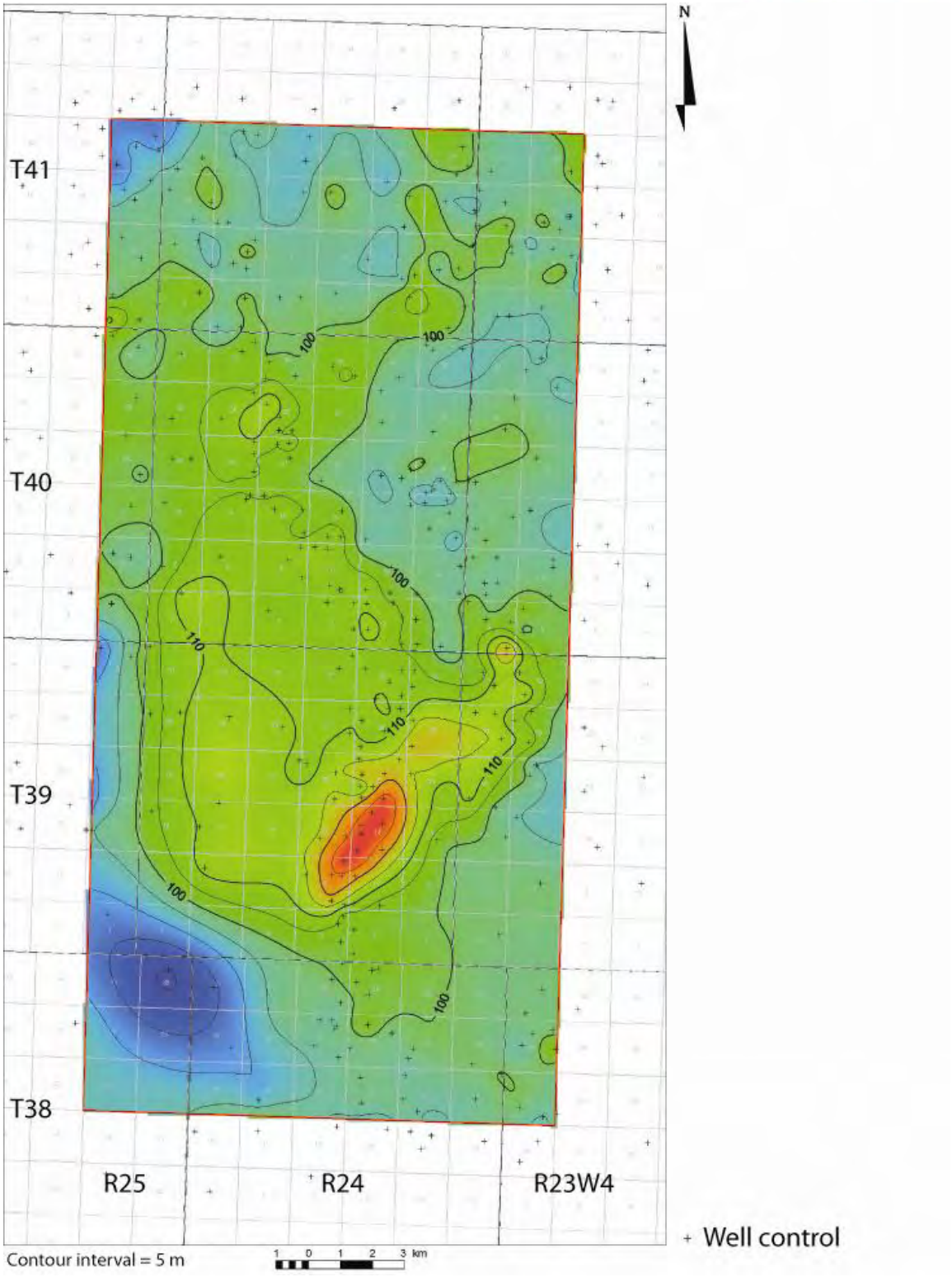

Figure A.18: Isopach of the Upper Mannville Group in the Enhance Clive study area.

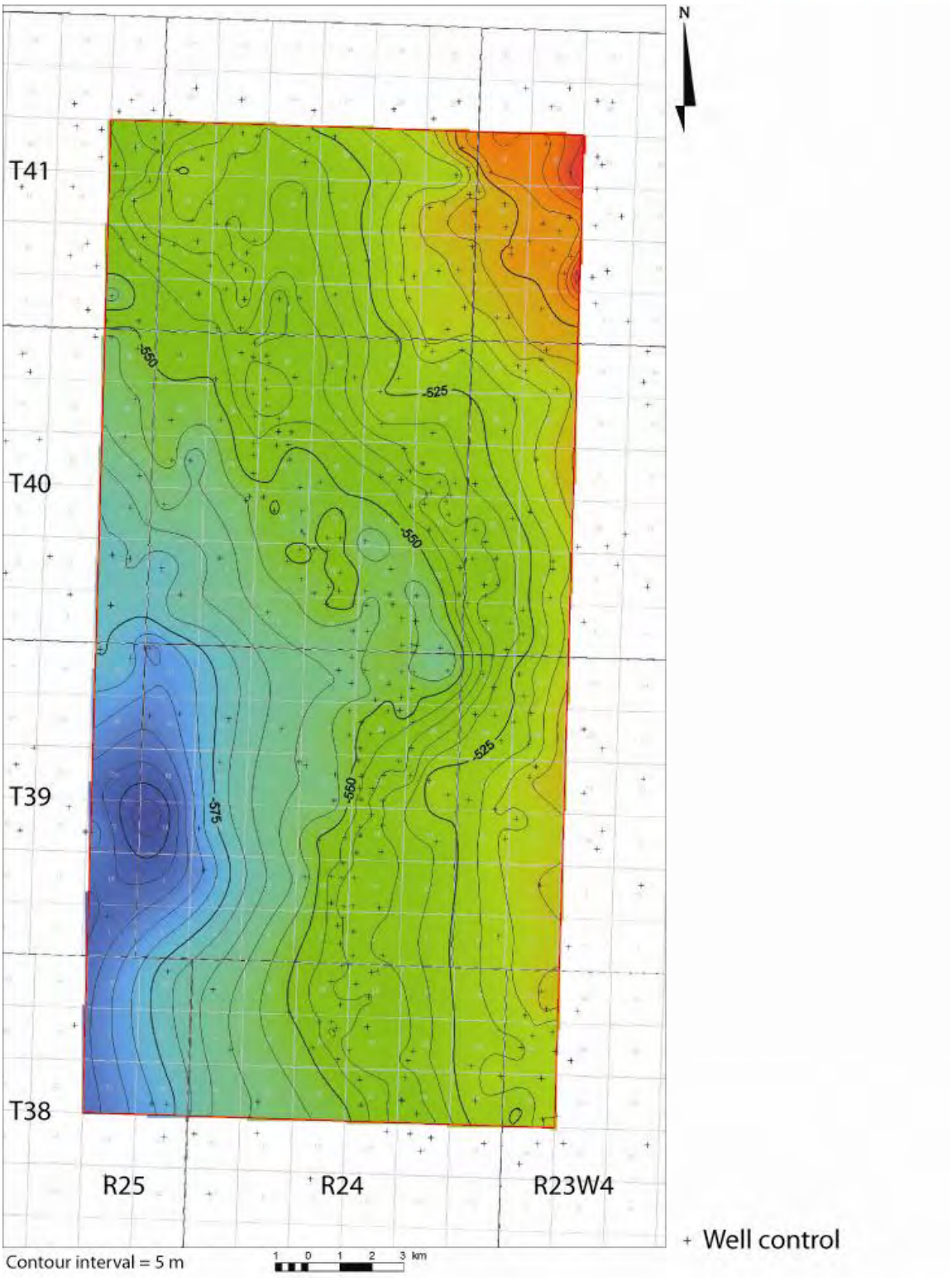

Figure A.19: Structural elevation of the top of the Joli Fou Formation in the Enhance Clive study area.

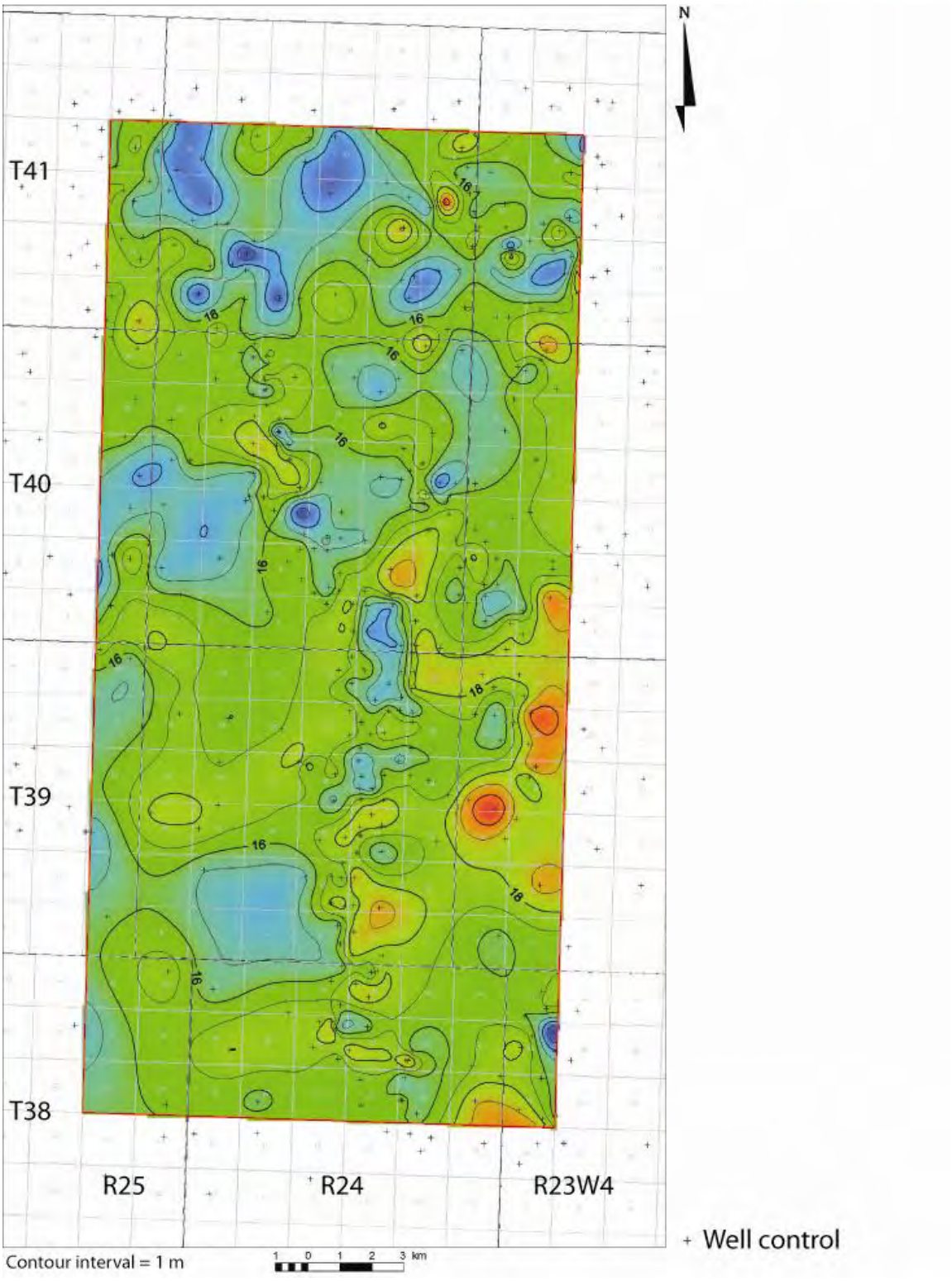

Figure A.20: Isopach of the Joli Fou Formation in the Enhance Clive study area.

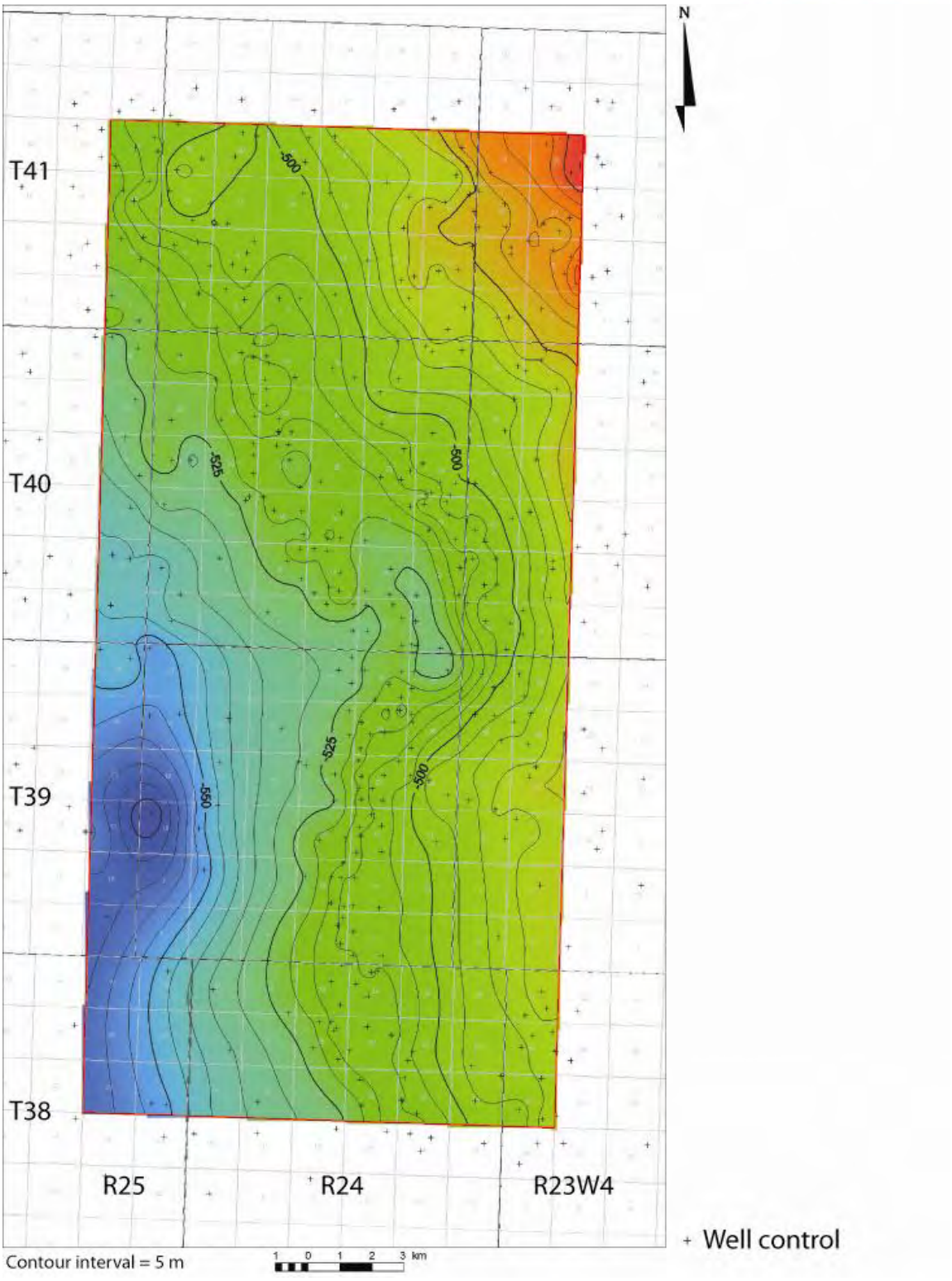

Figure A.21: Structural elevation of the Viking Sandstone in the Enhance Clive study area.

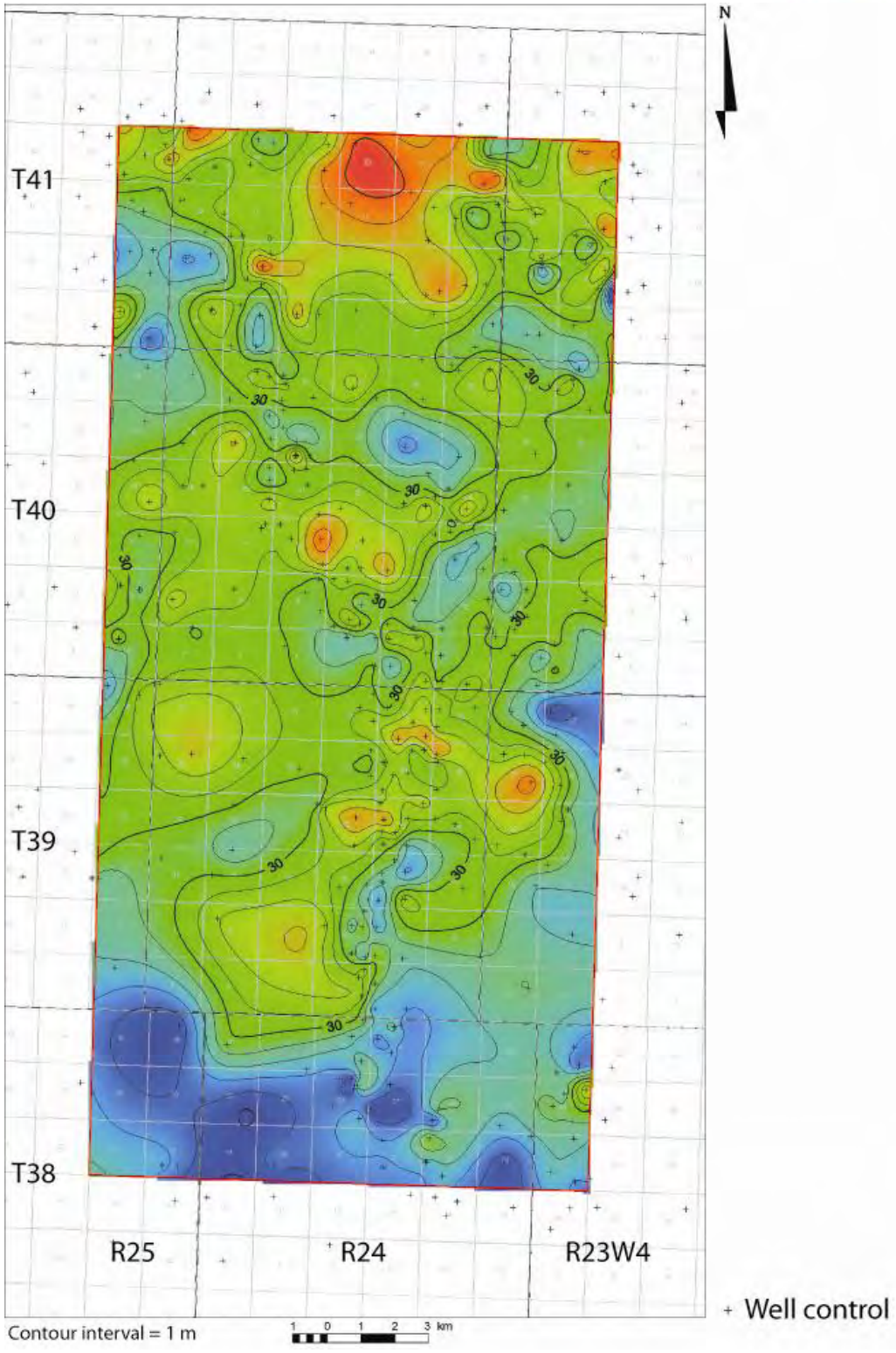

Figure A.22: Isopach of the Viking Sandstone in the Enhance Clive study area.

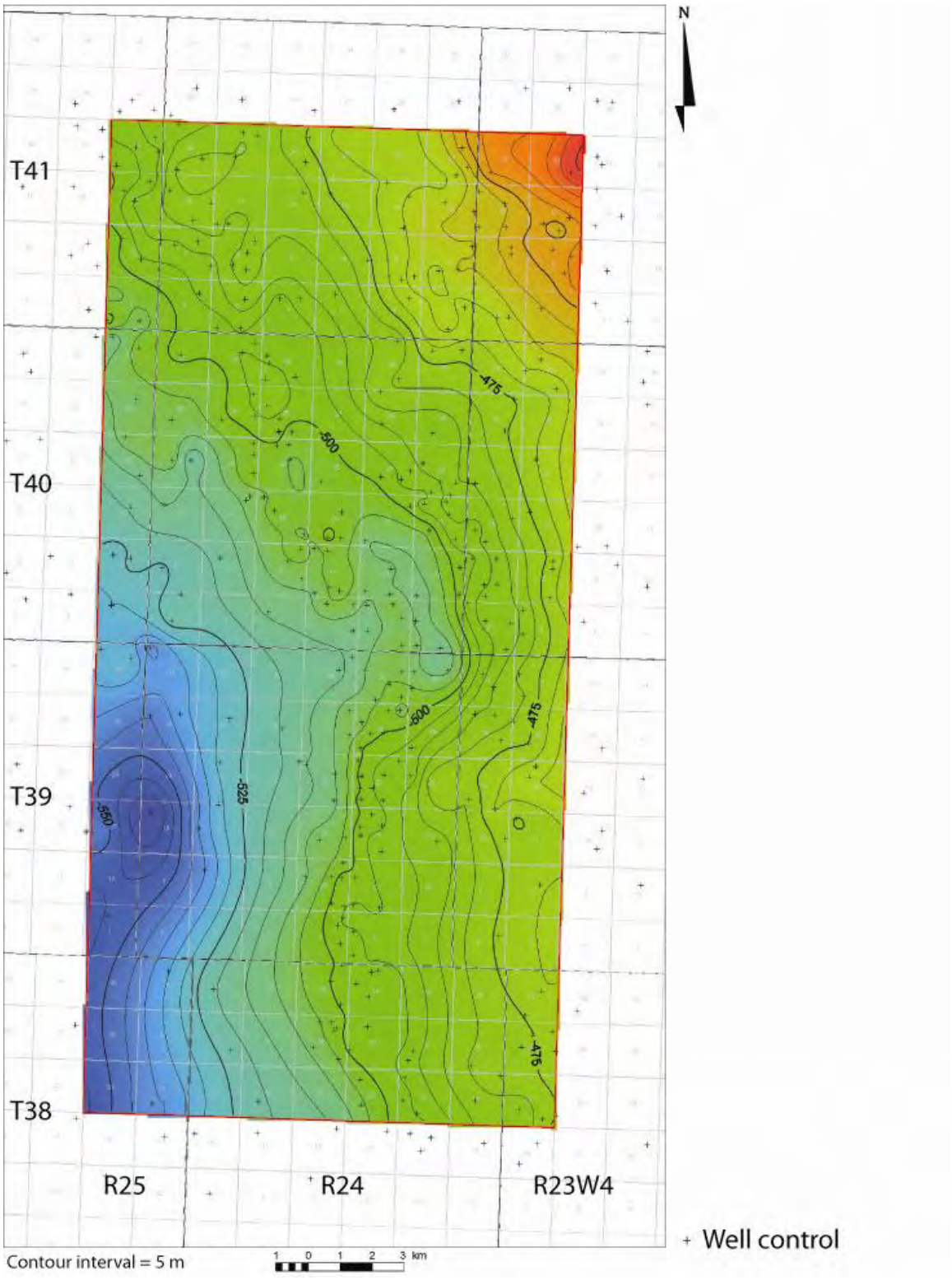

Figure A.23: Structural elevation of the Viking Formation ("shaly" Viking) in the Enhance Clive study area.

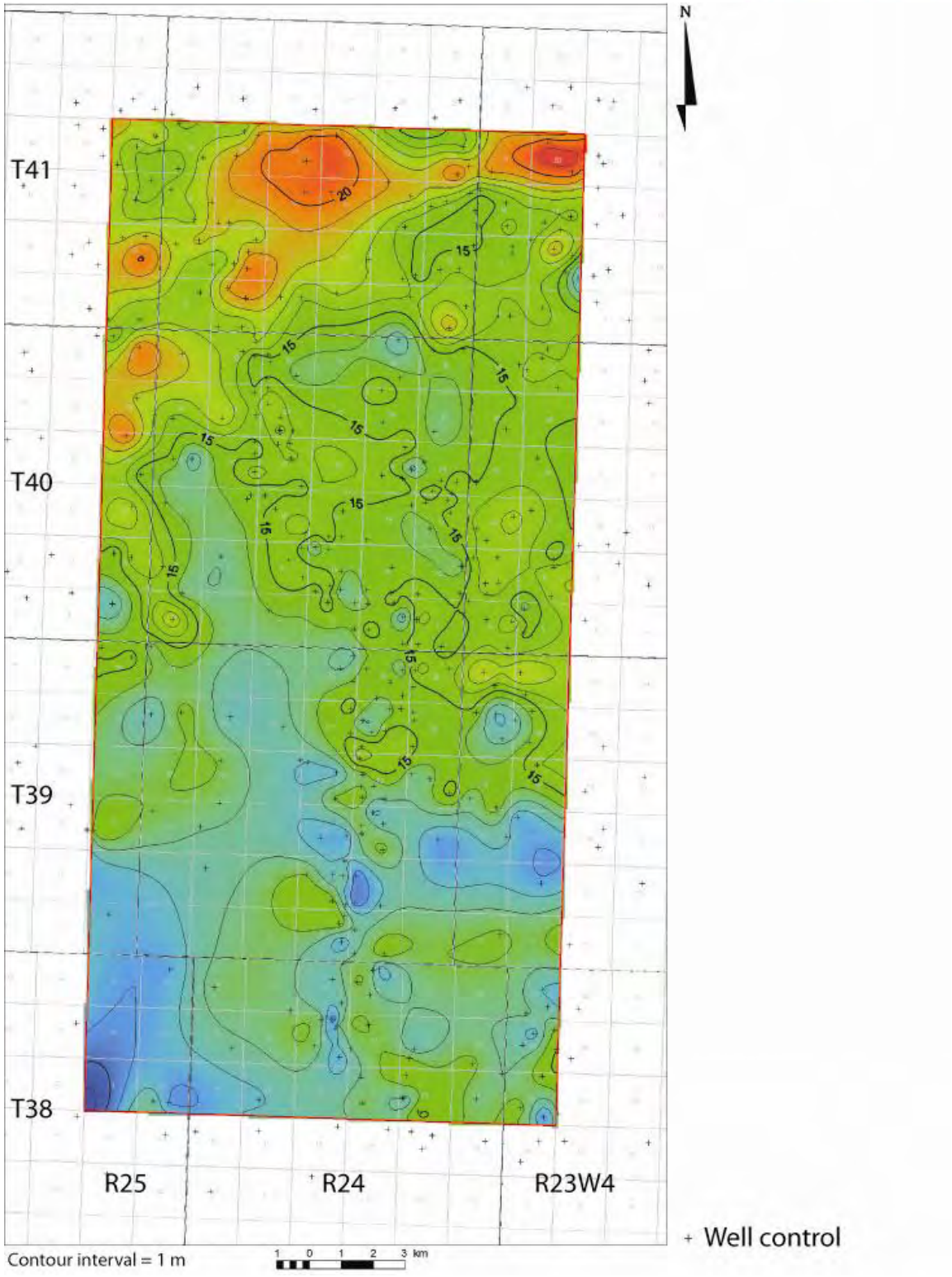

Figure A.24: Isopach of the "shaly" Viking unit in the Enhance Clive study area.

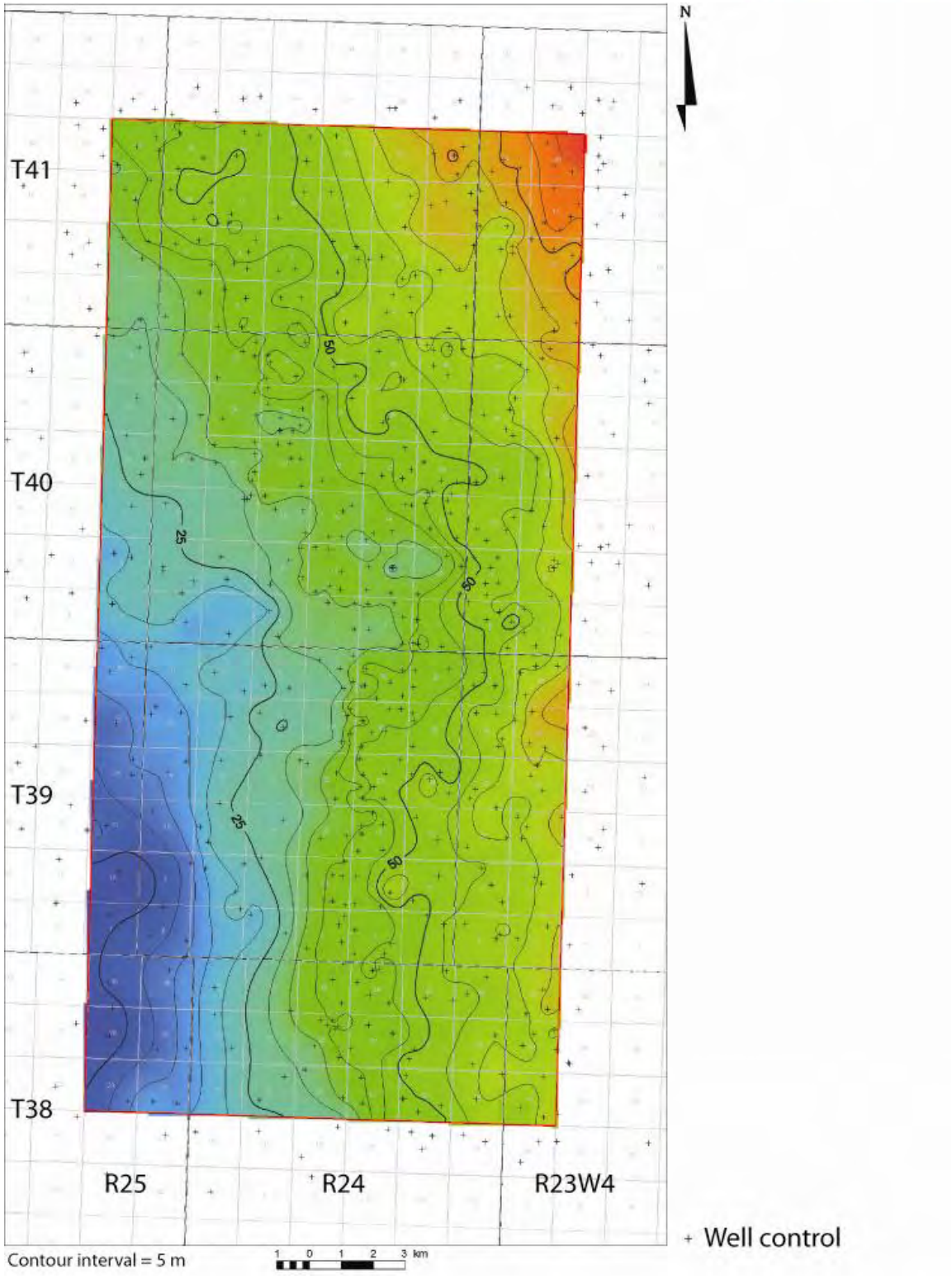

Figure A.25: Structural elevation of the top of the Lea Park Formation in the Enhance Clive study area.

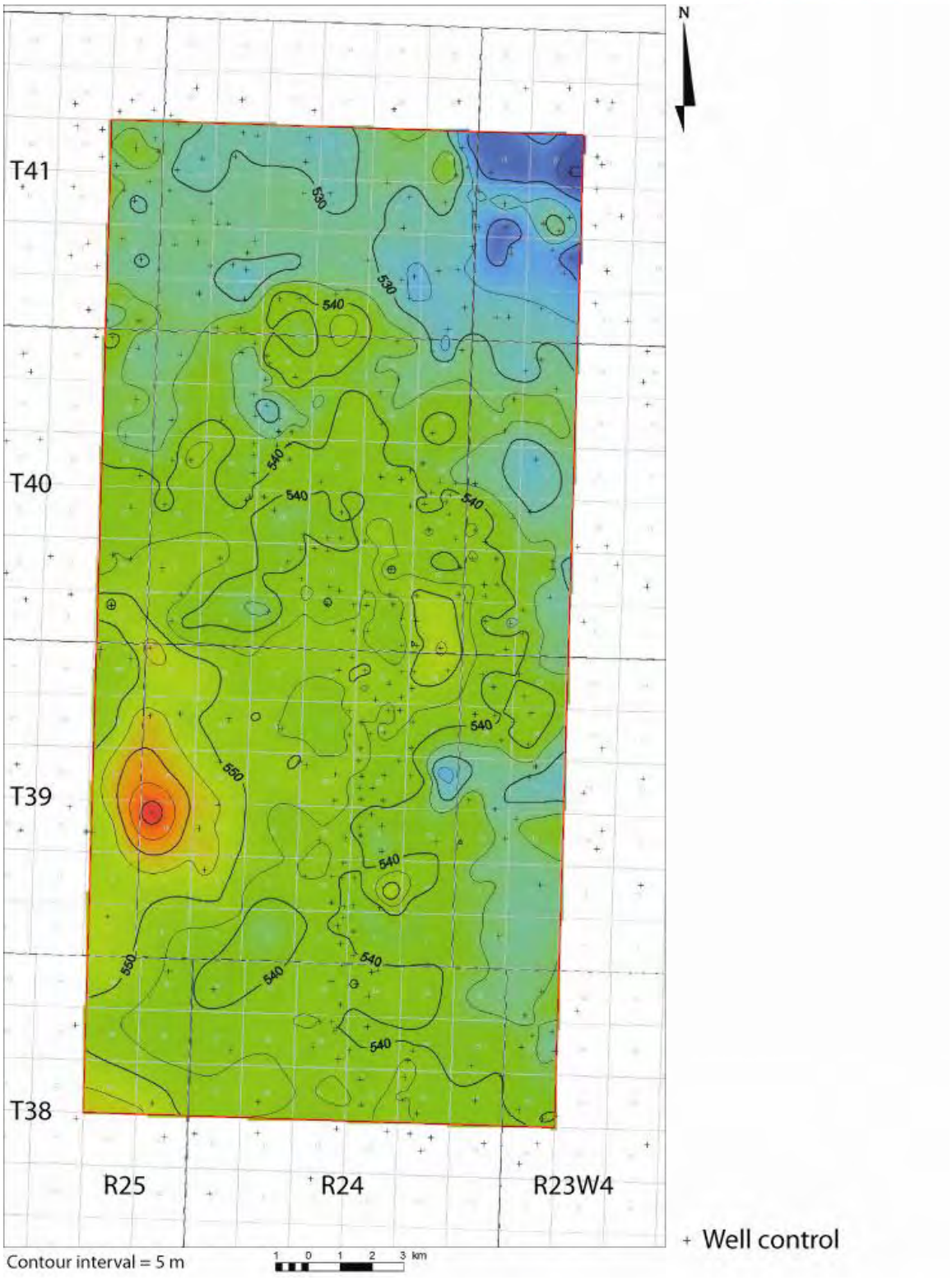

Figure A.26: Isopach of the sedimentary succession from the top of the Viking Sandstone Unit to top of the Lea Park Formation in the Enhance Clive study area.

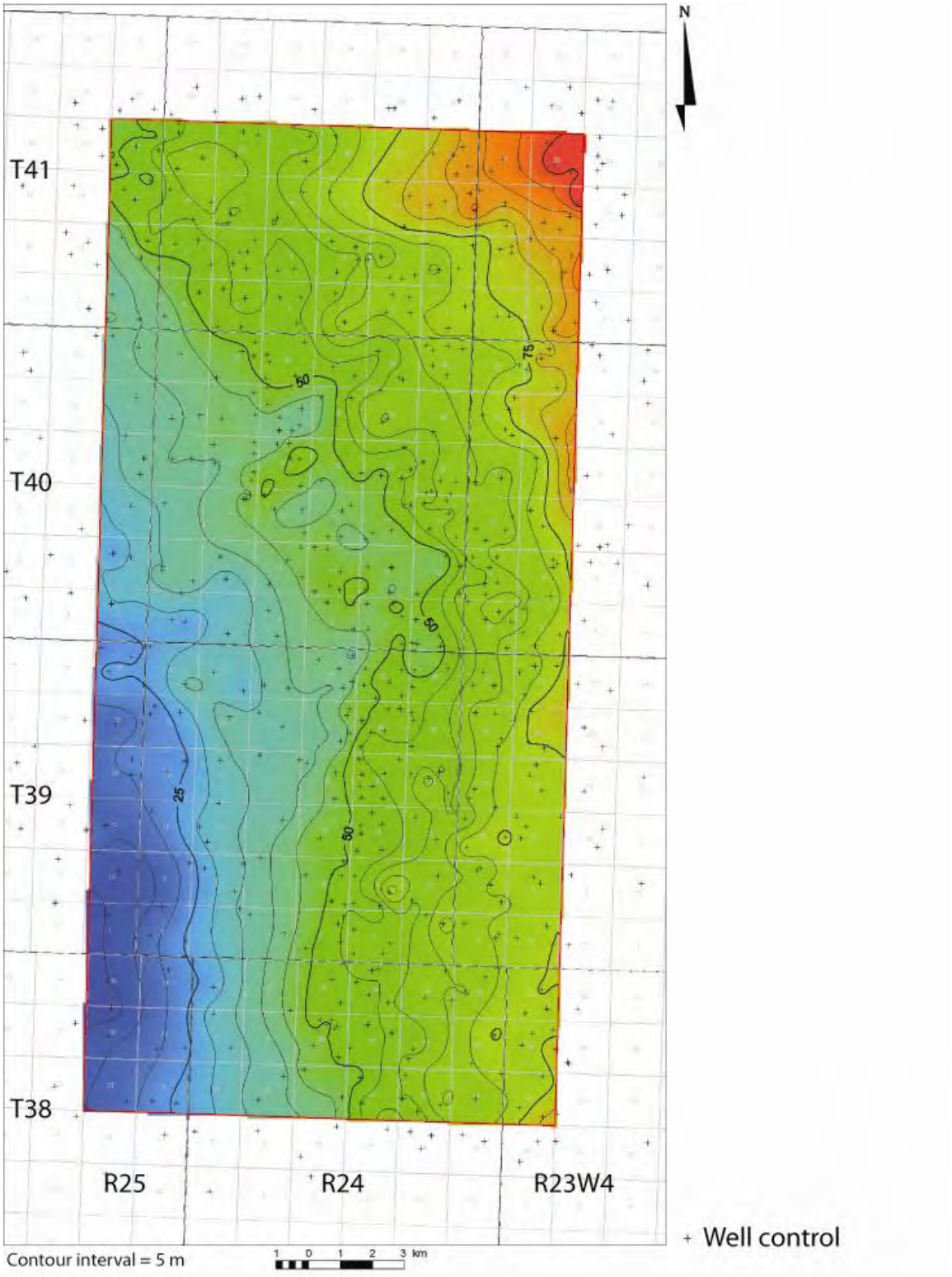

Figure A.27: Structural elevation of the top of the Basal Belly River Sandstone unit of the Foremost Formation in the Enhance Clive study area.

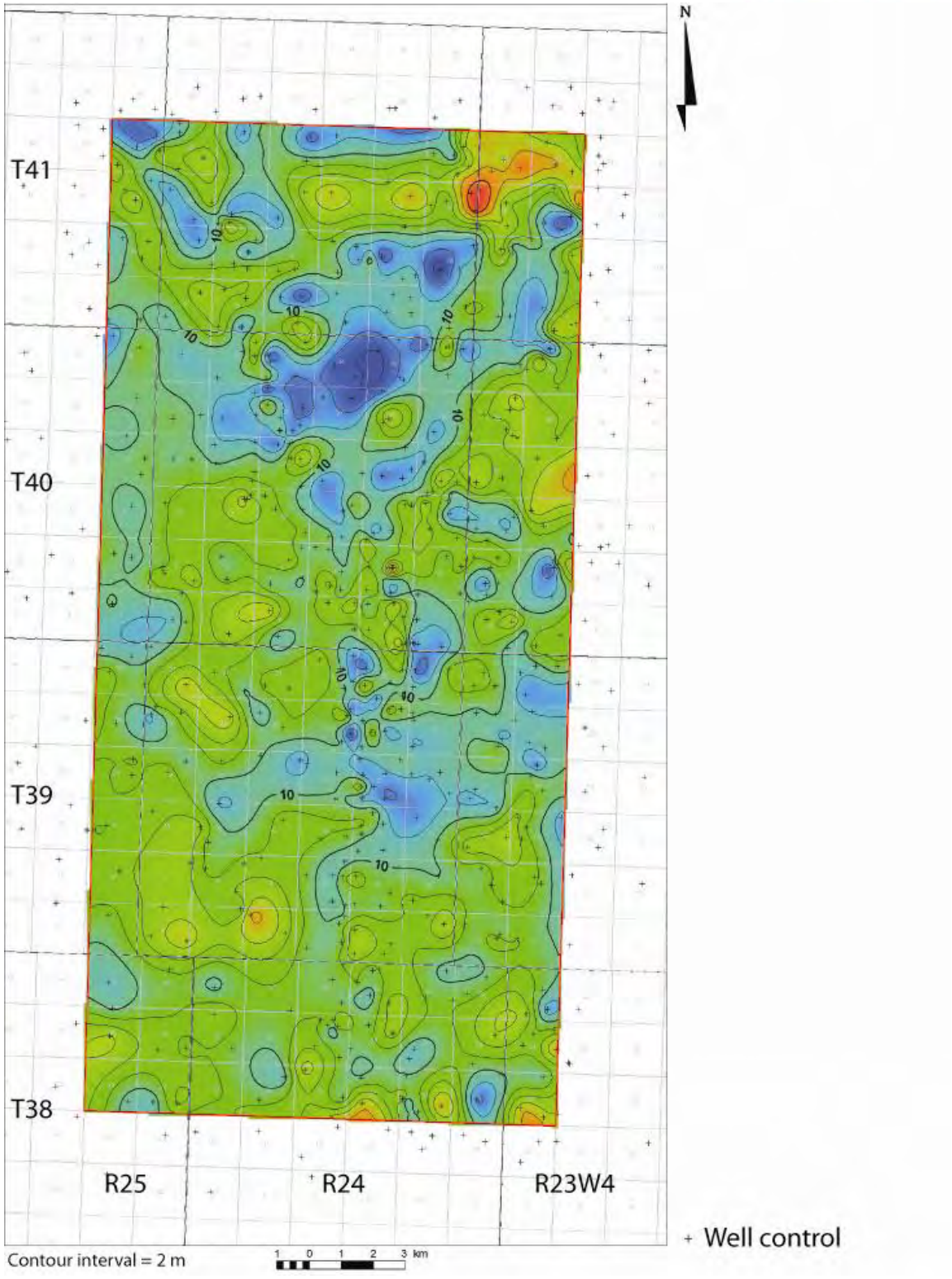

Figure A.28: Isopach of the Basal Belly River Sandstone unit in the Enhance Clive study area.

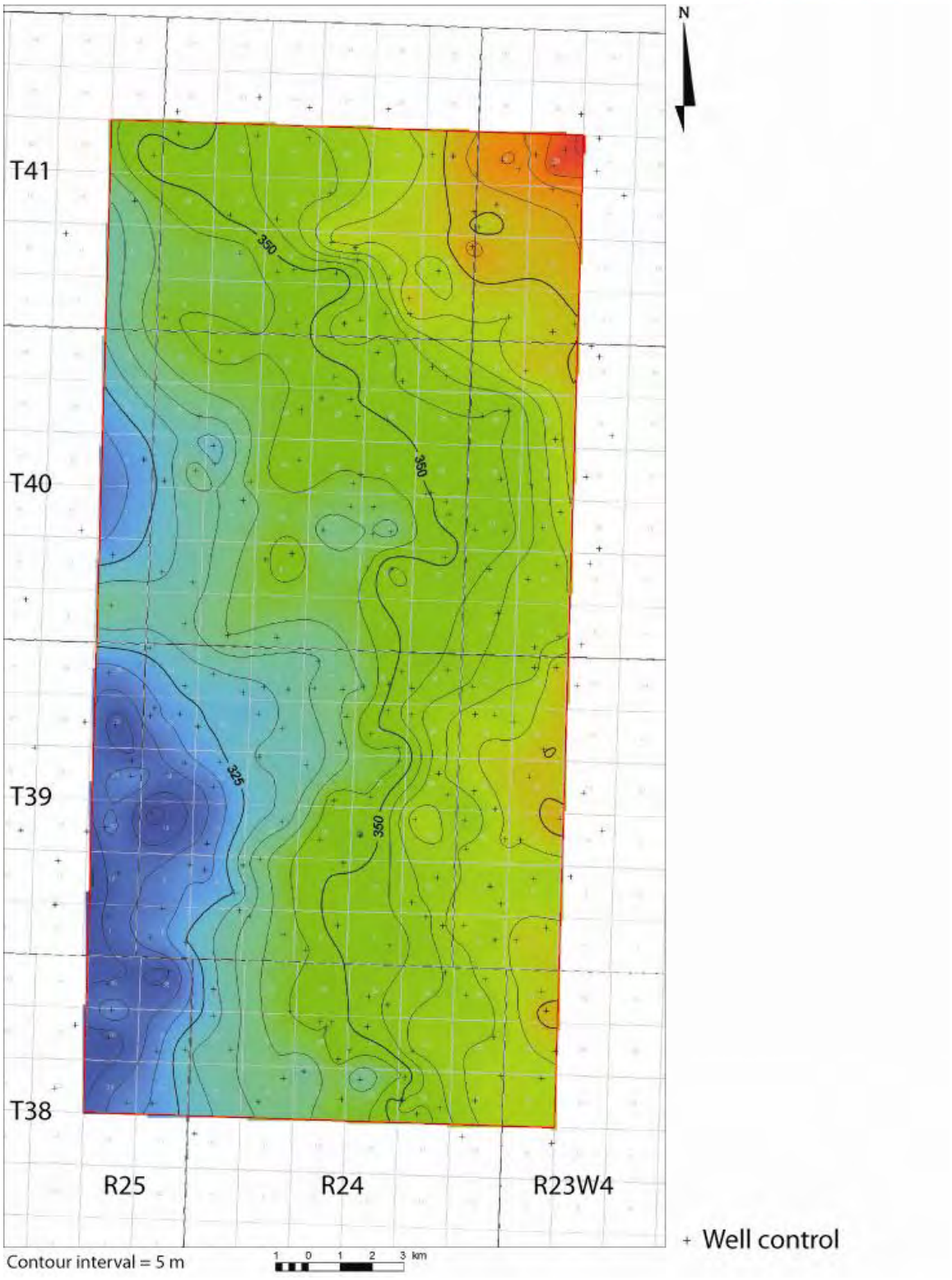

Figure A.29: Structural elevation of the top of the Belly River Group in the Enhance Clive study area.

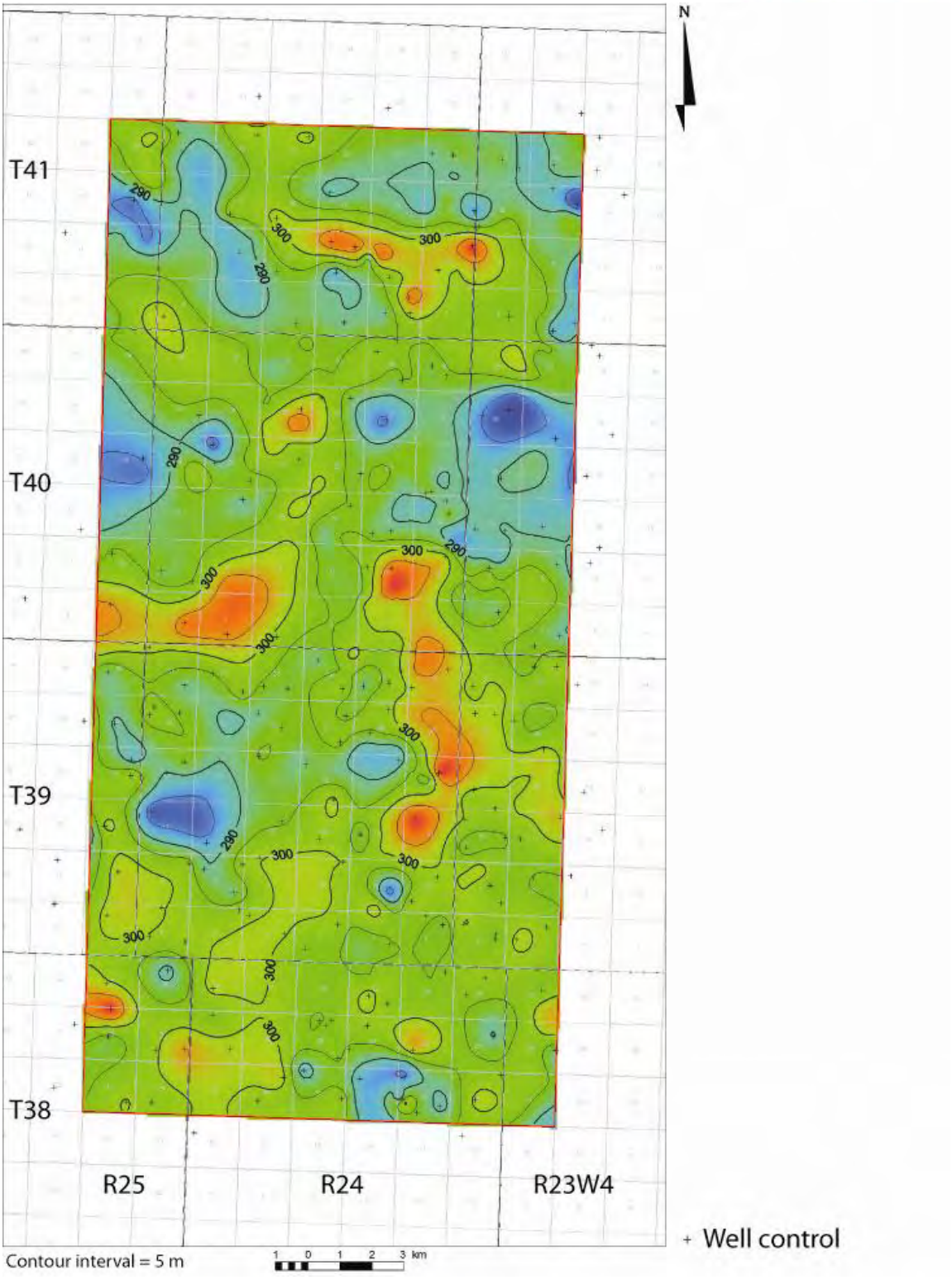

Figure A.30: Isopach of the undifferentiated Upper Belly River Group in the Enhance Clive study area.

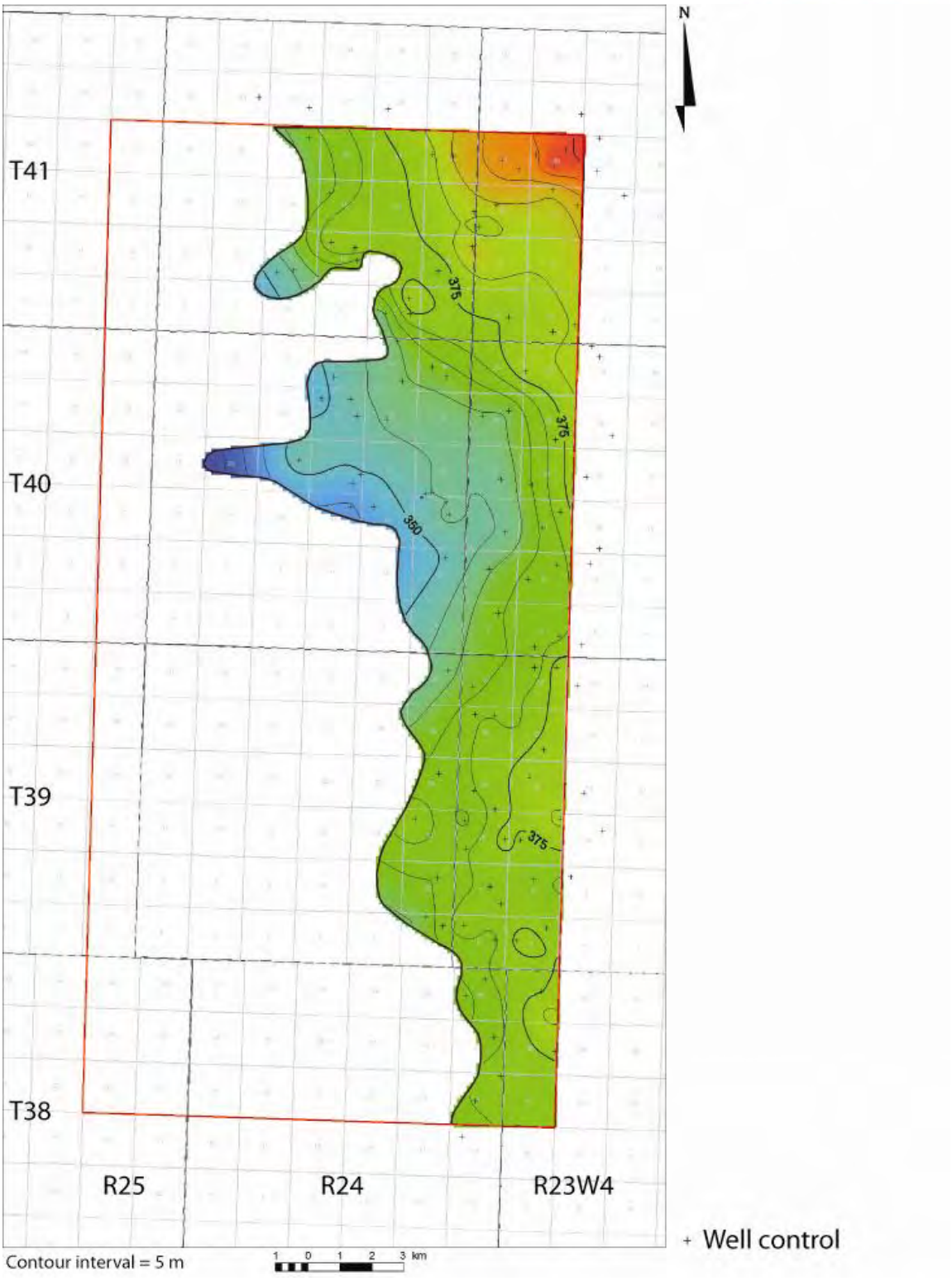

Figure A.31: Structural elevation of the top of the Bearpaw Formation in the Enhance Clive study area.

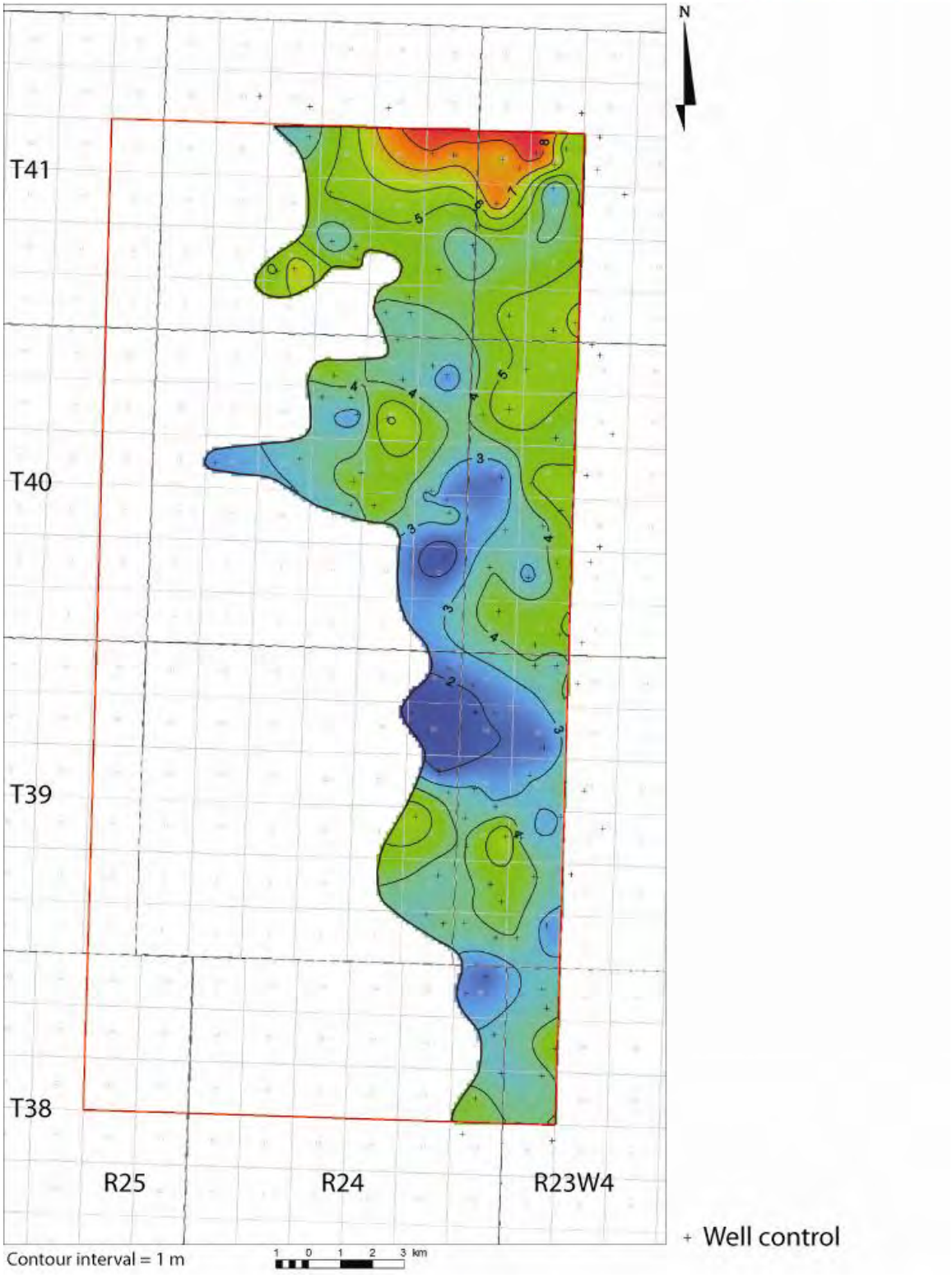

Figure A.32: Isopach of the Bearpaw Formation in the Enhance Clive study area.

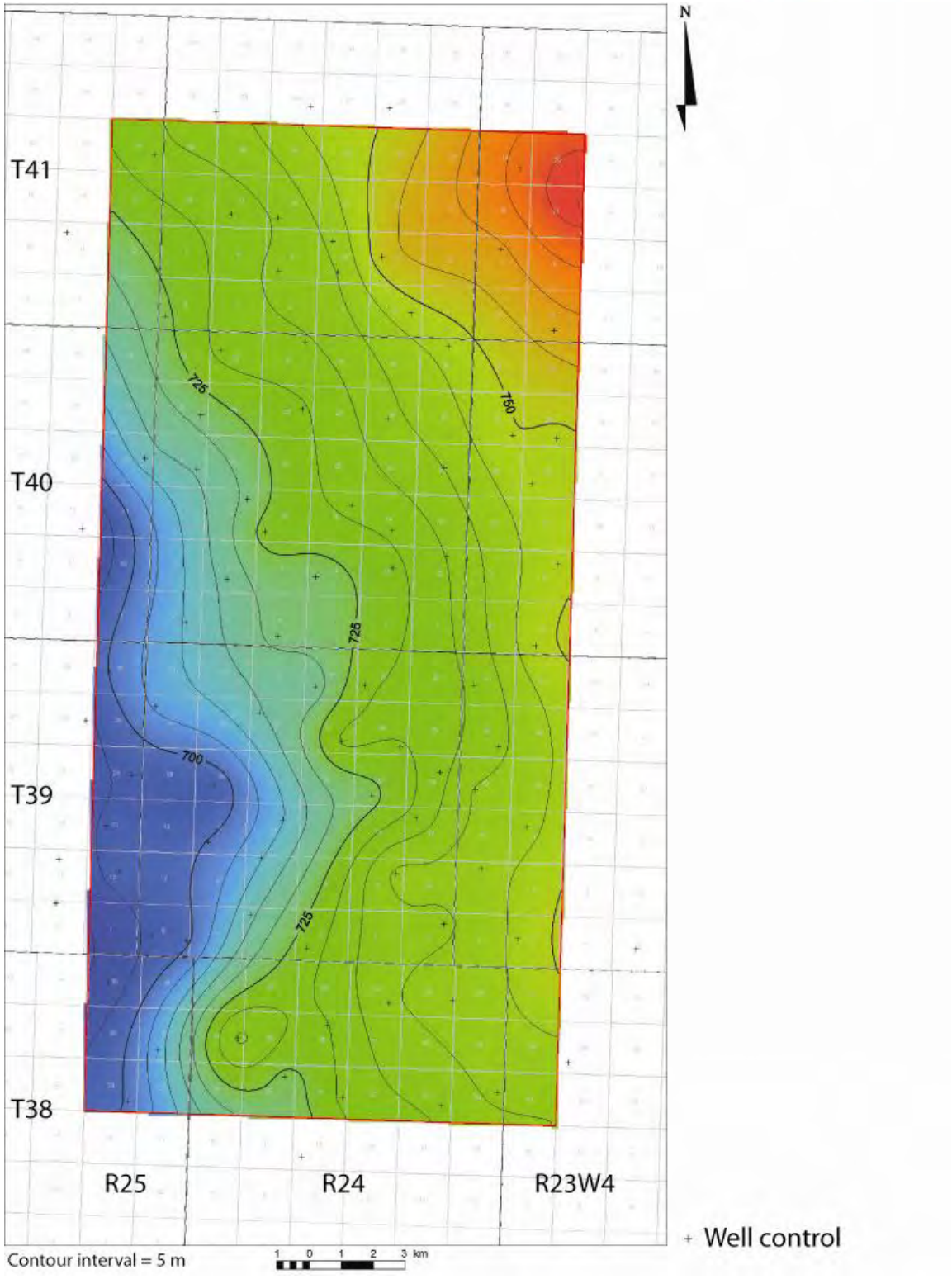

Figure A.33: Structural elevation of the top of the Horseshoe Canyon Formation in the Enhance Clive study area.

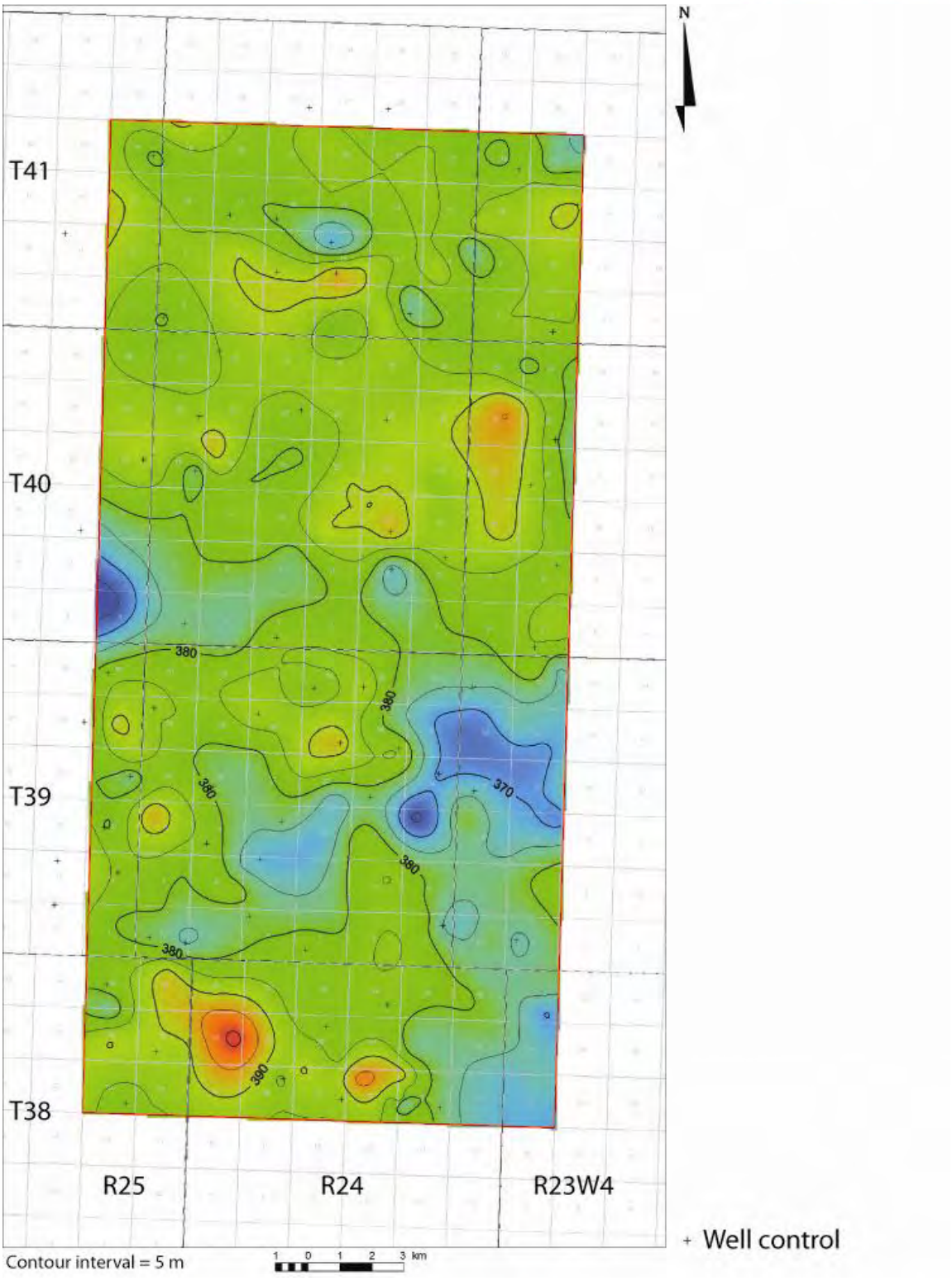

Figure A.34: Isopach of the Horseshoe Canyon Formation in the Enhance Clive study area.

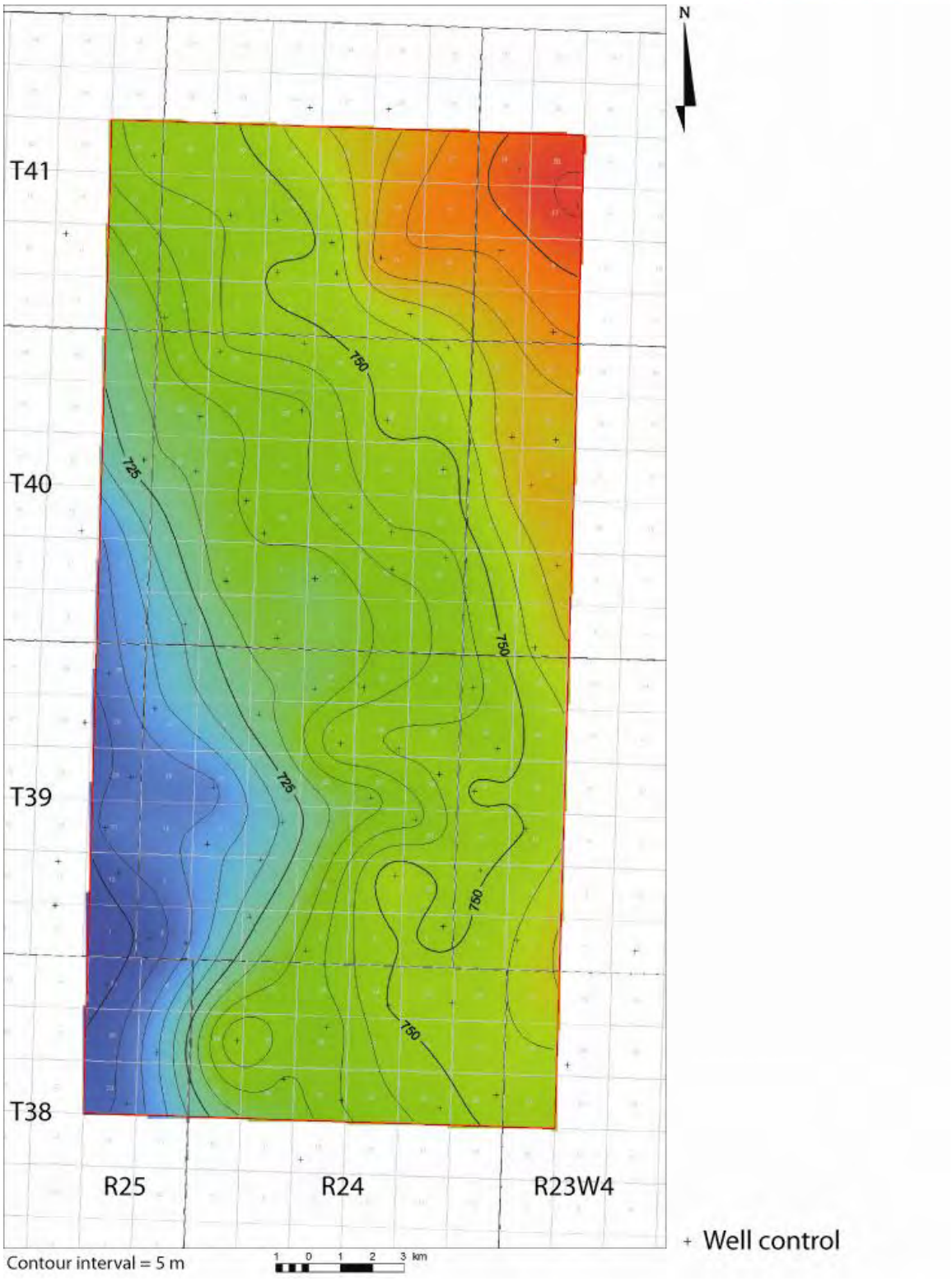

Figure A.35: Structural elevation of the top of the Whitemud and Battle formations in the Enhance Clive study area.

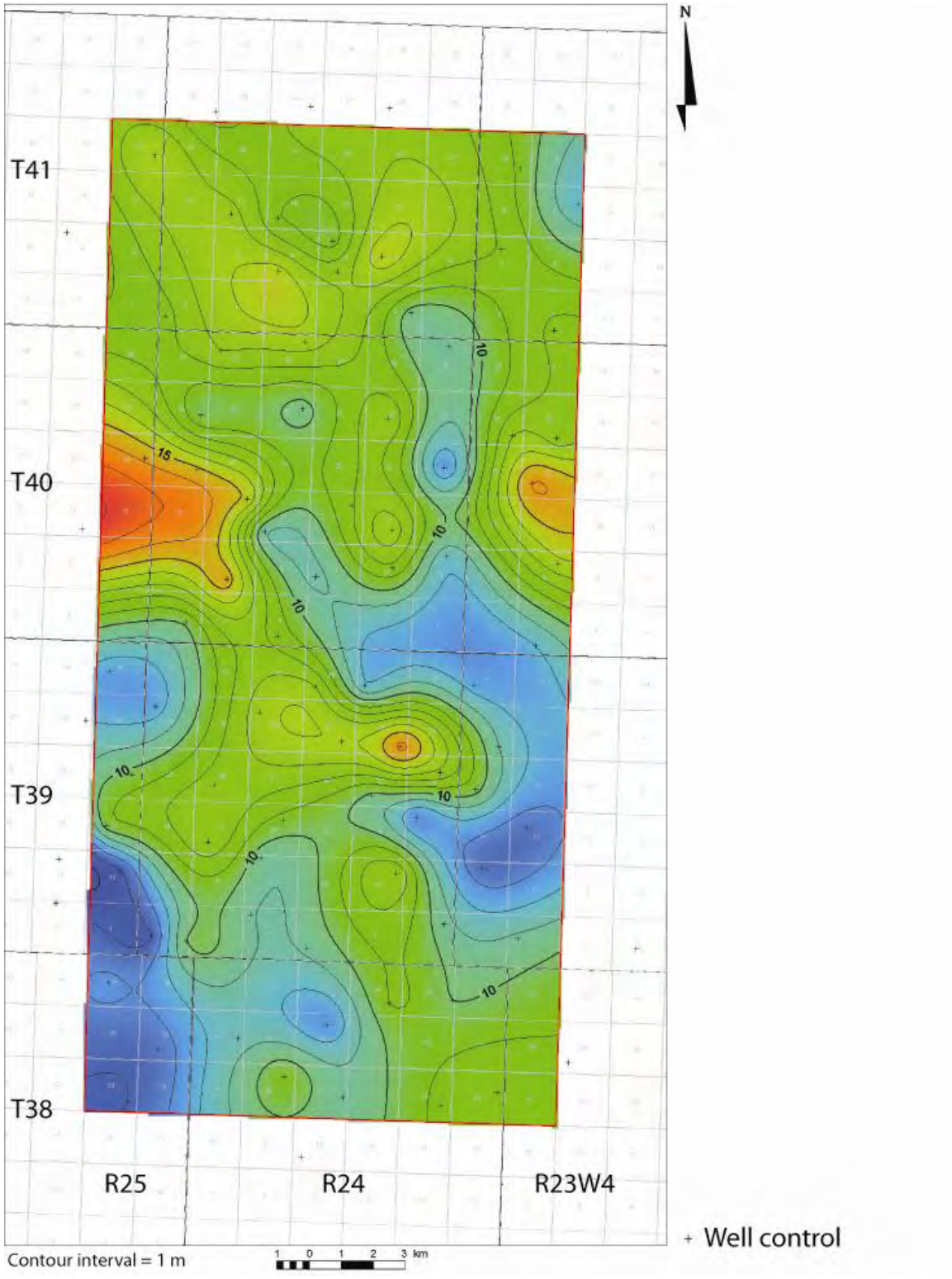

Figure A.36: Isopach of the Whitemud-and Battle formations in the Enhance Clive study area.

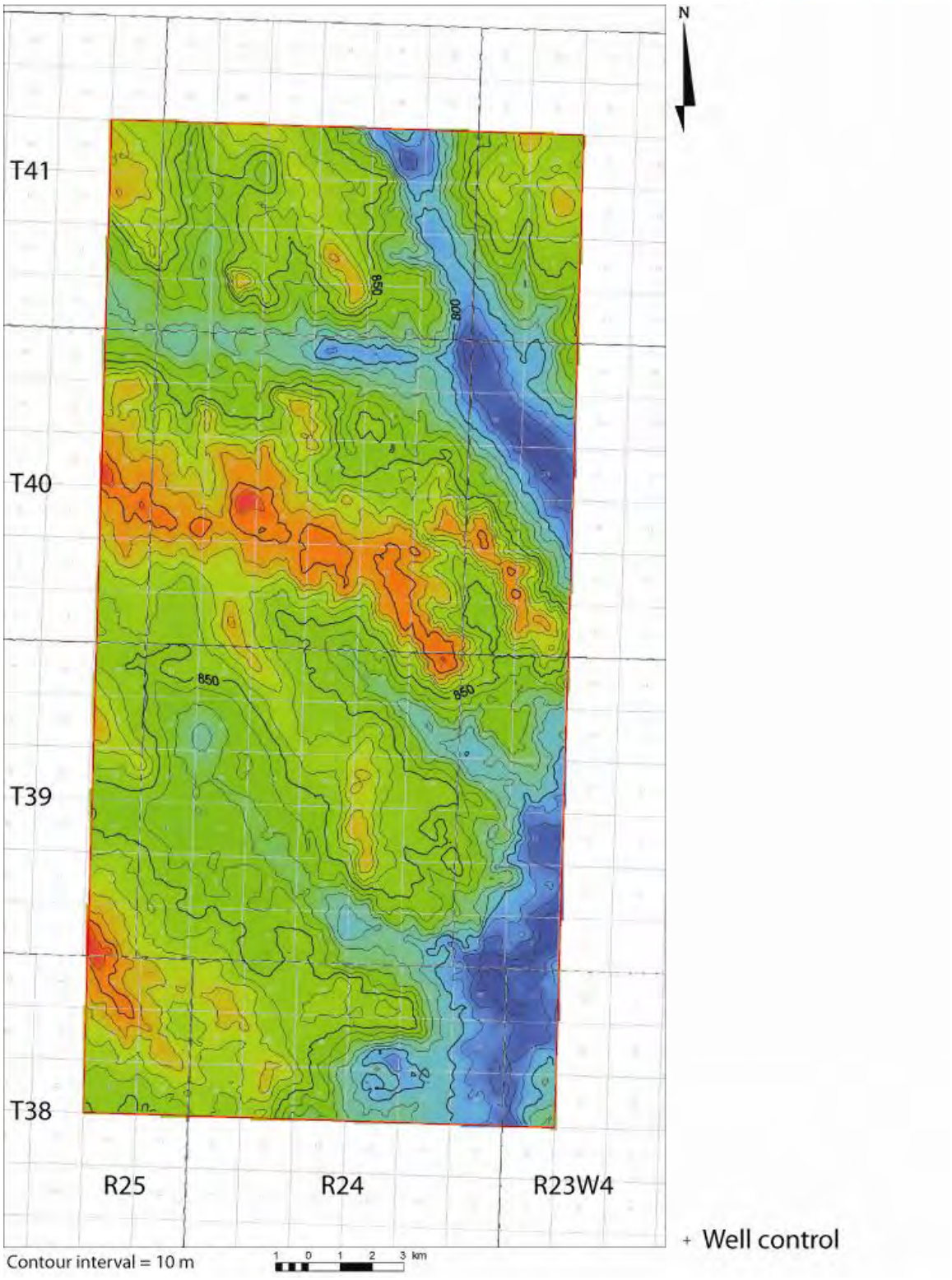

Figure A.37: Structural elevation of the top of the bedrock surface (subcrop of the Scollard and Paskapoo formations) in the Enhance Clive study area.

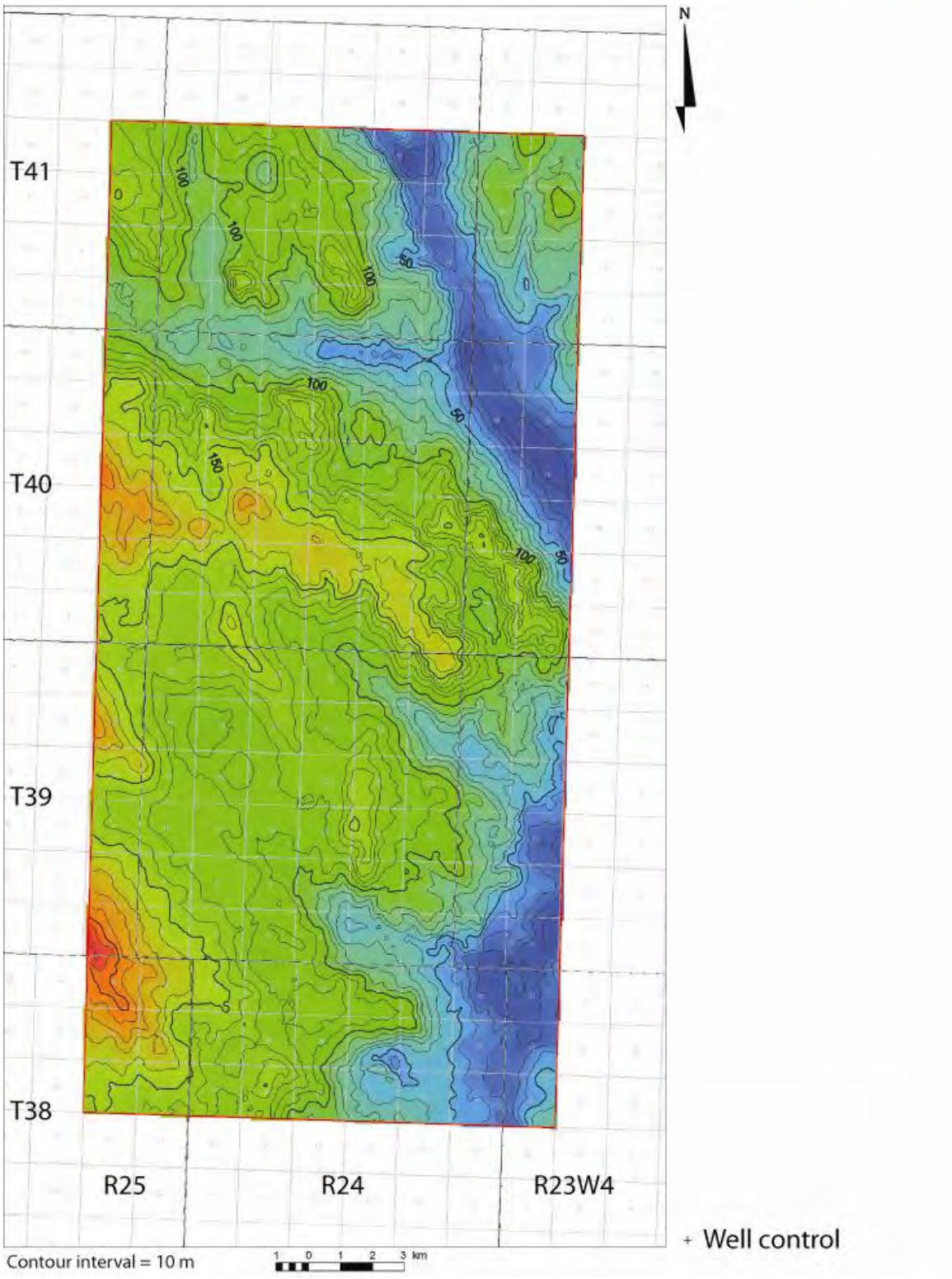

Figure A.38: Isopach of the Scollard and Paskapoo formations in the Enhance Clive study area. Bedrock well control comes from the Alberta Water Well Database. Battle Fm. well control comes from hydrocarbon wells.

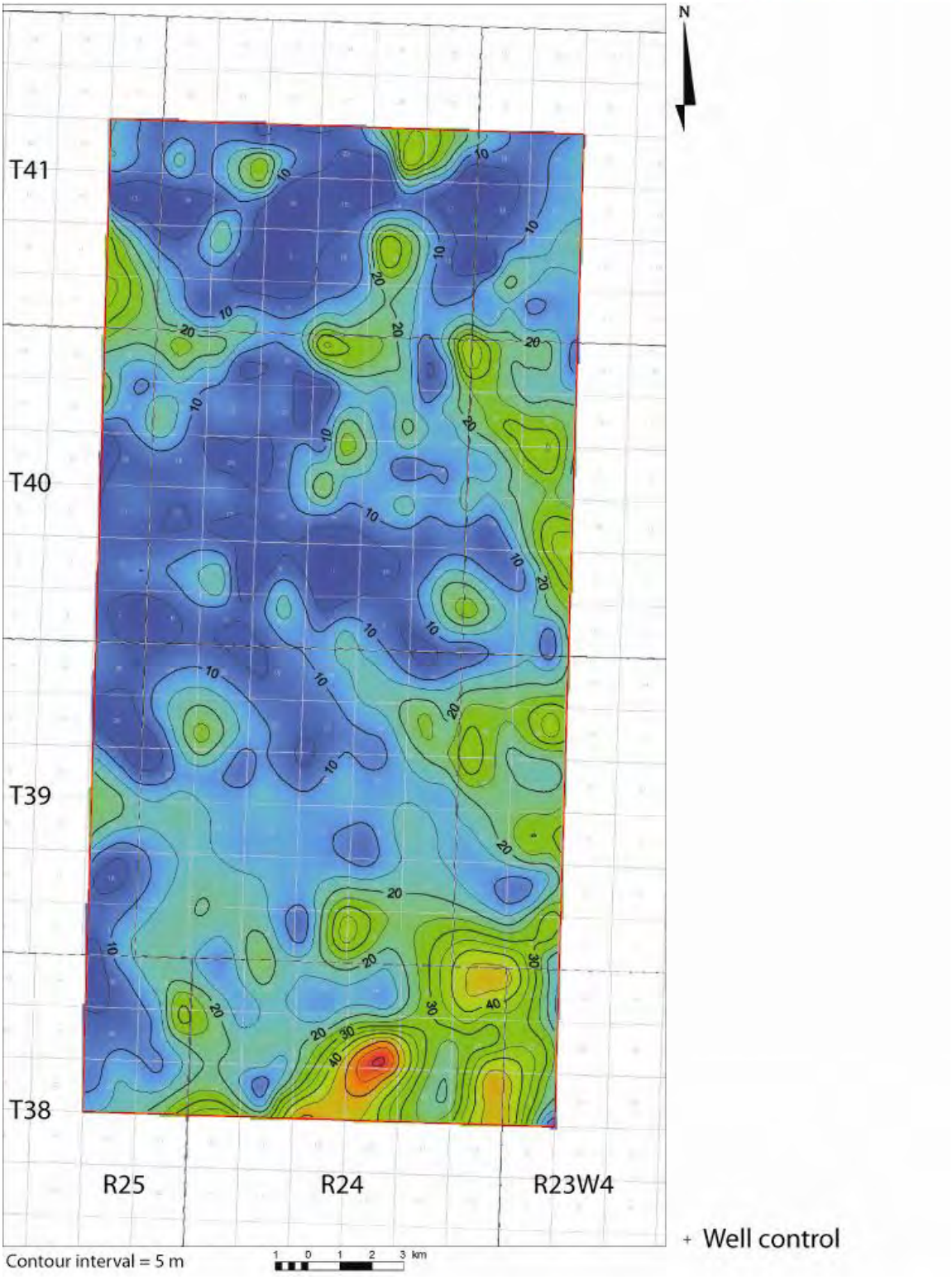

Figure A.39: Isopach of the unconsolidated Tertiary and Quaternary deposits in the Enhance Clive study area.

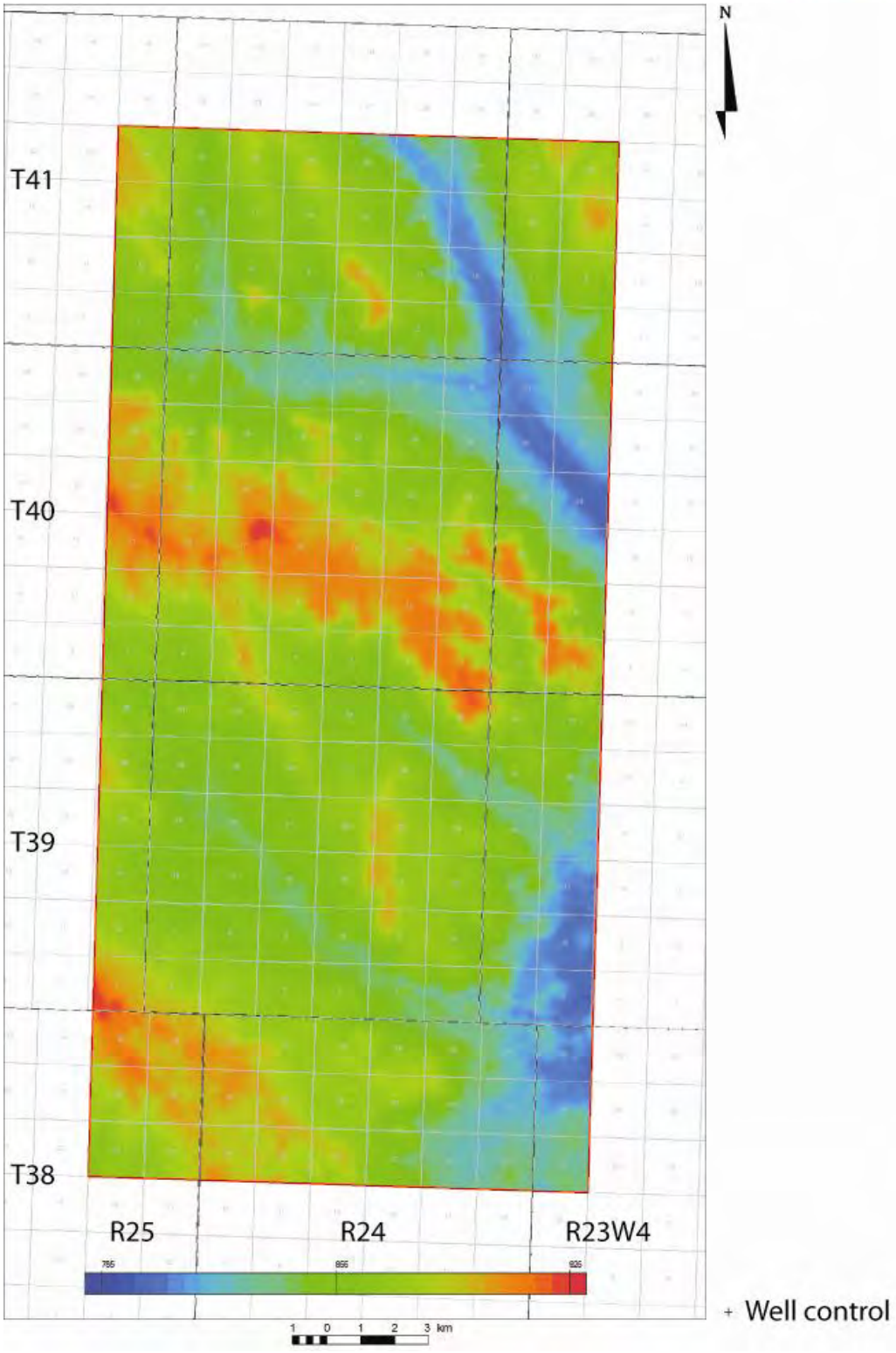

Figure A.40: Ground elevation (surface topography) in the Enhance Clive study area.

9. APPENDIX B – Culling Methods for Hydrogeological Data

9.1 Chemistry

The following are additional culling criteria for chemistry data:

Incomplete Analyses
Many chemical analyses are incomplete or have missing information (such as test interval, pH, and type of test). All water samples must be analysed for major ionic species: chloride (Cl^-), bicarbonate (HCO_3^-), sulphate (SO_4^{2-}), sodium (Na^+), Calcium (Ca^{2+}), and Magnesium (Mg^{2+}). Analyses that are missing any one of these ions were removed from database or flagged as potentially erroneous. However, certain chemical species are not reported due to their very low concentrations (bellow the detection limit). This does not mean that the entire analysis is invalid and manual examination is required.

Charge Balance Error
Charge Balance Error (CBE) is a fundamental parameter in the quality control of chemical analyses (Davis, 1988). Poor quality analyses can be detected by a simple calculation based on the fact that dissolved chemical species exist in equilibrium (by molar mass and charge). The % CBE is calculated using the following equation (Freeze and Cherry, 1979):

$$\%\mathrm{CBE} = \left[\frac{\sum \mathrm{Z}\times \mathrm{m_c} - \sum \mathrm{Z}\times \mathrm{m_a}}{\sum \mathrm{Z}\times \mathrm{m_c} + \sum \mathrm{Z}\times \mathrm{m_a}}\right]\times 100\% \qquad (7)$$

where: Z is the absolute value of ion's charge, m_c is the molar mass of cations, and m_a is the molar mass of anions. Analyses with CBE greater than 10% were flagged and subsequently eliminated from further consideration.

Identification of Contaminated Samples
The following are diagnostic criteria used to identify contaminated water samples (e.g. Hitchon and Brulotte, 1994; Rostron, 1994; Khan, 2006; Palombi, 2008):

a) General Criteria
   - pH < 5 or > 8: generally formation water falls within this pH boundary. Any samples with pH from outside of this range could potentially be contaminated by completion fluid or corrosion inhibitor.

- Hydroxide reported (OH^-): presence of hydroxide may indicate large amount of mud recovery during the test.
- Carbonate reported (CO_3^{2-}): dissolved CO_3^{2-} cannot exist in a pH environment below 8.1 (Langmuir, 1997). Most subsurface brines do not contain CO_3^{2-}, therefore, its presence may indicate potential contamination with drilling fluid.
- Density <1 g/cm^3 (1000 kg/m^3): measured water density of less than 1 g/cm^3 may indicate contamination by an alcohol-based drilling fluid.
- Recovery <100 m (measured in drill-pipe stands during DSTs only): drill-stem tests with low recoveries were avoided whenever possible due their higher risk of contamination with drilling fluid ("filter cake").

b) Acid Water/Completion Fluid Criteria
   - pH <4.5
   - Ratio Ca/Cl >0.3 and pH <5.7
   - Ratio Na/Ca <1.2
   - Ratios Na/Ca <5 and Na/Mg <10 and pH <6
   - Ratio Na/Cl <0.4 and pH <6.8

c) Corrosion Inhibitor Criteria
   - pH >9
   - Ratios Na/Cl >3.5 and SO_4/Cl >1.5
   - SO_4/Cl >10

d) Mud Filtrate/GelChem Criteria
   - Ratio Na/Cl >5
   - Ratios Na/Cl >3.5 and SO_4/Cl >1.5

e) KCl Mud Filtrate (“Kill Fluid”) Criterion
   - Ratio Na/K <20

In addition to the above criteria, a number of other parameters were used to assess the quality of the water analyses. First, the location of the sampling point was used to identify where in the fluid column a sample has been taken. Typically locations described in the water analysis report include: the top; middle; and bottom of fluid recovery; specified distance above the tool; top of tool (above the down-hole sampler); and the down-hole sampler. The lower in the fluid column the sample was taken, the better ("cleaner") the sample is likely to have been recovered since larger volume of formation water has entered the drill pipe and flushed the drilling fluid (filter cake) up the tool string. Thus, the bottom of the fluid recovery and top of tool are the preferred locations. Samples from the down-hole sampler are generally good but it is often found that drilling fluid is erroneously sampled instead of the formation water. The least favourable sampling locations include the top and middle of the fluid recovery, but sometimes they can also produce representative water samples in DSTs with large water recoveries (hundreds of metres).

A water cushion, a volume of water placed in the tubing prior to flow, is often used in deep drill-stem tests to avoid wellbore damage due to high pressure differential. Water cushion can significantly dilute the sample, therefore, it is important to know which DSTs contained them and take precautions.

For the final culling stage the TDS and chemistry of each analysis were manually examined to ensure a fit with the general data trend. Previous work has shown that formation water chemistry is locally consistent, i.e. does not vary (Benn and Rostron, 1998; Khan, 2006; Palombi, 2008). Data points with anomalous TDS were further examined. In cases where TDS values were similar, ionic ratios were calculated and samples with anomalous ratios were identified as contaminated or being from a different formation.

9.2 Pressure

The following are additional culling criteria for pressure data:

a) Interval Length: The length of tested interval can often be too large and straddle over several formations or aquifers with different pressure regimes. Tests with intervals greater than 50 m were manually examined and generally culled.

b) Quality Code: Data vendors assign a code to subjectively assess the quality of the pressure test. Both Hydrofax and CIFE have similar quality codes: (A) best quality; (B) nearing stabilization; (C) caution (possible tool plugging); (D) questionable or misrun; (E) low permeability and low pressure; (F) low permeability and high pressure; (G) misrun. Data with quality from A to C were generally retained for further mapping. Quality-D data were also used in areas where better quality data were not available or areas of sparse data. Very poor quality tests (E to G) were discarded. Additional verification and manual culling was performed on lesser-quality data (C and D).

c) Qualitative Permeability: This code provides a permeability rating based on subjective examination of the DST chart(s) by the database vendors. The following are the assigned codes: excellent (EX) – final flow has stabilized with the final shut-in pressures; high (HI) final flow nearing stabilization with the final shut-in pressures; relatively high (RH) – final flow and shut-in are still building up slightly; average (AV) - final flow and shut-in are still building up rapidly; relatively low (RL) – flow pressure is low and shut-in pressure is building rapidly; low (LO) – very low flowing pressure with rapidly building-up shut-in pressure; virtually none (VN) – almost no flow and rapidly building pressure. DSTs with qualitative permeabilities of lower than average (AV) were generally culled.

d) Qualitative Hydro-Factor: This code indicates the type of fluid recovered: water, oil, gas, mud, or water cushion. With a mixed recovery the larger amount of fluid is taken to be the representative fluid type. For example “Gas-cut water” will be marked as W (water). DSTs with water recoveries were preferred. However, most DSTs with oil and water cushion recoveries were used since they still represent flow conditions in the formation. Mud and gas recoveries were generally not used.

e) Flow and Shut-In Times: These are the times allowed for the fluid to flow into the drill-pipe and then stabilize during the shut-in time. Tests with longer flow and shut-in times are likely to better represent true formation pressure or provide more accurate extrapolation results.

f) Recovery and Blow Description: on-site operator’s comments can often be useful in determining the quality of the test. Those comments could include any breakdown events during the test, equipment malfunctions, tool skids, and mud leaks all of which could affect pressure measurements.

g) DST chart: Visual examination of a DST chart can give a firsthand impression about the quality of the test if no addition information or interpretation is given. Certain older tests also require proper Horner extrapolation directly from the DST chart due to the lack of digital pressure readings.

10. APPENDIX C – Piper Plots for the Paskapoo Aquifer

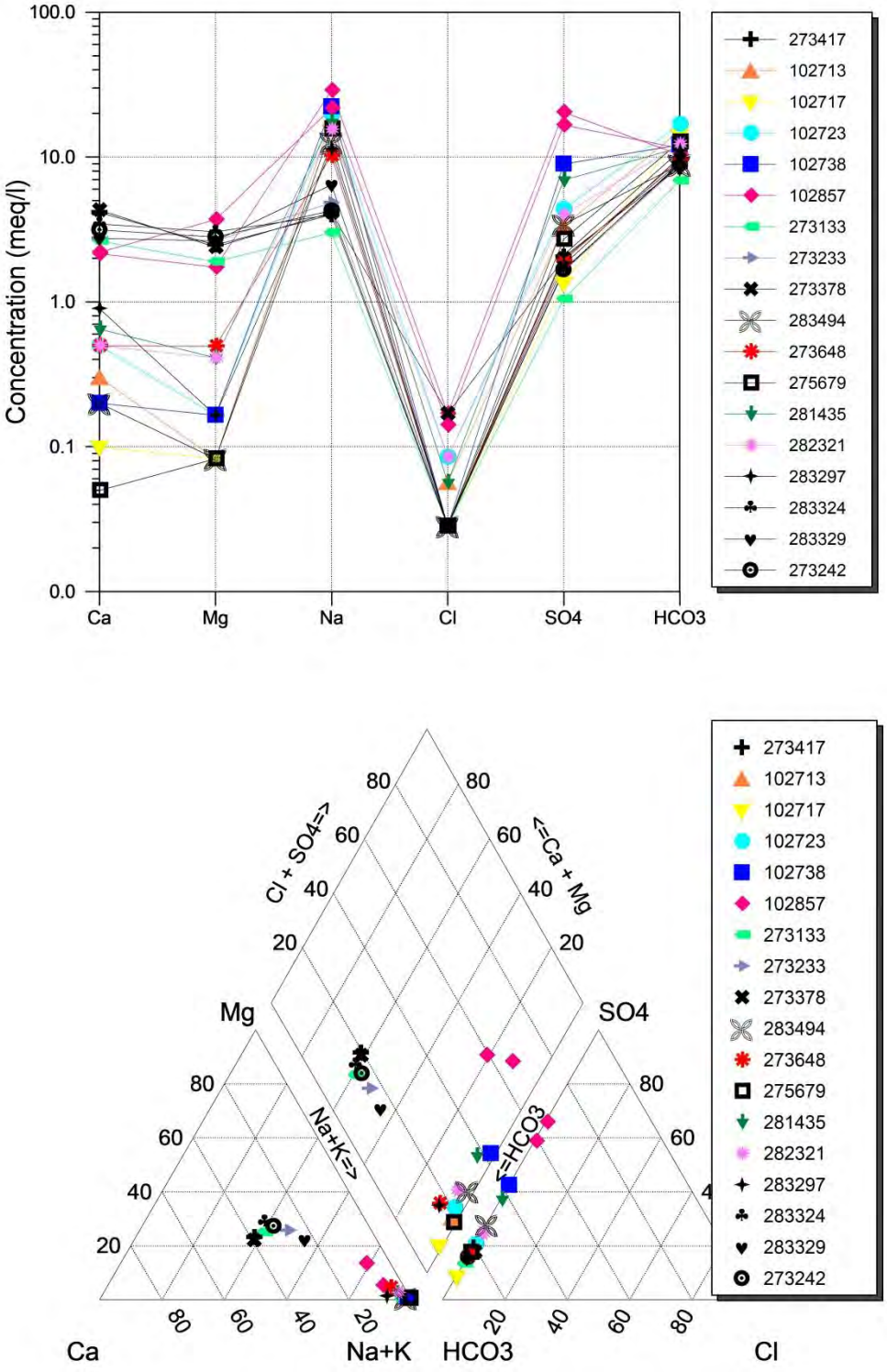

Figure C.1: Paskapoo Formation Well Chemistry.

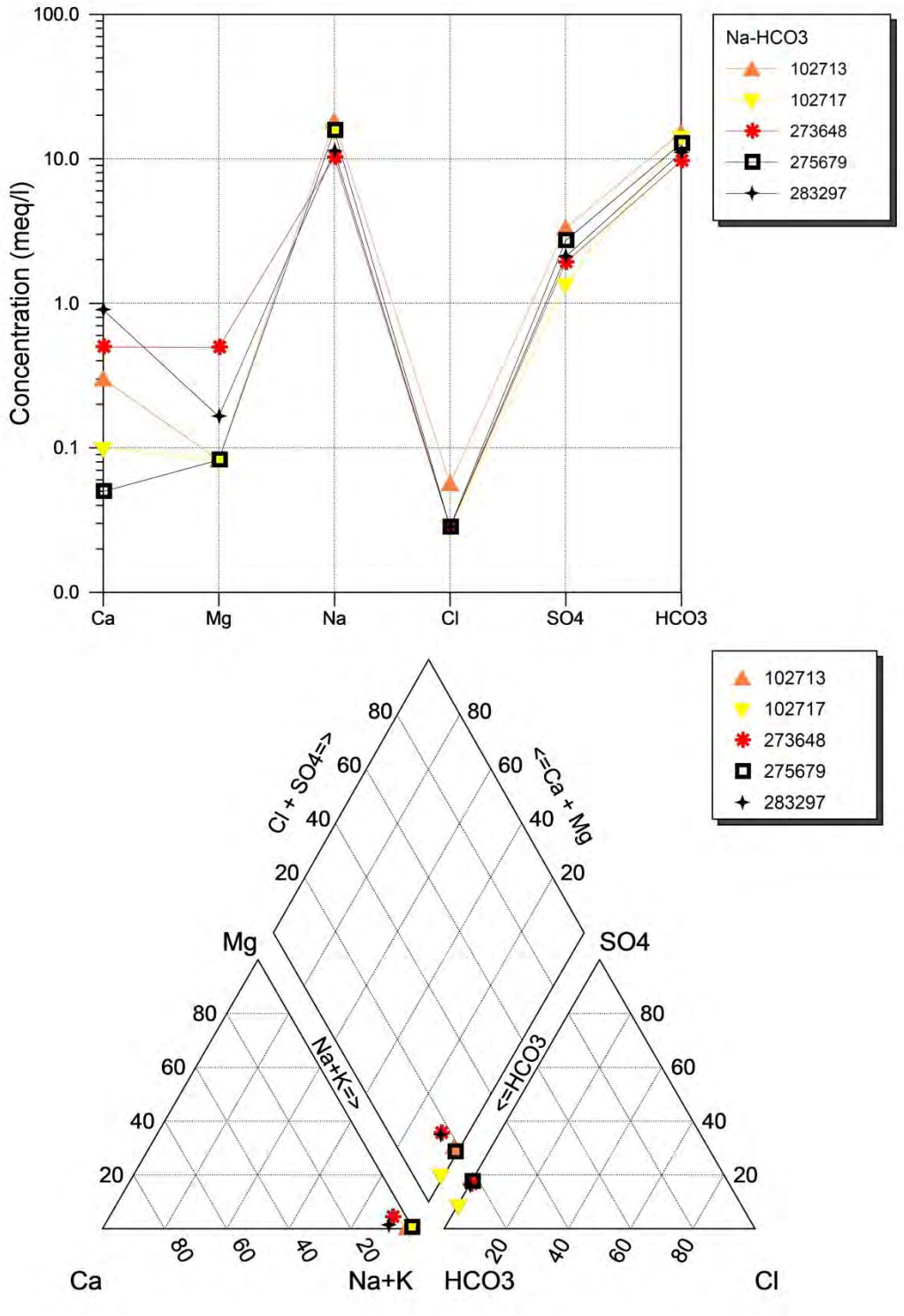

Figure C.2: Paskapoo Formation Wells – Na-HCO_3 Water.

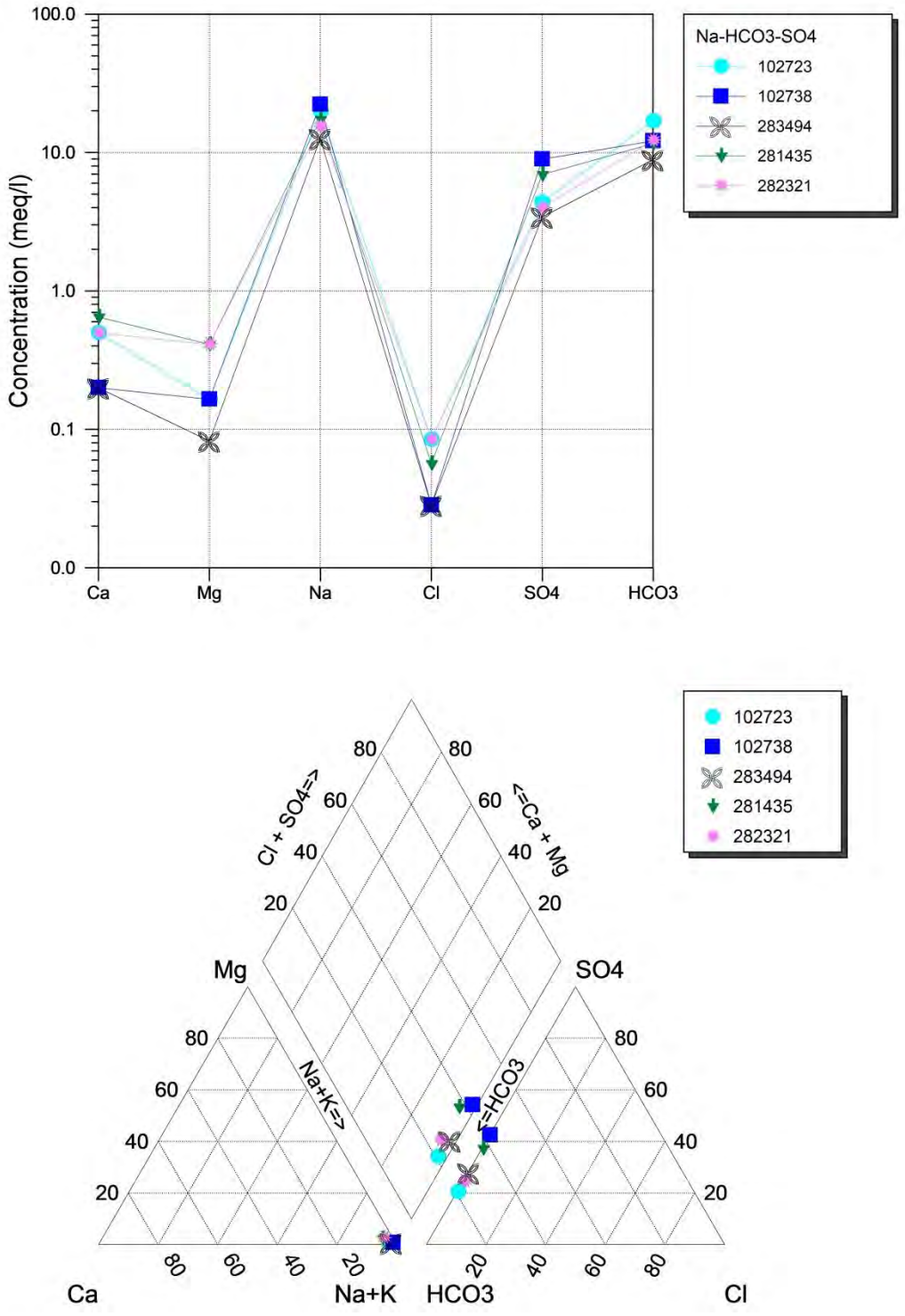

Figure C.3: Paskapoo Formation Wells – Na-HCO_3-SO_4 Water.

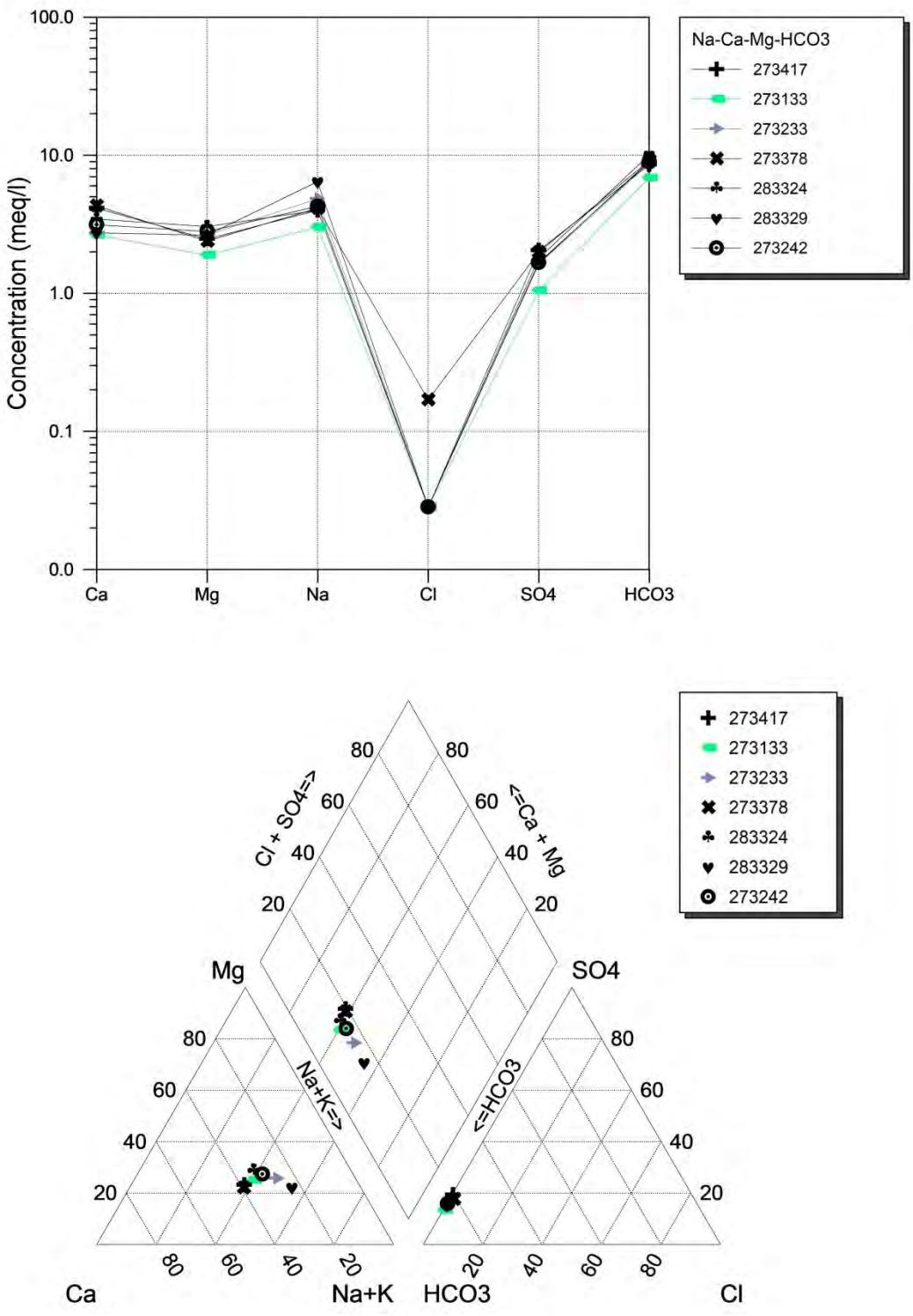

Figure C.4: Paskapoo Formation Wells – Na-Ca-Mg-HCO_3 Water.

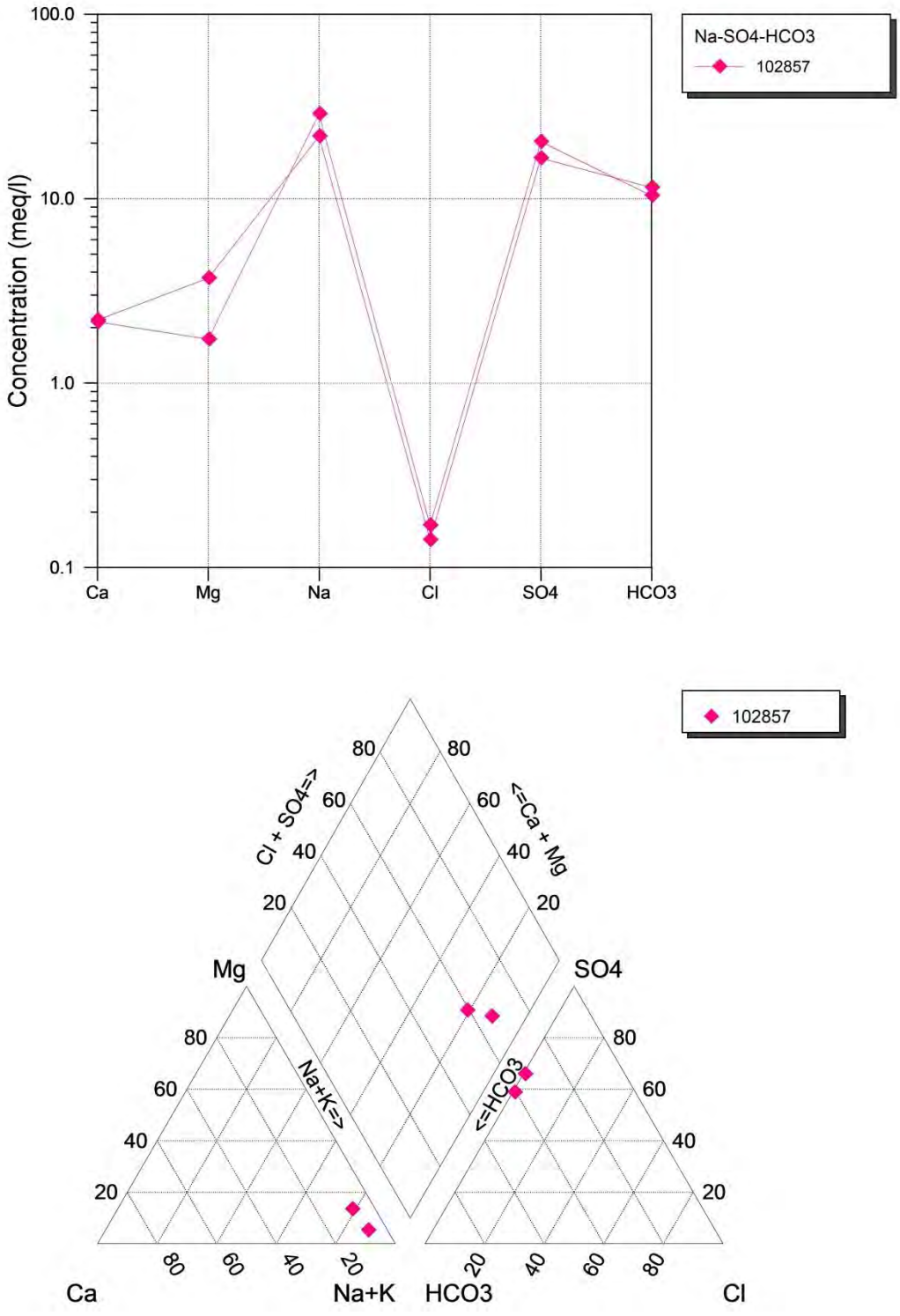

Figure C.5: Paskapoo Formation Wells – Na-SO_4-HCO_3 Water.

Alberta Innovates Technology Futures

Well Number	Bicarbonate (mg/L)	Calcium (mg/L)	Carbonate (mg/L)	Chloride (mg/L)	Electrical Conductivity (µS/cm)	Fluoride (mg/L)	Ion Balance	Iron (mg/L)	Magnesium (mg/L)	pH	Potassium (mg/L)	Silica (mg/L)	Sodium (mg/L)	Sulphate (mg/L)	Total Alkalinity (mEq/L)	Total Dissolved Solids (mg/L)	Total Hardness (mg/L as CaCO3)	Water Type
102713	926.09396	5.99998	21.999	2.0022	1740	1.21	0.97	2.75	<1.000768	8.6	2.148	5.5	420	160.236	797	1068	15	Na-HCO3
102717	868.08265	1.99999		<1.0011	1378	1.06	1.01	0.62	<1.000768	8.1	1.228	9.6	360	65.0937	712	857	10	Na-HCO3
102723	1027.0981	9.99996	6.999	3.0033	1906	0.91	0.95	0.69	2.001536	8.4	1.944	8	454	209.302	854	1193	33	Na-HCO3-SO4
102738	739.07368	3.99998	12.999	<1.0011	2200	0.45	1.05	<0.05	2.001536	8.6	1.328	9.3	511	428.624	629	1325	18	Na-HCO3-SO4
102857	633.05931	42.9998	81.999	6.01015	2700	0.88	0.98	0.3	21.017344	8.5	2.048		663	976.42	653	2102	195	Na-SO4-HCO3
102857	701.06669	43.9998	32.001	5.0055	2700	0.38	0.95	0.8	45.036992	8.7	2.66		500	796.161	629	1770	296	Na-SO4-HCO3
273133	418.04031	52.9998		<1.0011	705	0.17	0.96	0.45	23.01888	7.9	2.252	10.8	69	50.0721	343	404	227	Na-Ca-Mg-HCO3
273233	533.04991	54.9998		1.0011	890	0.13	0.98	0.3	32.025792	7.3	2.556		111	78.1144	437	546	267	Na-Ca-Mg-HCO3
273242	544.05289	62.9997		<1.0011	917	0.16	0.97	2.55	34.028544	8.2	2.556	12.8	98.001	80.1154	446	546	297	Na-Ca-Mg-HCO3
273378	558.05226	85.9997		6.01015	1000	0.17	0.96	3.9	29.023488	8.1	1.944		94.999	95.137	458	595	331	Na-Ca-Mg-HCO3
273417	520.05137	82.9997		1.0011	850	0.15	1	<0.05	30.024256	7.9	2.66		92	98.1432	427	567	330	Na-Ca-Mg-HCO3
273648	590.06039	9.99996	6.999	<1.0011	1057	0.51	0.95	<0.02	6.004608	8.4	1.024	7.2	235	92.1356	495	642	50	Na-HCO3
275679	776.07375	1	9	1.0011	1399	0.82	1	0.5	1.000768	8.5	1.024	19.6	360	130.187	651	884	5	Na-HCO3
281435	709.0672	12.9999	12.999	2.0022	1744	0.27	0.97	0.25	5.00384	8.7	1.536	10.8	400	332.482	604	1116	54	Na-HCO3-SO4
282321	748.07502	9.99996	24	3.0033	1520	0.44	0.96	11.35	5.00384	8.6	2.252	12.8	355	192.28	654	960	46	Na-HCO3-SO4
283297	672.06713	17.9999		<1.0011	1129	0.19	0.94	0.56	2.001536	8	2.148	22	260	101.149	551	715	53	Na-HCO3
283324	553.05423	68.9997		<1.0011	894	0.18	0.98	0.56	37.030848	7.9	2.148	13.7	92	79.1149	454	552	323	Na-Ca-Mg-HCO3
283329	611.05944	54.9998		<1.0011	1008	0.2	1	0.22	32.025792	8.1	2.148	10.7	148	86.1231	501	625	269	Na-Ca-Mg-HCO3
283494	542.05124	3.99998	18.999	<1.0011	1213	1.15	0.99	<0.02	<1.000768	8.7	1.024	7.1	290	164.237	477	746	10	Na-HCO3-SO4

11. APPENDIX D – Mineralogical Analyses

The following is a record of the SEM microphotographs, the EDX analyses, the ICP-ms analyses, LECO and XRD analyses for the following samples collected form the sedimentary succession from the Leduc (D3-A) and Nisku (D2) reservoirs to Upper Belly River in the Clive oil field, and include both the aquifers and aquitards in the succession.

Sample #	Well Location	Depth (m)	Formation
EN-1	6-13-41-25W4	~ 1864.00	Calmar
EN-2	6-13-41-25W4	~ 1860.50	Calmar
EN-3	6-13-41-25W4	~1855.00	Wabamun
EN-4	11-5-41-23W4	~ 1492.00	Ellerslie
EN-5	11-5-41-23W4	~ 1478.00	Ostracod
EN-6	11-5-41-23W4	~1474.00	Ostracod
EN-7	11-5-41-23W4	~ 1463.30	Glauconitic Sandstone
EN-8	11-12-41-25W4	~ 1388.00	Viking
EN-9	9-35-41-23W4	~695.25	Basal Belly River Sandstone
EN-10	9-35-39-24W4	~1847.00	Nisku
EN-11	9-35-39-24W4	~1876.50	Leduc
EN-30	6-7-40-24W4	~1570.50	lowermost Upper Mannville
EN-31	8-6-40-25W4	~1448.00	Colorado shales
EN-32	12-17-39-24W4	~1401.90	Viking Fm. shale
EN-33	7-14-41-23W4	~548.00	Upper Belly River Sst.
EN-34	12-5-39-23W4	~748.50	lowermost Upper Belly River

11.1 Sample EN-1

Sample EN-1 was sampled from core extracted from the Calmar Formation at a depth of approximately 1864 meters in well 6-13-41-25W4.

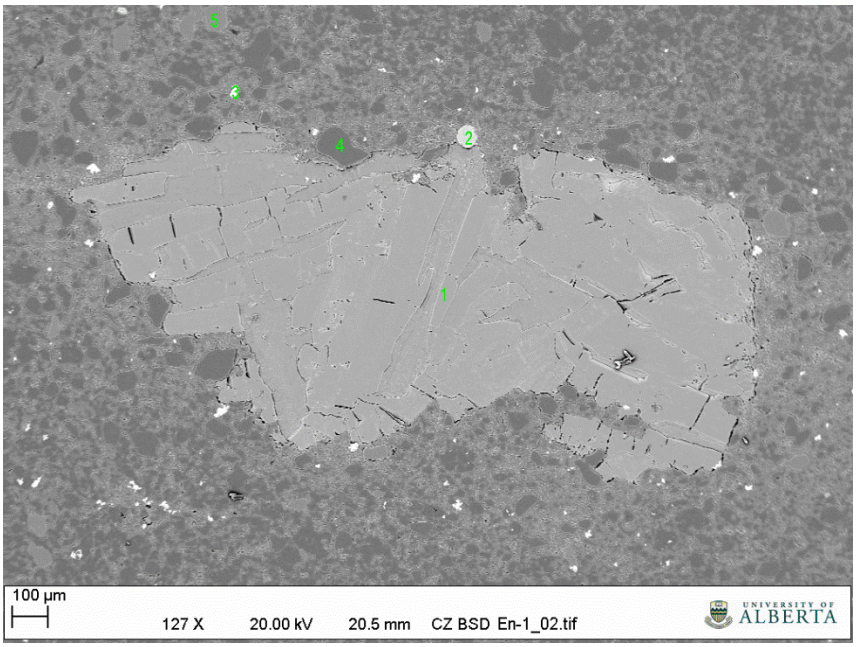

Figure D 1: A 100X image of the central grain in sample EN-1, with the EDX analyses positions identified.

The large central grain in Figure D 1 is a calcium sulphate mineral, and is probably anhydrite.

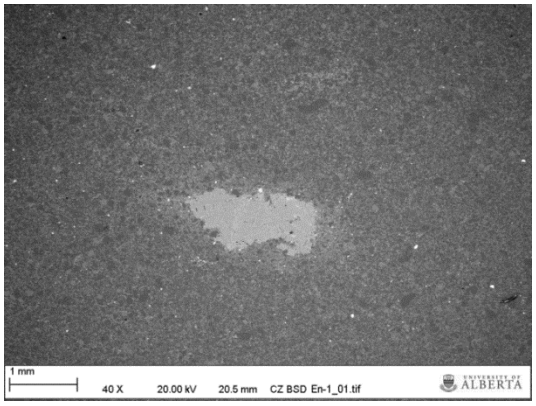

Figure D 2: A 40X magnification of sample EN-1.

Figure D 2 is at lower magnification than Figure D 1. No other grains of anhydrite can be seen.

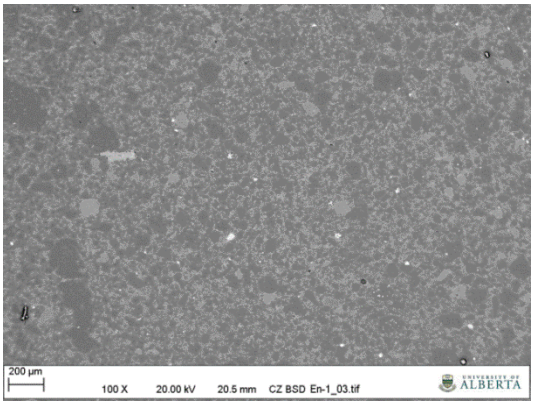

Figure D 3: A 100 X magnification of the matrix.

Figure D 3 is a 100 X magnification of the matrix, which can be seen in Figure D 2 and Figure D 1. A mineralogical assessment would be predominately quartz with significant potassium feldspar. There are large, but isolated calcium sulphate grains (anhydrite) occurring infrequently

through the matrix. The matrix was found to be visually consistent across the remained of the sample, suggesting that it (the matrix) is relatively mineralogical homogeneous.

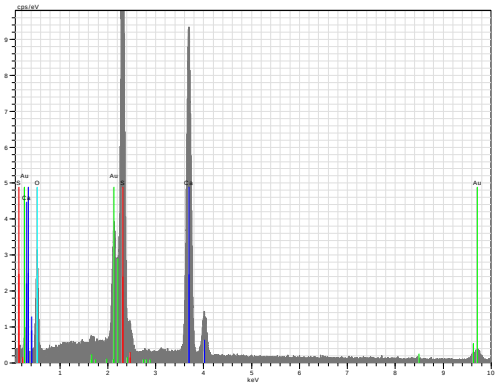

Figure D 4: An EDX analysis of point 1.

This mineral is a calcium sulphate phase, most likely anhydrite.

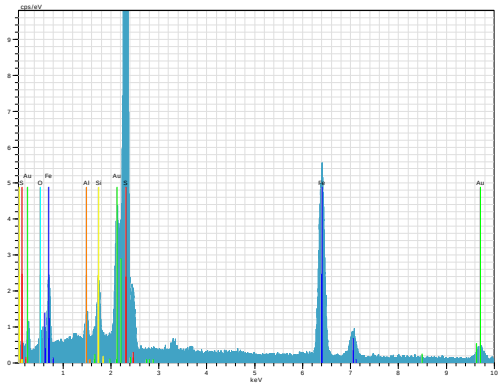

Figure D 6: An EDX analysis of point 3.

This mineral is an iron sulphide, either pyrite (most likely) or pyrrhotite.

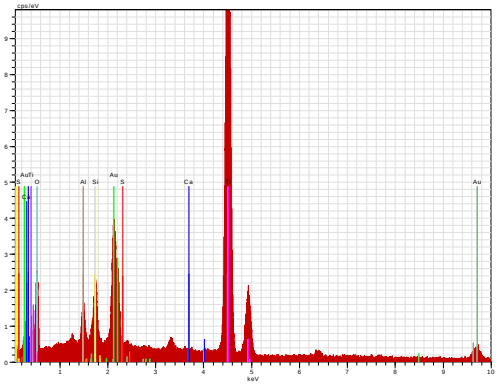

Figure D 5: An EDX analysis of point 2.

This mineral is a titanium oxide, either rutile or anatase.

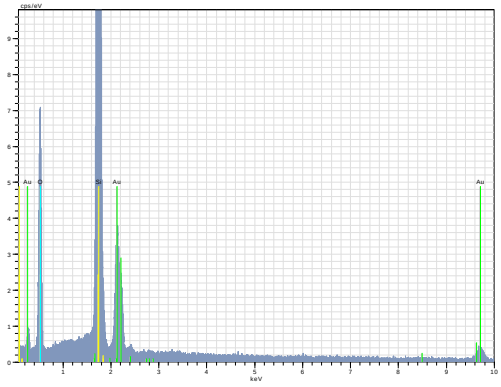

Figure D 7: An EDX analysis of point 4.

This mineral is quartz.

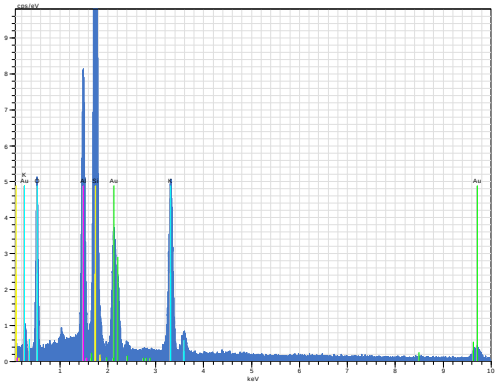

Figure D 8: An EDX analysis of point 5.

This mineral is potassium feldspar. Other spot analysis were made and identified additional grains of quartz, iron sulphide and potassium feldspar.

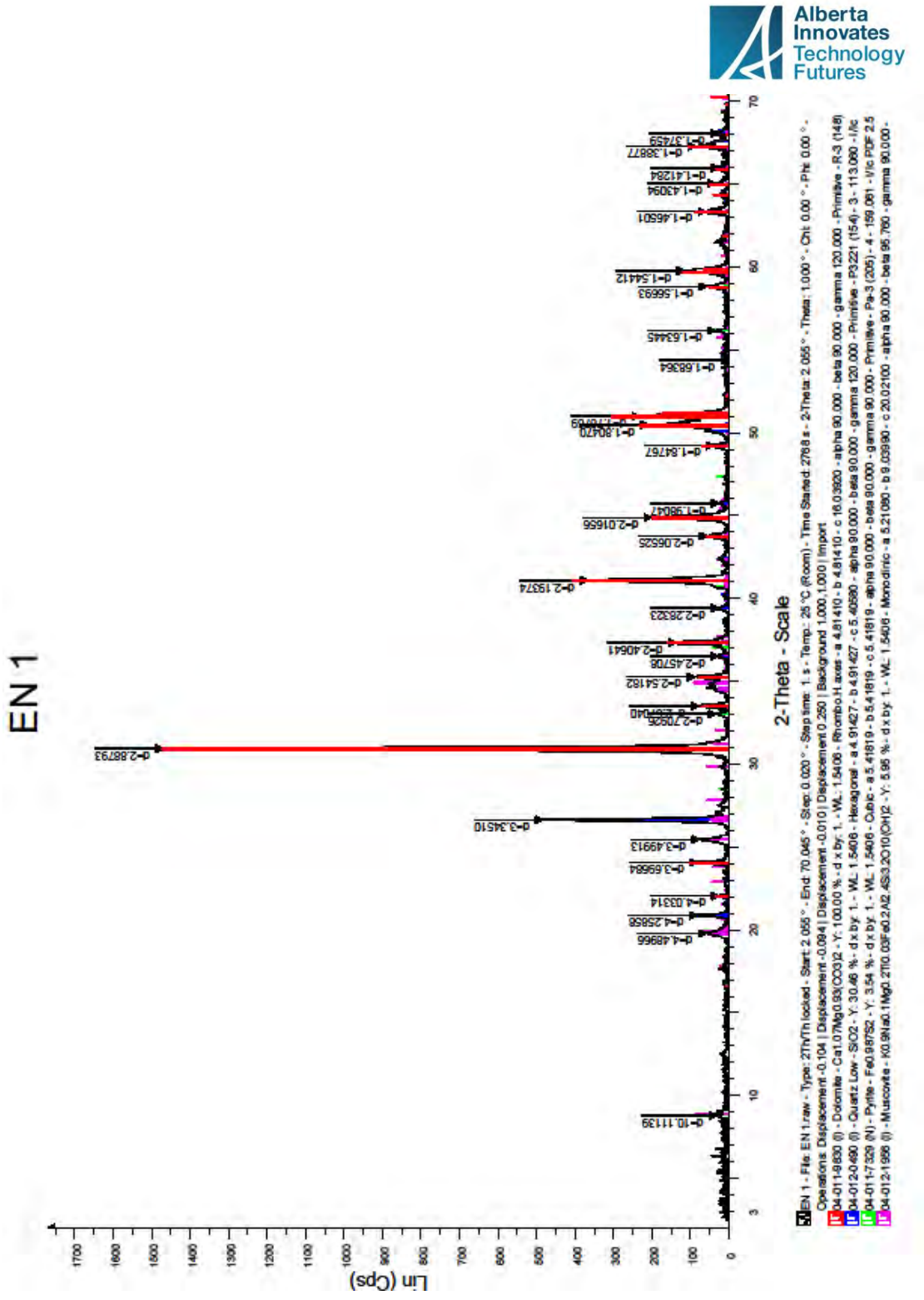

Figure D 9: X-Ray Diffraction pattern for sample EN-1.

Based on the XRD data, the relative proportions and identity of the minerals are: 70% dolomite, 20% quartz, 5% pyrite and 5% illite.

11.2 Sample EN-2

Sample EN-2 was sampled from core at a depth of approximately 1860.5 meters form the Calmar Formation in well 6-13-41-25W4.

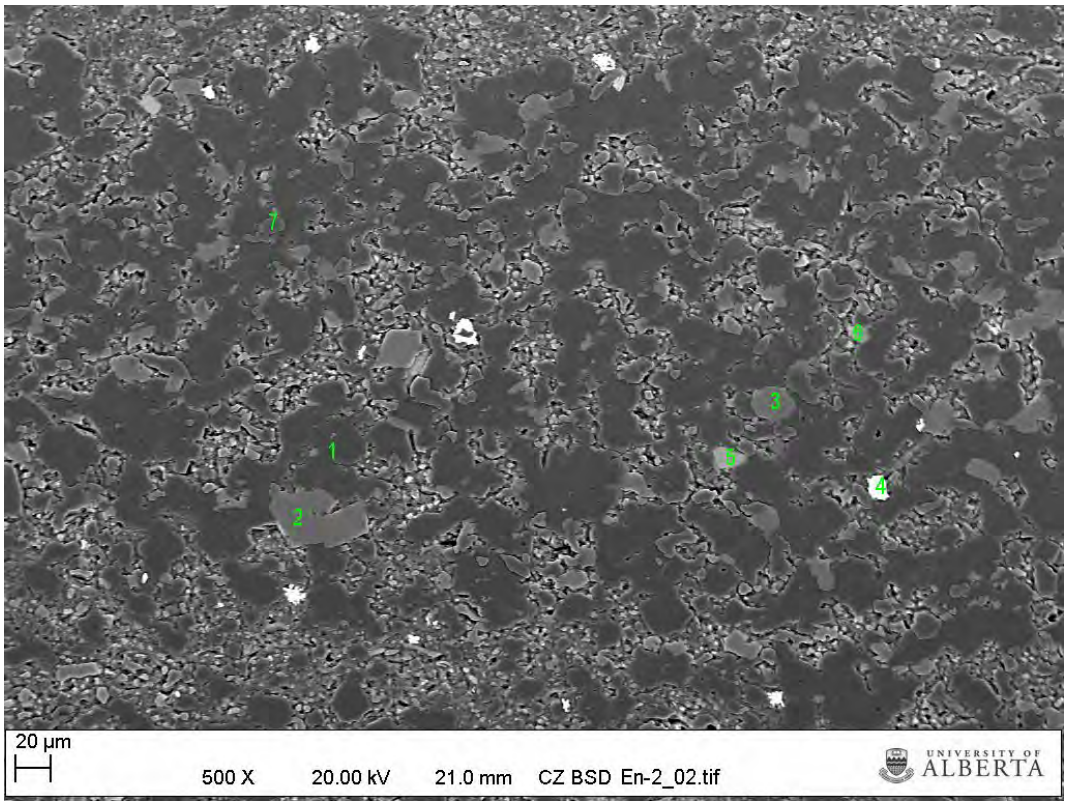

Figure D 10: A 500X magnification of sample EN-2. The green numbers refer to the location of the EDX analyses.

The sample did not polish as well as sample EN-1. The EDX analysis at point 2 was not recorded, however, the mineral was noted to be potassium feldspar and the same as point 3.

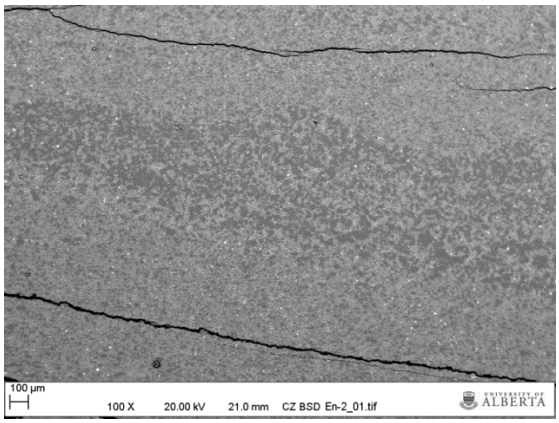

Figure D 11: A 100X magnification of sample EN-2.

Bedding effects can be clearly seen in this figure.

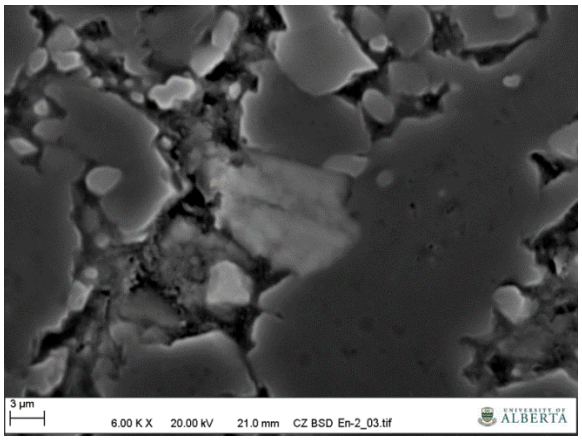

Figure D 12: A high magnification of the minerals at EDX analysis point 6.

The principal grain in the center of

Figure D 12 (point 6) is smaller than the effective beam diameter, thus the analysis at point 6 contains elemental signals from other mineral grains.

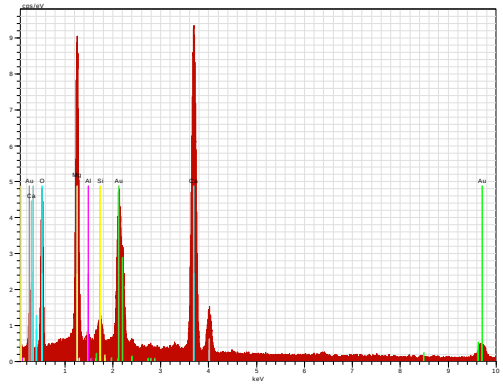

Figure D 13: Point 1 in Figure 10.

The mineral is a grain of dolomite.

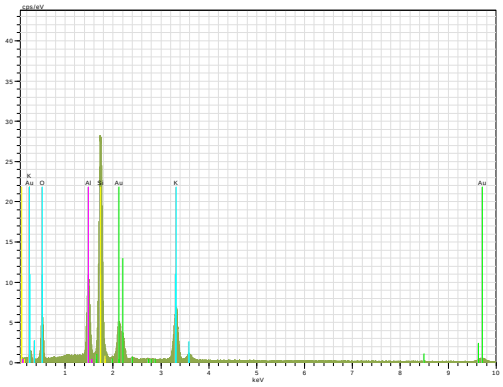

Figure D 14: EDX analysis at point 3.

The mineral is a grain of potassium feldspar.

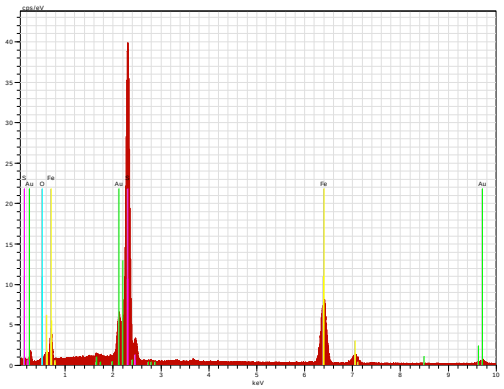

Figure D 15: EDX analysis at point 4.

The mineral is a grain of iron sulphide, probably pyrite.

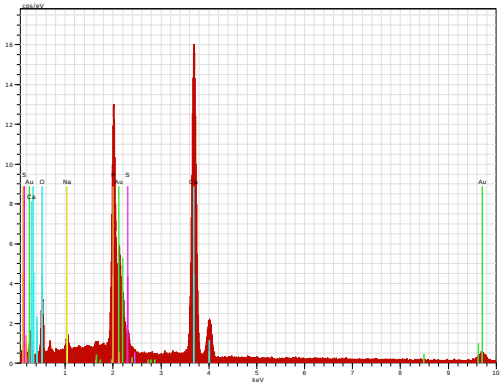

Figure D 16: EDX analysis at point 5.

The mineral is a grain of calcium phosphate, probably apatite.

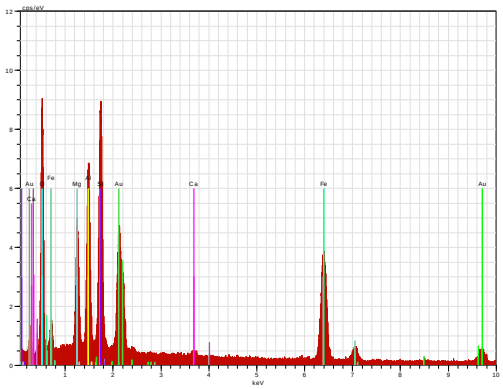

Figure D 17: EDX analysis at point 6.

As was noted in the text following

Figure D 12, the minerals examined and analyzed at point 6 are smaller than the beam size. Thus, it is not clear from Figure D 17 what the identity and composition of the mineral is, and it is believe that more than one mineral was included in the analytical results.

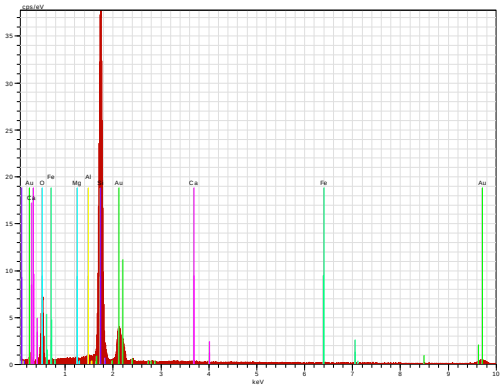

Figure D 18: EDX analysis at Point 7.

The mineral is quartz.

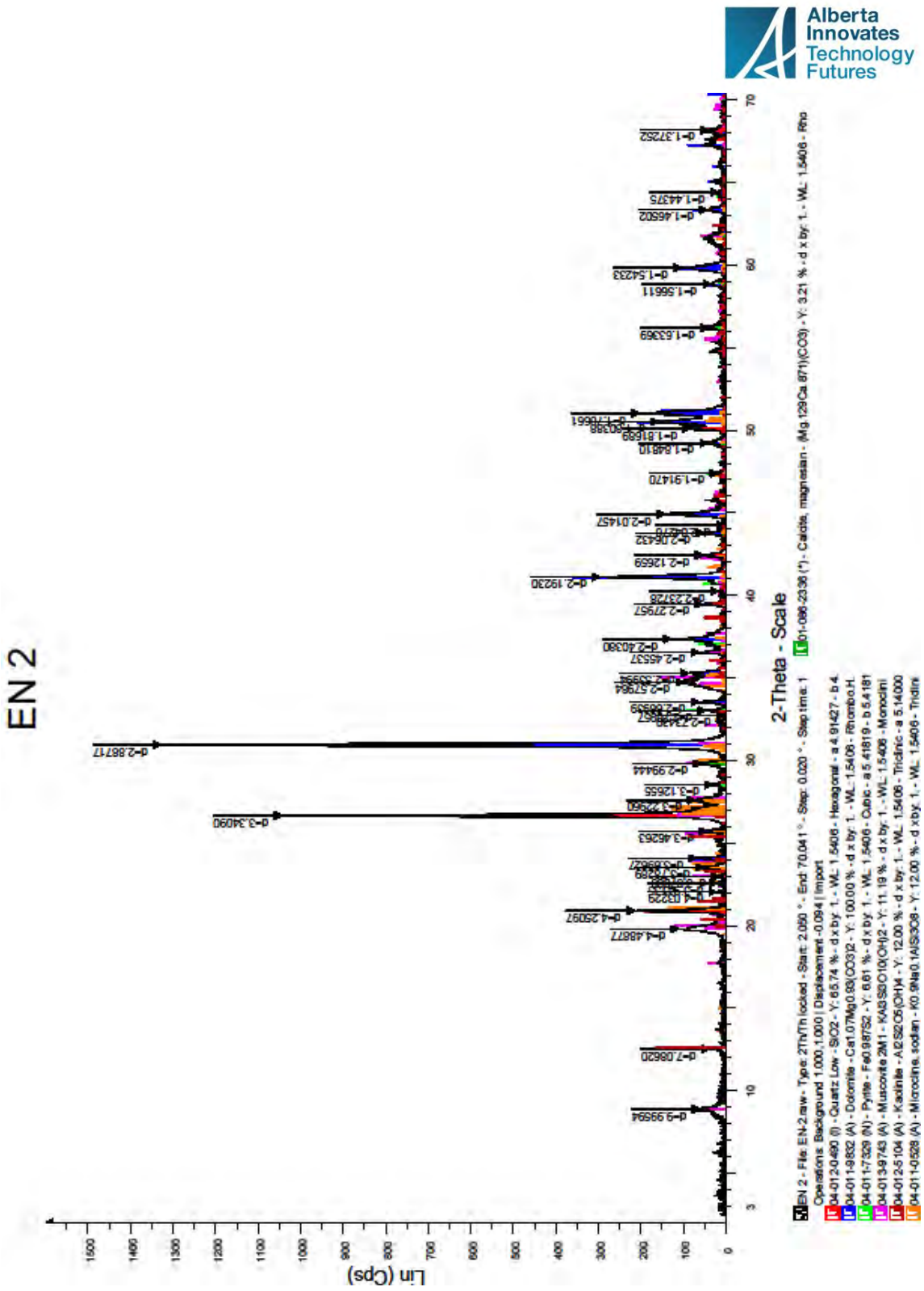

Figure D 19: X-Ray Diffraction pattern for sample EN-2.

Based on the XRD results, the mineralogy and the relative phase abundance is 50% dolomite, 30% quartz, 5% illite, 5% potassium feldspar, 5% calcite and 5% pyrite. A trace amount of kaolinite is also present.

11.3 Sample EN-3

Sample EN-3 was sampled from core at a depth of approximately 1855 meters, at well location 6-13-41-25W4. The formation is the Wabamun formation.

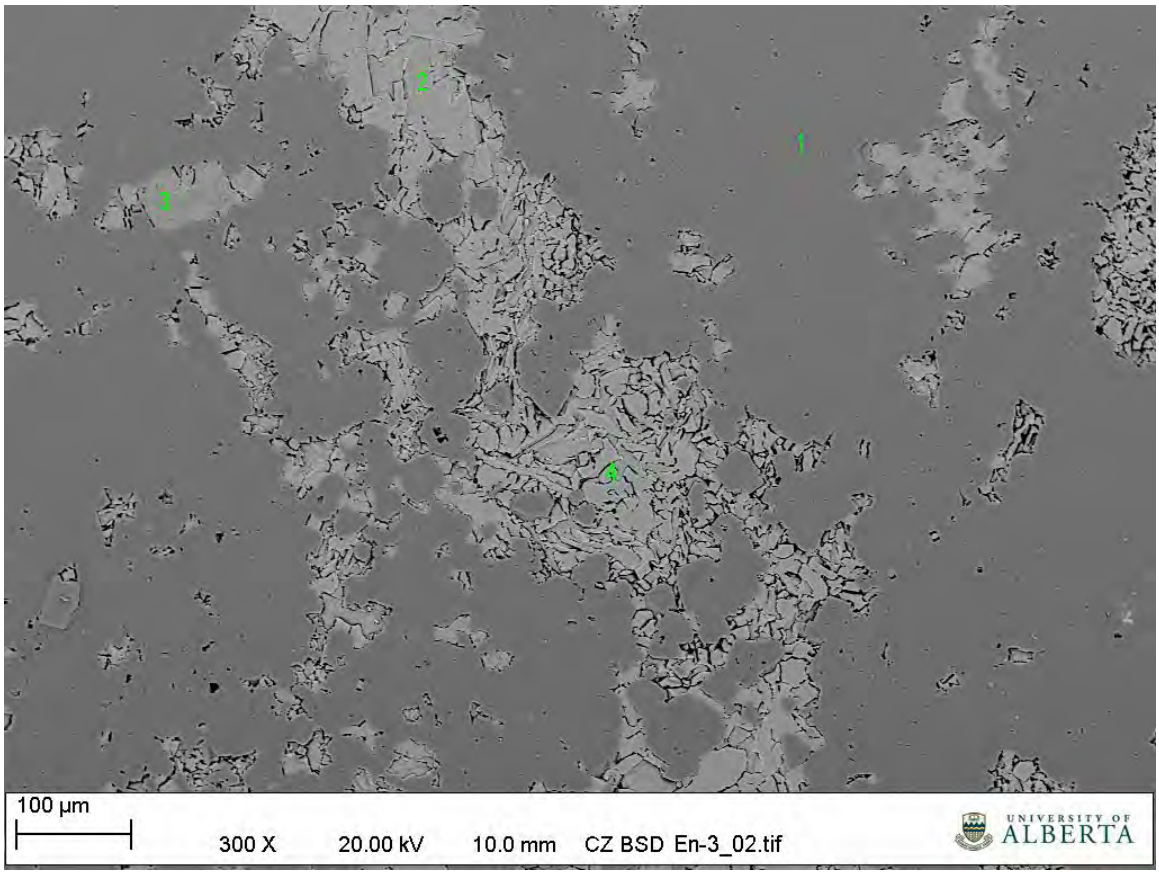

Figure D 20: A 300x magnification of sample EN-3. The green numbers refer to the spot EDX analyses reported below.

Note the lack of visible grain boundaries in the matrix in Figure D 20.

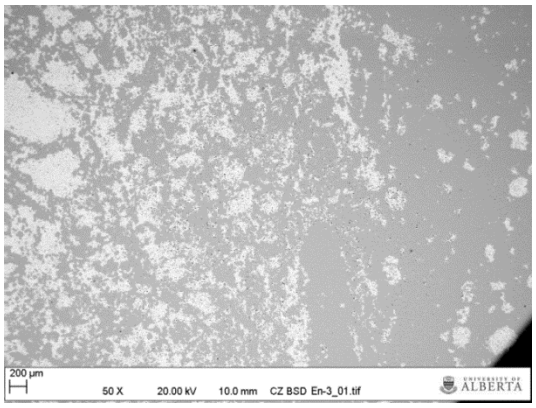

Figure D 21: A 50X magnification of sample EN-3.

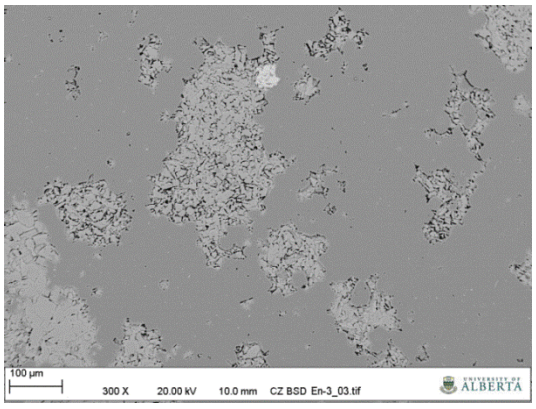

Figure D 22: A 300X magnification of a portion of EN-3.

In Figure D 22, a large grain of iron sulphide (pyrite) was observed in the upper center portion of the slide. Although it was analyzed, the EDX spectrum was not kept. Pyrite was not noticed elsewhere on the slide.

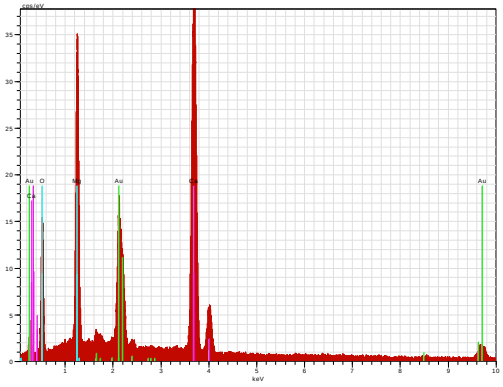

Figure D 23: EDX analysis at point 1.

The grain is dolomite.

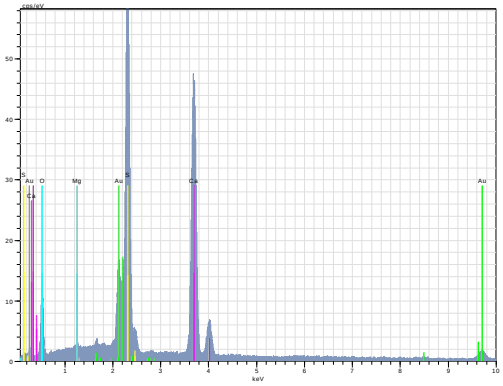

Figure D 24: EDX analysis at point 2.

The grain is calcium sulphate (anhydrite).

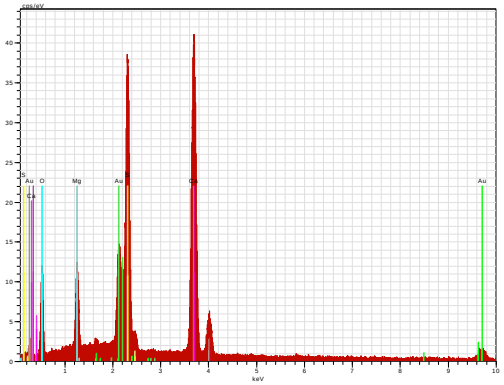

Figure D 25: EDX analysis at point 3.

The grain is calcium sulphate (anhydrite) with some magnesium present.

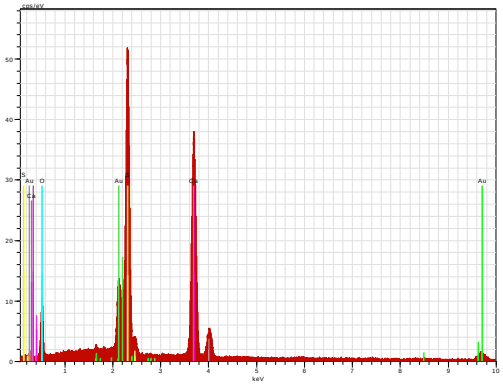

Figure D 26: EDX analysis at point 4.

The grain is calcium sulphate (anhydrite) with some magnesium present.

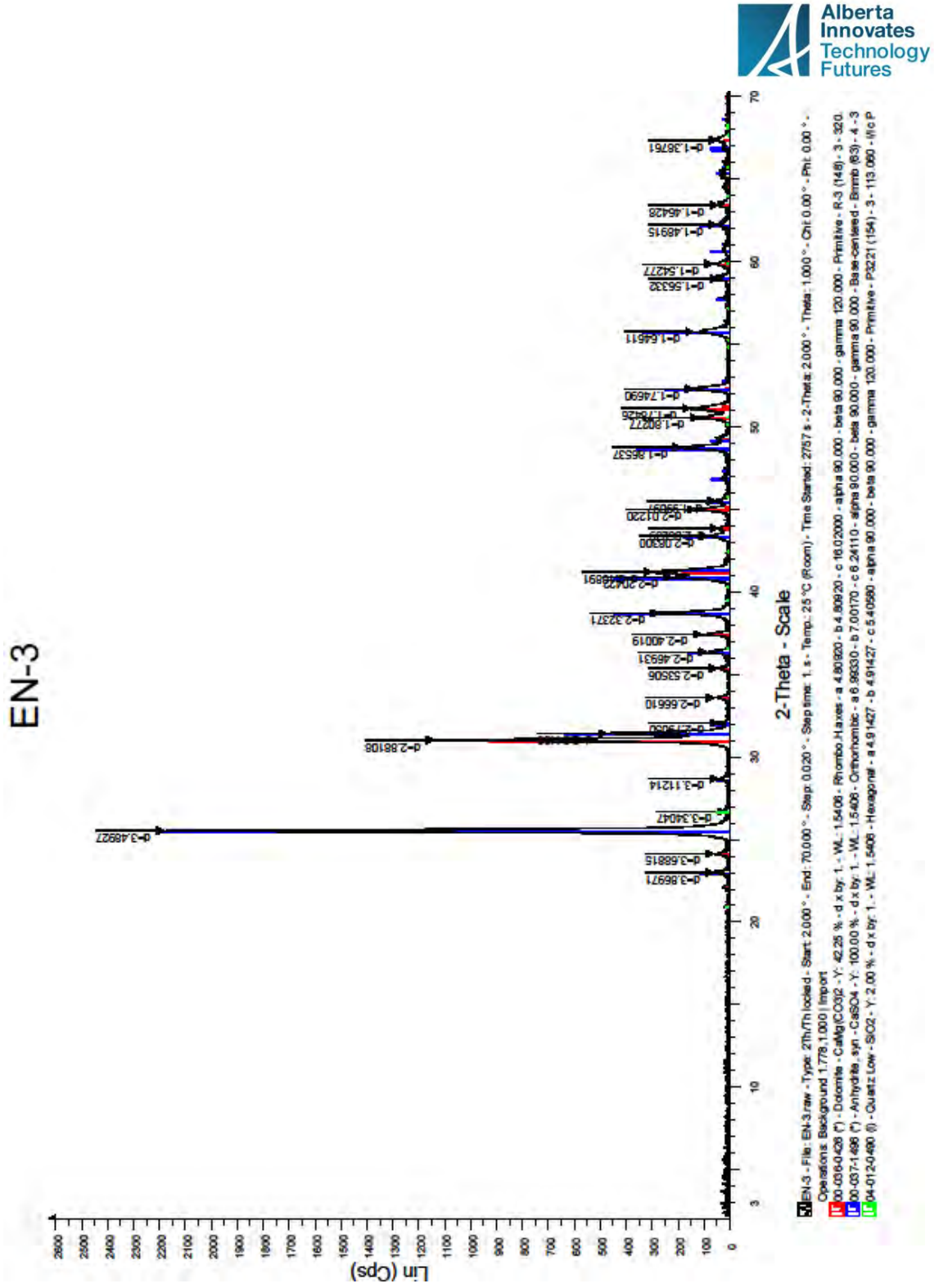

Figure D 27: X-Ray Diffraction pattern for sample EN-3.

Based on the XRD results, the mineralogy is primarily anhydrite (65%), with the remainder dolomite (35%). A trace amount of quartz (< 1%) was also noted.

11.4 Sample EN-4

Sample EN-4 was sampled from Ellerslie Formation core at a depth of approximately 1492 meters in well location 11-5-41-23W4.

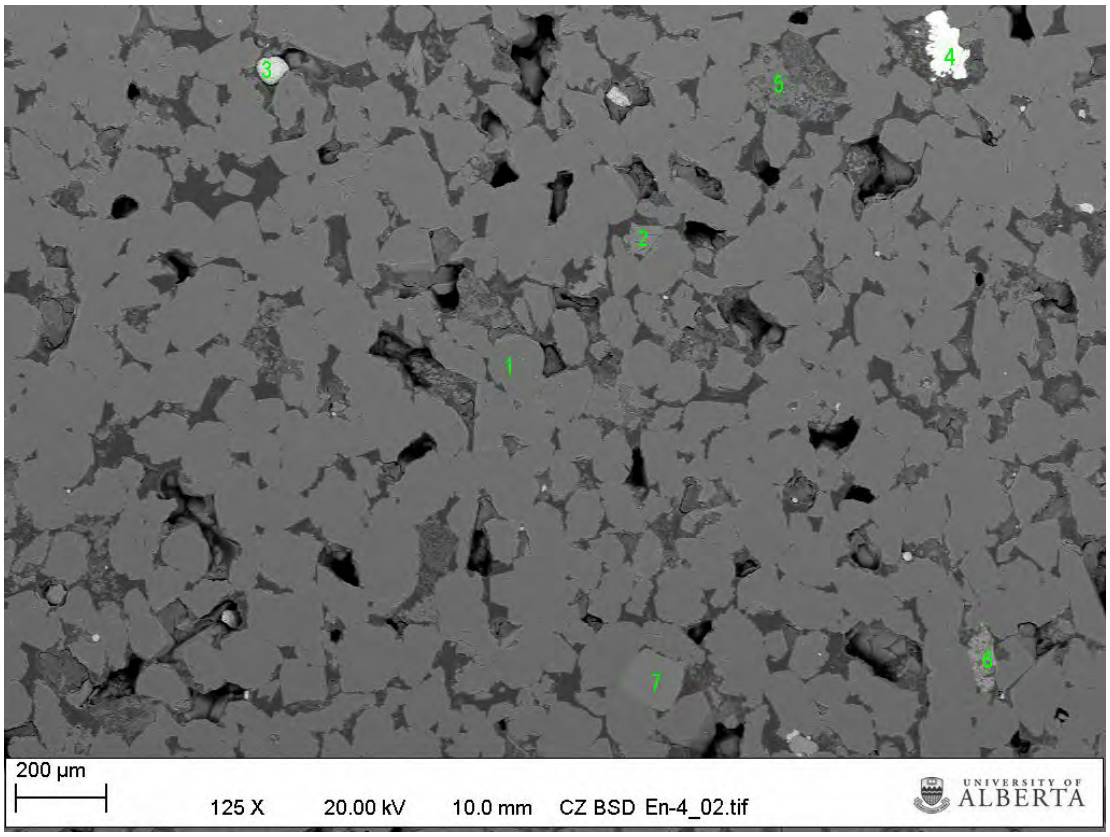

Figure D 28: A 125X view of sample EN-4, with the EDX analytical positions identified.

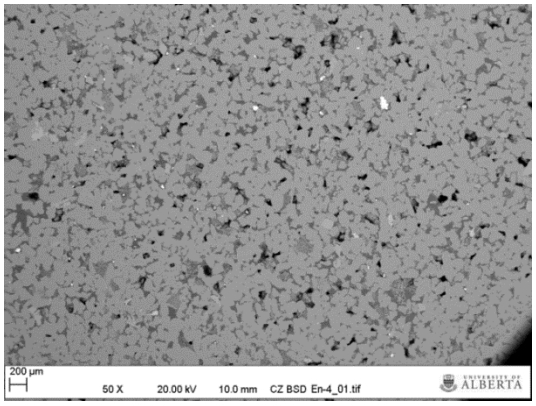

Figure D 29: A 50X overview of sample EN-4

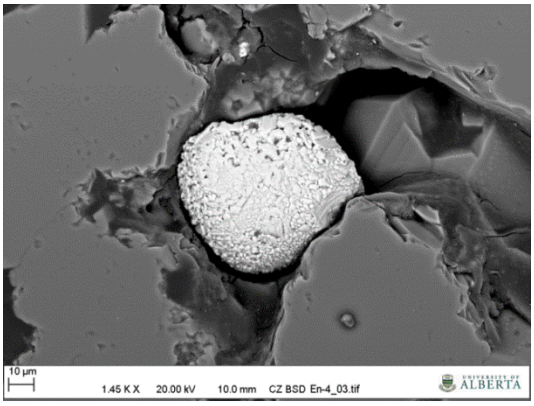

Figure D 30: A high magnification of an unusual mineral grain at position 3.

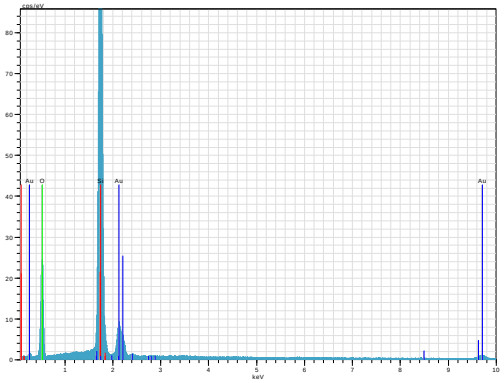

Figure D 31: EDX analysis of position 1.

The mineral is quartz.

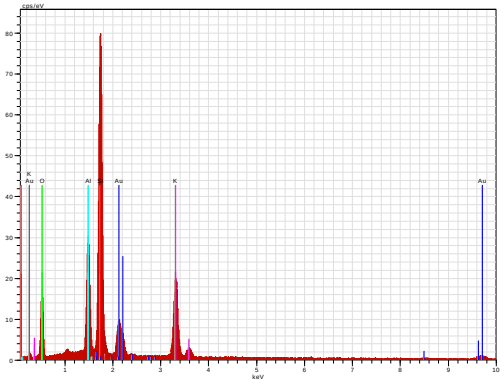

Figure D 32: EDX analysis of position 2.

The mineral is potassium feldspar.

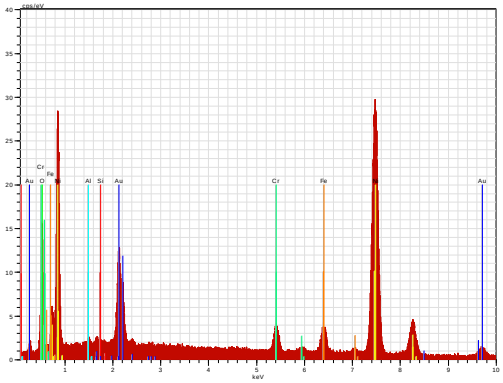

Figure D 33: EDX analysis of position 3.

The analysis of point 3, shown in more detail in Figure D 30, is composed of nickel and other metals. There is a similar grain about 2/3 of the distance from point 3 to point 5 in Figure D 28. Because of its unique composition, it is probably the result contamination either during drilling or sample preparation of the slide.

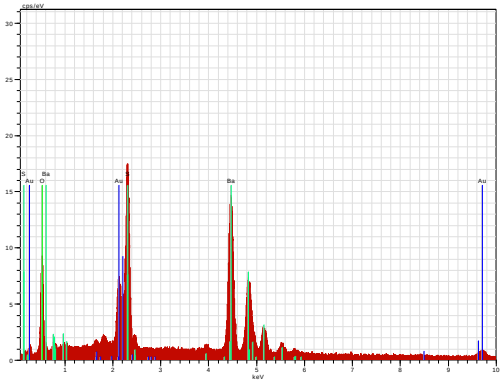

Figure D 34: EDX analysis of position 4.

The mineral phase is barite.

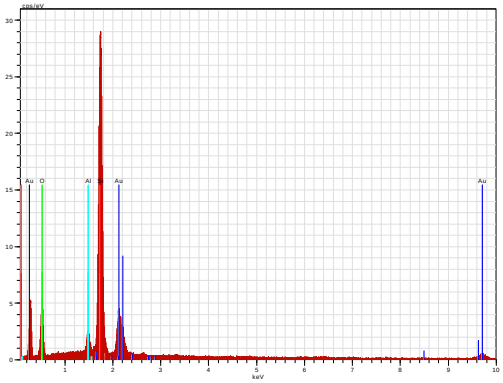

Figure D 35: EDX analysis of position 5.

The mineral phase is quartz, as are the grains surrounding it.

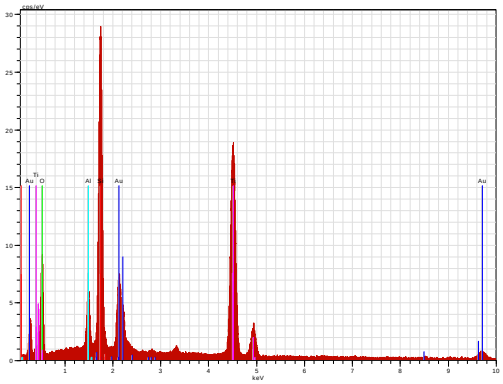

Figure D 36: EDX analysis of position 6.

The mineral phase is a mixture of quartz and titanium oxide (rutile or anatase).

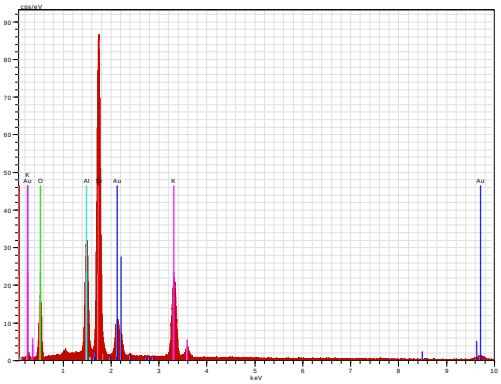

Figure D 37: EDX analysis of position 7.

The mineral phase is potassium feldspar.

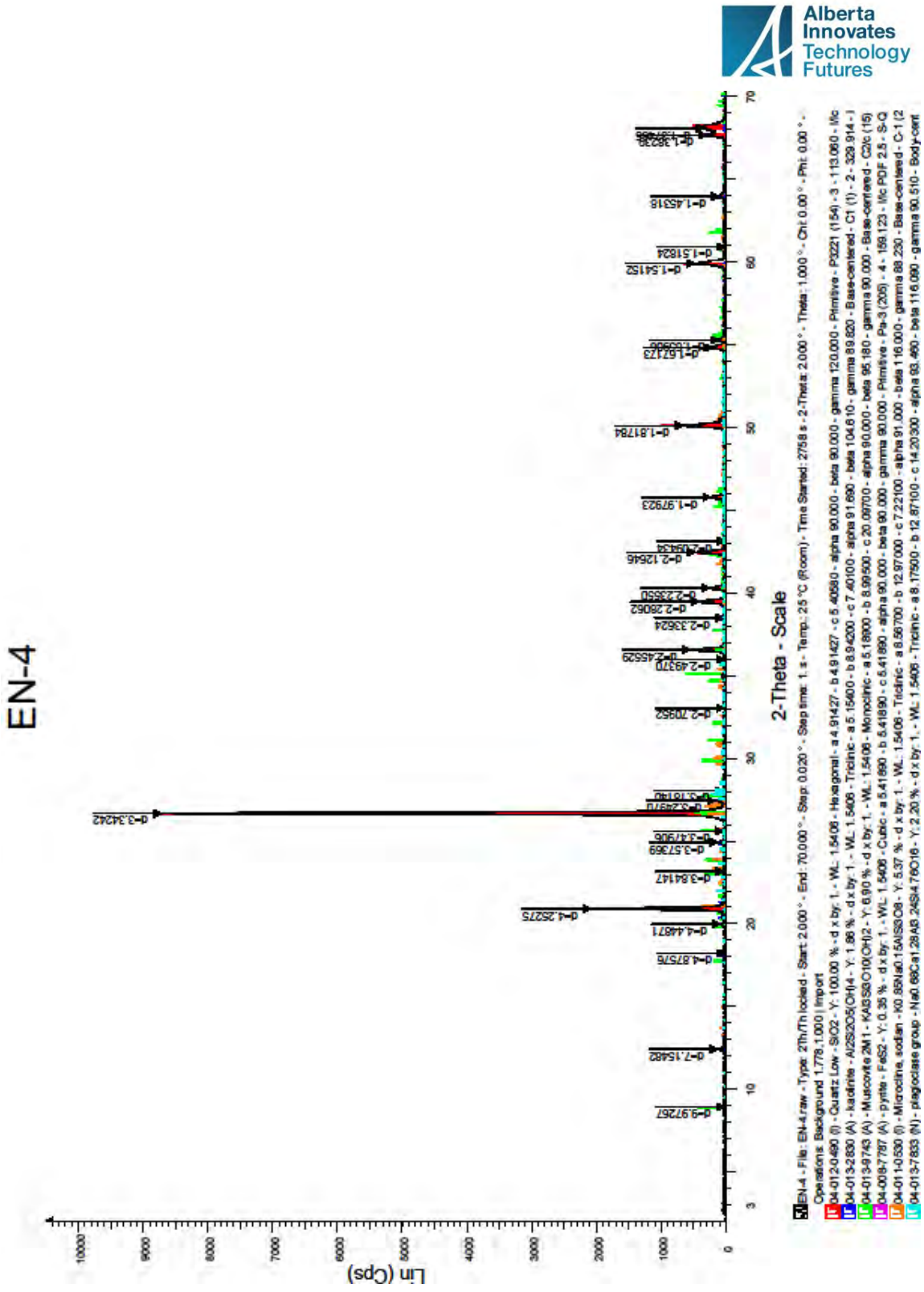

Figure D 38: X-Ray Diffraction pattern for sample EN-4.

Based on the XRD results, this sample is predominately quartz (90%). Kaolinite at 5% and 5% potassium feldspar was also noted. Trace amounts (< 1%) of illite, plagioclase and pyrite were also noted.

11.5 Sample EN-5

Sample EN-5 was sampled from core from the Ostracod Formation at a depth of approximately 1478 meters in well 11-5-41-23W4.

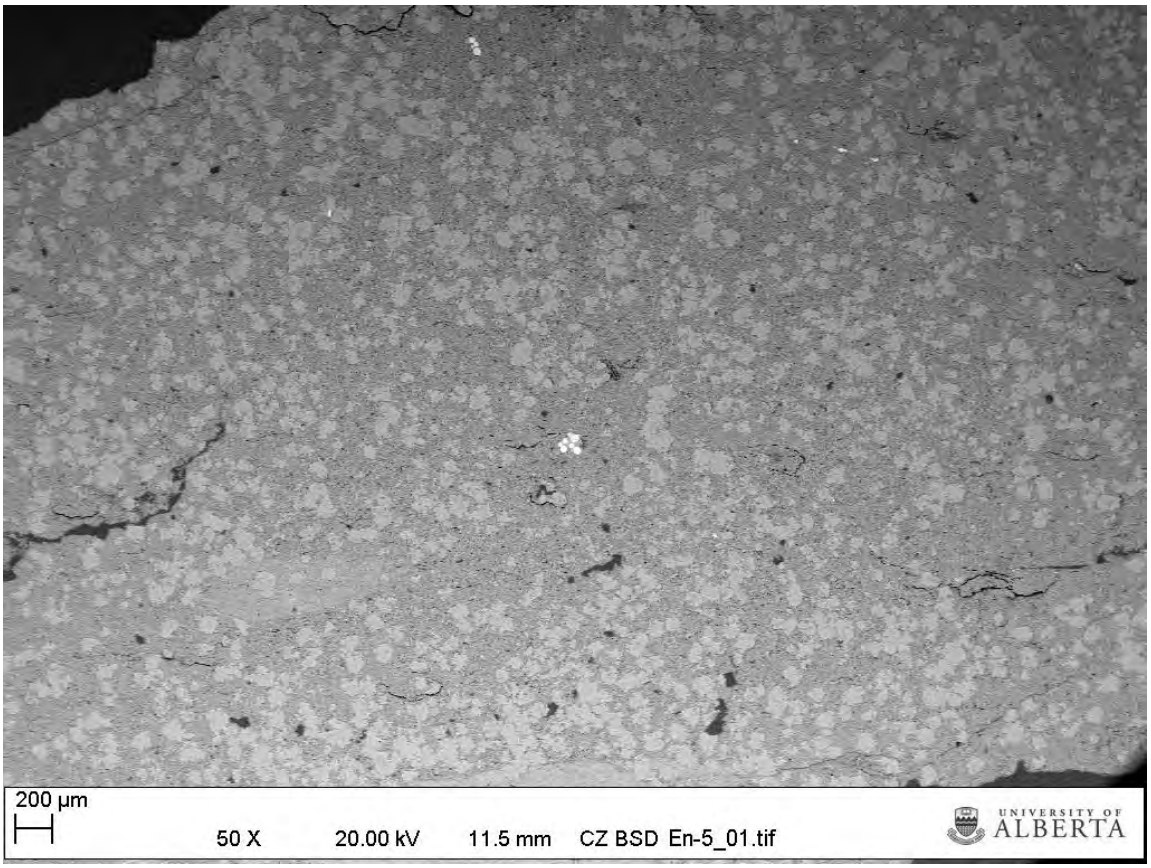

Figure D 39: 50X magnification of sample EN-5.

Unfortunately, the SEM image showing the locations of the EDX analyses was corrupted and could not be used. As a result, the location of the analytical EDX that follow could not be located on this image.

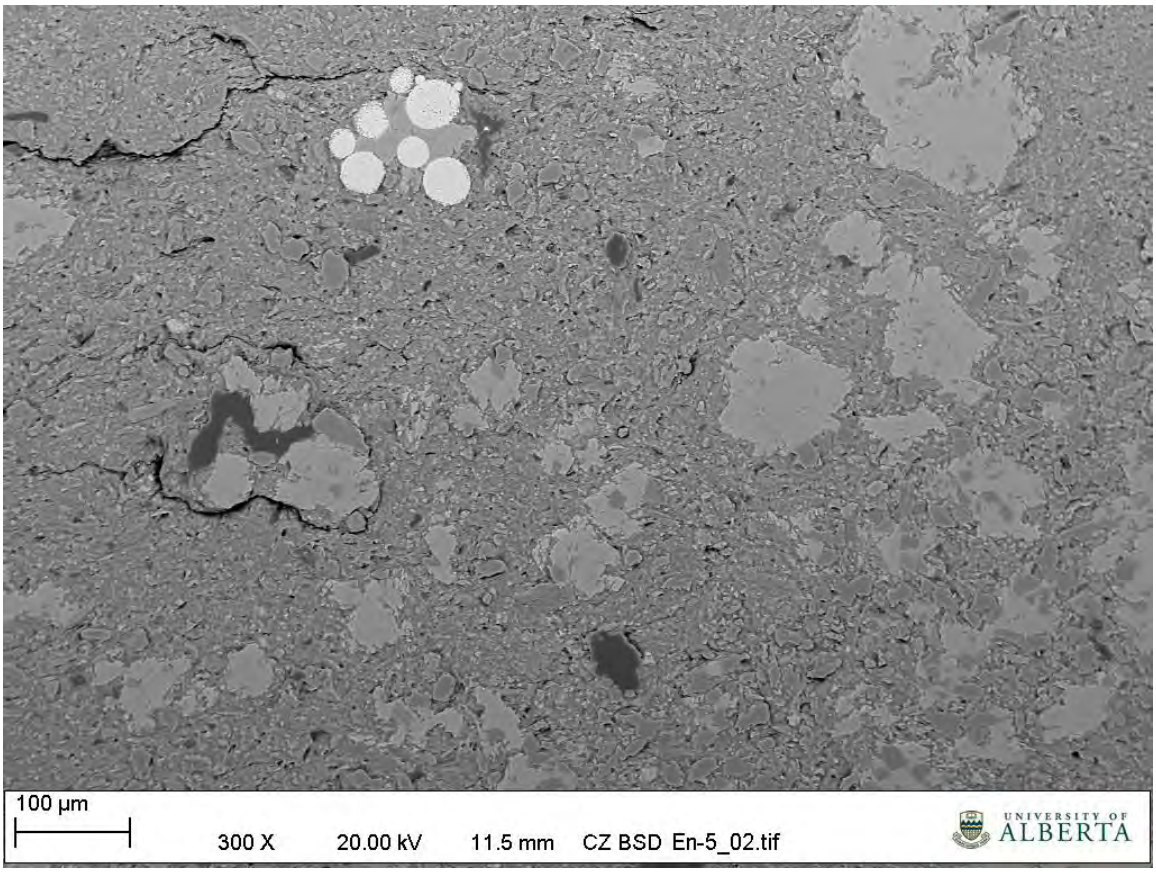

Figure D 40: 300X magnification of the framboidal pyrite at the center of the previous figure.

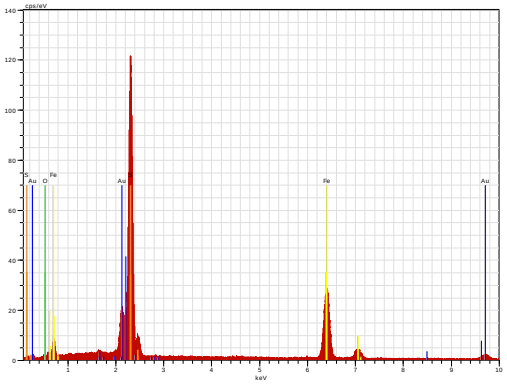

Figure D 41: EDX of the framboidal pyrite balls in the upper portion of the figure.

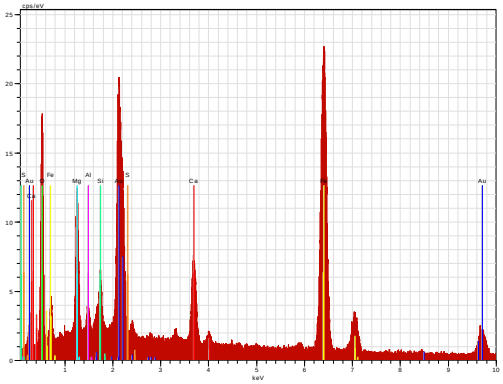

Figure D 42: EDX analysis of the matrix.

It is a complex mixture with major constituents being calcium, iron and magnesium. A smaller amount of silicon is present. The minerals could not be identified.

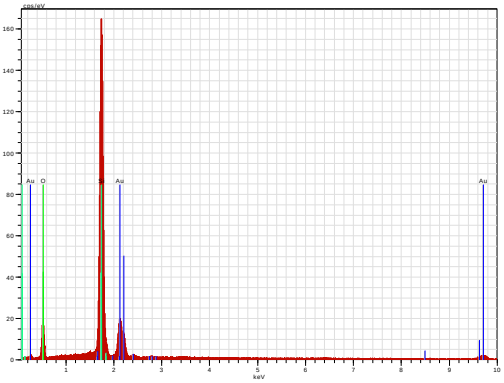

Figure D 43: EDX analysis of the large grains in the matrix.

The mineral is quartz.

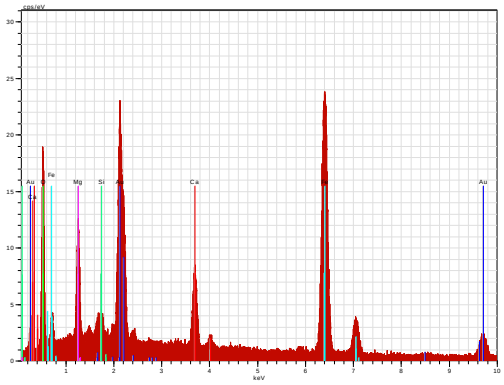

Figure D 44: A second EDX analysis of the matrix.

It is a complex mixture with major constituents being calcium, iron and magnesium. A smaller amount of silicon is present. The mineral(s) could not be identified.

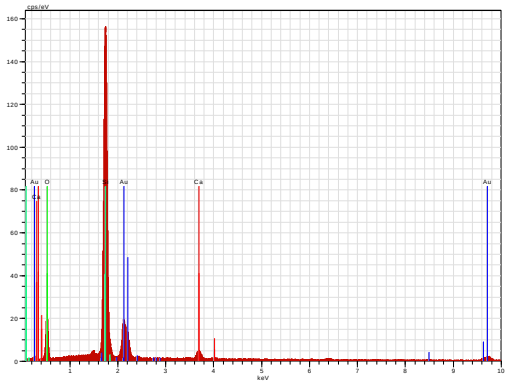

Figure D 45: A second EDX analysis of the large grains in the matrix.

The mineral is quartz.

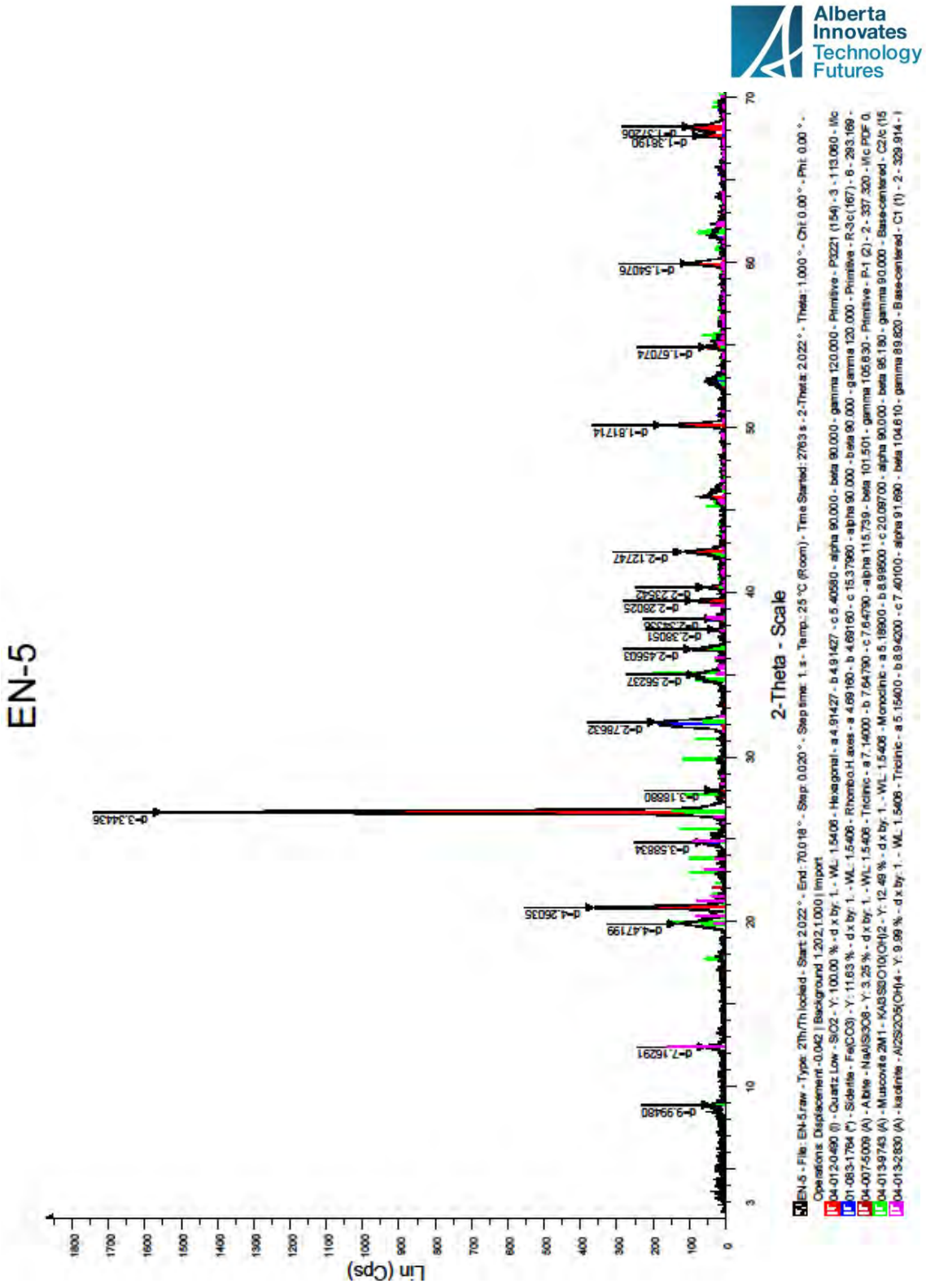

Figure D 46: X-Ray Diffraction pattern for sample EN-5.

Based on the XRD results, this sample is primarily composed of quartz (75%) and siderite (15%). Illite and kaolinite comprise 5% of the sample each. Trace amounts of plagioclase were also noted.

11.6 Sample EN-6

Sample EN-6 was sampled from core at a depth of approximately 1474 meters form the Ostracod Formation in well 11-5-41-23W4.

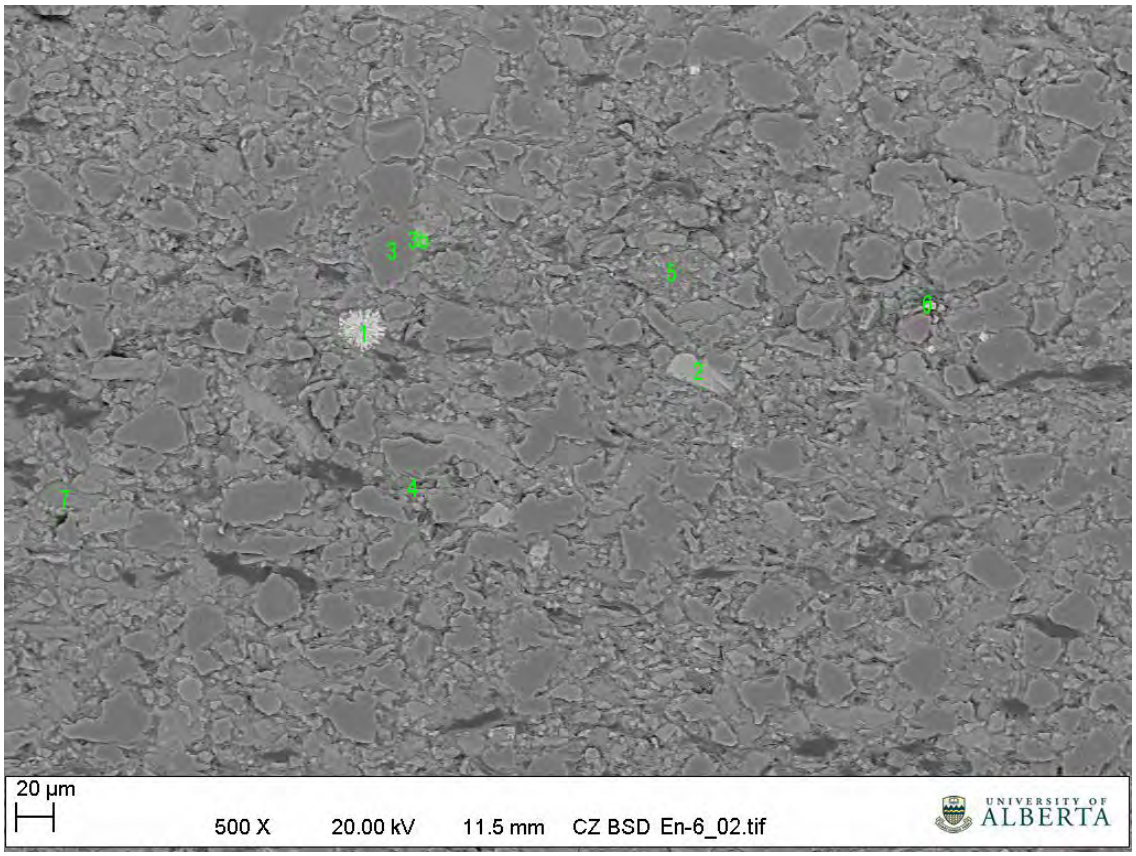

Figure D 47: A 500X view of Sample **EN-6, with the EDX analytical positions identified by numbers.**

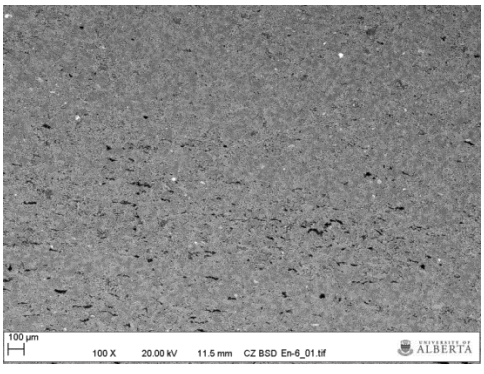

Figure D 48: 100X magnification of Sample EN-6.

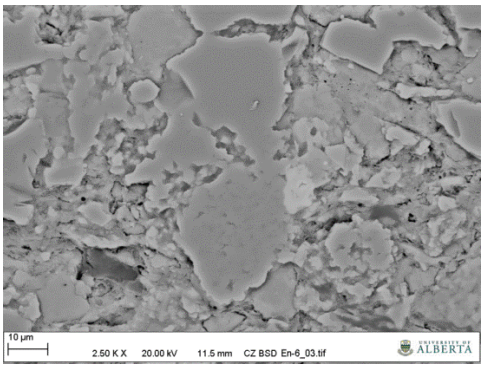

Figure D 49: Further magnification of the area around samples 3 and 3b. The location of Figure D 49 is slightly to the upper left of the center of Figure D 47.

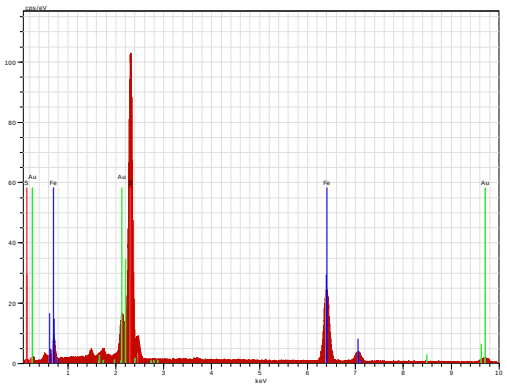

Figure D 50: EDX analysis at position 1.

The phase is pyrite.

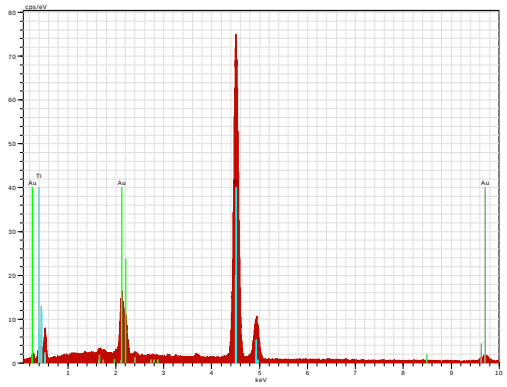

Figure D 51: EDX analysis at position 2.

The phase is composed of titanium and oxygen, and is either rutile or anatase.

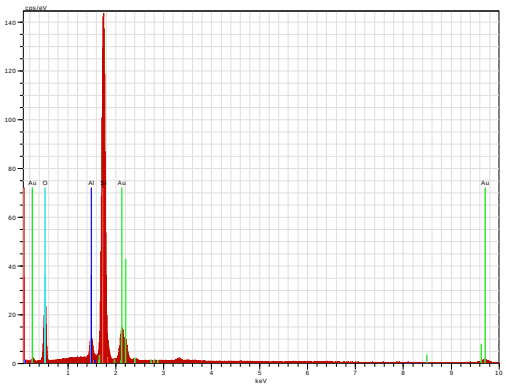

Figure D 52: EDX analysis at position 3.

The phase is quartz.

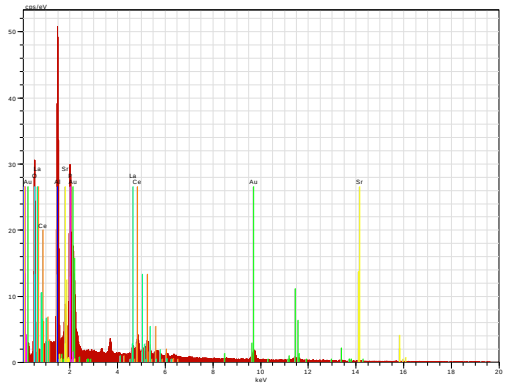

Figure D 53: EDX analysis at position 3b.

The high magnification resulted in a beam size greater than the mineral grains; hence the phases could not be identified.

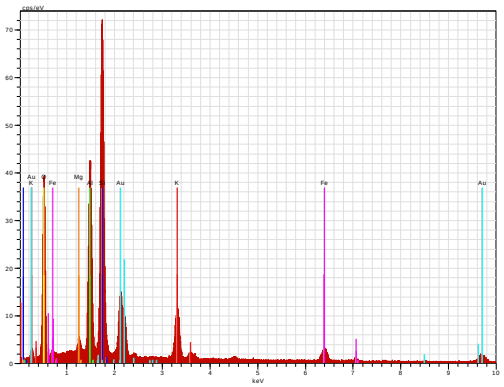

Figure D 54: EDX analysis at position 4.

The area analyzed comprises two or more phases, one is composed of titanium and oxygen, and the other is either a potassium clay or potassium feldspar.

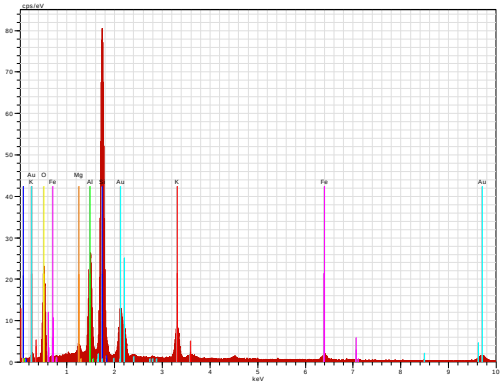

Figure D 55: EDX analysis at position 5.

The phase is composed of titanium and oxygen, and is either potassium clay or potassium feldspar. This is very similar to analytical position 4.

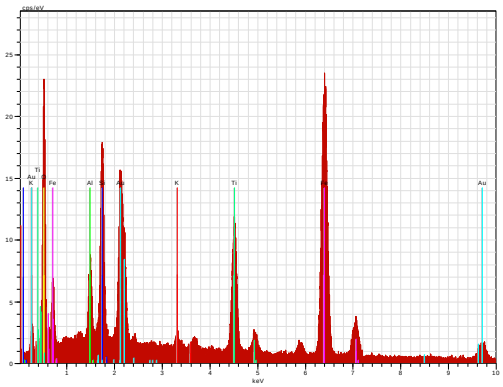

Figure D 56: EDX analysis at position 6.

The phases are too small to be accurately analyzed, but they appear to be a mixture of ilmenite and potassium feldspar.

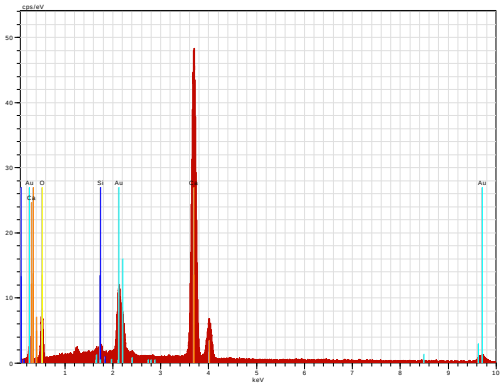

Figure D 57: EDX analysis at position 7.

The phase is calcite.

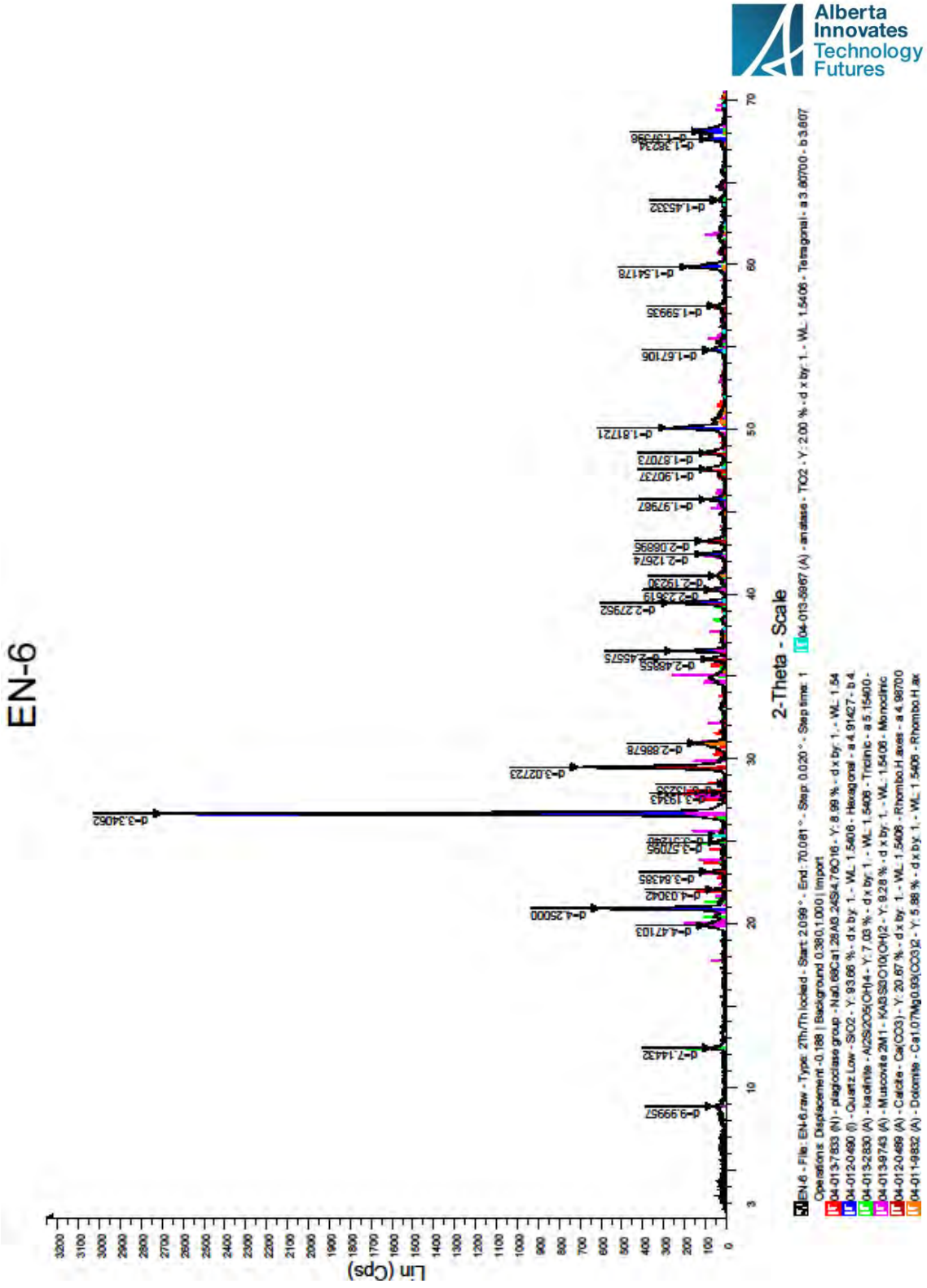

Figure D 58: X-Ray Diffraction pattern for sample EN-6.

Based on the XRD results, the most abundant mineral is quartz (65%). Calcite is present (20%), with 5% of dolomite, illite and kaolinite, respectively, also present. Trace amounts of anatase and plagioclase were also noted.

11.7 Sample EN 7

Sample EN-7 was sampled from core at a depth of approximately 1463.3 meters from the Glauconitic Sandstone in well 11-5-41-23W4.

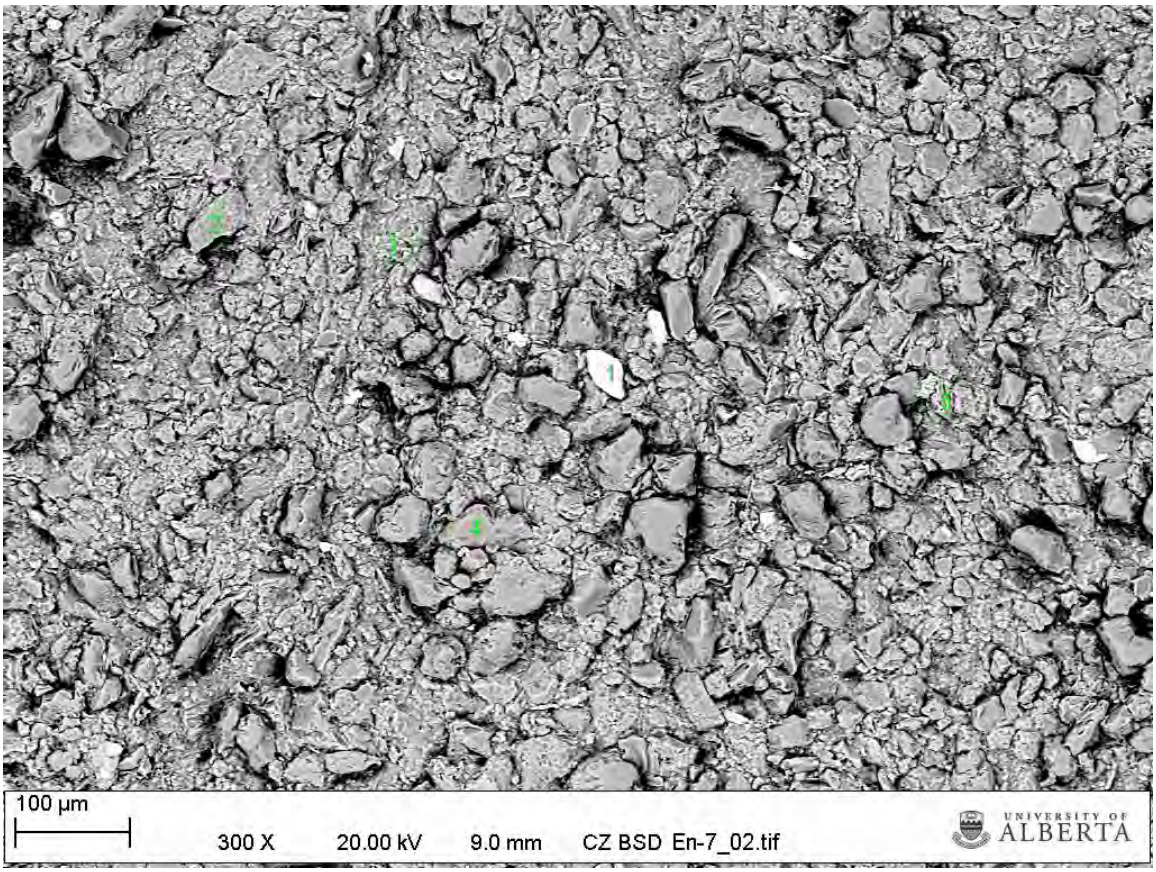

Figure D 59: A 300X magnification of sample EN-7. The annotations refer to the positions of the EDX analyses.

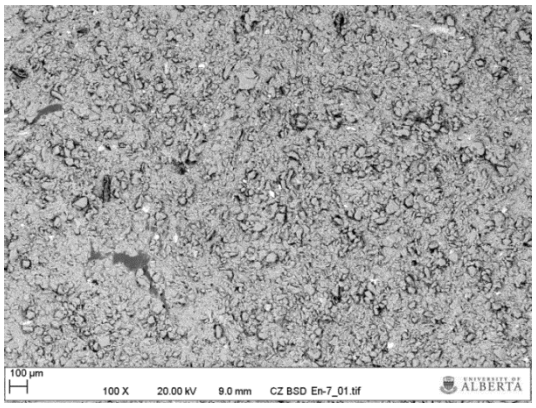

Figure D 60: A 100X magnification / overview of sample EN-7

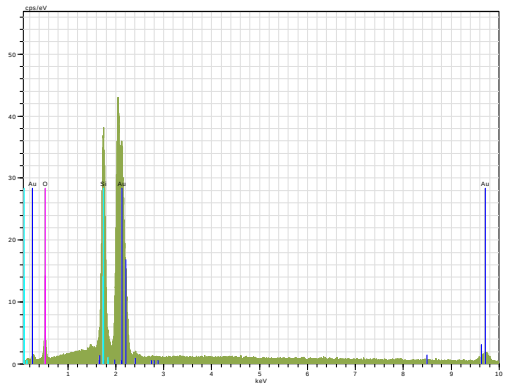

Figure D 61: EDX analysis of position 1.

The minerial is a zircon.

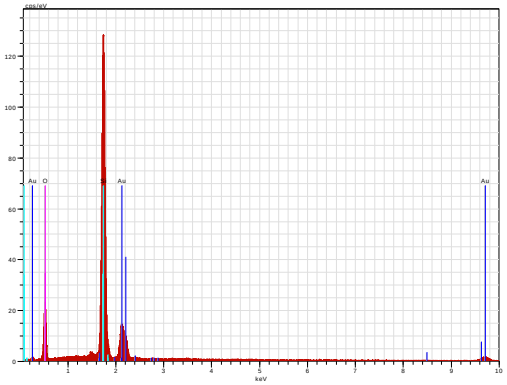

Figure D 62: EDX analysis of position 2.

The mineral is quartz.

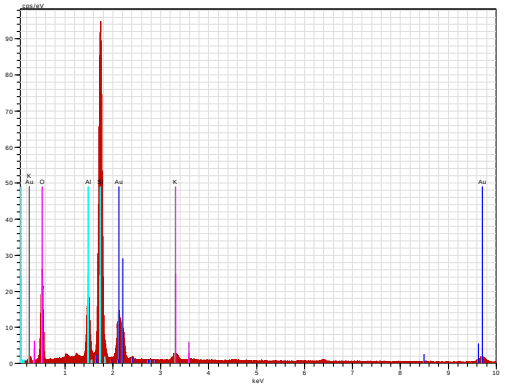

Figure D 63: EDX analysis of position 3.

The mineral is either an illite or fine grained potassium feldspar, probably with minor amounts of kaolinite present.

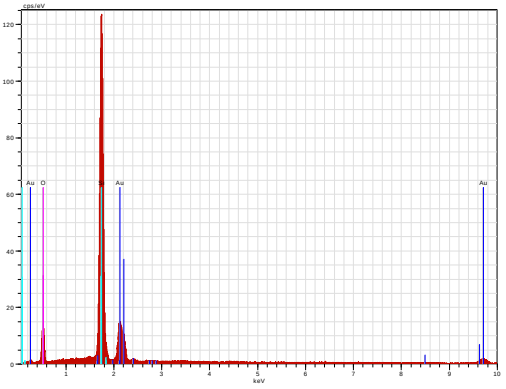

Figure D 64: EDX analysis of position 4.

The mineral is quartz.

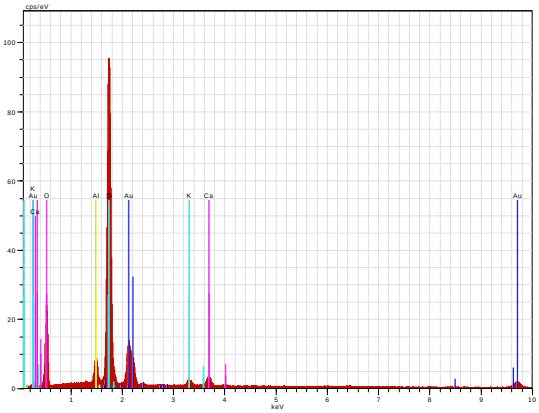

Figure D 65: EDX analysis of position 4.

The mineral(s) are predominately quartz.

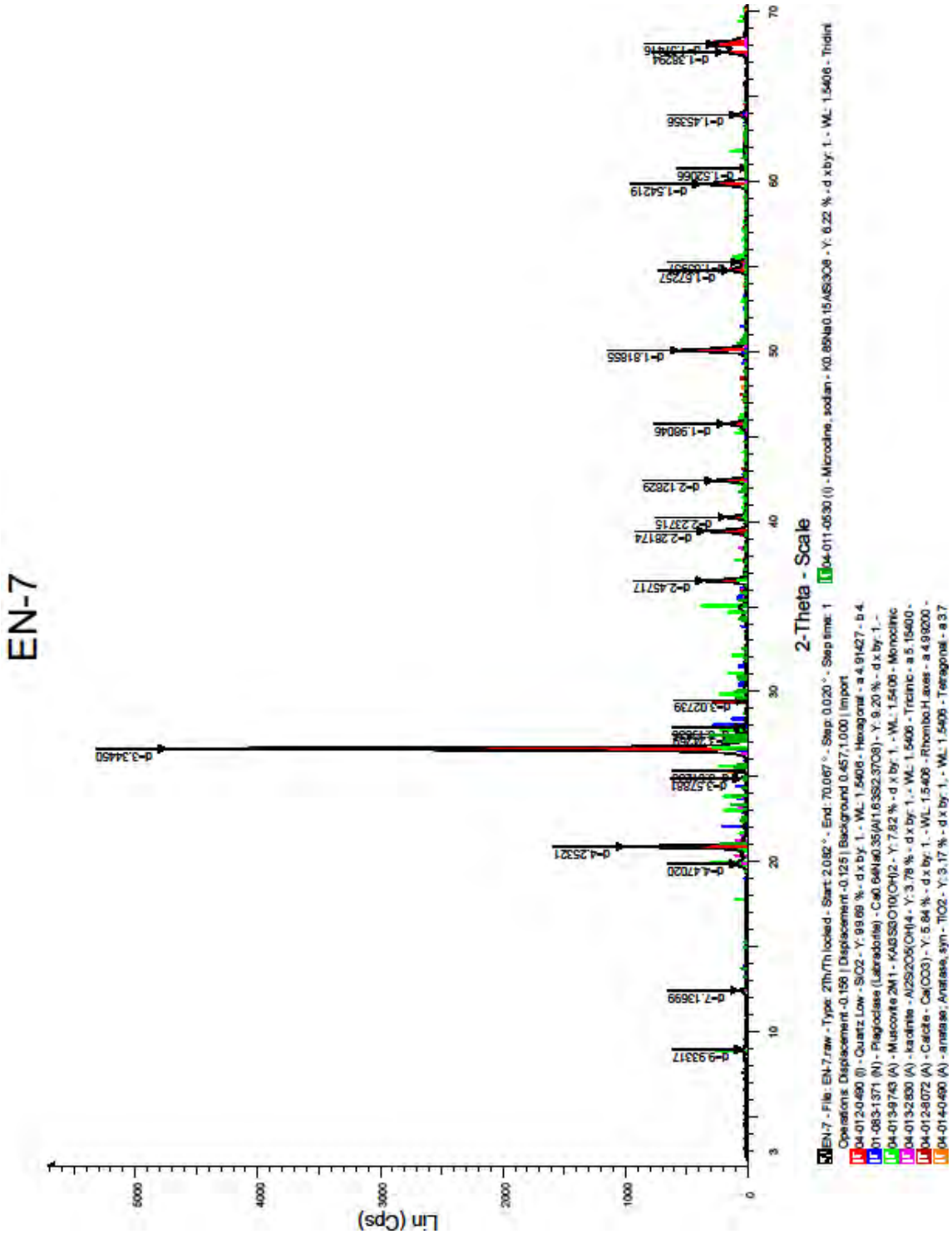

Figure D 66: X-Ray Diffraction pattern for sample EN-7.

Based on the XRD results, the primary mineral present is quartz (90%). Illite and kaolinite are both present at approximately 5%. Trace amounts of anatase, potassium feldspar, plagioclase and calcite were also noted.

11.8 Sample EN-8

Sample EN-8 was sampled from core at a depth of approximately 1388 meters from the Viking sandstone in well 11-12-41-25W4.

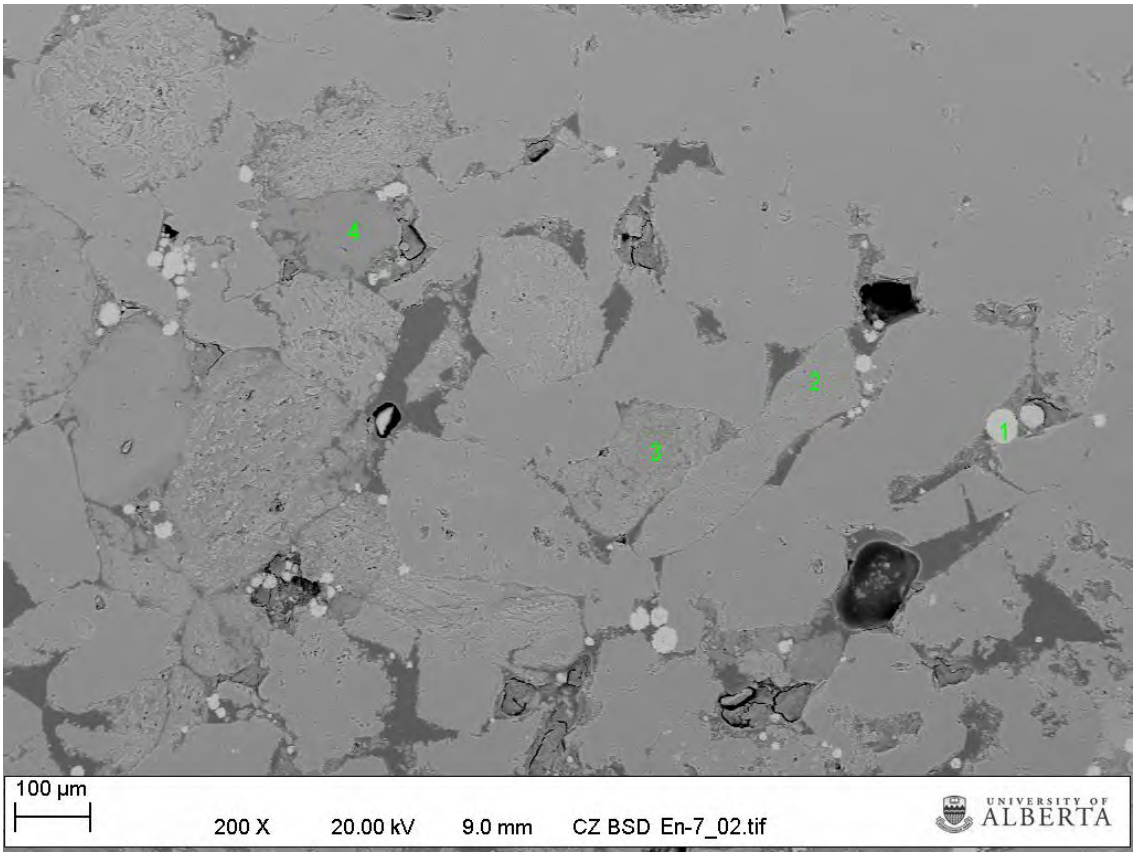

Figure D 67: 200X magnification of Sample En-8. The numbers refer to the points at which an EDX analysis was made.

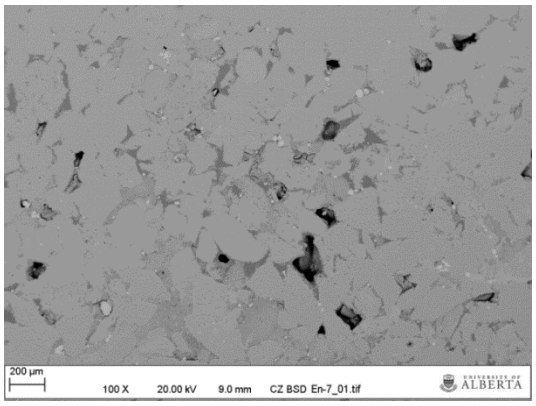

Figure D 68: 100X magnification of sample EN-8

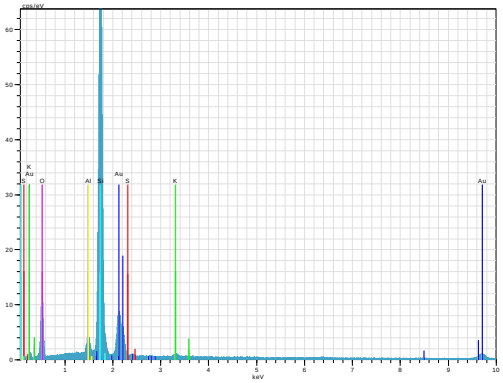

Figure D 70: EDX analysis at position 2.

The grains are quartz with minor amounts of aluminium and iron. The aluminum and iron is either due to inclusions or other grains.

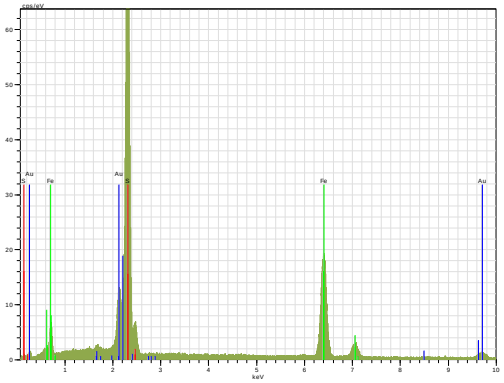

Figure D 69: EDX analysis at position 1, Error! eference source not found.**. 67.**

The grains are framboidal pyrite.

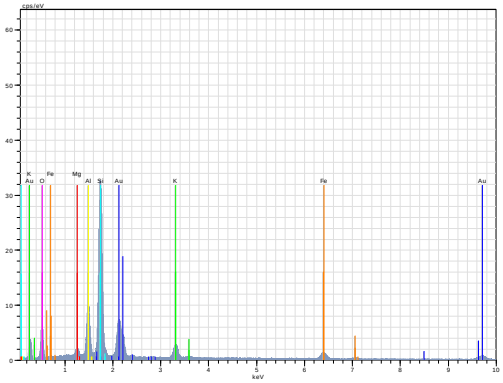

Figure D 71: EDX analysis at position 3.

The grains are either a feldspar or clay, and appear that they have undergone digenetic reactions.

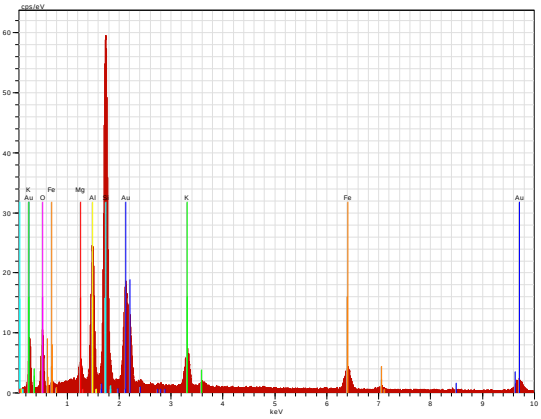

Figure D 72: EDX analysis at position 4.

The grains are most likely feldspar with minor amounts of magnesium and iron present, probably due to other grains.

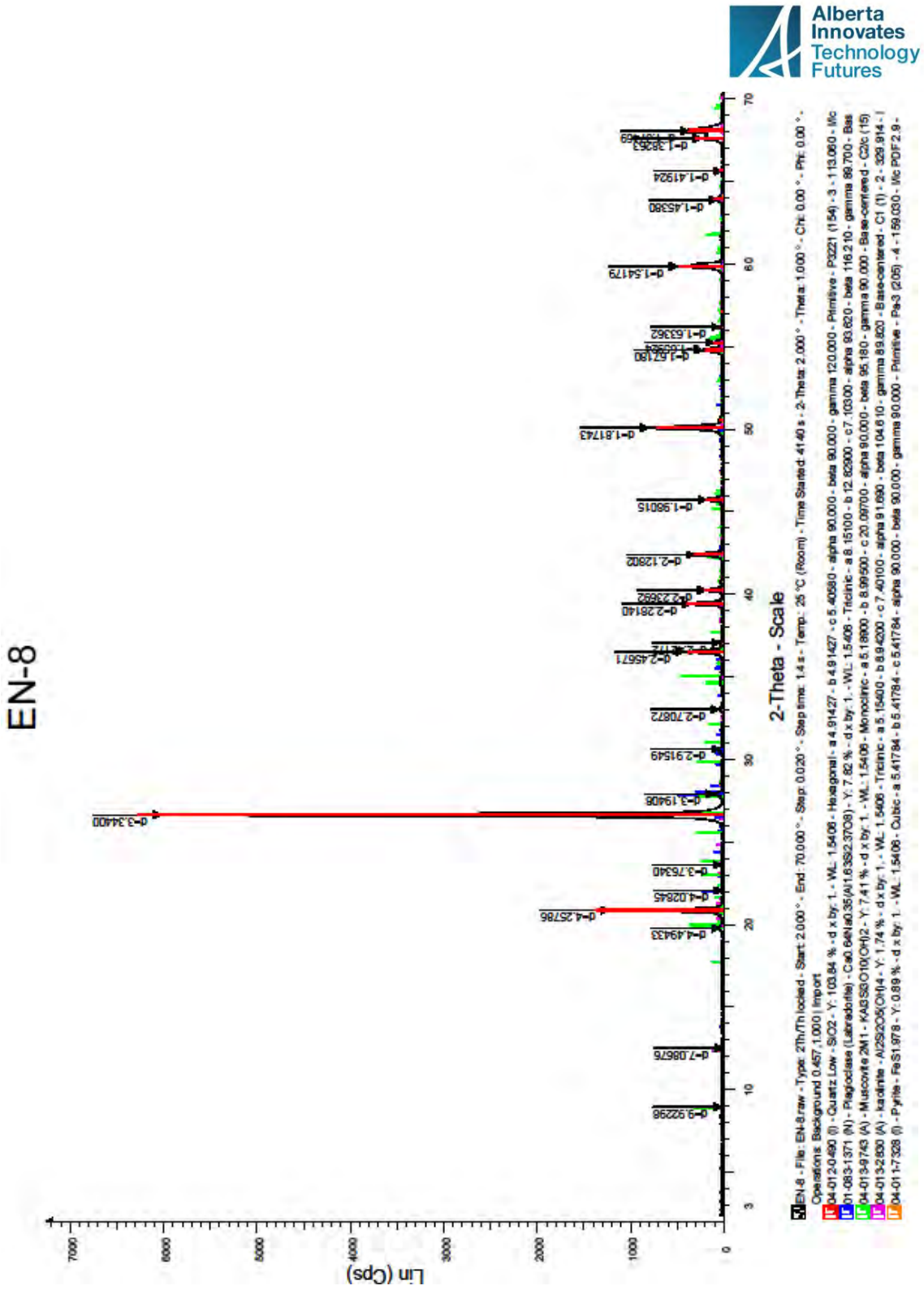

Figure D 73: X-Ray Diffraction pattern for sample EN-8

Based on the XRD data, the mineralogy of this sample is dominantly quartz (95%). Plagioclase is present at 5%. Trace amounts (< 1%) of illite, kaolinite and pyrite were also observed.

11.9 Sample EN-9

Sample EN-9 was sampled from core at a depth of approximately 695.25 meters from the Basal Belly River sandstone in well 9-35-41-23W4.

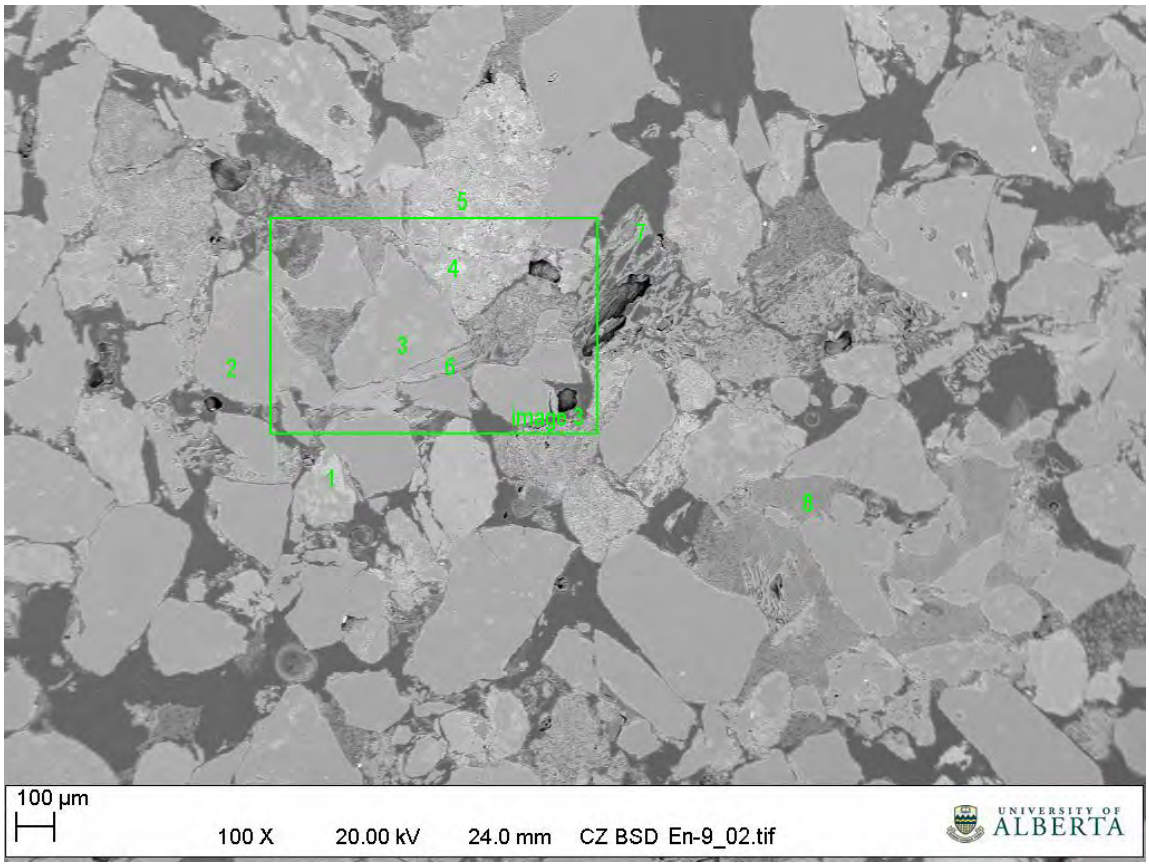

Figure D 74: A 100X magnification of Sample EN-9. The numbers refer to the points at which an EDX analyses were made.

In Figure D 74, the square box labeled ***image 3*** refers to Figure D 77.

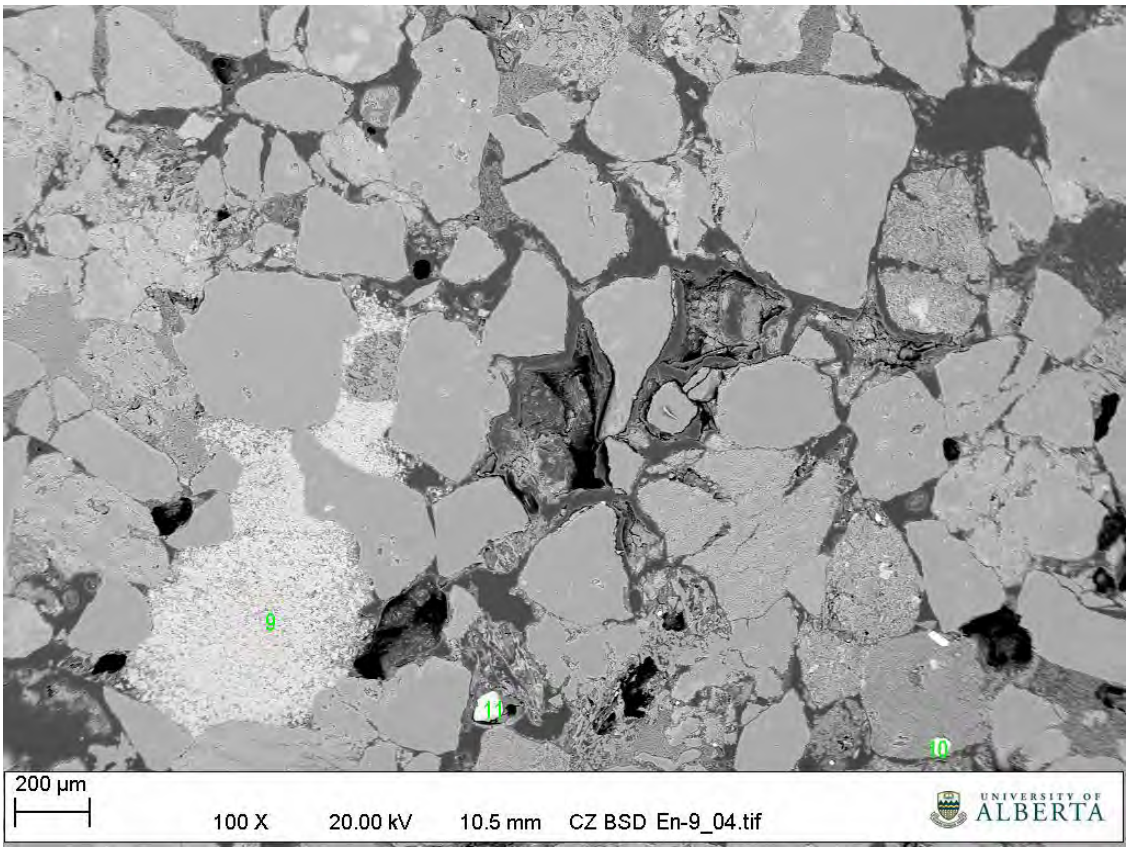

Figure D 75: A 100X magnification of Sample EN-9. The numbers refer to the points at which an EDX analyses were made.

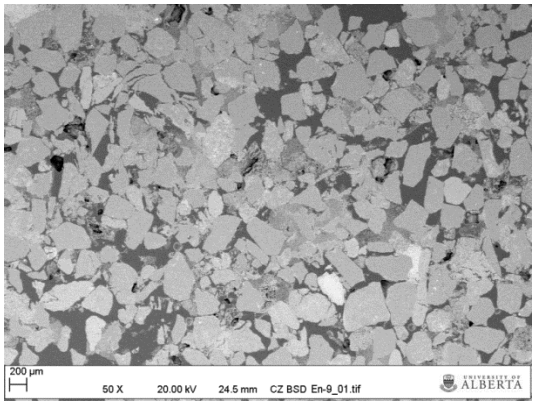

Figure D 76: A 50X magnification of Sample EN-9.

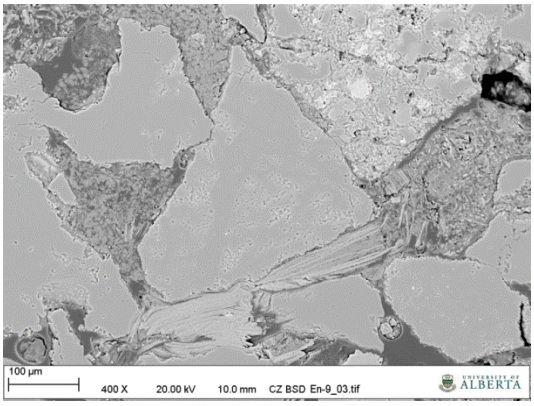

Figure D 77: A 400X magnification of the area identified as image 3.

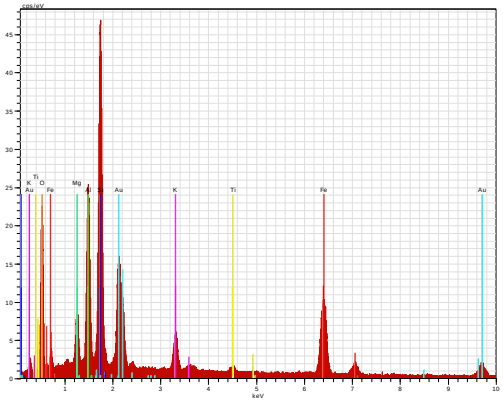

Figure D 78: An EDX analysis at point 1.

The primary mineral is an illite with some intergrowths of other phases containing iron, magnesium and oxygen

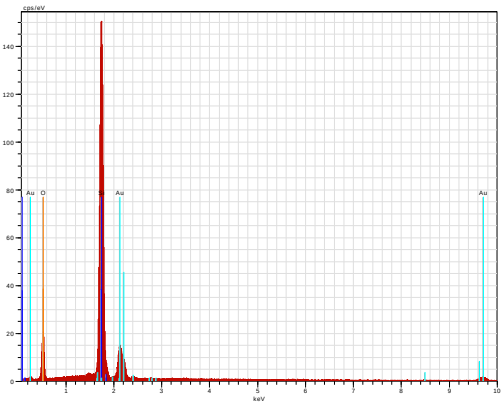

Figure D 79: An EDX analysis at point 20.

The mineral grain is quartz.

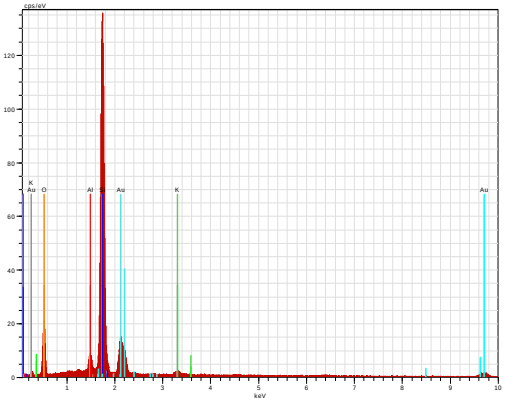

Figure D 80: An EDX analysis at point 3.

The large mineral grain is quartz.

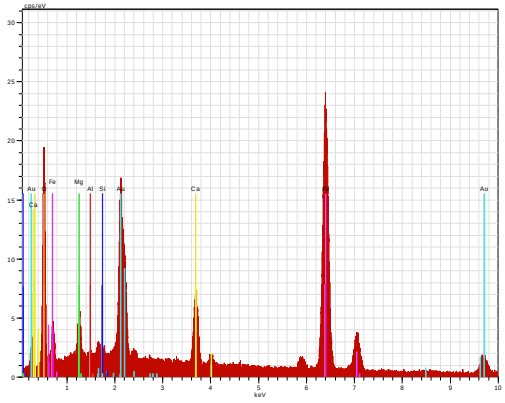

Figure D 81: An EDX analysis at point 4.

The main mineral is iron oxide or siderite, with small amounts of other phases such as calcite.

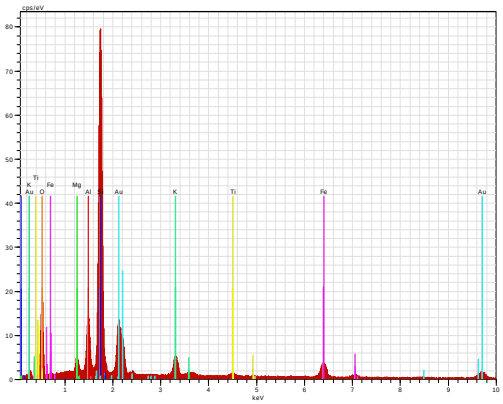

Figure D 82: An EDX analysis at point 5.

The principle grain is quartz with some clays and iron oxides present.

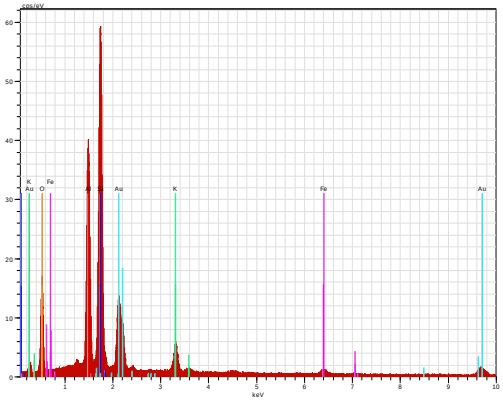

Figure D 83: An EDX analysis at point 6.

The principal mineral is kaolinite with some minor illite present.

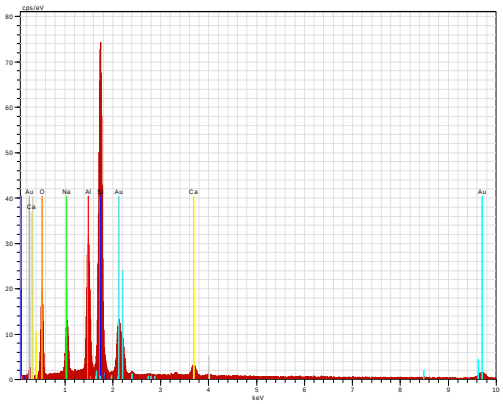

Figure D 84: An EDX analysis at point 7.

The mineralogy is comprised of intergrowths of kaolinite and a minor amount of plagioclase.

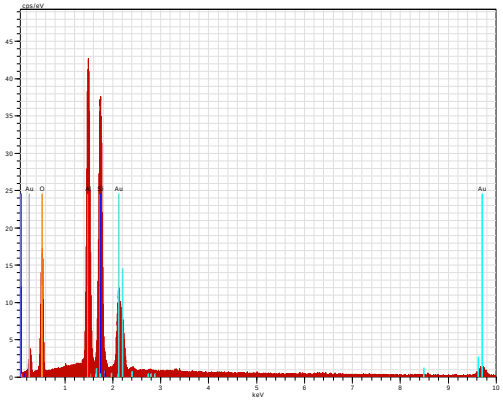

Figure D 85: An EDX analysis at point 8.

The principal mineral is kaolinite.

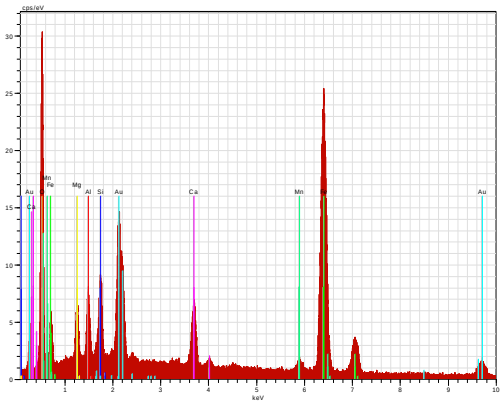

Figure D 86: An EDX analysis at point 9.

This large grain is a complex intergrowth of various clays, plagioclase and probably iron-manganese oxides.

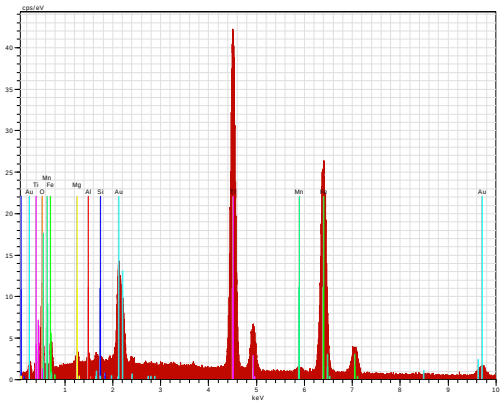

Figure D 87: An EDX analysis at point 10.

The mineral analyzed is ilimenite.

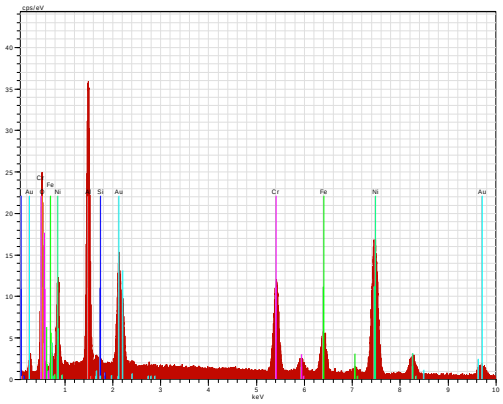

Figure D 88: An EDX analysis at point 11.

The high concentrations of nickel, chromium and aluminum suggest that this material is either a polishing compound or contamination.

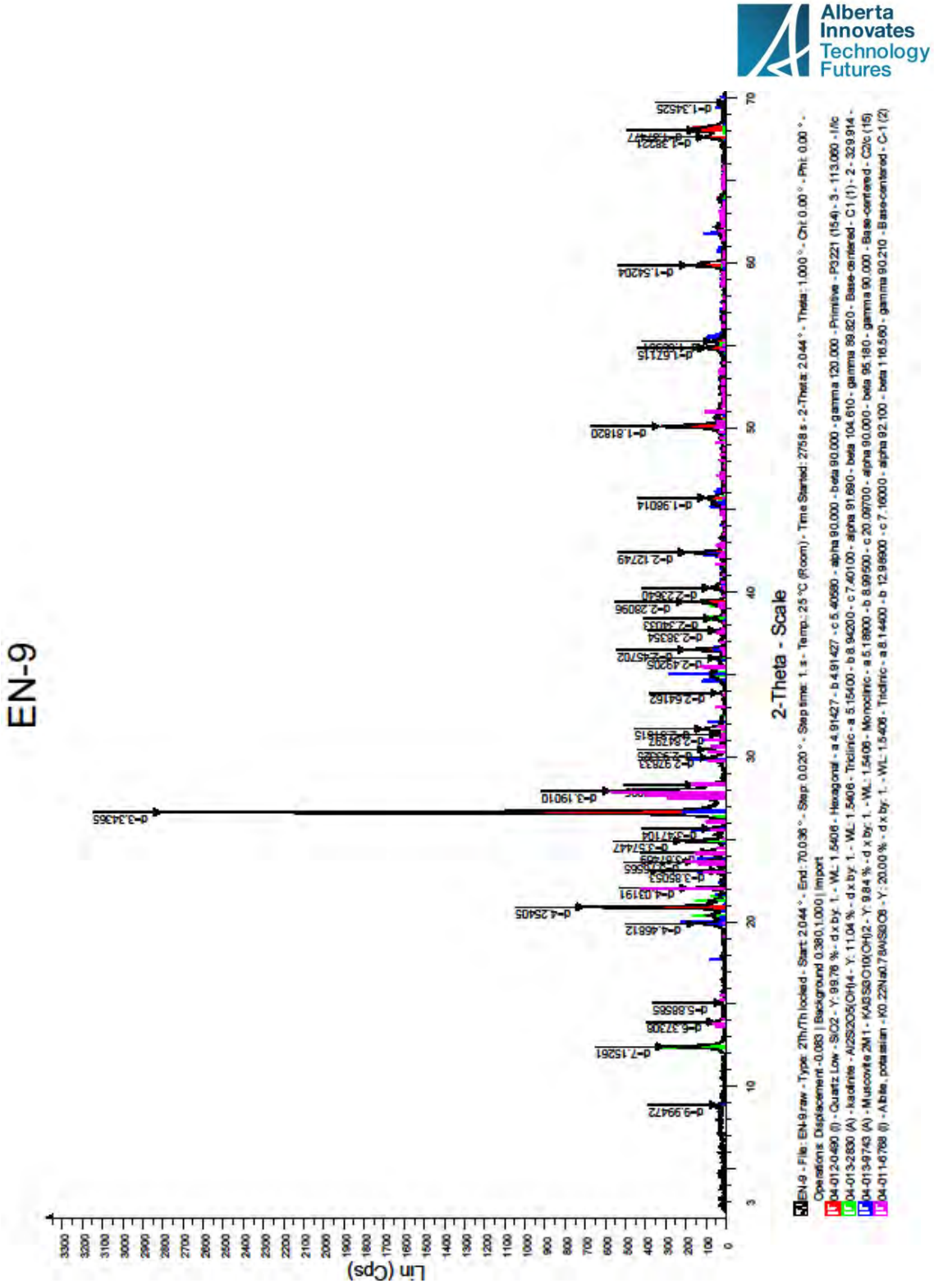

Figure D 89: X-Ray Diffraction pattern for sample EN-9

Based on the X-ray Diffraction results, the main mineralogy can assumed to be mostly quartz (65%), approximately 20% plagioclase, 10% kaolinite and 5% illite.

11.10 Sample EN-10

Sample EN-10 was sampled from core at a depth of approximately 1847.0 meters from the Nisku Formation in well 9-35-39-24W4.

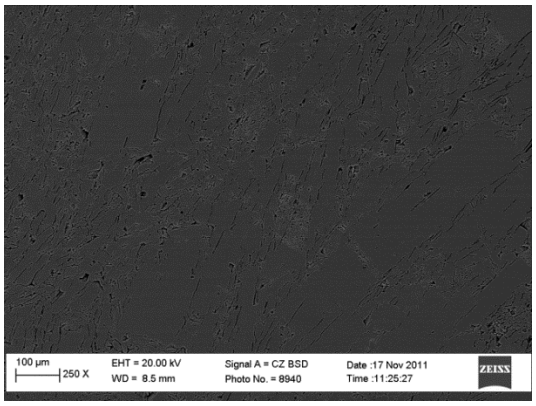

Figure D 90: A 250X magnification of Sample EN-10. At this scale, the sample appears homogeneous.

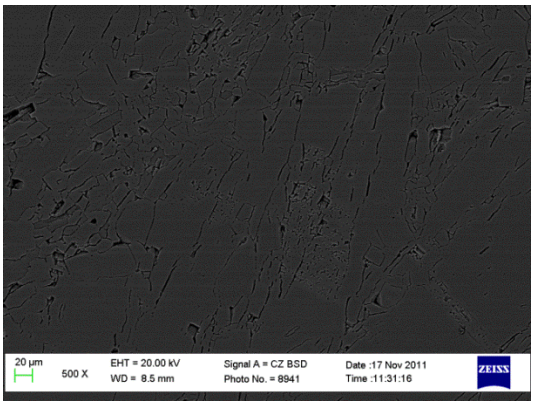

Figure D 91: A 500X magnification of Sample EN-10. At this scale, the sample appears homogeneous

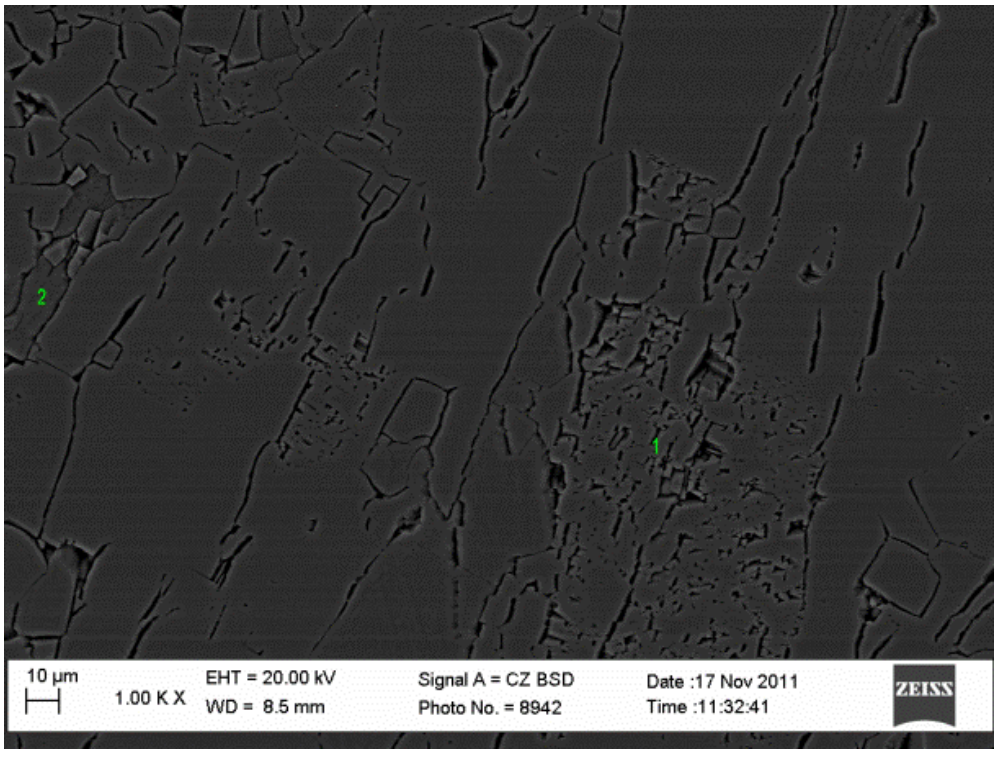

Figure D 92: A 1000X magnification of Sample EN-10. Once again, the sample appears homogeneous. The green annotations refer to the following EDX analysis.

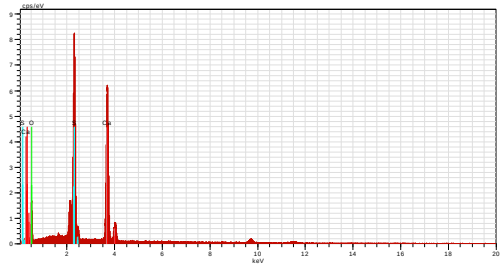

Figure D 93: An EDX analysis at point 1. The mineral is calcium sulphate

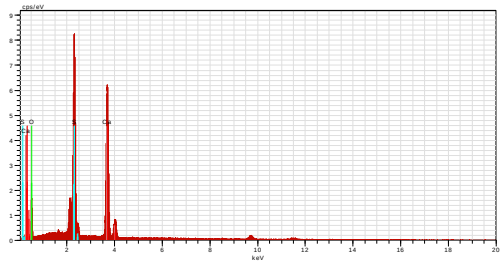

Figure D 94: An EDX analysis at point 2. The mineral is calcium sulphate.

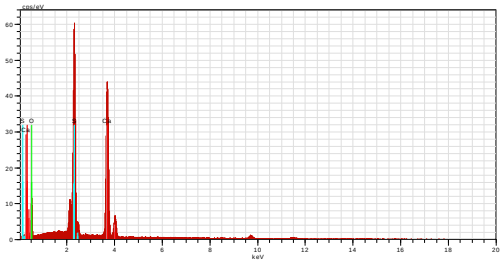

Figure D 95: An EDX analysis at point 3. The mineral is calcium sulphate.

All three analyses are identical. No other minerals were observed in the SEM sample.

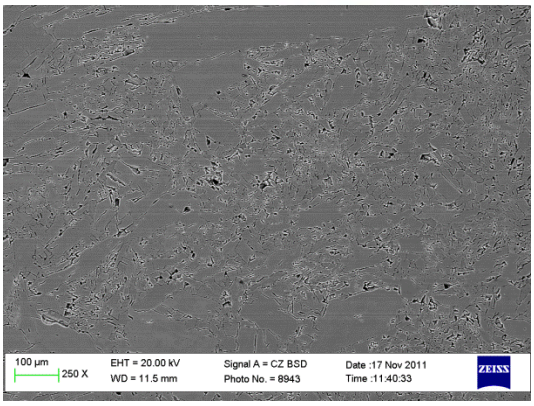

Figure D 96: A 250X magnification of another area on the sample. The mineralogy and texture is essentially the same as the previous images.

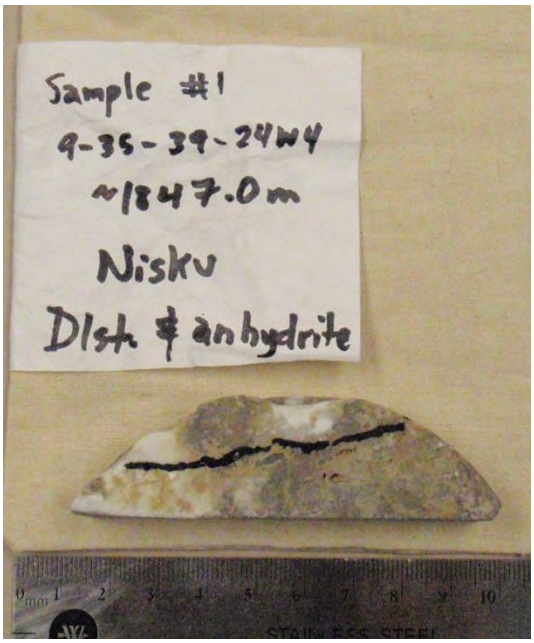

Figure D 97: Photograph of the Nisku sample which has been used for analytical purposes.

The solid line on the same indicates where the cut was to be made for the SEM sample. Based on the SEM results, it appears that only the “white” vein portion of the sample was used for the SEM sample, thus resulting in the “pure” anhydrite sample.

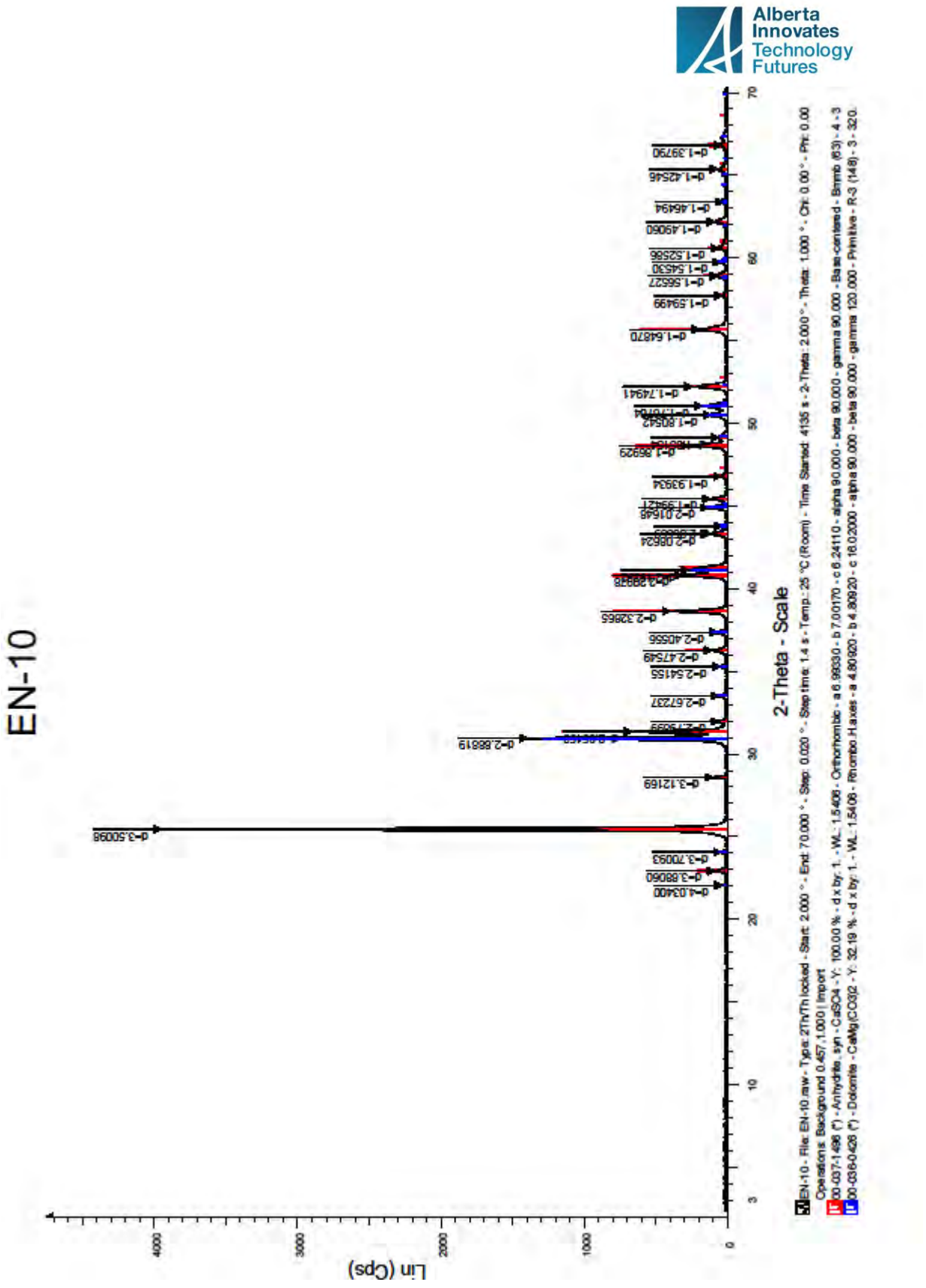

Figure D 98: X-Ray Diffraction pattern for sample EN-10

Based on the X-Ray Diffraction (XRD) results, the minerals observed are anhydrite (calcium sulphate – 70%) and dolomite 30%. This indicates that the XRD sample consisted mostly of vein material with a smaller portion of matrix material.

11.11 Sample EN-11

Sample EN-11 was sampled from core at a depth of approximately 1876.50 meters from the Leduc Formation in well 9-35-39-24W4.

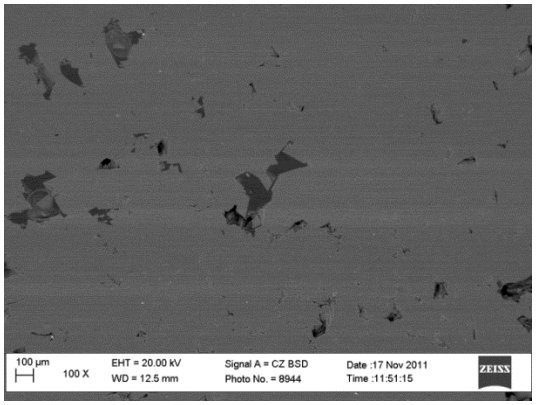

Figure D 99: A 100X magnification of Sample EN-11. At this scale, the sample appears relatively homogeneous.

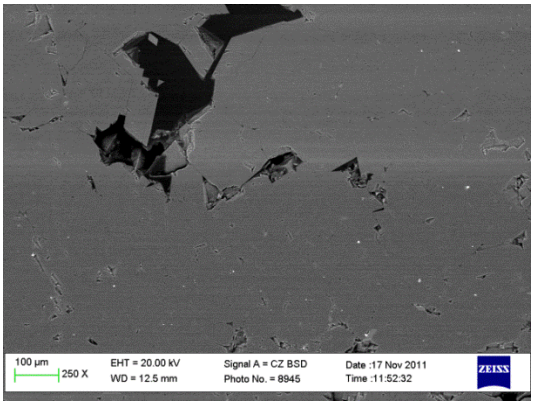

Figure D 100: A 250X magnification of Sample EN-11. Sharp grain edges in the pores show no evidence of dissolution.

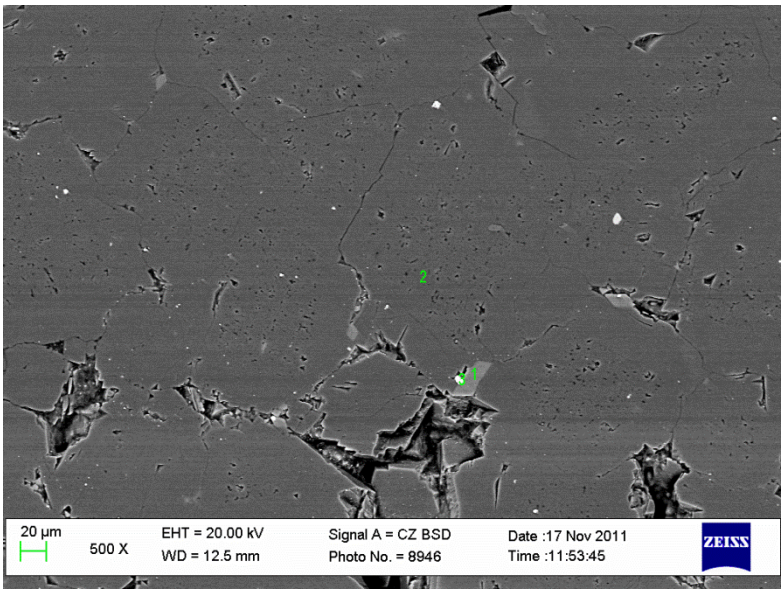

Figure D 101: A 500X magnification of Sample EN-11. The two green annotations refer to the following EDX analysis

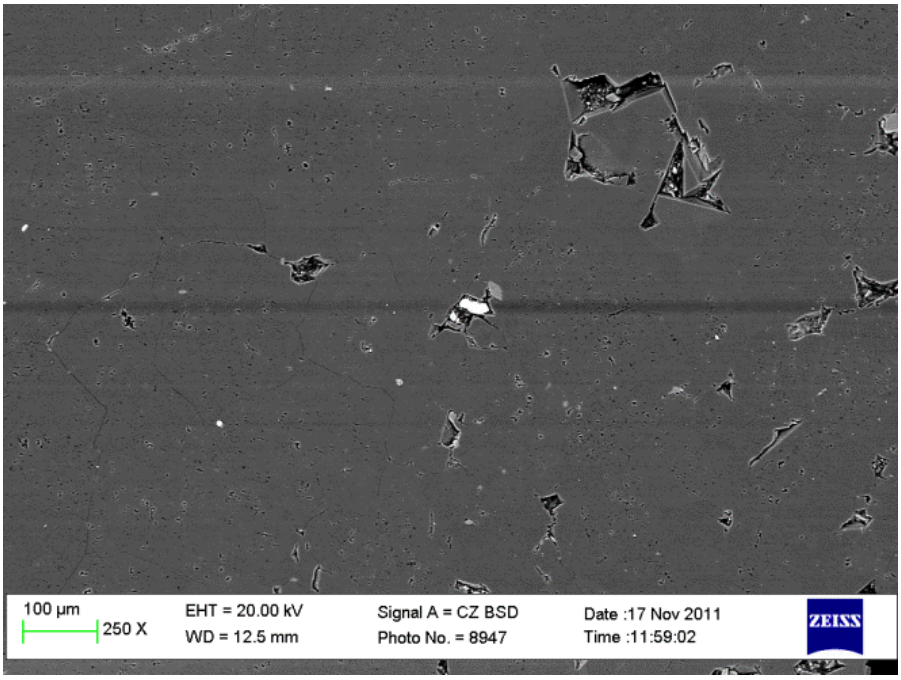

Figure D 102: A 250X magnification of another area on the sample.

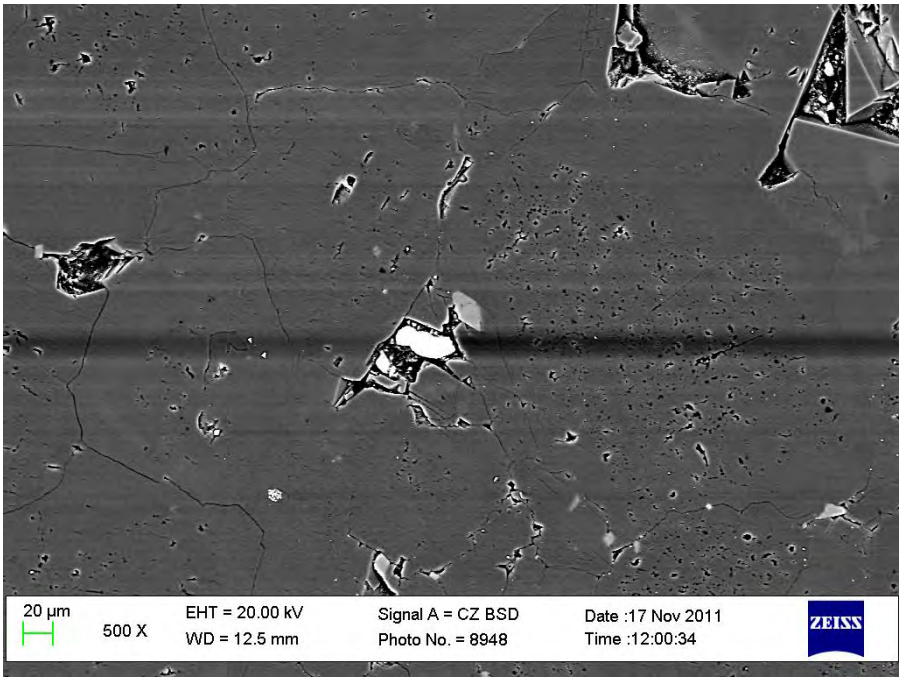

Figure D 103: A 500X magnification near the center of the preceding image. Three analysis (identified as 4, 5 and 6) shown in the followed EDX spectrum were made.

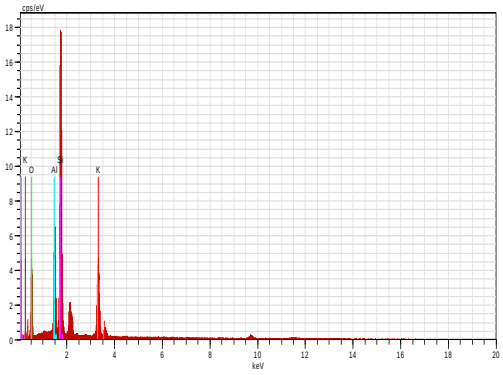

Figure D 104: An EDX analysis at point 1. The mineral is a potassium feldspar.

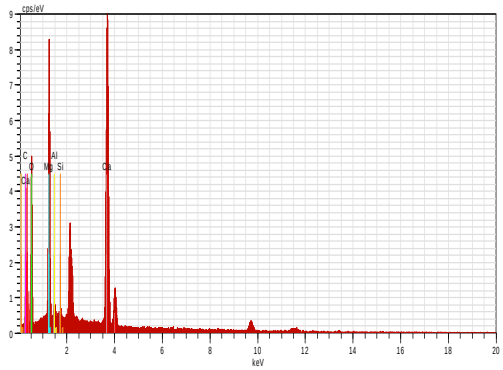

Figure D 105: An EDX analysis at point 2. The mineral is Dolomite and comprises the matrix material.

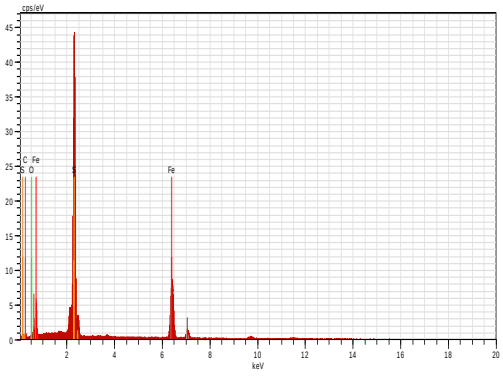

Figure D 106: An EDX analysis at point 3. The mineral is pyrite and can be seen in other locations as a bright spot.

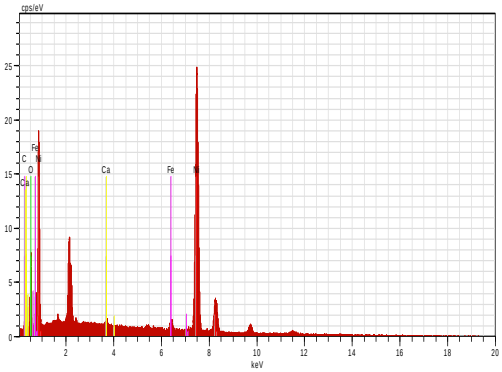

Figure D 107: One of the small bright grains turned out to be almost pure nickel. It is mostly contamination.

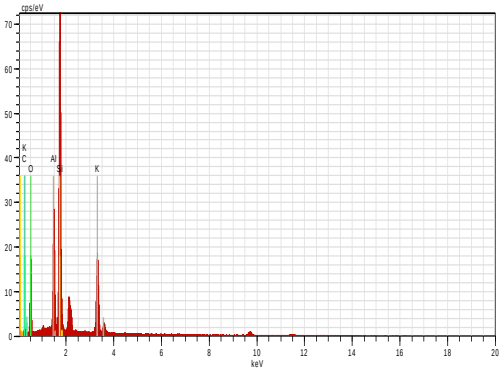

Figure D 108: Several small grains of potassium feldspar were identified at high magnification.

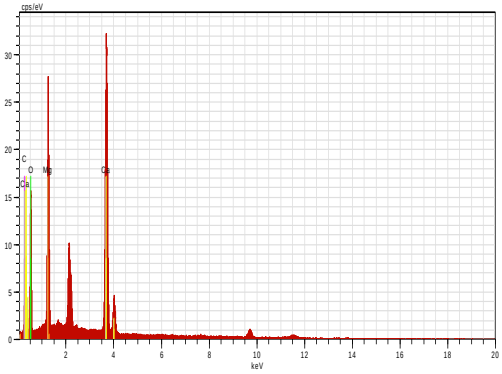

Figure D 109: The matrix is dolomite, as was identified from this EDX analysis.

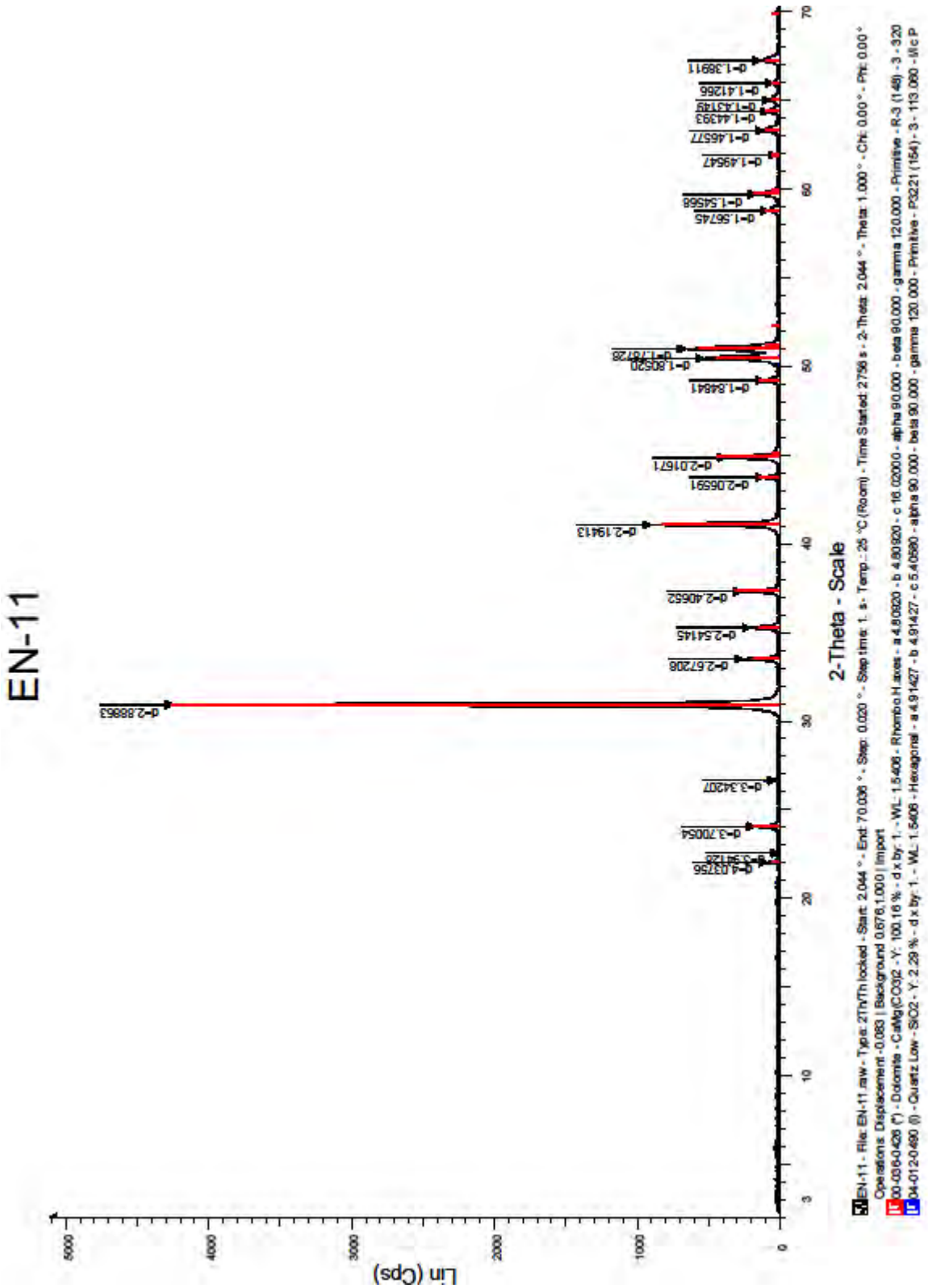

Figure D 110: X-Ray Diffraction pattern for sample EN-11.

Based on the X-ray Diffraction results, the main mineral is dolomite. A trace of quartz (less than 1%) was also measured. No other minerals were identified by XRD.

11.12 Sample EN-30

Sample EN-30 was sampled from core at a depth of approximately 1570.50 meters from the lowermost upper Mannville in well 6-7-40-24W4.

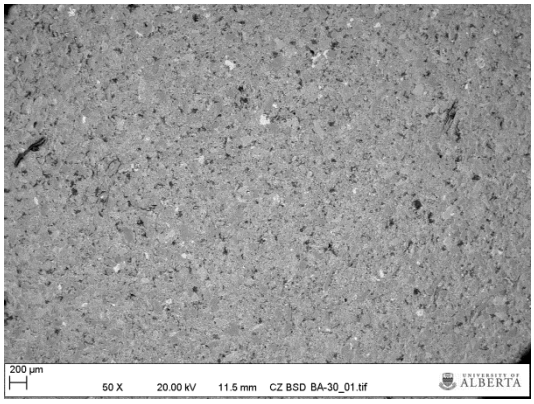

Figure D 111: A 50X magnification of Sample EN-30. At this scale, the sample appears relatively homogeneous although composed of a number of different minerals.

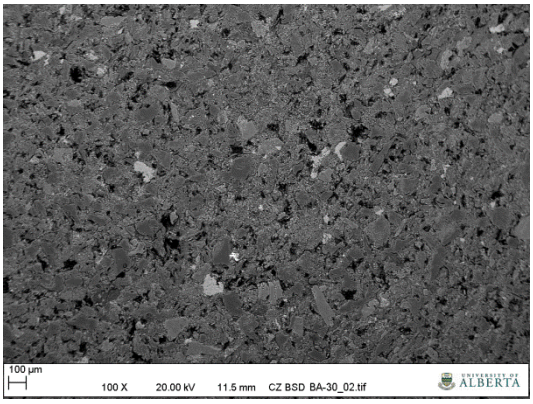

Figure D 112: A 100X magnification of Sample EN-30.

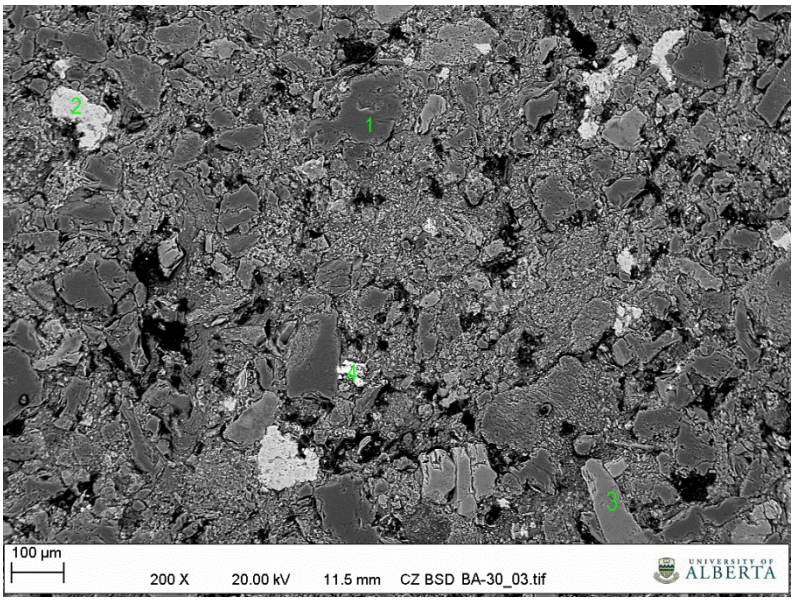

Figure D 113: A 200X magnification of Sample EN-30. The green annotations refer to the following EDX analysis.

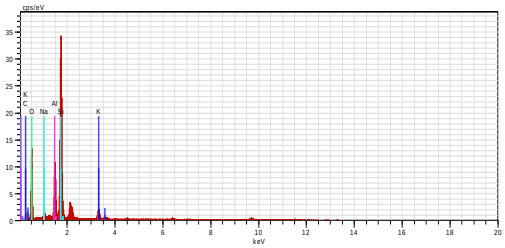

Figure D 114: An EDX analysis/scan of the entire sample. Quartz with smaller amounts of illite/k-spar appear to be the dominate mineralogy.

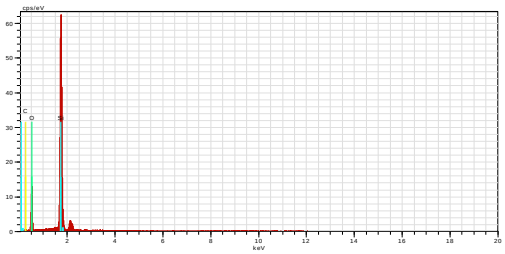

Figure D 115: An EDX analysis at point 1. The mineral is Quartz and comprises the matrix material.

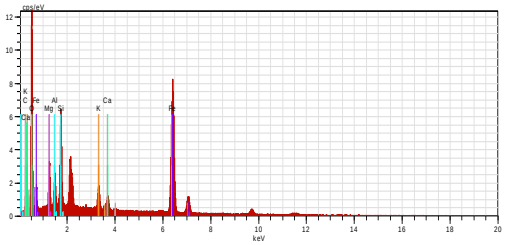

Figure D 116: An EDX analysis at point 2. There is no clear indication of the identity of the mineral(s).

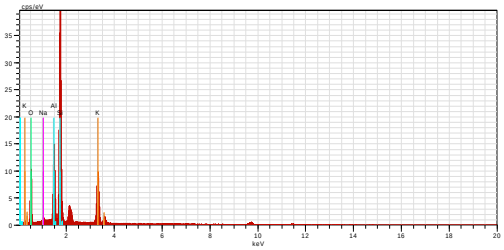

Figure D 117: An EDX analysis at point 3. The mineral is most likely K-spar with some minor kaolinite.

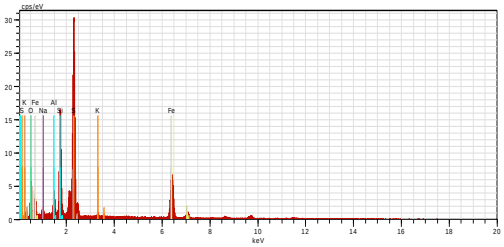

Figure D 118: An EDX analysis at point 4. The mineral is pyrite with some background bleed through.

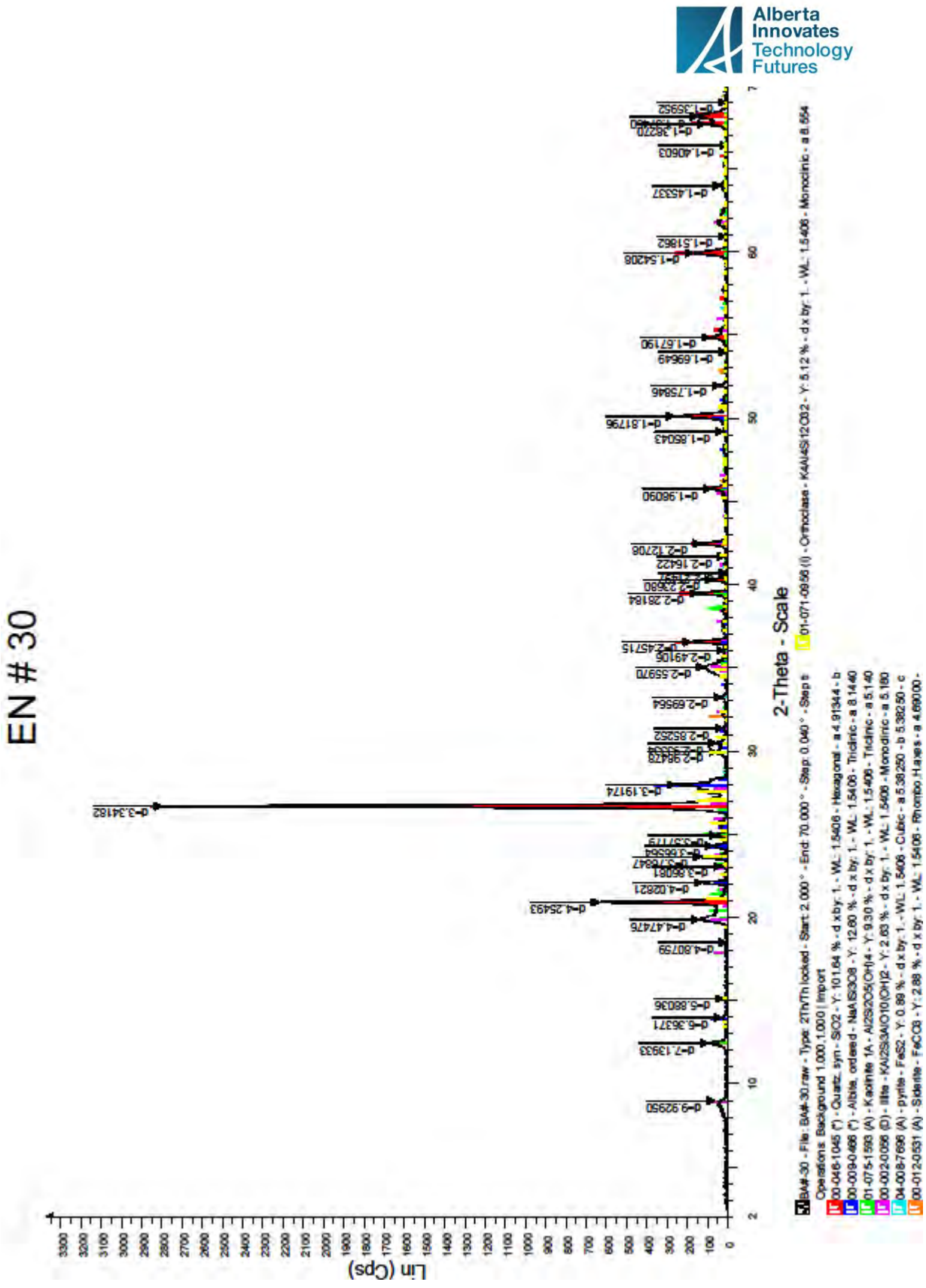

Figure D 119: X-Ray Diffraction pattern for sample EN-30.

Based on the X-ray Diffraction results, the main mineral is quartz (75%). Plagioclase (10%), illite (5%), kaolinite (5%) and potassium feldspar (5%) are the other major components. Siderite and pyrite were present as trace amounts.

11.13 Sample EN-31

Sample EN-31 was sampled from core at a depth of approximately 1448.0 meters from the Colorado shales in well 8-6-40-25W4.

Figure D 120: A 50X magnification of Sample EN-31. At this scale, the layering can be clearly seen.

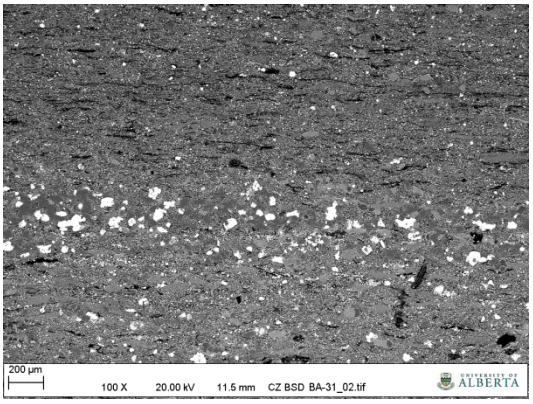

Figure D 121: A 100X magnification of Sample EN-30, located slightly to the right of center of the previous image. The bright grains are quartz.

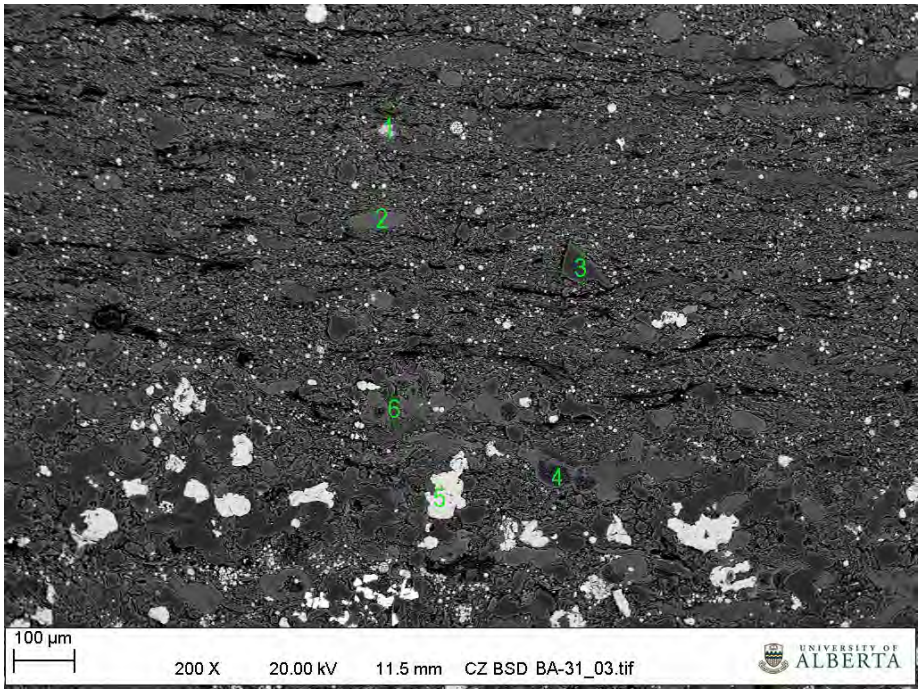

Figure D 122: A 200X magnification of Sample EN-31. The green annotations refer to the following EDX analysis

Figure D 123: A 3000X magnification of the area identified as point 1 on the annotated sample.

The small grains in the center of the image are pyrite. It is surrounded by calcite and fine grained clays.

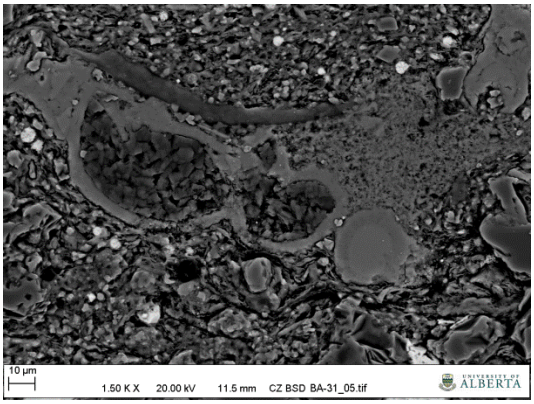

Figure D 124: A 1500X magnification of the area identified as point 4 on the annotated sample.

The area in the center of the figure are kaolinite, which are surrounded by calcite This relationship was observed throughout the slide.

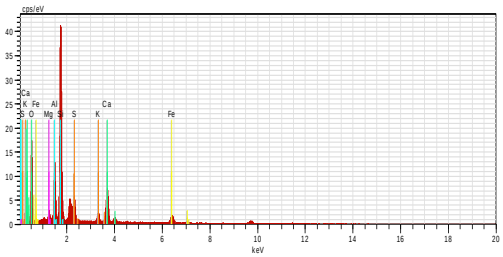

Figure D 125: An EDX overview analysis, indicateing that pyrite,quartz and plagioclase are present. There is an indication of illite and/or potassium feldspar.

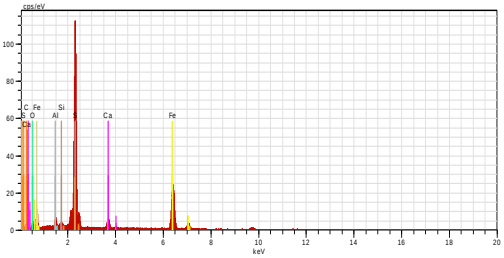

Figure D 126: An EDX analysis at point 1. The bright central mineral is Pyrite and is surrounded by calcite and clays.

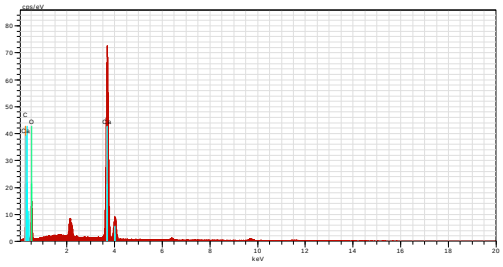

Figure D 127: An EDX analysis at point 2. The mineral is calcite.

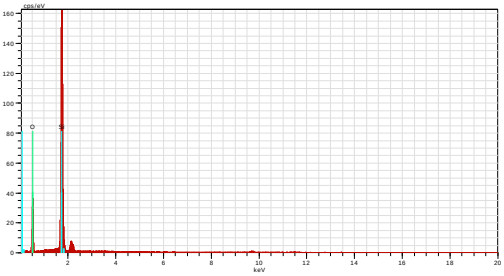

Figure D 128: An EDX analysis at point 3. The mineral is quartz.

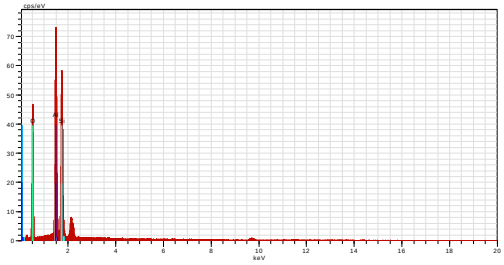

Figure D 129: An EDX analysis at point 4. The mineral in the center is kaoloinite with calcite surrounding it. An SEM image showing this point precedes this EDX section.

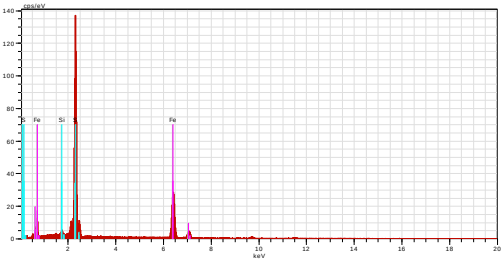

Figure D 130: An EDX analysis at point 5. The mineral is pyrite.

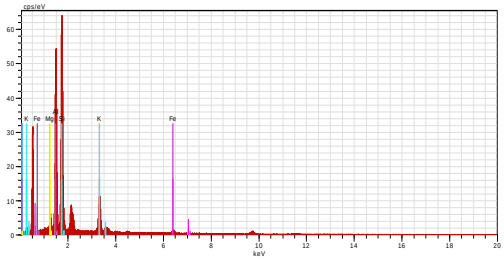

Figure D 131: An EDX analysis at point 6. The mineral is a clay, but could not be further identified.

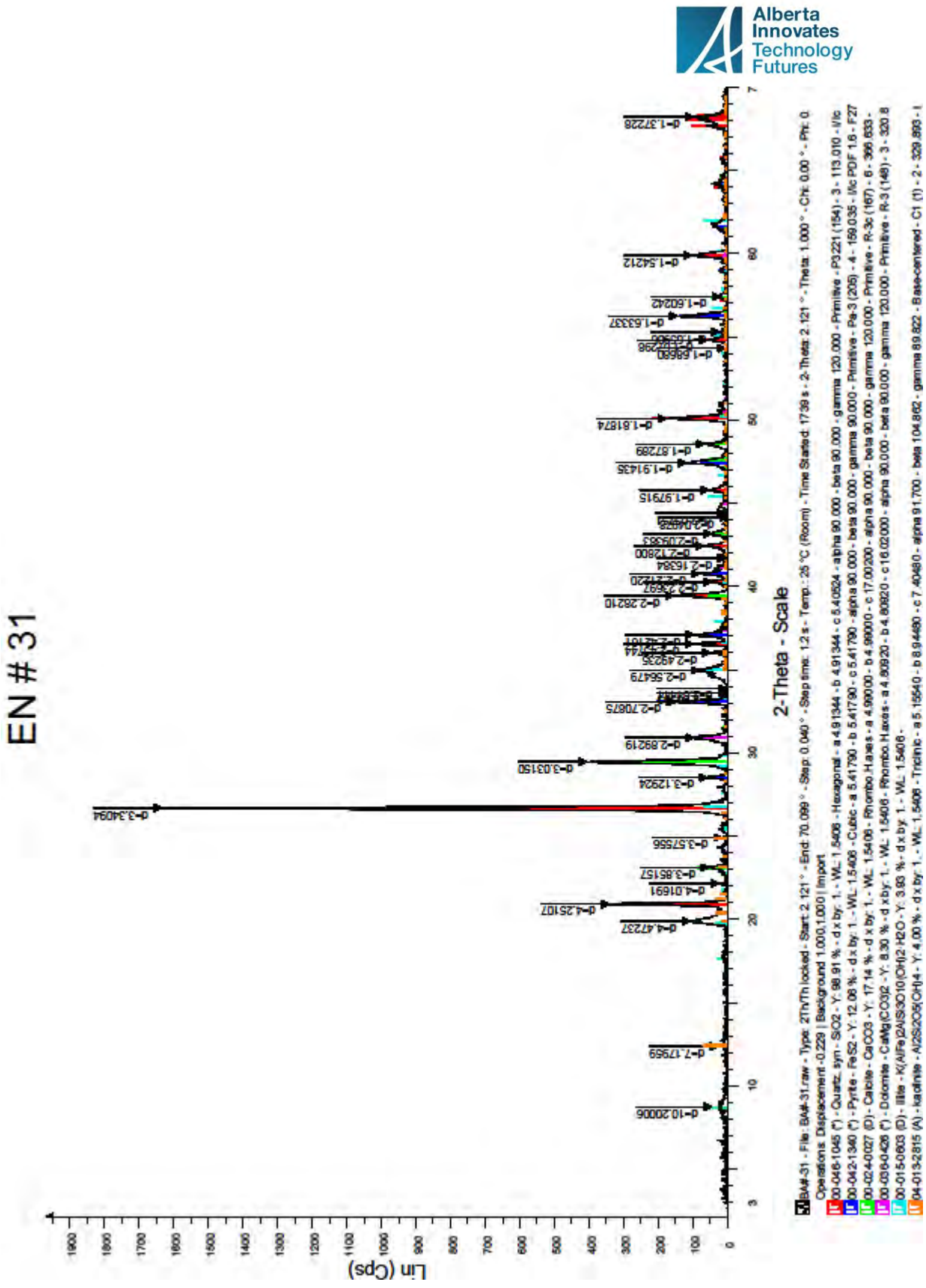

Figure D 132: X-Ray Diffraction pattern for sample EN-31.

Based on the X-ray Diffraction results, the main mineral is quartz (65%). Calcite is present at 20%. Illite, dolomite and pyrite are present each in the amount of 5%. A trace of kaolinite (less than 1%) was also observed.

11.14 Sample EN-32

Sample EN-32 was sampled from core at a depth of approximately 1401.90 meters from the Viking Formation shales in well 12-17-39-24W4.

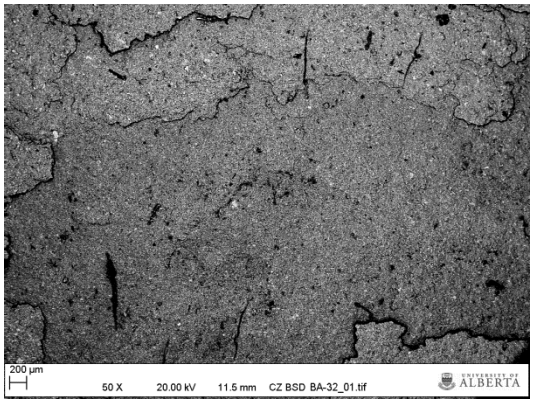

Figure D 133: A 50X magnification of Sample EN-32.

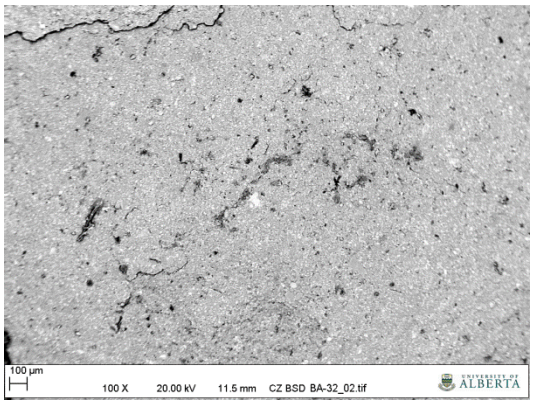

Figure D 134: A 100X magnification of Sample EN-32.

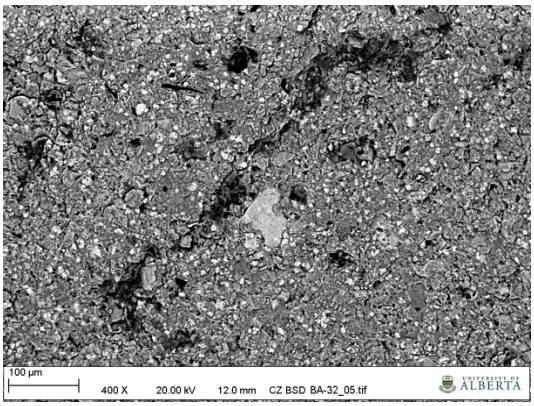

Figure D 135: A 400X magnification near the center of the preceding image

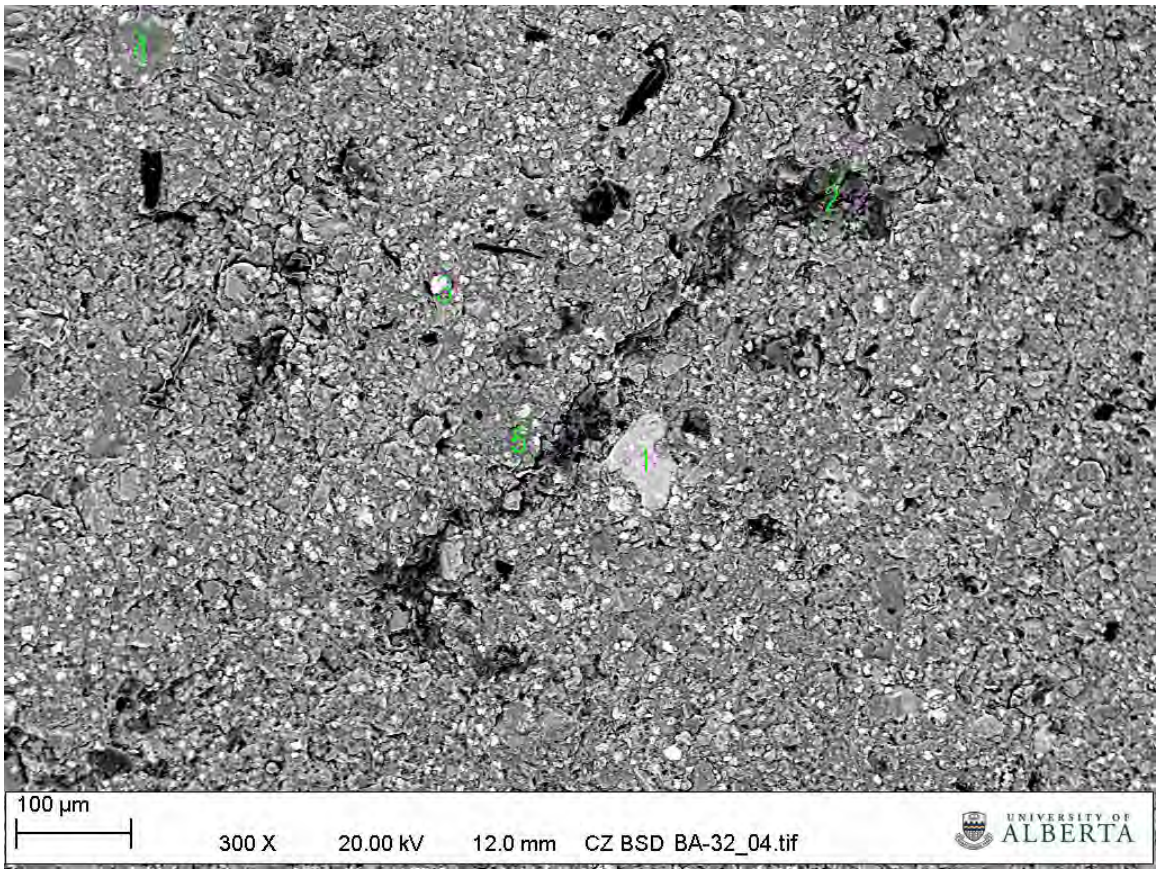

Figure D 136: A 300X magnification sample EN-32. The green numbers refer to the points at which the following EDX analyses were made on the sample.

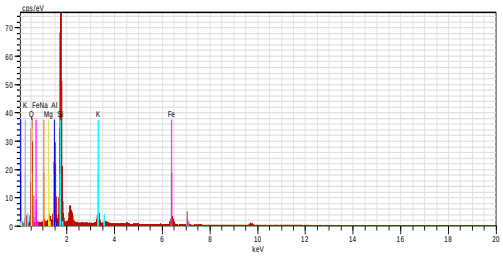

Figure D 137: An EDX overview analysis of the 100X image. It indicates that Quartz is the major mineral.

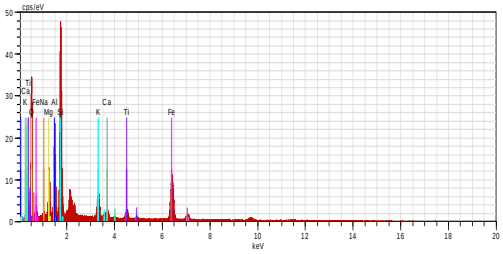

Figure D 138: An EDX analysis at point 1. The principle elements are oxygen, iron, silica and aluminum. The other common cations are present from .5 to 4 %.The mineral identities are not clear.

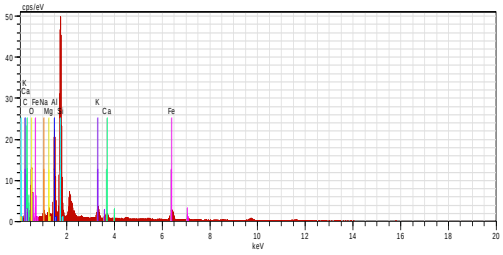

Figure D 139: An EDX analysis at point 2. The main mineral is calcite.

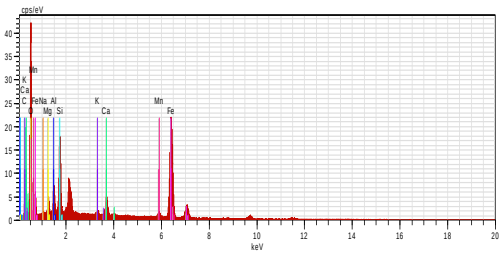

Figure D 140: An EDX analysis at point 3. The mineral appears to be clay or perhaps a chlorite.

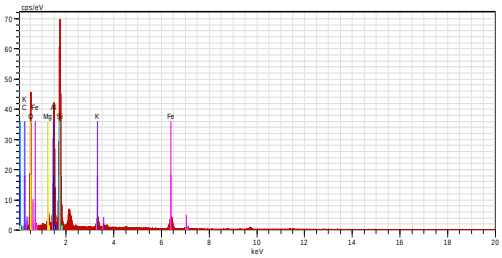

Figure D 141: An EDX analysis at point 4. The mineral appears to be clay.

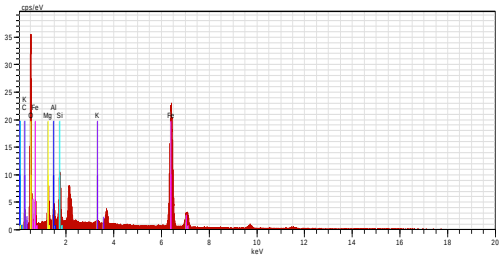

Figure D 142: An EDX analysis at point 5. The analysis is of the matrix material, and apears to be a clay or perhaps a chlorite.

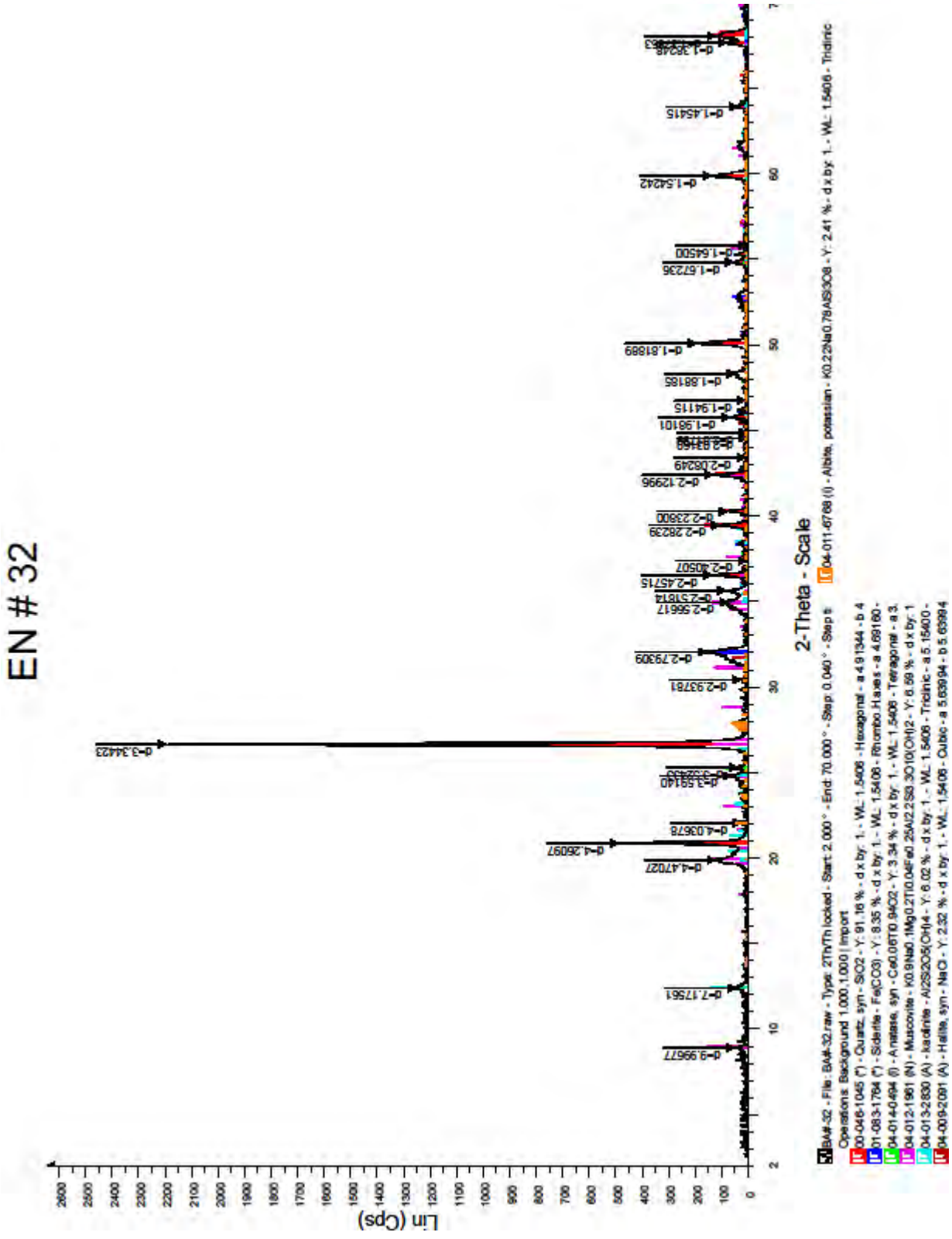

Figure D 143: X-Ray Diffraction pattern for sample EN-32.

Based on the X-ray Diffraction results, the main mineral is quartz (70%). Siderite was present at approximately 10%. Muscovite, kaolinite, plagioclase and halite were all present at 5% each. A trace of Anatase was present.

11.15 Sample EN-33

Sample EN-33 was sampled from core at a depth of approximately 548.00 meters from the upper Belly River sandstone in well 7-14-41-23W4.

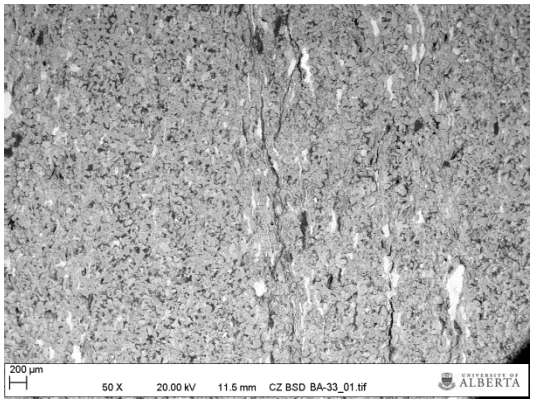

Figure D 144: A 50X magnification of Sample EN-33. The layering is very clear.

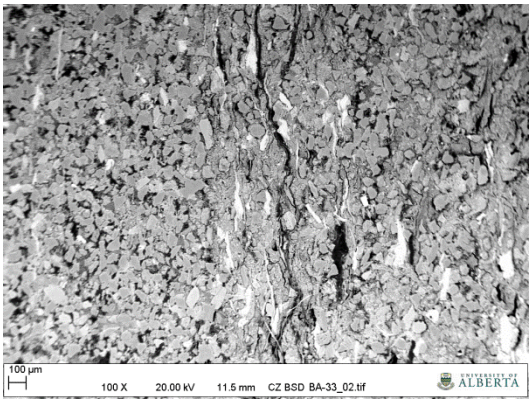

Figure D 145: A 100X magnification of Sample EN-33.

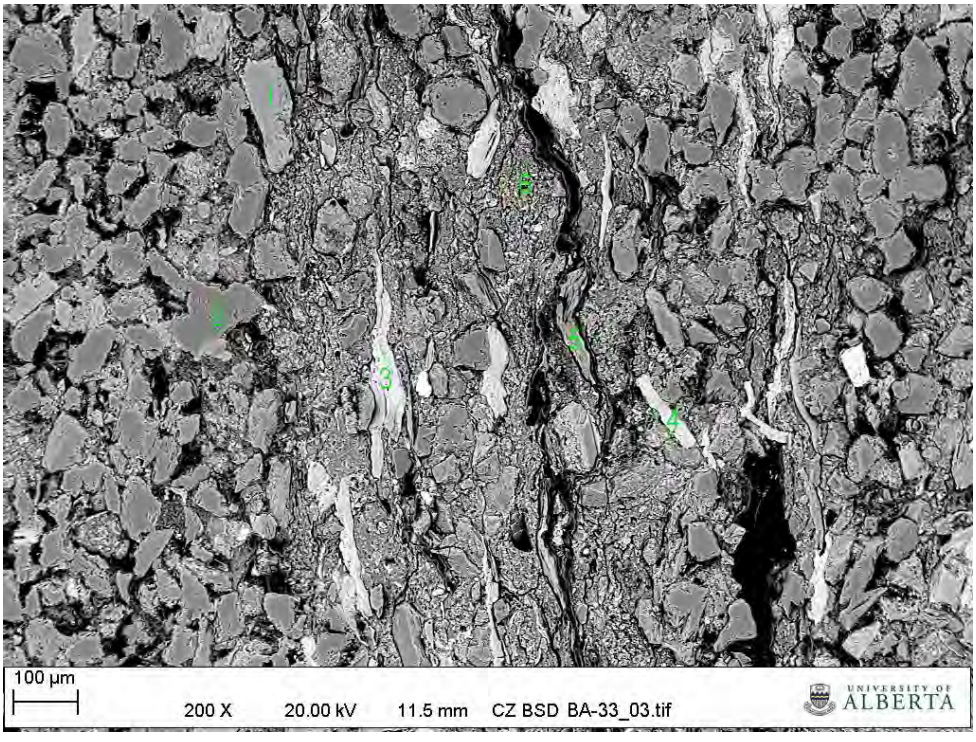

Figure D 146: A 200X magnification of Sample EN-33. The green annotations refer to the following EDX analyses 1 through 6.

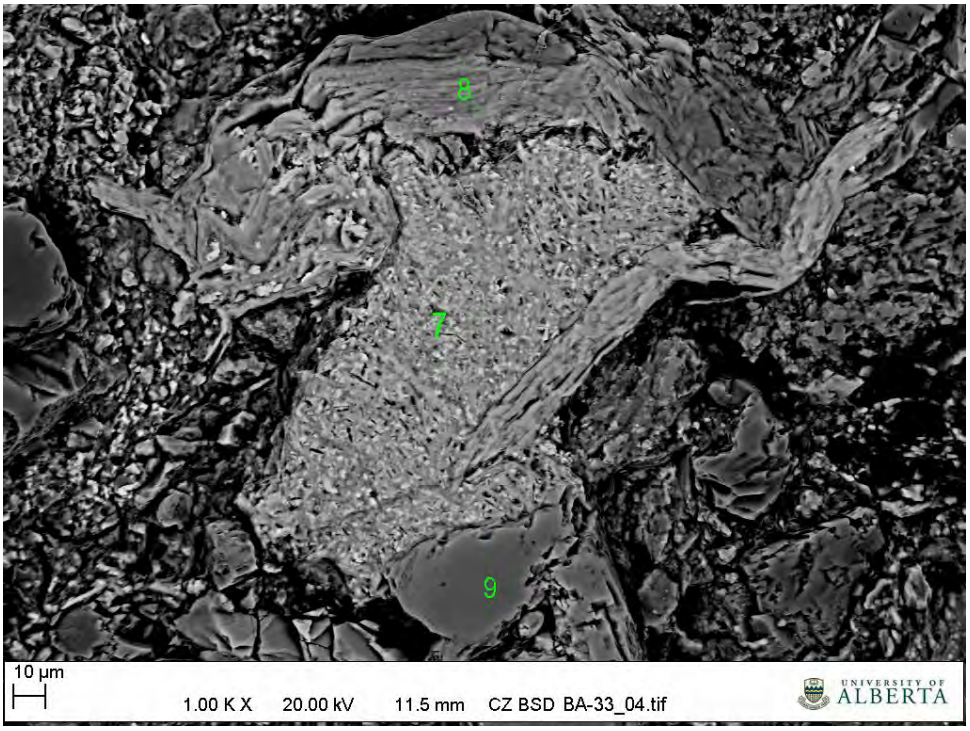

Figure D 147: A 1000X magnification of another area on the sample, annotated showing the locations of EDX analyses 7, 8 and 9.

.

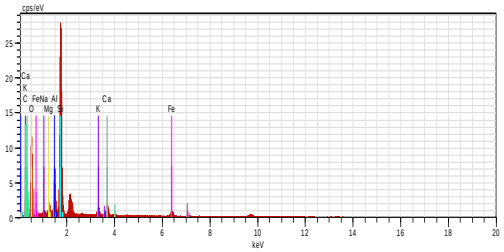

Figure D 148: An EDX overview analysis. High oxygen, carbon, silica (all exceeding 10%). About 4% aluminium and other major cations in the range of 1% to 2%.

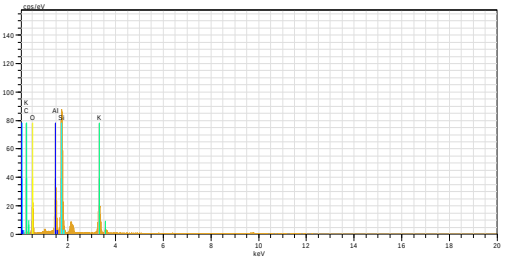

Figure D 149: An EDX analysis at point 1. The mineral is illite.

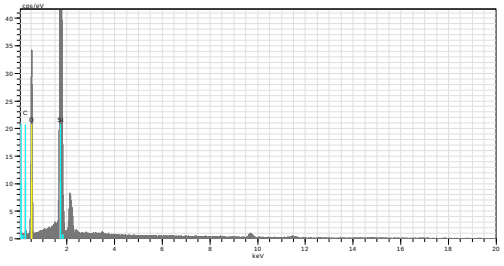

Figure D 150: An EDX analysis at point 2. The mineral is Quartz.

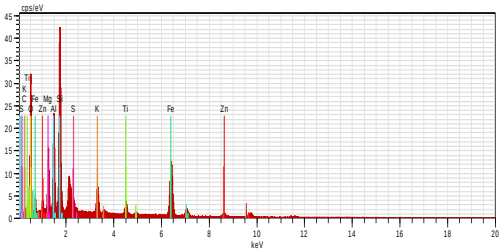

Figure D 151: An EDX analysis at point 3. The mineral is a clay, with the possible presence of some pyrite.

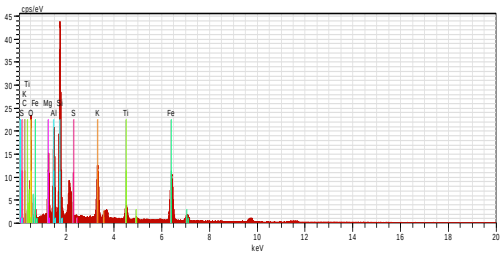

Figure D 152: An EDX analysis at point 4. The mineral in a clay with high magnesium, potassium, aluminum and silica.

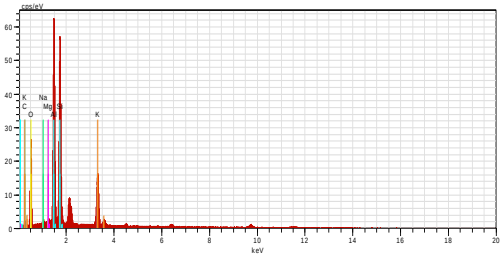

Figure D 153: An EDX analysis at point 5. The mineral is a clay, and appears to be illite.

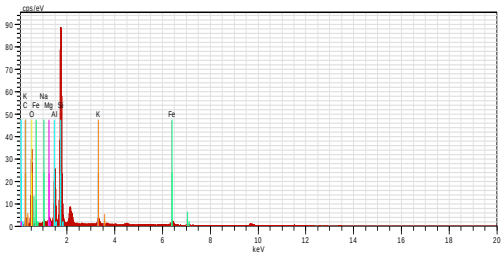

Figure D 154: An EDX analysis at point 6. The mineral appears to be an illilte with minor amounts of iron present.

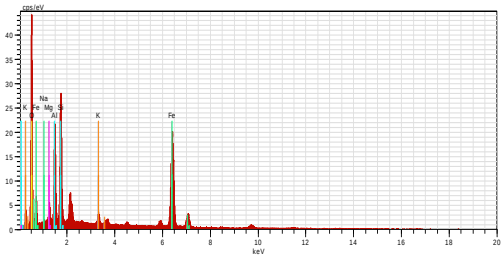

Figure D 155: An EDX analysis at point 7. The mineral is probably an Illite, but could be a glauconite.

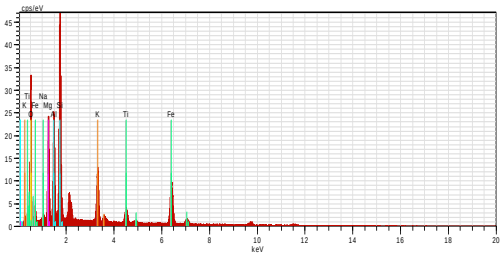

Figure D 156: An EDX analysis at point 8. The mineral is high in magnesium and iron but was not identified.

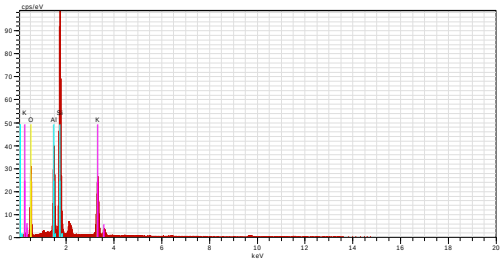

Figure D 157: An EDX analysis at point 9. The mineral is potassium feldspar.

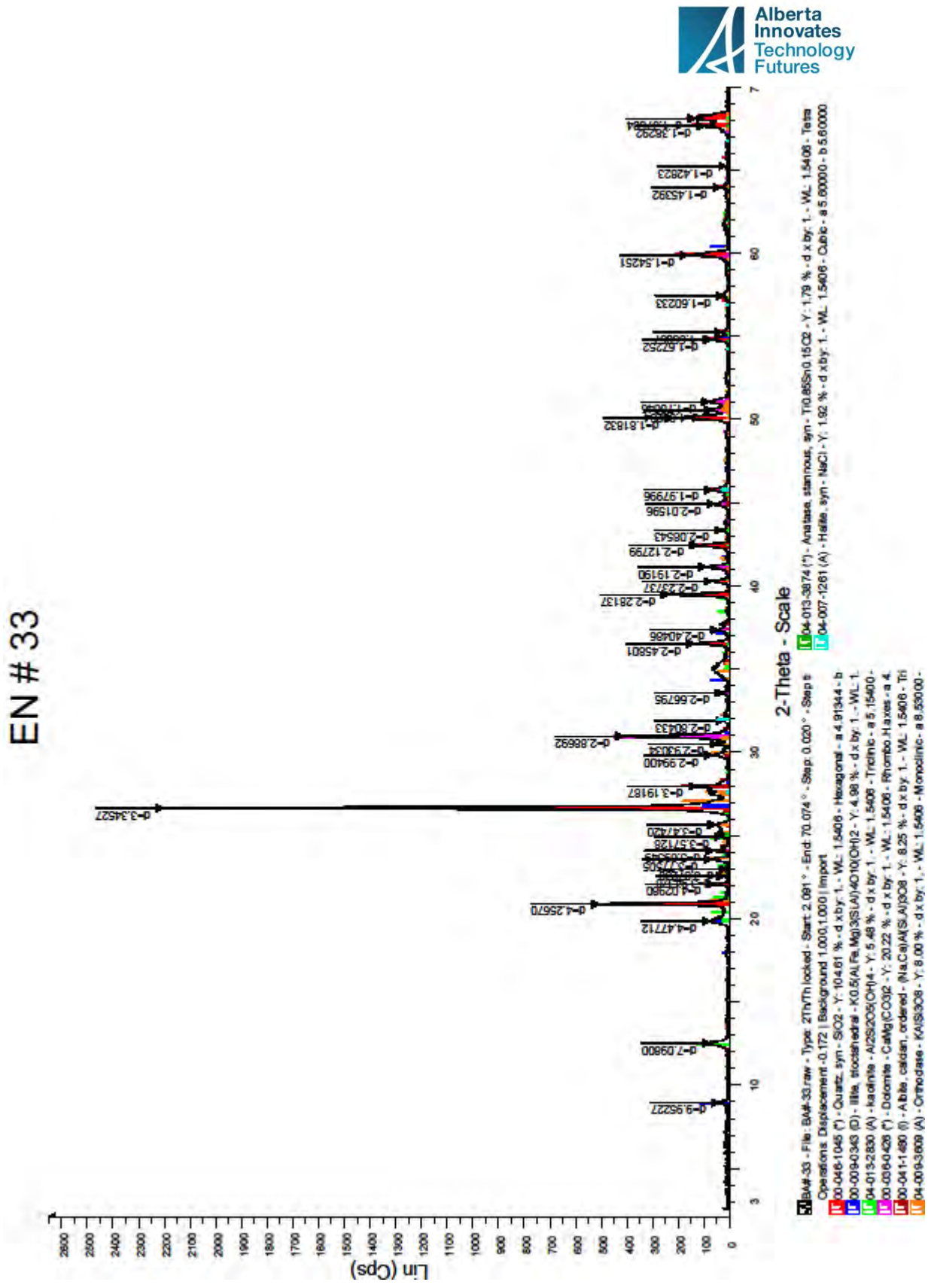

Figure D 158: X-Ray Diffraction pattern for sample EN-33.

Based on the X-Ray Diffraction results, the main mineral is quartz (65%). 15% of the sample is dolomite. Illite, kaolinite, potassium feldspar and plagioclase are present in the amount of 5% each. Traces of anatase and of halite (less than 1% each) were also identified. The Halite is probably drilling mud fluid contamination.

11.16 Sample EN-34

Sample EN-34 was sampled from core at a depth of approximately 748.50 meters from the lowermost Upper Belly River formation in well 12-5-39-23W4.

During the preparation, the sample was found to be water sensitive and proved very difficult to mount. Thus the SEM slide consists of grains epoxied onto the slide and then prepared.

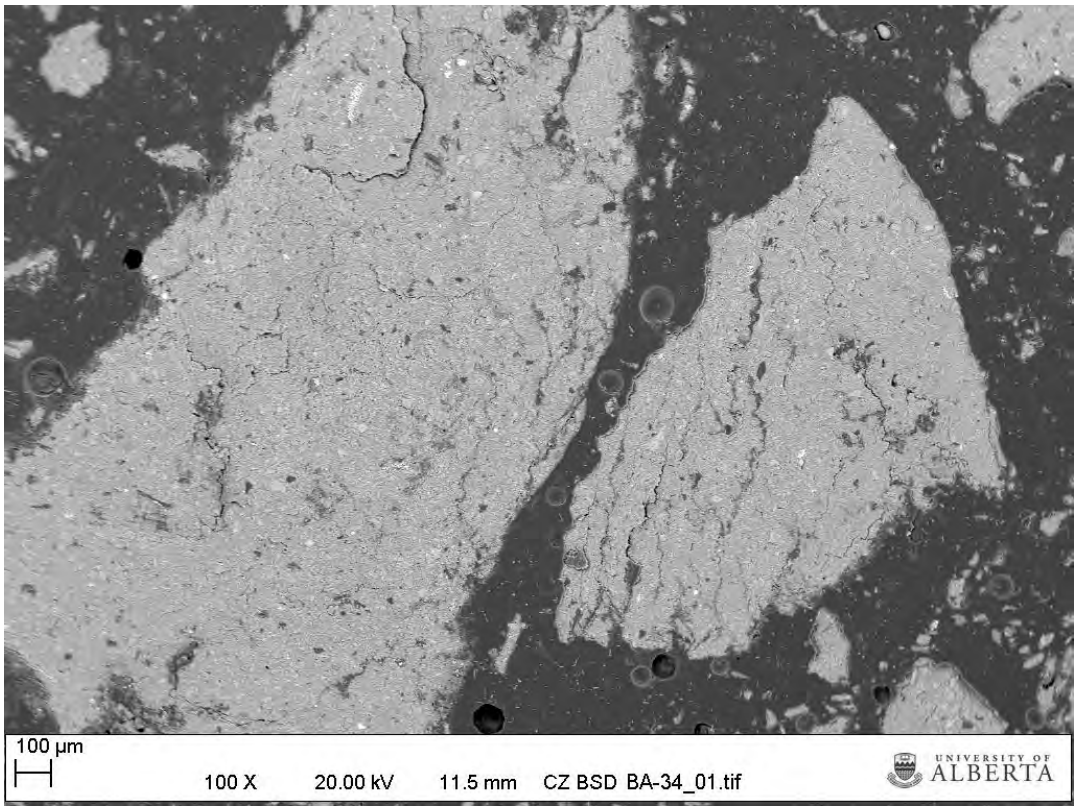

Figure D 159: A 100X magnification of Sample EN-34, shows that the slide is glued on fragments.

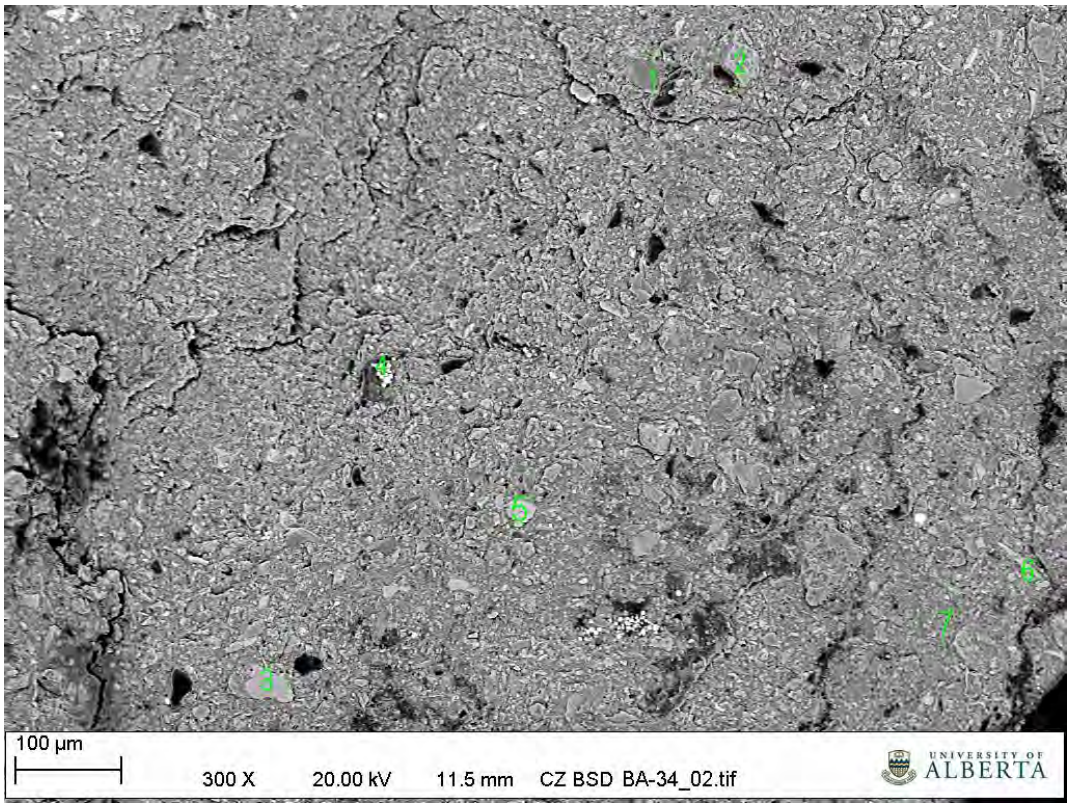

Figure D 160: A 300X magnification of Sample EN-34. The green annotations refer to the following EDX analysis. Quartz, illite and pyrite can be easily identified in this slide.

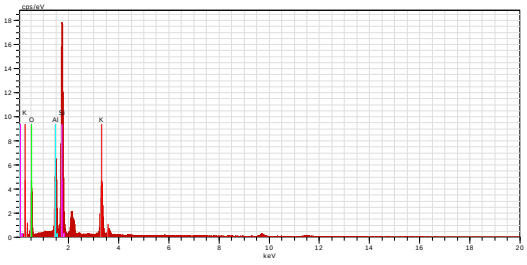

.

Figure D 161: An EDX overview analysis. The dominate minerals appear to be quartz and illite.

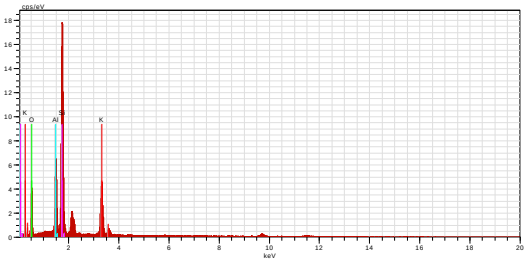

Figure D 162: An EDX analysis at point 1. The mineral is a clay, perhaps a chlorite.

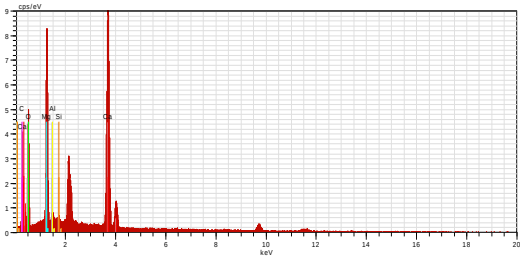

Figure D 163: An EDX analysis at point 2. The mineral is potassium feldspar.

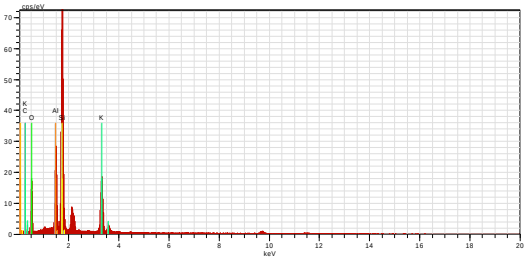

Figure D 166: An EDX analysis at point 5. The mineralogy is basically the same as at points 1 and 3.

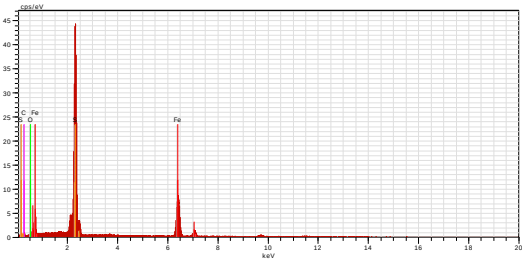

Figure D 164: An EDX analysis at point 3. The mineral is probably clay or a chlorite.

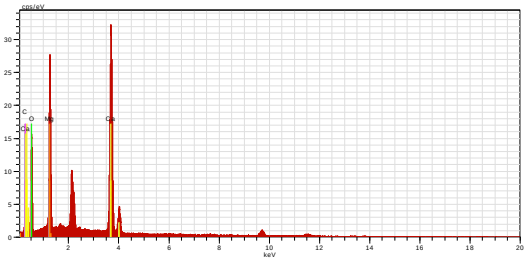

Figure D 167: An EDX analysis at point 6. This analysis is similar to the previous ones but the potassium levels are higher. Some illite may be present.

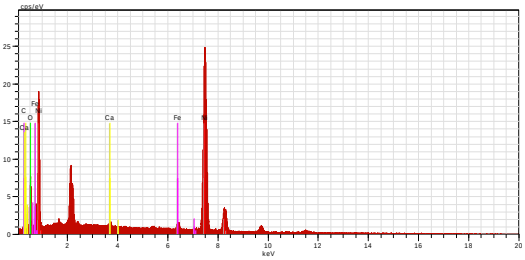

Figure D 165: An EDX analysis at point 4. The mineral is Pyrite with some background silicates indicating bleeding through.

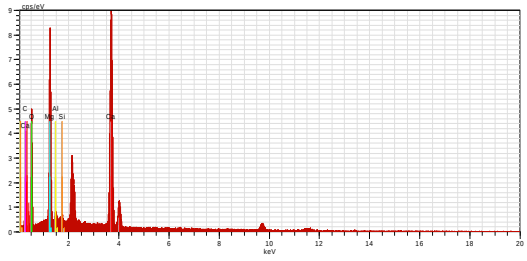

Figure D 168: An EDX analysis at point 7. This is an analysis of the very fine matrix and appears to be kaolinite with perhaps some illite.

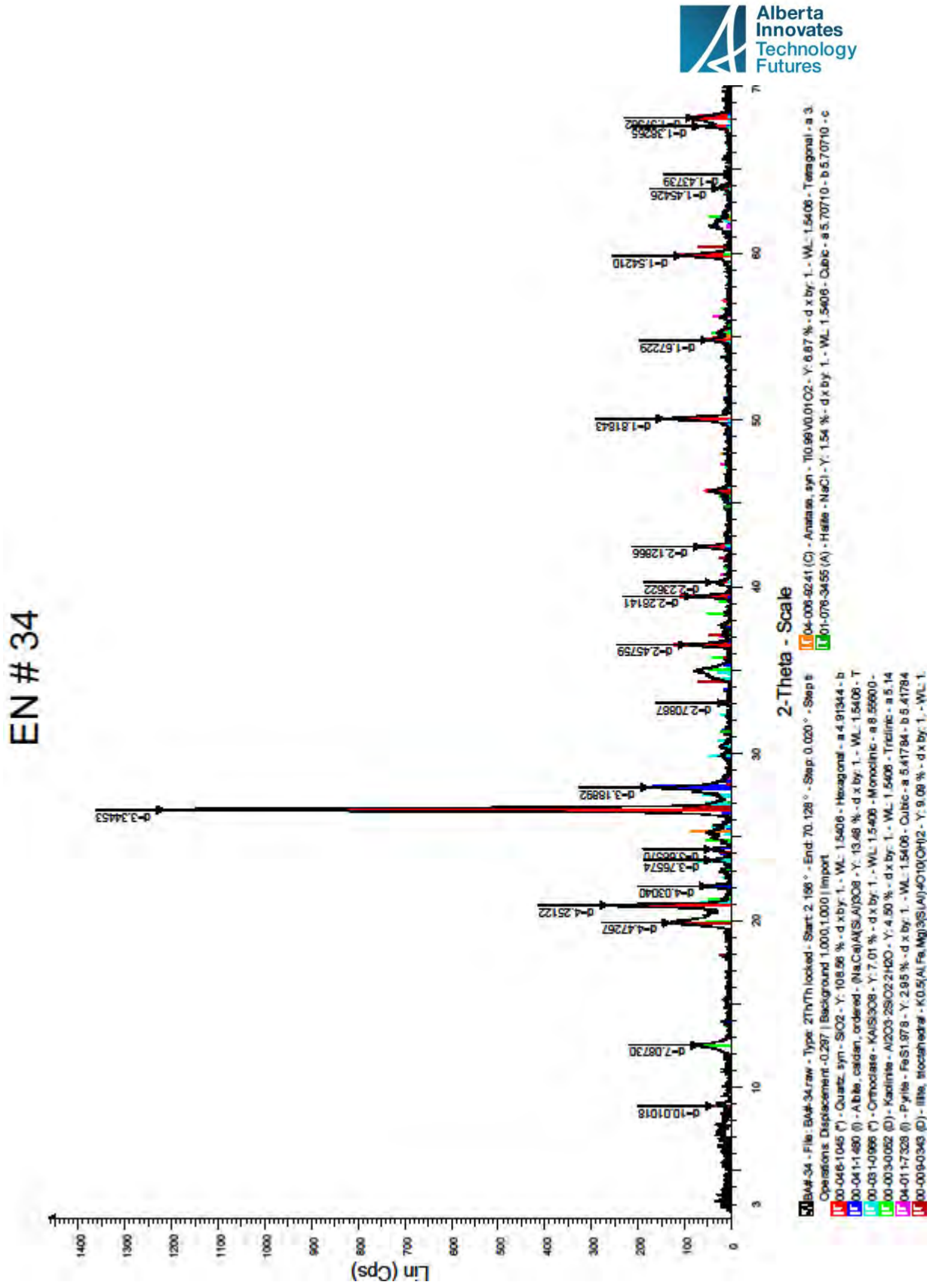

Figure D 169: X-Ray Diffraction pattern for sample EN-34.

Based on the X-Ray Diffraction results, the main mineral is Quartz (70%). 10% Plagioclase was also measured. Illite, kaolinite, potassium feldspar and anatase were present at 5% each. A trace of pyrite and hyalite (less than 1%) was also measured.

Alberta Innovates Technology Futures

11.17 ICP-MS, LECO & XRF analyses of all samples.

AcmeLabs Acme Analytical Laboratories (Vancouver) Ltd.
1020 Cordova St. East Vancouver BC V6A 4A3 Canada

Client: Alberta Innovates Technology Futures
250 Karl Clark Road
Edmonton AB T6N 1E4 Canada

Submitted By: Ernie Perkins
Receiving Lab: Canada-Vancouver
Received: May 26, 2011
Report Date: June 06, 2011
Page: 1 of 2

www.acmelab.com

CERTIFICATE OF ANALYSIS VAN11002216.1

CLIENT JOB INFORMATION

Project:	Enhance
Shipment ID:	
P.O. Number	E000065547
Number of Samples:	9

SAMPLE DISPOSAL

R TRN-PLP	Return
R TRN-RJT	Return

Acme does not accept responsibility for samples left at the laboratory after 90 days without prior written instructions for sample storage or return.

SAMPLE PREPARATION AND ANALYTICAL PROCEDURES

Method Code	Number of Samples	Code Description	Test Wgt (g)	Report Status	Lab
R200-250	9	Crush, split and pulverize 250 g rock to 200 mesh			VAN
1E	9	4 Add digestion ICP-ES analysis	0.25	Completed	VAN
Group 1T	9	4 Add digestion Ultratrace ICP-MS analysis	0.25	Completed	VAN
2A12	9	Analysis by Leco	0.1	Completed	VAN
4X02	9	Li2B4O7/LiBO2 fusion, analysis by XRF		Completed	VAN

ADDITIONAL COMMENTS

Invoice To: Alberta Innovates Technology Futures
250 Karl Clark Road
Edmonton AB T6N 1E4
Canada

CC: Trish Rattray

This report supersedes all previous preliminary and final reports with this file number dated prior to the date on this certificate. Signature indicates final approval; preliminary reports are unsigned and should be used for reference only.
All results are considered the confidential property of the client. Acme assumes the liabilities for actual cost of analysis only.
** asterisk indicates that an analytical result could not be provided due to unusually high levels of interference from other elements.

Acme Analytical Laboratories (Vancouver) Ltd.
1020 Cordova St. East Vancouver BC V6A 4A3 Canada
Phone (604) 253-3158 Fax (604) 253-1716
www.acmelab.com

Client: **Alberta Innovates Technology Futures**
250 Karl Clark Road
Edmonton AB T6N 1E4 Canada

Project: Enhance
Report Date: June 06, 2011

CERTIFICATE OF ANALYSIS VAN11002216.1

	Method	WGHT	1E	1E	1E	1E	1E	1E	1E	1E	1E	1E	1E	1E	1E	1E	1E	1E	1E	1E
	Analyte	Wgt	Mo	Cu	Pb	Zn	Ag	Ni	Co	Mn	Fe	As	U	Au	Th	Sr	Cd	Sb	Bi	V	Ca
	Unit	kg	ppm	ppm	ppm	ppm	ppm	ppm	ppm	ppm	%	ppm	ppm	ppm	ppm	ppm	ppm	ppm	ppm	ppm	%
	MDL	0.01	2	2	5	2	0.5	2	2	5	0.01	5	20	4	2	2	0.4	5	5	2	0.01
1	Rock	0.02	2	22	53	21	<0.5	24	11	157	1.34	14	<20	<4	2	111	<0.4	<5	<5	38	13.27
2	Rock	0.02	11	5	19	31	<0.5	22	6	223	1.73	<5	<20	<4	5	79	<0.4	<5	<5	68	9.17
3	Rock	0.03	<2	<2	7	30	<0.5	<2	<2	30	0.06	<5	<20	<4	<2	829	<0.4	<5	8	3	15.27
4	Rock	0.02	2	7	84	24	<0.5	23	17	104	0.86	<5	<20	<4	<2	67	<0.4	<5	<5	11	0.62
5	Rock	0.02	<2	24	25	52	<0.5	14	<2	981	8.05	<5	<20	<4	7	165	<0.4	<5	<5	115	1.73
6	Rock	0.02	5	13	13	59	<0.5	20	4	591	1.38	<5	<20	<4	5	348	0.5	<5	<5	85	8.95
7	Rock	0.02	2	11	20	47	<0.5	6	2	58	0.79	<5	<20	<4	7	101	<0.4	<5	<5	70	0.33
8	Rock	0.02	2	6	34	48	<0.5	10	5	72	1.06	<5	<20	<4	<2	55	<0.4	<5	<5	37	0.29
9	Rock	0.02	<2	12	19	54	<0.5	35	13	186	1.45	20	<20	<4	<2	161	<0.4	<5	<5	57	0.32

Acme Analytical Laboratories (Vancouver) Ltd.
1020 Cordova St. East Vancouver BC V6A 4A3 Canada
Phone (604) 253-3158 Fax (604) 253-1716
www.acmelab.com

Client: **Alberta Innovates Technology Futures**
250 Karl Clark Road
Edmonton AB T6N 1E4 Canada

Project: Enhance
Report Date: June 06, 2011

CERTIFICATE OF ANALYSIS VAN11002216.1

	Method	1E	1E	1E	1E	1E	1E	1E	1E	1E	1E	1E	1E	1E	1E	1E	1E	1T	1T	1T
	Analyte	P	La	Cr	Mg	Ba	Ti	Al	Na	K	W	Zr	Sn	Y	Nb	Be	Sc	S	Mo	Cu	Pb
	Unit	%	ppm	ppm	%	ppm	%	%	%	%	ppm	ppm	ppm	ppm	ppm	ppm	ppm	%	ppm	ppm	ppm
	MDL	0.002	2	2	0.01	1	0.01	0.01	0.01	0.01	4	2	2	2	2	1	1	0.1	0.05	0.02	0.02
1	Rock	0.020	11	19	7.90	118	0.13	2.97	0.12	1.91	<4	47	<2	8	5	<1	4	0.8	1.61	22.96	58.60
2	Rock	0.039	16	39	6.47	156	0.21	4.82	0.16	2.63	<4	53	<2	11	7	1	8	0.2	9.60	5.94	20.94
3	Rock	0.002	<2	<2	4.85	<1	<0.01	0.13	0.02	0.08	<4	<2	<2	<2	<2	<1	<1	5.6	0.46	0.84	6.54
4	Rock	0.004	9	11	0.15	103	0.08	0.71	0.04	0.22	<4	23	<2	3	3	<1	<1	0.8	1.98	9.56	92.82
5	Rock	0.470	28	73	1.58	365	0.29	6.20	0.30	2.23	<4	78	<2	28	12	2	13	<0.1	0.93	27.30	29.14
6	Rock	0.122	27	56	1.01	352	0.25	4.84	0.27	1.48	<4	79	<2	23	11	1	7	0.6	4.66	15.80	21.71
7	Rock	0.057	34	37	0.24	1554	0.38	4.04	0.41	1.20	<4	115	<2	18	16	<1	5	0.2	2.04	10.66	29.38
8	Rock	0.044	9	19	0.15	337	0.04	1.08	0.27	0.32	<4	15	3	8	2	<1	1	0.4	1.62	7.19	37.39
9	Rock	0.040	12	35	0.37	807	0.20	4.48	1.43	1.58	<4	41	<2	9	5	<1	6	<0.1	1.65	13.80	25.73

Acme Analytical Laboratories (Vancouver) Ltd.
1020 Cordova St. East Vancouver BC V6A 4A3 Canada
Phone (604) 253-3158 Fax (604) 253-1716
www.acmelab.com

Client: **Alberta Innovates Technology Futures**
250 Karl Clark Road
Edmonton AB T6N 1E4 Canada

Project: Enhance
Report Date: June 06, 2011

CERTIFICATE OF ANALYSIS VAN11002216.1

	Method	1T	1T	1T	1T	1T	1T	1T	1T	1T	1T	1T	1T	1T	1T	1T	1T	1T	1T	1T	1T
	Analyte	Zn	Ag	Ni	Co	Mn	Fe	As	U	Au	Th	Sr	Cd	Sb	Bi	V	Ca	P	La	Cr	Mg
	Unit	ppm	ppb	ppm	ppm	ppm	%	ppm	ppm	ppm	ppm	ppm	ppm	ppm	ppm	ppm	%	%	ppm	ppm	%
	MDL	0.2	20	0.1	0.2	2	0.02	0.2	0.1	0.1	0.1	1	0.02	0.02	0.04	1	0.02	0.001	0.1	1	0.02
1	Rock	29.1	89	24.0	10.3	147	1.30	13.1	2.1	<0.1	3.6	117	0.22	1.94	0.21	39	11.44	0.023	10.9	18	7.78
2	Rock	39.9	36	21.3	7.1	215	1.72	1.7	2.5	<0.1	5.6	85	0.08	0.73	0.10	70	8.29	0.038	15.5	31	6.50
3	Rock	31.2	52	0.9	0.6	34	0.06	<0.2	0.2	<0.1	0.1	1080	0.10	0.14	<0.04	3	16.98	0.003	1.1	2	4.85
4	Rock	26.6	75	26.4	18.8	108	0.93	5.2	0.5	<0.1	1.8	76	0.19	1.85	<0.04	12	0.65	0.005	10.1	11	0.15
5	Rock	67.8	144	16.5	2.9	1025	8.63	1.8	2.6	<0.1	9.4	194	0.41	0.48	0.30	128	1.88	0.505	35.5	80	1.89
6	Rock	65.3	191	22.6	4.3	599	1.44	7.7	3.0	<0.1	7.7	356	0.66	0.74	0.18	89	8.46	0.130	29.5	55	1.05
7	Rock	47.4	121	7.3	2.4	63	0.82	1.6	2.2	<0.1	8.9	118	0.15	1.54	0.14	72	0.40	0.060	37.7	30	0.25
8	Rock	51.8	172	10.0	6.0	79	1.11	5.0	0.7	<0.1	1.6	60	0.09	0.92	0.05	40	0.32	0.045	9.7	17	0.16
9	Rock	52.2	146	33.9	13.3	181	1.48	20.7	1.1	<0.1	2.7	175	0.10	1.11	0.05	63	0.37	0.040	14.3	34	0.35

Acme Analytical Laboratories (Vancouver) Ltd.
1020 Cordova St. East Vancouver BC V6A 4A3 Canada
Phone (604) 253-3158 Fax (604) 253-1716
www.acmelab.com

Client: **Alberta Innovates Technology Futures**
250 Karl Clark Road
Edmonton AB T6N 1E4 Canada

Project: Enhance
Report Date: June 06, 2011

CERTIFICATE OF ANALYSIS VAN11002216.1

	Method	1T	1T	1T	1T	1T	1T	1T	1T	1T	1T	1T	1T	1T	1T	1T	1T	1T	1T	1T	1T
	Analyte	Ba	Ti	Al	Na	K	W	Zr	Sn	Be	Sc	S	Y	Ce	Pr	Nd	Sm	Eu	Gd	Tb	Dy
	Unit	ppm	%	%	%	%	ppm	ppm	ppm	ppm	ppm	%	ppm	ppm	ppm	ppm	ppm	ppm	ppm	ppm	ppm
	MDL	1	0.001	0.02	0.002	0.02	0.1	0.2	0.1	1	0.1	0.04	0.1	0.02	0.1	0.1	0.1	0.1	0.1	0.1	0.1
1	Rock	128	0.132	2.74	0.111	1.78	0.4	41.6	0.9	1	4.2	0.76	7.7	22.21	2.7	9.3	1.9	0.4	1.5	0.3	1.4
2	Rock	164	0.201	4.64	0.164	3.41	0.5	46.0	1.3	1	8.2	0.25	10.8	31.89	4.0	13.9	2.4	0.5	2.0	0.3	2.0
3	Rock	6	0.005	0.11	0.017	0.08	<0.1	0.9	<0.1	<1	0.4	8.13	0.6	2.07	0.3	0.7	<0.1	<0.1	0.2	<0.1	<0.1
4	Rock	218	0.082	0.71	0.033	0.23	0.2	20.1	0.5	<1	0.8	0.83	3.2	22.50	2.6	9.1	1.6	0.3	1.1	0.2	0.7
5	Rock	404	0.306	7.00	0.314	2.47	1.0	68.7	1.8	2	14.2	0.11	31.7	66.60	8.5	29.7	6.0	1.2	5.3	0.9	4.7
6	Rock	371	0.246	4.83	0.270	1.50	0.8	63.8	1.1	1	7.7	0.62	23.0	55.53	6.6	24.2	4.8	1.2	4.5	0.7	3.9
7	Rock	956	0.371	3.97	0.416	1.27	0.9	93.4	1.6	1	5.1	0.24	19.1	73.79	9.2	33.6	6.5	1.2	5.0	0.8	3.7
8	Rock	309	0.038	1.03	0.255	0.33	0.2	11.9	0.6	1	1.1	0.38	7.6	18.28	2.3	8.8	1.6	0.4	1.7	0.3	1.5
9	Rock	768	0.195	4.50	1.419	1.56	0.6	36.8	1.0	<1	5.3	0.05	9.7	25.56	3.4	12.8	2.5	0.6	1.7	0.3	1.6

Acme Analytical Laboratories (Vancouver) Ltd.
1020 Cordova St. East Vancouver BC V6A 4A3 Canada
Phone (604) 253-3158 Fax (604) 253-1716
www.acmelab.com

Client: **Alberta Innovates Technology Futures**
250 Karl Clark Road
Edmonton AB T6N 1E4 Canada

Project: Enhance
Report Date: June 06, 2011

CERTIFICATE OF ANALYSIS VAN11002216.1

	Method	1T	1T	1T	1T	1T	1T	1T	1T	1T	1T	1T	1T	2A Leco	2A Leco	4X	4X	4X	4X	4X	4X
	Analyte	Ho	Er	Tm	Yb	Lu	Hf	Li	Rb	Ta	Nb	Cs	Ga	TOT/C	TOT/S	SiO2	Al2O3	Fe2O3	CaO	MgO	Na2O
	Unit	ppm	ppm	ppm	ppm	ppm	ppm	ppm	ppm	ppm	ppm	ppm	ppm	%	%	%	%	%	%	%	%
	MDL	0.1	0.1	0.1	0.1	0.1	0.02	0.1	0.1	0.1	0.04	0.1	0.02	0.02	0.02	0.1	0.01	0.01	0.01	0.01	0.01
1	Rock	0.3	0.9	0.1	0.8	0.1	1.21	141.6	66.5	0.3	3.69	2.3	6.68	8.06	0.79	24.1	5.24	2.05	19.61	14.48	0.34
2	Rock	0.4	1.0	0.2	1.0	0.2	1.29	276.6	103.4	0.4	5.38	4.5	10.72	6.03	0.25	33.9	8.94	2.72	13.92	12.02	0.34
3	Rock	<0.1	<0.1	<0.1	<0.1	<0.1	0.03	9.5	2.3	<0.1	0.16	0.1	0.24	5.49	13.93	0.8	0.21	0.09	36.83	8.76	<0.01
4	Rock	0.1	0.4	<0.1	0.3	<0.1	0.56	12.5	8.6	<0.1	2.24	0.3	1.34	1.78	0.79	90.8	1.32	1.25	0.91	0.29	0.04
5	Rock	1.1	2.8	0.4	2.4	0.3	2.07	51.1	122.4	0.7	10.32	9.3	17.22	3.75	0.09	49.7	13.00	12.49	2.64	2.81	0.41
6	Rock	0.8	2.3	0.3	1.8	0.3	1.79	35.8	71.2	0.6	9.15	5.0	11.33	5.11	0.58	53.4	9.08	2.11	12.88	1.87	0.39
7	Rock	0.7	2.0	0.3	1.8	0.3	2.85	32.7	75.8	0.7	12.86	3.2	10.01	0.51	0.22	82.8	7.74	1.14	0.49	0.41	0.53
8	Rock	0.2	0.7	<0.1	0.5	<0.1	0.37	18.1	16.4	<0.1	1.74	0.7	3.06	0.59	0.35	92.2	2.02	1.54	0.41	0.28	0.31
9	Rock	0.3	0.9	0.2	0.9	0.1	1.06	16.3	34.4	0.2	3.60	1.1	9.44	0.33	0.04	79.3	8.94	2.10	0.49	0.65	1.92

Acme Analytical Laboratories (Vancouver) Ltd.
1020 Cordova St. East Vancouver BC V6A 4A3 Canada
Phone (604) 253-3158 Fax (604) 253-1716
www.acmelab.com

Client: **Alberta Innovates Technology Futures**
250 Karl Clark Road
Edmonton AB T6N 1E4 Canada

Project: Enhance
Report Date: June 06, 2011

CERTIFICATE OF ANALYSIS VAN11002216.1

	Method	4X	4X	4X	4X	4X	4X	4X	4X
	Analyte	K2O	MnO	TiO2	P2O5	Cr2O3	Ba	LOI	SUM
	Unit	%	%	%	%	%	%	%	%
	MDL	0.01	0.01	0.01	0.01	0.001	0.01	-5.11	0.01
1	Rock	2.01	0.02	0.28	0.05	0.004	0.01	29.91	98.02
2	Rock	3.78	0.03	0.41	0.09	0.005	0.02	23.74	99.87
3	Rock	0.02	<0.01	<0.01	<0.01	<0.001	<0.01	19.25	65.96
4	Rock	0.27	0.02	0.23	0.01	<0.001	0.04	3.93	99.10
5	Rock	2.94	0.13	0.55	1.07	0.011	0.04	14.39	100.2
6	Rock	1.75	0.08	0.48	0.28	0.006	0.04	16.76	99.14
7	Rock	1.49	0.01	0.81	0.13	0.008	0.17	3.61	99.38
8	Rock	0.39	0.01	0.09	0.10	<0.001	0.03	1.82	99.25
9	Rock	1.98	0.03	0.39	0.09	0.006	0.07	3.10	99.13

Acme Analytical Laboratories (Vancouver) Ltd.
1020 Cordova St. East Vancouver BC V6A 4A3 Canada
Phone (604) 253-3158 Fax (604) 253-1716
www.acmelab.com

Client: **Alberta Innovates Technology Futures**
250 Karl Clark Road
Edmonton AB T6N 1E4 Canada

Project: Enhance
Report Date: June 06, 2011

QUALITY CONTROL REPORT VAN11002216.1

	Method	WGHT	1E	1E	1E	1E	1E	1E	1E	1E	1E	1E	1E	1E	1E	1E	1E	1E	1E	1E
	Analyte	Wgt	Mo	Cu	Pb	Zn	Ag	Ni	Co	Mn	Fe	As	U	Au	Th	Sr	Cd	Sb	Bi	V	Ca
	Unit	kg	ppm	ppm	ppm	ppm	ppm	ppm	ppm	ppm	%	ppm	ppm	ppm	ppm	ppm	ppm	ppm	ppm	ppm	%
	MDL	0.01	2	2	5	2	0.5	2	2	5	0.01	5	20	4	2	2	0.4	5	5	2	0.01
Pulp Duplicates																					
2	Rock	0.02	11	5	19	31	<0.5	22	6	223	1.73	<5	<20	<4	5	79	<0.4	<5	<5	68	9.17
REP 2	QC		11	5	13	33	<0.5	22	6	228	1.75	<5	<20	<4	3	81	<0.4	<5	5	68	9.40
3	Rock	0.03	<2	<2	7	30	<0.5	<2	<2	30	0.06	<5	<20	<4	<2	829	<0.4	<5	8	3	15.27
REP 3	QC																				
4	Rock	0.02	2	7	84	24	<0.5	23	17	104	0.86	<5	<20	<4	<2	67	<0.4	<5	<5	11	0.62
REP 4	QC																				
5	Rock	0.02	<2	24	25	52	<0.5	14	<2	981	8.05	<5	<20	<4	7	165	<0.4	<5	<5	115	1.73
REP 5	QC																				
Reference Materials																					
STD CSC	Standard																				
STD NBS-86A (D)	Standard																				
STD OREAS24P	Standard																				
STD OREAS24P	Standard		<2	47	<5	112	<0.5	142	44	1118	7.45	<5	<20	<4	<2	386	<0.4	<5	<5	156	5.70
STD OREAS45C	Standard																				
STD OREAS45C	Standard		2	650	21	82	<0.5	339	106	1228	17.74	12	<20	<4	10	37	<0.4	<5	<5	276	0.50
STD OREAS76A	Standard																				
STD SO-18	Standard																				
STD SY-4(D)	Standard																				
STD CSC Expected																					
STD OREAS76A Expected																					
STD OREAS24P Expected			1.5	52	2.9	119	0.06	141	44	1100	7.53	1.2	0.75		2.85	403	0.15	0.09		158	5.83
STD OREAS45C Expected			2.26	620	24	83	0.28	333	104	1160	16.33	10.1	2.4	0.045	10.2	36.4	0.15	0.79	0.21	270	0.482
STD SY-4(D) Expected																					
STD SO-18 Expected																					
STD NBS-86A (D) Expected																					
BLK	Blank																				
BLK	Blank																				
BLK	Blank		<2	<2	<5	<2	<0.5	<2	<2	<5	<0.01	<5	<20	<4	<2	<2	<0.4	<5	<5	<2	<0.01

Acme Analytical Laboratories (Vancouver) Ltd.
1020 Cordova St. East Vancouver BC V6A 4A3 Canada
Phone (604) 253-3158 Fax (604) 253-1716
www.acmelab.com

Client: **Alberta Innovates Technology Futures**
250 Karl Clark Road
Edmonton AB T6N 1E4 Canada

Project: Enhance
Report Date: June 06, 2011

QUALITY CONTROL REPORT VAN11002216.1

	Method	1E	1E	1E	1E	1E	1E	1E	1E	1E	1E	1E	1E	1E	1E	1E	1E	1T	1T	1T
	Analyte	P	La	Cr	Mg	Ba	Ti	Al	Na	K	W	Zr	Sn	Y	Nb	Be	Sc	S	Mo	Cu	Pb
	Unit	%	ppm	ppm	%	ppm	%	%	%	%	ppm	ppm	ppm	ppm	ppm	ppm	ppm	%	ppm	ppm	ppm
	MDL	0.002	2	2	0.01	1	0.01	0.01	0.01	0.01	4	2	2	2	2	1	1	0.1	0.05	0.02	0.02
Pulp Duplicates																					
2	Rock	0.039	16	39	6.47	156	0.21	4.82	0.16	2.63	<4	53	<2	11	7	1	8	0.2	9.60	5.94	20.94
REP 2	QC	0.038	16	35	6.61	158	0.21	4.90	0.16	2.92	<4	53	3	11	7	1	8	0.2			
3	Rock	0.002	<2	<2	4.85	<1	<0.01	0.13	0.02	0.08	<4	<2	<2	<2	<2	<1	<1	5.6	0.46	0.84	6.54
REP 3	QC																		0.53	0.78	6.95
4	Rock	0.004	9	11	0.15	103	0.08	0.71	0.04	0.22	<4	23	<2	3	3	<1	<1	0.8	1.98	9.56	92.82
REP 4	QC																				
5	Rock	0.470	28	73	1.58	385	0.29	6.20	0.30	2.23	<4	78	<2	28	12	2	13	<0.1	0.93	27.30	29.14
REP 5	QC																				
Reference Materials																					
STD CSC	Standard																				
STD NBS-88A (D)	Standard																				
STD OREAS24P	Standard																		1.31	46.13	278
STD OREAS24P	Standard	0.135	18	199	4.02	274	1.02	7.59	2.33	0.70	<4	149	<2	21	24	1	20	<0.1			
STD OREAS45C	Standard																		2.15	649.2	27.45
STD OREAS45C	Standard	0.052	25	1021	0.25	298	1.17	7.35	0.09	0.36	<4	192	<2	12	29	1	61	<0.1			
STD OREAS76A	Standard																				
STD SO-18	Standard																				
STD SY-4(D)	Standard																				
STD CSC Expected																					
STD OREAS76A Expected																					
STD OREAS24P Expected		0.136	17.4	196	4.13	285	1.1	7.66	2.34	0.7	0.5	141	1.6	21.3	21		20		1.5	52	29
STD OREAS45C Expected		0.051	26.2	962	0.25	270	1.1313	7.59	0.097	0.36	1.06	169.7	2.9	12.9	23.05		59.03	0.021	2.26	620	36
STD SY-4(D) Expected																					
STD SO-18 Expected																					
STD NBS-88A (D) Expected																					
BLK	Blank																				
BLK	Blank																		<0.05	<0.02	<0.02
BLK	Blank	<0.002	<2	<2	<0.01	<1	<0.01	<0.01	<0.01	<0.01	<4	<2	<2	<2	<2	<1	<1	<0.1			

Acme Analytical Laboratories (Vancouver) Ltd.
1020 Cordova St. East Vancouver BC V6A 4A3 Canada
Phone (604) 253-3158 Fax (604) 253-1716
www.acmelab.com

Client: **Alberta Innovates Technology Futures**
250 Karl Clark Road
Edmonton AB T6N 1E4 Canada

Project: Enhance
Report Date: June 06, 2011

QUALITY CONTROL REPORT VAN11002216.1

	Method	1T	1T	1T	1T	1T	1T	1T	1T	1T	1T	1T	1T	1T	1T	1T	1T	1T	1T	1T
	Analyte	Zn	Ag	Ni	Co	Mn	Fe	As	U	Au	Th	Sr	Cd	Sb	Bi	V	Ca	P	La	Cr	Mg
	Unit	ppm	ppb	ppm	ppm	ppm	%	ppm	ppm	ppm	ppm	ppm	ppm	ppm	ppm	ppm	%	%	ppm	ppm	%
	MDL	0.2	20	0.1	0.2	2	0.02	0.2	0.1	0.1	0.1	1	0.02	0.02	0.04	1	0.02	0.001	0.1	1	0.02
Pulp Duplicates																					
2	Rock	39.9	36	21.3	7.1	215	1.72	1.7	2.5	<0.1	5.6	85	0.08	0.73	0.10	70	8.29	0.036	15.5	31	6.50
REP 2	QC																				
3	Rock	31.2	52	0.9	0.6	34	0.06	<0.2	0.2	<0.1	0.1	1080	0.10	0.14	<0.04	3	16.98	0.003	1.1	2	4.86
REP 3	QC	35.8	27	1.1	0.3	36	0.08	0.6	0.2	<0.1	<0.1	1065	0.07	0.16	<0.04	3	16.99	0.003	1.1	1	4.86
4	Rock	26.6	75	26.4	18.8	108	0.93	5.2	0.5	<0.1	1.8	76	0.19	1.85	<0.04	12	0.65	0.005	10.1	11	0.15
REP 4	QC																				
5	Rock	67.8	144	16.5	2.9	1025	8.63	1.8	2.6	<0.1	9.4	194	0.41	0.48	0.30	126	1.88	0.505	35.5	80	1.69
REP 5	QC																				
Reference Materials																					
STD CSC	Standard																				
STD NBS-88A (D)	Standard																				
STD OREAS24P	Standard	114.0	45	135.7	46.2	1033	7.17	1.0	0.7	<0.1	2.7	379	0.10	0.10	<0.04	159	5.33	0.134	18.1	182	3.96
STD OREAS24P	Standard																				
STD OREAS45C	Standard	89.6	416	349.4	104.9	1177	18.80	11.9	2.4	<0.1	11.4	42	0.16	0.92	0.25	276	0.52	0.057	27.9	987	0.26
STD OREAS45C	Standard																				
STD OREAS76A	Standard																				
STD SO-18	Standard																				
STD SY-4(D)	Standard																				
STD CSC Expected																					
STD OREAS76A Expected																					
STD OREAS24P Expected		119	60	141	44	1100	7.53	1.2	0.75		2.85	403	0.15	0.09		158	5.83	0.136	17.4	196	4.13
STD OREAS45C Expected		83	280	333	104	1160	18.33	10.1	2.4	0.045	10.2	36.4	0.15	0.79	0.21	270	0.482	0.051	26.2	962	0.25
STD SY-4(D) Expected																					
STD SO-18 Expected																					
STD NBS-88A (D) Expected																					
BLK	Blank																				
BLK	Blank	<0.2	<20	<0.1	<0.2	<2	<0.02	<0.2	<0.1	<0.1	<0.1	<1	<0.02	<0.02	<0.04	<1	<0.02	<0.001	<0.1	<1	<0.02
BLK	Blank																				

Acme Analytical Laboratories (Vancouver) Ltd.
1020 Cordova St. East Vancouver BC V6A 4A3 Canada
Phone (604) 253-3158 Fax (604) 253-1716
www.acmelab.com

Client: **Alberta Innovates Technology Futures**
250 Karl Clark Road
Edmonton AB T6N 1E4 Canada

Project: Enhance
Report Date: June 06, 2011

QUALITY CONTROL REPORT VAN11002216.1

	Method	1T	1T	1T	1T	1T	1T	1T	1T	1T	1T	1T	1T	1T	1T	1T	1T	1T	1T	1T
	Analyte	Ba	Ti	Al	Na	K	W	Zr	Sn	Be	Sc	S	Y	Ce	Pr	Nd	Sm	Eu	Gd	Tb	Dy
	Unit	ppm	%	%	%	%	ppm	ppm	ppm	ppm	ppm	%	ppm	ppm	ppm	ppm	ppm	ppm	ppm	ppm	ppm
	MDL	1	0.001	0.02	0.002	0.02	0.1	0.2	0.1	1	0.1	0.04	0.1	0.02	0.1	0.1	0.1	0.1	0.1	0.1	0.1
Pulp Duplicates																					
2	Rock	164	0.201	4.64	0.164	3.41	0.5	46.0	1.3	1	8.2	0.25	10.8	31.89	4.0	13.9	2.4	0.5	2.0	0.3	2.0
REP 2	QC																				
3	Rock	6	0.005	0.11	0.017	0.08	<0.1	0.9	<0.1	<1	0.4	8.13	0.6	2.07	0.3	0.7	<0.1	<0.1	0.2	<0.1	<0.1
REP 3	QC	5	0.005	0.12	0.018	0.08	<0.1	1.0	<0.1	<1	0.3	8.21	0.7	2.07	0.3	0.8	0.2	<0.1	<0.1	<0.1	<0.1
4	Rock	218	0.082	0.71	0.033	0.23	0.2	20.1	0.5	<1	0.8	0.83	3.2	22.50	2.6	9.1	1.6	0.3	1.1	0.2	0.7
REP 4	QC																				
5	Rock	404	0.306	7.00	0.314	2.47	1.0	68.7	1.8	2	14.2	0.11	31.7	66.60	8.5	29.7	6.0	1.2	5.3	0.9	4.7
REP 5	QC																				
Reference Materials																					
STD CSC	Standard																				
STD NBS-88A (D)	Standard																				
STD OREAS24P	Standard	279	0.992	7.45	2.340	0.67	0.4	131.5	1.6	1	19.3	<0.04	21.5	35.96	4.8	19.2	4.9	1.9	4.6	0.8	4.4
STD OREAS24P	Standard																				
STD OREAS45C	Standard	290	1.173	7.47	0.092	0.38	1.0	172.1	3.1	<1	61.3	<0.04	13.6	54.31	6.3	24.0	4.7	1.2	4.1	0.6	3.7
STD OREAS45C	Standard																				
STD OREAS76A	Standard																				
STD SO-18	Standard																				
STD SY-4(D)	Standard																				
STD CSC Expected																					
STD OREAS76A Expected																					
STD OREAS24P Expected		285	1.1	7.66	2.34	0.7	0.5	141	1.6		20		21.3	37.6	4.7	22	4.7	1.6	5.3	0.81	4.6
STD OREAS45C Expected		270	1.1313	7.59	0.097	0.36	1.06	169.7	2.9		59.03	0.021	12.9	54	6.31	24.49	4.3	1.13	3.64	0.6	3.41
STD SY-4(D) Expected																					
STD SO-18 Expected																					
STD NBS-88A (D) Expected																					
BLK	Blank																				
BLK	Blank	<1	<0.001	<0.02	<0.002	<0.02	<0.1	<0.2	<0.1	<1	<0.1	<0.04	<0.1	<0.02	<0.1	<0.1	<0.1	<0.1	<0.1	<0.1	<0.1
BLK	Blank																				

Acme Analytical Laboratories (Vancouver) Ltd.
1020 Cordova St. East Vancouver BC V6A 4A3 Canada
Phone (604) 253-3158 Fax (604) 253-1716
www.acmelab.com

Client: **Alberta Innovates Technology Futures**
250 Karl Clark Road
Edmonton AB T6N 1E4 Canada

Project: Enhance
Report Date: June 06, 2011

QUALITY CONTROL REPORT VAN11002216.1

	Method	1T	1T	1T	1T	1T	1T	1T	1T	1T	1T	1T	1T	2A Leco	2A Leco	4X	4X	4X	4X	4X	4X
	Analyte	Ho	Er	Tm	Yb	Lu	Hf	Li	Rb	Ta	Nb	Cs	Ga	TOT/C	TOT/S	SiO2	Al2O3	Fe2O3	CaO	MgO	Na2O
	Unit	ppm	ppm	ppm	ppm	ppm	ppm	ppm	ppm	ppm	ppm	ppm	ppm	%	%	%	%	%	%	%	%
	MDL	0.1	0.1	0.1	0.1	0.1	0.02	0.1	0.1	0.1	0.04	0.1	0.02	0.02	0.02	0.1	0.01	0.01	0.01	0.01	0.01
Pulp Duplicates																					
2	Rock	0.4	1.0	0.2	1.0	0.2	1.29	276.6	103.4	0.4	5.38	4.5	10.72	6.03	0.25	33.9	8.94	2.72	13.92	12.02	0.34
REP 2	QC																				
3	Rock	<0.1	<0.1	<0.1	<0.1	<0.1	0.03	9.5	2.3	<0.1	0.16	0.1	0.24	5.49	13.93	0.8	0.21	0.09	36.83	8.76	<0.01
REP 3	QC	<0.1	<0.1	<0.1	<0.1	<0.1	0.02	10.2	2.6	<0.1	0.20	0.1	0.34								
4	Rock	0.1	0.4	<0.1	0.3	<0.1	0.56	12.5	8.6	<0.1	2.24	0.3	1.34	1.78	0.79	90.8	1.32	1.25	0.91	0.29	0.04
REP 4	QC															90.8	1.30	1.26	0.90	0.27	0.01
5	Rock	1.1	2.8	0.4	2.4	0.3	2.07	51.1	122.4	0.7	10.32	9.3	17.22	3.75	0.09	49.7	13.00	12.49	2.64	2.61	0.41
REP 5	QC													3.73	0.09						
Reference Materials																					
STD CSC	Standard													3.11	4.29						
STD NBS-88A (D)	Standard															1.3	0.22	0.28	30.14	21.11	<0.01
STD OREAS24P	Standard	0.9	2.1	0.3	1.8	0.3	3.38	7.2	21.8	1.1	17.63	0.8	19.38								
STD OREAS24P	Standard																				
STD OREAS45C	Standard	0.6	1.7	0.3	1.6	0.2	4.37	16.7	24.3	1.5	22.35	2.3	25.52								
STD OREAS45C	Standard																				
STD OREAS76A	Standard													0.16	17.72						
STD SO-18	Standard															58.2	14.04	7.59	6.38	3.37	3.81
STD SY-4(D)	Standard															50.1	20.81	6.27	8.06	0.53	7.23
STD CSC Expected														2.94	4.25						
STD OREAS76A Expected														0.16	18						
STD OREAS24P Expected		0.8	2.2	0.3	1.83	0.25	3.6	8.7	22.4	1.04	21	0.8	19.43								
STD OREAS45C Expected		0.64	1.52	0.21	1.51	0.23	4.27	15.69	24	1.43	23.05	2.3	24.8								
STD SY-4(D) Expected																49.9	20.69	6.21	8.05	0.54	7.1
STD SO-18 Expected																58.47		7.67	6.42	3.35	3.71
STD NBS-88A (D) Expected																1.2	0.19	0.28	30.1	21.3	
BLK	Blank													<0.02	<0.02						
BLK	Blank	<0.1	<0.1	<0.1	<0.1	<0.1	<0.02	<0.1	<0.1	<0.1	<0.04	<0.1	<0.02								
BLK	Blank																				

Acme Analytical Laboratories (Vancouver) Ltd.
1020 Cordova St. East Vancouver BC V6A 4A3 Canada
Phone (604) 253-3158 Fax (604) 253-1716
www.acmelab.com

Client: **Alberta Innovates Technology Futures**
250 Karl Clark Road
Edmonton AB T6N 1E4 Canada

Project: Enhance
Report Date: June 06, 2011

QUALITY CONTROL REPORT VAN11002216.1

	Method	4X	4X	4X	4X	4X	4X	4X	4X
	Analyte	K2O	MnO	TiO2	P2O5	Cr2O3	Ba	LOI	SUM
	Unit	%	%	%	%	%	%	%	%
	MDL	0.01	0.01	0.01	0.01	0.001	0.01	-5.11	0.01
Pulp Duplicates									
2	Rock	3.78	0.03	0.41	0.09	0.005	0.02	23.74	99.87
REP 2	QC								
3	Rock	0.02	<0.01	<0.01	<0.01	<0.001	<0.01	19.25	65.96
REP 3	QC								
4	Rock	0.27	0.02	0.23	0.01	<0.001	0.04	3.93	99.10
REP 4	QC	0.27	0.02	0.21	0.01	<0.001	0.04	3.93	99.03
5	Rock	2.94	0.13	0.55	1.07	0.011	0.04	14.39	100.2
REP 5	QC								
Reference Materials									
STD CSC	Standard								
STD NBS-88A (D)	Standard	0.13	0.03	0.01	<0.01	<0.001	<0.01	46.70	99.91
STD OREAS24P	Standard								
STD OREAS24P	Standard								
STD OREAS45C	Standard								
STD OREAS45C	Standard								
STD OREAS76A	Standard								
STD SO-18	Standard	2.26	0.40	0.72	0.81	0.577	0.06	1.91	99.57
STD SY-4(D)	Standard	1.69	0.11	0.27	0.13	0.001	0.05	4.56	99.82
STD CSC Expected									
STD OREAS76A Expected									
STD OREAS24P Expected									
STD OREAS45C Expected									
STD SY-4(D) Expected		1.66	0.108	0.287	0.131		0.034	4.56	
STD SO-18 Expected		2.17	0.39	0.69	0.83				
STD NBS-88A (D) Expected		0.12	0.03	0.02	0.01			46.7	
BLK	Blank								
BLK	Blank								
BLK	Blank								

Acme Analytical Laboratories (Vancouver) Ltd.
1020 Cordova St. East Vancouver BC V6A 4A3 Canada
Phone (604) 253-3158 Fax (604) 253-1716
www.acmelab.com

Client: **Alberta Innovates Technology Futures**
250 Karl Clark Road
Edmonton AB T6N 1E4 Canada

Project: Enhance
Report Date: June 06, 2011

QUALITY CONTROL REPORT VAN11002216.1

		WGHT	1E	1E	1E	1E	1E	1E	1E	1E	1E	1E	1E	1E	1E	1E	1E	1E	1E	1E
		Wgt	Mo	Cu	Pb	Zn	Ag	Ni	Co	Mn	Fe	As	U	Au	Th	Sr	Cd	Sb	Bi	V	Ca
		kg	ppm	ppm	ppm	ppm	ppm	ppm	ppm	ppm	%	ppm	ppm	ppm	ppm	ppm	ppm	ppm	ppm	ppm	%
		0.01	2	2	5	2	0.5	2	2	5	0.01	5	20	4	2	2	0.4	5	5	2	0.01
BLK	Blank																				
Prep Wash																					
G1	Prep Blank	<0.01	<2	2	83	48	<0.5	4	4	708	2.16	<5	<20	<4	6	670	<0.4	5	<5	49	2.22

Acme Analytical Laboratories (Vancouver) Ltd.
1020 Cordova St. East Vancouver BC V6A 4A3 Canada
Phone (604) 253-3158 Fax (604) 253-1716
www.acmelab.com

Client: **Alberta Innovates Technology Futures**
250 Karl Clark Road
Edmonton AB T6N 1E4 Canada

Project: Enhance
Report Date: June 06, 2011

QUALITY CONTROL REPORT VAN11002216.1

		1E P % 0.002	1E La ppm 2	1E Cr ppm 2	1E Mg % 0.01	1E Ba ppm 1	1E Ti % 0.01	1E Al % 0.01	1E Na % 0.01	1E K % 0.01	1E W ppm 4	1E Zr ppm 2	1E Sn ppm 2	1E Y ppm 2	1E Nb ppm 2	1E Be ppm 1	1E Sc ppm 1	1E S % 0.1	1T Mo ppm 0.05	1T Cu ppm 0.02	1T Pb ppm 0.02
BLK	Blank																				
Prep Wash																					
G1	Prep Blank	0.086	18	5	0.63	998	0.24	6.65	2.65	2.64	5	12	<2	14	27	2	5	<0.1	0.61	4.74	95.04

Alberta Innovates Technology Futures

Acme Analytical Laboratories (Vancouver) Ltd.
1020 Cordova St. East Vancouver BC V6A 4A3 Canada
Phone (604) 253-3158 Fax (604) 253-1716
www.acmelab.com

Client: **Alberta Innovates Technology Futures**
250 Karl Clark Road
Edmonton AB T6N 1E4 Canada

Project: Enhance
Report Date: June 06, 2011

QUALITY CONTROL REPORT VAN11002216.1

		1T Zn ppm 0.2	1T Ag ppb 20	1T Ni ppm 0.1	1T Co ppm 0.2	1T Mn ppm 2	1T Fe % 0.02	1T As ppm 0.2	1T U ppm 0.1	1T Au ppm 0.1	1T Th ppm 0.1	1T Sr ppm 1	1T Cd ppm 0.02	1T Sb ppm 0.02	1T Bi ppm 0.04	1T V ppm 1	1T Ca % 0.02	1T P % 0.001	1T La ppm 0.1	1T Cr ppm 1	1T Mg % 0.02
BLK	Blank																				
Prep Wash																					
G1	Prep Blank	49.8	<20	4.0	5.4	709	2.29	1.3	3.0	<0.1	7.2	727	0.15	1.93	0.19	53	2.33	0.089	21.2	5	0.64

Acme Analytical Laboratories (Vancouver) Ltd.
1020 Cordova St. East Vancouver BC V6A 4A3 Canada
Phone (604) 253-3158 Fax (604) 253-1716
www.acmelab.com

Client: **Alberta Innovates Technology Futures**
250 Karl Clark Road
Edmonton AB T6N 1E4 Canada

Project: Enhance
Report Date: June 06, 2011

QUALITY CONTROL REPORT VAN11002216.1

		1T Ba ppm 1	1T Ti % 0.001	1T Al % 0.02	1T Na % 0.002	1T K % 0.02	1T W ppm 0.1	1T Zr ppm 0.2	1T Sn ppm 0.1	1T Be ppm 1	1T Sc ppm 0.1	1T S % 0.04	1T Y ppm 0.1	1T Ce ppm 0.02	1T Pr ppm 0.1	1T Nd ppm 0.1	1T Sm ppm 0.1	1T Eu ppm 0.1	1T Gd ppm 0.1	1T Tb ppm 0.1	1T Dy ppm 0.1
BLK	Blank																				
Prep Wash																					
G1	Prep Blank	981	0.245	7.39	2.698	3.05	0.2	11.5	1.5	3	5.1	<0.04	14.2	47.74	5.5	19.5	3.6	0.9	2.5	0.4	2.6

Acme Analytical Laboratories (Vancouver) Ltd.
1020 Cordova St. East Vancouver BC V6A 4A3 Canada
Phone (604) 253-3158 Fax (604) 253-1716
www.acmelab.com

Client: **Alberta Innovates Technology Futures**
250 Karl Clark Road
Edmonton AB T6N 1E4 Canada

Project: Enhance
Report Date: June 06, 2011

QUALITY CONTROL REPORT VAN11002216.1

		1T Ho ppm 0.1	1T Er ppm 0.1	1T Tm ppm 0.1	1T Yb ppm 0.1	1T Lu ppm 0.1	1T Hf ppm 0.02	1T Li ppm 0.1	1T Rb ppm 0.1	1T Ta ppm 0.1	1T Nb ppm 0.04	1T Cs ppm 0.1	1T Ga ppm 0.02	2A Leco TOT/C % 0.02	2A Leco TOT/S % 0.02	4X SiO2 % 0.1	4X Al2O3 % 0.01	4X Fe2O3 % 0.01	4X CaO % 0.01	4X MgO % 0.01	4X Na2O % 0.01
BLK	Blank															<0.1	<0.01	<0.01	<0.01	<0.01	<0.01
Prep Wash																					
G1	Prep Blank	0.5	1.7	0.2	1.6	0.3	0.73	35.1	122.3	1.4	24.06	4.0	18.56	<0.02	<0.02	66.6	15.71	3.40	3.51	1.22	3.74

Acme Analytical Laboratories (Vancouver) Ltd.
1020 Cordova St. East Vancouver BC V6A 4A3 Canada
Phone (604) 253-3158 Fax (604) 253-1716
www.acmelab.com

Client: **Alberta Innovates Technology Futures**
250 Karl Clark Road
Edmonton AB T6N 1E4 Canada

Project: Enhance
Report Date: June 06, 2011

QUALITY CONTROL REPORT VAN11002216.1

		4X K2O % 0.01	4X MnO % 0.01	4X TiO2 % 0.01	4X P2O5 % 0.01	4X Cr2O3 % 0.001	4X Ba % 0.01	4X LOI % -5.11	4X SUM % 0.01
BLK	Blank	<0.01	<0.01	<0.01	<0.01	<0.001	<0.01		
Prep Wash									
G1	Prep Blank	3.80	0.10	0.42	0.20	<0.001	0.11	0.64	99.44

Alberta Innovates Technology Futures

APPENDIX B

Acme Analytical Laboratories (Vancouver) Ltd.
1020 Cordova St. East Vancouver BC V6A 4A3 Canada
www.acmelab.com

Client: **Alberta Innovates Technology Futures**
250 Karl Clark Road
Edmonton AB T6N 1E4 Canada

Submitted By: Ernie Perkins
Receiving Lab: Canada-Vancouver
Received: October 28, 2011
Report Date: November 04, 2011
Page: 1 of 2

CERTIFICATE OF ANALYSIS VAN11005834.1

CLIENT JOB INFORMATION

Project: Enhance
Shipment ID:
P.O. Number E000057972
Number of Samples:

SAMPLE DISPOSAL

RTRN-PLP Return

SAMPLE PREPARATION AND ANALYTICAL PROCEDURES

Method Code	Number of Samples	Code Description	Test Wgt (g)	Report Status	Lab
P200	2	Pulverize to 85% passing 200 mesh			VAN
Group 1T	2	4 Acid digestion Ultratrace ICP-MS analysis	0.25	Completed	VAN
2A12	2	Analysis by Leco	0.1	Completed	VAN

ADDITIONAL COMMENTS

Acme does not accept responsibility for samples left at the laboratory after 90 days without prior written instructions for sample storage or return.

Invoice To: Alberta Innovates Technology Futures
250 Karl Clark Road
Edmonton AB T6N 1E4
Canada

CC: Trish Rattray
Mark Olson

This report supersedes all previous preliminary and final reports with this file number dated prior to the date on this certificate. Signature indicates final approval; preliminary reports are unsigned and should be used for reference only.
All results are considered the confidential property of the client. Acme assumes the liabilities for actual cost of analysis only. Results apply to samples as submitted.
*** asterisk indicates that an analytical result could not be provided due to unusually high levels of interference from other elements.

Acme Analytical Laboratories (Vancouver) Ltd.
1020 Cordova St. East Vancouver BC V6A 4A3 Canada
Phone (604) 253-3158 Fax (604) 253-1716
www.acmelab.com

Client: **Alberta Innovates Technology Futures**
250 Karl Clark Road
Edmonton AB T6N 1E4 Canada

Project: Enhance
Report Date: November 04, 2011

CERTIFICATE OF ANALYSIS VAN11005834.1

	Method	1T	1T	1T	1T	1T	1T	1T	1T	1T	1T	1T	1T	1T	1T	1T	1T	1T	1T	1T
	Analyte	Mo	Cu	Pb	Zn	Ag	Ni	Co	Mn	Fe	As	U	Au	Th	Sr	Cd	Sb	Bi	V	Ca	P
	Unit	ppm	ppm	ppm	ppm	ppb	ppm	ppm	ppm	%	ppm	ppm	ppm	ppm	ppm	ppm	ppm	ppm	ppm	%	%
	MDL	0.05	0.02	0.02	0.2	20	0.1	0.2	2	0.02	0.2	0.1	0.1	0.1	1	0.02	0.02	0.04	1	0.02	0.001
G1	Prep Blank	0.95	3.79	22.61	53.5	73	4.2	4.7	768	2.40	1.0	2.8	<0.1	10.5	729	0.07	0.23	0.16	48	2.45	0.066
EN-10	Core Chip	0.55	1.38	11.12	2.8	31	2.0	0.6	98	0.15	1.3	0.3	<0.1	0.3	104	0.08	0.21	0.05	3	16.80	0.001
EN-11	Core Chip	0.48	1.31	2.77	1.9	36	3.1	0.7	66	0.13	1.0	0.5	<0.1	0.3	93	<0.02	0.10	<0.04	4	16.61	<0.001

AcmeLabs
Acme Analytical Laboratories (Vancouver) Ltd.
1020 Cordova St. East Vancouver BC V6A 4A3 Canada
Phone (604) 253-3158 Fax (604) 253-1716
www.acmelab.com

Client: **Alberta Innovates Technology Futures**
250 Karl Clark Road
Edmonton AB T6N 1E4 Canada

Project: Enhance
Report Date: November 04, 2011

CERTIFICATE OF ANALYSIS VAN11005834.1

	Method	1T	1T	1T	1T	1T	1T	1T	1T	1T	1T	1T	1T	1T	1T	1T	1T	1T	1T	1T
	Analyte	La	Cr	Mg	Ba	Ti	Al	Na	K	W	Zr	Sn	Be	Sc	S	Y	Ce	Pr	Nd	Sm	Eu
	Unit	ppm	ppm	%	ppm	%	%	%	%	ppm	ppm	ppm	ppm	ppm	%	ppm	ppm	ppm	ppm	ppm	ppm
	MDL	0.1	1	0.02	1	0.001	0.02	0.002	0.02	0.1	0.2	0.1	1	0.1	0.04	0.1	0.02	0.1	0.1	0.1	0.1
G1	Prep Blank	31.7	61	0.56	1078	0.296	8.11	2.625	3.36	0.2	11.4	1.4	2	4.5	<0.04	14.3	66.99	7.6	27.2	4.4	1.2
EN-10	Core Chip	0.9	12	11.88	17	0.007	0.18	0.072	0.10	1.0	1.2	0.2	<1	<0.1	0.10	0.8	1.81	0.2	0.7	0.2	<0.1
EN-11	Core Chip	1.3	13	11.74	8	0.006	0.14	0.053	0.08	0.2	1.9	0.1	<1	0.2	0.07	1.2	2.57	0.3	1.1	0.3	<0.1

Alberta Innovates Technology Futures

Acme Analytical Laboratories (Vancouver) Ltd.
1020 Cordova St. East Vancouver BC V6A 4A3 Canada
Phone (604) 253-3158 Fax (604) 253-1716
www.acmelab.com

Client: **Alberta Innovates Technology Futures**
250 Karl Clark Road
Edmonton AB T6N 1E4 Canada

Project: Enhance
Report Date: November 04, 2011

QUALITY CONTROL REPORT VAN11005834.1

	Method	1T	1T	1T	1T	1T	1T	1T	1T	1T	1T	1T	1T	1T	1T	1T	2A Leco	2A Leco
	Analyte	Gd	Tb	Dy	Ho	Er	Tm	Yb	Lu	Hf	Li	Rb	Ta	Nb	Cs	Ga	TOT/C	TOT/S
	Unit	ppm	ppm	ppm	ppm	ppm	ppm	ppm	ppm	ppm	ppm	ppm	ppm	ppm	ppm	ppm	%	%
	MDL	0.1	0.1	0.1	0.1	0.1	0.1	0.1	0.1	0.02	0.1	0.1	0.1	0.04	0.1	0.02	0.02	0.02
Pulp Duplicates																		
EN-10	Core Chip	0.1	<0.1	<0.1	<0.1	0.1	<0.1	<0.1	<0.1	0.04	2.9	3.4	<0.1	0.40	0.2	0.45	12.86	0.03
REP EN-10	QC	<0.1	<0.1	<0.1	<0.1	<0.1	<0.1	<0.1	<0.1	0.03	1.9	3.6	<0.1	0.45	0.2	0.41		
Reference Materials																		
STD CSC	Standard																2.95	4.34
STD OREAS24P	Standard	5.7	0.9	5.0	1.0	2.5	0.3	1.9	0.3	3.58	8.6	22.1	1.1	20.31	0.8	20.01		
STD OREAS45C	Standard	3.7	0.8	3.7	0.7	1.9	0.3	1.6	0.2	5.18	15.5	26.4	1.7	25.46	2.4	25.49		
STD OREAS76A	Standard																0.14	18.07
STD CSC Expected																	2.94	4.25
STD OREAS76A Expected																	0.16	18
STD OREAS24P Expected		5.3	0.81	4.6	0.8	2.2	0.3	1.83	0.25	3.6	8.7	22.4	1.04	21	0.8	19.43		
STD OREAS45C Expected		3.64	0.6	3.41	0.64	1.52	0.21	1.51	0.23	4.27	15.69	24	1.43	23.05	2.3	24.8		
BLK	Blank																<0.02	<0.02
BLK	Blank	<0.1	<0.1	<0.1	<0.1	<0.1	<0.1	<0.1	<0.1	<0.02	<0.1	<0.1	<0.1	<0.04	<0.1	<0.02		
Prep Wash																		
G1	Prep Blank	3.4	0.5	2.8	0.7	1.5	0.2	1.8	0.3	0.71	32.6	116.2	1.2	22.49	3.8	19.28	<0.02	<0.02

Acme Analytical Laboratories (Vancouver) Ltd.
1020 Cordova St. East Vancouver BC V6A 4A3 Canada
Phone (604) 253-3158 Fax (604) 253-1716
www.acmelab.com

Client: **Alberta Innovates Technology Futures**
250 Karl Clark Road
Edmonton AB T6N 1E4 Canada

Project: Enhance
Report Date: November 04, 2011

QUALITY CONTROL REPORT VAN11005834.1

	Method	1T	1T	1T	1T	1T	1T	1T	1T	1T	1T	1T	1T	1T	1T	1T	1T	1T	1T	1T
	Analyte	La	Cr	Mg	Ba	Ti	Al	Na	K	W	Zr	Sn	Be	Sc	S	Y	Ce	Pr	Nd	Sm	Eu
	Unit	ppm	ppm	%	ppm	%	%	%	%	ppm	ppm	ppm	ppm	ppm	%	ppm	ppm	ppm	ppm	ppm	ppm
	MDL	0.1	1	0.02	1	0.001	0.02	0.002	0.02	0.1	0.2	0.1	1	0.1	0.04	0.1	0.02	0.1	0.1	0.1	0.1
Pulp Duplicates																					
EN-10	Core Chip	0.9	12	11.88	17	0.007	0.18	0.072	0.10	1.0	1.2	0.2	<1	<0.1	0.10	0.8	1.81	0.2	0.7	0.2	<0.1
REP EN-10	QC	1.0	21	11.95	17	0.007	0.18	0.074	0.11	0.9	1.3	0.1	<1	<0.1	0.10	0.8	1.73	0.3	0.9	0.2	<0.1
Reference Materials																					
STD CSC	Standard																				
STD OREAS24P	Standard	20.4	213	4.03	288	1.098	7.70	2.547	0.66	0.5	137.0	1.8	1	19.2	<0.04	22.6	44.50	5.7	21.1	5.5	1.8
STD OREAS45C	Standard	30.4	1002	0.25	284	1.232	7.38	0.103	0.35	1.2	181.9	2.9	<1	56.1	<0.04	14.3	62.22	7.0	24.4	5.4	1.4
STD OREAS76A	Standard																				
STD CSC Expected																					
STD OREAS76A Expected																					
STD OREAS24P Expected		17.4	196	4.13	285	1.1	7.66	2.34	0.7	0.5	141	1.6		20		21.3	37.6	4.7	22	4.7	1.6
STD OREAS45C Expected		26.2	962	0.25	270	1.1313	7.59	0.097	0.36	1.06	169.7	2.9		59.03	0.021	12.9	54	6.31	24.49	4.3	1.13
BLK	Blank																				
BLK	Blank	<0.1	<1	<0.02	<1	<0.001	<0.02	<0.002	<0.02	<0.1	<0.2	<0.1	<1	<0.1	<0.04	<0.1	<0.02	<0.1	<0.1	<0.1	<0.1
Prep Wash																					
G1	Prep Blank	31.7	61	0.56	1078	0.236	8.11	2.825	3.36	0.2	11.4	1.4	2	4.5	<0.04	14.3	66.99	7.6	27.2	4.4	1.2

Acme Analytical Laboratories (Vancouver) Ltd.
1020 Cordova St. East Vancouver BC V6A 4A3 Canada
Phone (604) 253-3158 Fax (604) 253-1716
www.acmelab.com

Client: **Alberta Innovates Technology Futures**
250 Karl Clark Road
Edmonton AB T6N 1E4 Canada

Project: Enhance
Report Date: November 04, 2011

CERTIFICATE OF ANALYSIS VAN11005834.1

	Method	1T	1T	1T	1T	1T	1T	1T	1T	1T	1T	1T	1T	1T	1T	1T	2A Leco	2A Leco
	Analyte	Gd	Tb	Dy	Ho	Er	Tm	Yb	Lu	Hf	Li	Rb	Ta	Nb	Cs	Ga	TOT/C	TOT/S
	Unit	ppm	ppm	ppm	ppm	ppm	ppm	ppm	ppm	ppm	ppm	ppm	ppm	ppm	ppm	ppm	%	%
	MDL	0.1	0.1	0.1	0.1	0.1	0.1	0.1	0.1	0.02	0.1	0.1	0.1	0.04	0.1	0.02	0.02	0.02
G1	Prep Blank	3.4	0.5	2.8	0.7	1.5	0.2	1.8	0.3	0.71	32.6	116.2	1.2	22.49	3.8	19.28	<0.02	<0.02
EN-10	Core Chip	0.1	<0.1	<0.1	<0.1	0.1	<0.1	<0.1	<0.1	0.04	2.9	3.4	<0.1	0.40	0.2	0.45	12.86	0.03
EN-11	Core Chip	0.2	<0.1	0.2	<0.1	0.1	<0.1	<0.1	<0.1	0.06	1.3	2.3	<0.1	0.27	0.1	0.39	13.04	0.03

Acme Analytical Laboratories (Vancouver) Ltd.
1020 Cordova St. East Vancouver BC V6A 4A3 Canada
Phone (604) 253-3158 Fax (604) 253-1716
www.acmelab.com

Client: **Alberta Innovates Technology Futures**
250 Karl Clark Road
Edmonton AB T6N 1E4 Canada

Project: Enhance
Report Date: November 04, 2011

QUALITY CONTROL REPORT VAN11005834.1

	Method	1T	1T	1T	1T	1T	1T	1T	1T	1T	1T	1T	1T	1T	1T	1T	1T	1T	1T	1T	1T
	Analyte	Mo	Cu	Pb	Zn	Ag	Ni	Co	Mn	Fe	As	U	Au	Th	Sr	Cd	Sb	Bi	V	Ca	P
	Unit	ppm	ppm	ppm	ppm	ppb	ppm	ppm	ppm	%	ppm	ppm	ppm	ppm	ppm	ppm	ppm	ppm	ppm	%	%
	MDL	0.05	0.02	0.02	0.2	20	0.1	0.2	2	0.02	0.2	0.1	0.1	0.1	1	0.02	0.02	0.04	1	0.02	0.001
Pulp Duplicates																					
EN-10	Core Chip	0.55	1.38	11.12	2.8	31	2.0	0.6	98	0.15	1.3	0.3	<0.1	0.3	104	0.08	0.21	0.05	3	16.80	0.001
REP EN-10	QC	0.52	1.27	11.56	2.9	45	1.8	0.6	98	0.14	1.7	0.3	<0.1	0.3	106	0.05	0.19	<0.04	3	16.64	0.001
Reference Materials																					
STD CSC	Standard																				
STD OREAS24P	Standard	1.55	51.89	3.32	107.5	76	146.0	46.9	1056	7.37	1.5	0.8	<0.1	3.4	425	0.08	0.09	0.05	162	5.39	0.124
STD OREAS45C	Standard	2.59	632.3	28.87	92.0	354	343.2	106.5	1143	19.16	12.6	2.8	<0.1	13.3	42	0.07	0.87	0.29	279	0.50	0.045
STD OREAS76A	Standard																				
STD CSC Expected																					
STD OREAS76A Expected																					
STD OREAS24P Expected		1.5	52	2.9	119	60	141	44	1100	7.53	1.2	0.75		2.85	403	0.15	0.09		158	5.83	0.136
STD OREAS45C Expected		2.26	620	24	83	280	333	104	1160	18.33	10.1	2.4	0.045	10.2	36.4	0.15	0.79	0.21	270	0.482	0.051
BLK	Blank																				
BLK	Blank	<0.05	<0.02	<0.02	<0.2	<20	<0.1	<0.2	<2	<0.02	<0.2	<0.1	<0.1	<0.1	<1	<0.02	<0.02	<0.04	<1	<0.02	<0.001
Prep Wash																					
G1	Prep Blank	0.95	3.79	22.61	53.5	73	4.2	4.7	768	2.40	1.0	2.8	<0.1	10.5	729	0.07	0.23	0.16	48	2.45	0.066

Acme Analytical Laboratories (Vancouver) Ltd.
1020 Cordova St. East Vancouver BC V6A 4A3 Canada
www.acmelab.com

Client: **Alberta Innovates Technology Futures**
250 Karl Clark Road
Edmonton AB T6N 1E4 Canada

Submitted By: Ernie Perkins
Receiving Lab: Canada-Vancouver
Received: August 19, 2011
Report Date: October 23, 2011
Page: 1 of 2

CERTIFICATE OF ANALYSIS VAN11004088.1

CLIENT JOB INFORMATION

Project: Enhance
Shipment ID:
P.O. Number E000057258
Number of Samples: 5

SAMPLE DISPOSAL

RTRN-PLP Return

SAMPLE PREPARATION AND ANALYTICAL PROCEDURES

Method Code	Number of Samples	Code Description	Test Wgt (g)	Report Status	Lab
P200	5	Pulverize to 85% passing 200 mesh			VAN
1E	5	4 Acid digestion ICP-ES analysis	0.25	Completed	VAN
Group 1T	5	4 Acid digestion Ultratrace ICP-MS analysis	0.25	Completed	VAN
2A12	5	Analysis by Leco	0.1	Completed	VAN
4X02	5	U2B4O7/LiBO2 fusion, analysis by XRF		Completed	VAN

ADDITIONAL COMMENTS

Acme does not accept responsibility for samples left at the laboratory after 90 days without prior written instructions for sample storage or return.

Invoice To: Alberta Innovates Technology Futures
250 Karl Clark Road
Edmonton AB T6N 1E4
Canada

CC: Trish Rattray
Mark Olson

This report supersedes all previous preliminary and final reports with this file number dated prior to the date on this certificate. Signature indicates final approval; preliminary reports are unsigned and should be used for reference only.
All results are considered the confidential property of the client. Acme assumes the liabilities for actual cost of analysis only. Results apply to samples as submitted.
*** asterisk indicates that an analytical result could not be provided due to unusually high levels of interference from other elements.

Alberta Innovates Technology Futures

APPENDIX B

Acme Analytical Laboratories (Vancouver) Ltd.
1020 Cordova St. East Vancouver BC V6A 4A3 Canada
Phone (604) 253-3158 Fax (604) 253-1716
www.acmelab.com

Client: **Alberta Innovates Technology Futures**
250 Karl Clark Road
Edmonton AB T6N 1E4 Canada

Project: Enhance
Report Date: October 23, 2011

CERTIFICATE OF ANALYSIS VAN11004088.1

Method		1E	1E	1E	1E	1E	1E	1E	1E	1E	1E	1E	1E	1E	1E	1E	1E	1E	1E	1E
Analyte		Mo	Cu	Pb	Zn	Ag	Ni	Co	Mn	Fe	As	U	Au	Th	Sr	Cd	Sb	Bi	V	Ca	P
Unit		ppm	ppm	ppm	ppm	ppm	ppm	ppm	ppm	%	ppm	ppm	ppm	ppm	ppm	ppm	ppm	ppm	ppm	%	%
MDL		2	2	5	2	0.5	2	2	5	0.01	5	20	4	2	2	0.4	5	5	2	0.01	0.001
EN-30	Core	2	35	5	112	0.7	31	11	68	1.45	5	<20	<4	4	166	0.7	8	<5	135	0.10	0.007
EN-31	Core	9	41	17	150	0.8	56	15	120	3.71	10	<20	<4	9	250	1.9	7	<5	223	6.68	0.081
EN-32	Core	3	26	10	146	<0.5	31	11	751	5.76	<5	<20	<4	10	192	<0.4	<5	<5	150	0.38	0.112
EN-33	Core	2	27	10	73	<0.5	27	9	576	3.10	<5	<20	<4	7	124	1.2	<5	<5	77	2.52	0.070
EN-34	Core	2	54	5	138	1.1	60	19	198	3.83	7	<20	4	5	198	<0.4	<5	<5	171	0.24	0.045

Acme Analytical Laboratories (Vancouver) Ltd.
1020 Cordova St. East Vancouver BC V6A 4A3 Canada
Phone (604) 253-3158 Fax (604) 253-1716
www.acmelab.com

Client: **Alberta Innovates Technology Futures**
250 Karl Clark Road
Edmonton AB T6N 1E4 Canada

Project: Enhance
Report Date: October 23, 2011

CERTIFICATE OF ANALYSIS VAN11004088.1

Method		1E	1E	1E	1E	1E	1E	1E	1E	1E	1E	1E	1E	1E	1E	1E	1E	1T	1T	1T	1T
Analyte		La	Cr	Mg	Ba	Ti	Al	Na	K	W	Zr	Sn	Y	Nb	Be	Sc	S	Mo	Cu	Pb	Zn
Unit		ppm	ppm	%	ppm	%	%	%	%	ppm	ppm	ppm	ppm	ppm	ppm	ppm	%	ppm	ppm	ppm	ppm
MDL		2	2	0.01	1	0.01	0.01	0.01	0.01	4	2	2	2	2	1	1	0.1	0.05	0.02	0.02	0.2
EN-30	Core Chip	18	57	0.28	711	0.39	6.73	1.41	2.71	<4	52	3	11	8	1	11	0.6	1.59	36.25	14.80	109.1
EN-31	Core Chip	30	82	0.99	440	0.27	5.56	0.38	1.74	<4	68	<2	20	12	2	11	3.4	9.81	42.04	19.94	151.5
EN-32	Core Chip	32	83	0.88	726	0.34	6.07	0.71	1.76	<4	77	<2	20	14	2	12	0.3	0.98	28.74	17.14	146.0
EN-33	Core Chip	26	40	1.80	605	0.24	5.23	0.93	1.96	<4	73	<2	18	9	2	8	0.2	2.11	25.31	16.31	70.2
EN-34	Core Chip	12	84	1.10	1039	0.48	6.63	1.29	1.65	<4	79	3	15	8	2	14	0.5	2.11	56.29	13.48	135.4

Alberta Innovates Technology Futures

APPENDIX B

AcmeLabs
Acme Analytical Laboratories (Vancouver) Ltd.
1020 Cordova St. East Vancouver BC V6A 4A3 Canada
Phone (604) 253-3158 Fax (604) 253-1716
www.acmelab.com

Client: **Alberta Innovates Technology Futures**
250 Karl Clark Road
Edmonton AB T6N 1E4 Canada

Project: Enhance
Report Date: October 23, 2011

CERTIFICATE OF ANALYSIS VAN11004088.1

	Method	1T	1T	1T	1T	1T	1T	1T	1T	1T	1T	1T	1T	1T	1T	1T	1T	1T	1T	1T	1T
	Analyte	Ag	Ni	Co	Mn	Fe	As	U	Au	Th	Sr	Cd	Sb	Bi	V	Ca	P	La	Cr	Mg	Ba
	Unit	ppb	ppm	ppm	ppm	%	ppm	ppm	ppm	ppm	ppm	ppm	ppm	ppm	ppm	%	%	ppm	ppm	%	ppm
	MDL	20	0.1	0.2	2	0.02	0.2	0.1	0.1	0.1	1	0.02	0.02	0.04	1	0.02	0.001	0.1	1	0.02	1
EN-30	Core Chip	176	27.8	11.8	70	1.42	9.1	1.9	<0.1	4.7	155	0.26	1.13	0.20	136	0.21	0.013	19.3	61	0.29	715
EN-31	Core Chip	442	51.9	18.1	119	3.84	15.9	4.7	<0.1	8.9	243	1.69	2.16	0.29	233	6.99	0.098	31.8	73	1.11	213
EN-32	Core Chip	325	26.3	11.2	727	5.58	6.0	3.7	<0.1	9.7	174	0.56	0.46	0.35	147	0.48	0.116	30.4	79	0.90	720
EN-33	Core Chip	181	23.9	10.6	559	2.94	9.0	2.0	<0.1	7.3	110	1.02	0.94	0.27	72	2.49	0.071	23.7	40	1.76	564
EN-34	Core Chip	269	55.1	19.2	197	3.85	12.7	2.2	<0.1	4.8	185	0.43	1.10	0.27	163	0.39	0.048	13.9	92	1.13	1009

Alberta Innovates Technology Futures

AcmeLabs Acme Analytical Laboratories (Vancouver) Ltd.
1020 Cordova St. East Vancouver BC V6A 4A3 Canada
Phone (604) 253-3158 Fax (604) 253-1716
www.acmelab.com

Client: **Alberta Innovates Technology Futures**
250 Karl Clark Road
Edmonton AB T6N 1E4 Canada

Project: Enhance
Report Date: October 23, 2011

CERTIFICATE OF ANALYSIS VAN11004088.1

Method		1T	1T	1T	1T	1T	1T	1T	1T	1T	1T	1T	1T	1T	1T	1T	1T	1T	1T	1T	1T
Analyte		Tl	Al	Na	K	W	Zr	Sn	Be	Sc	S	Y	Ce	Pr	Nd	Sm	Eu	Gd	Tb	Dy	Ho
Unit		%	%	%	%	ppm	ppm	ppm	ppm	ppm	%	ppm	ppm	ppm	ppm	ppm	ppm	ppm	ppm	ppm	ppm
MDL		0.001	0.02	0.002	0.02	0.1	0.2	0.1	1	0.1	0.04	0.1	0.02	0.1	0.1	0.1	0.1	0.1	0.1	0.1	0.1
EN-30	Core Chip	0.362	6.82	1.466	2.61	1.2	50.6	1.4	<1	11.5	0.57	10.4	37.52	4.8	19.2	4.1	1.4	3.0	0.5	2.1	0.4
EN-31	Core Chip	0.244	5.92	0.424	1.84	1.3	59.5	1.6	2	10.9	3.50	19.8	57.35	7.3	26.1	4.9	1.2	4.7	0.8	3.8	0.8
EN-32	Core Chip	0.318	5.70	0.750	1.82	1.1	84.7	2.2	2	12.0	0.26	20.0	60.96	7.5	30.7	6.1	1.9	5.6	0.8	3.9	0.7
EN-33	Core Chip	0.186	5.02	0.942	1.91	1.2	60.5	1.4	2	7.9	0.22	15.2	46.28	5.5	22.6	4.3	1.4	3.7	0.6	3.2	0.6
EN-34	Core Chip	0.387	6.83	1.277	1.68	1.0	78.0	1.5	2	15.8	0.45	14.2	29.77	3.8	16.2	3.4	1.8	3.8	0.5	3.2	0.6

Acme Analytical Laboratories (Vancouver) Ltd.
1020 Cordova St. East Vancouver BC V6A 4A3 Canada
Phone (604) 253-3158 Fax (604) 253-1716
www.acmelab.com

Client: **Alberta Innovates Technology Futures**
250 Karl Clark Road
Edmonton AB T6N 1E4 Canada

Project: Enhance
Report Date: October 23, 2011

CERTIFICATE OF ANALYSIS VAN11004088.1

	Method	1T	1T	1T	1T	1T	1T	1T	1T	1T	1T	1T2A Leco	2A Leco	4X	4X	4X	4X	4X	4X	4X
	Analyte	Er	Tm	Yb	Lu	Hf	Li	Rb	Ta	Nb	Cs	Ga	TOT/C	TOT/S	SiO2	Al2O3	Fe2O3	CaO	MgO	Na2O	K2O
	Unit	ppm	ppm	ppm	ppm	ppm	ppm	ppm	ppm	ppm	ppm	ppm	%	%	%	%	%	%	%	%	%
	MDL	0.1	0.1	0.1	0.1	0.02	0.1	0.1	0.1	0.04	0.1	0.02	0.02	0.02	0.1	0.01	0.01	0.01	0.01	0.01	0.01
EN-30	Core Chip	1.3	0.2	1.1	0.2	1.68	39.4	76.7	0.5	7.79	5.1	16.10	0.43	0.56	69.9	16.15	2.05	0.16	0.52	2.03	3.41
EN-31	Core Chip	2.2	0.3	1.7	0.3	1.91	43.2	88.8	0.7	10.95	6.7	14.67	6.87	3.47	47.7	11.22	5.64	10.42	1.89	0.54	2.23
EN-32	Core Chip	2.2	0.3	1.9	0.3	2.35	57.3	79.6	0.8	13.32	5.7	17.48	2.64	0.27	60.4	13.82	8.70	0.63	1.65	1.02	2.33
EN-33	Core Chip	1.7	0.2	1.5	0.3	1.71	30.4	62.9	0.5	7.25	4.9	14.28	2.99	0.20	63.3	10.47	4.60	3.87	3.27	1.35	2.55
EN-34	Core Chip	1.8	0.2	1.5	0.3	2.34	42.7	61.2	0.5	7.51	4.7	19.51	1.47	0.43	59.4	16.97	5.80	0.45	2.07	1.80	2.12

Acme Analytical Laboratories (Vancouver) Ltd.
1020 Cordova St. East Vancouver BC V6A 4A3 Canada
Phone (604) 253-3158 Fax (604) 253-1716
www.acmelab.com

Client: **Alberta Innovates Technology Futures**
250 Karl Clark Road
Edmonton AB T6N 1E4 Canada

Project: Enhance
Report Date: October 23, 2011

CERTIFICATE OF ANALYSIS VAN11004088.1

	Method	4X	4X	4X	4X	4X	4X	4X
	Analyte	MnO	TiO2	P2O5	Cr2O3	Ba	LOI	SUM
	Unit	%	%	%	%	%	%	%
	MDL	0.01	0.01	0.01	0.001	0.01	-5.11	0.01
EN-30	Core Chip	0.01	0.77	0.03	0.011	0.07	5.13	100.3
EN-31	Core Chip	0.02	0.54	0.19	0.011	0.07	13.95	94.37
EN-32	Core Chip	0.11	0.72	0.27	0.015	0.08	10.51	100.3
EN-33	Core Chip	0.08	0.45	0.17	0.006	0.07	10.16	100.3
EN-34	Core Chip	0.03	0.76	0.11	0.015	0.11	9.83	99.43

Acme Analytical Laboratories (Vancouver) Ltd.
1020 Cordova St. East Vancouver BC V6A 4A3 Canada
Phone (604) 253-3158 Fax (604) 253-1716
www.acmelab.com

Client: **Alberta Innovates Technology Futures**
250 Karl Clark Road
Edmonton AB T6N 1E4 Canada

Project: Enhance
Report Date: October 23, 2011

QUALITY CONTROL REPORT VAN11004088.1

	Method	1E	1E	1E	1E	1E	1E	1E	1E	1E	1E	1E	1E	1E	1E	1E	1E	1E	1E	1E
	Analyte	Mo	Cu	Pb	Zn	Ag	Ni	Co	Mn	Fe	As	U	Au	Th	Sr	Cd	Sb	Bi	V	Ca	P
	Unit	ppm	ppm	ppm	ppm	ppm	ppm	ppm	ppm	%	ppm	ppm	ppm	ppm	ppm	ppm	ppm	ppm	ppm	%	%
	MDL	2	2	5	2	0.5	2	2	5	0.01	5	20	4	2	2	0.4	5	5	2	0.01	0.001
Pulp Duplicates																					
EN-33	Core Chip	2	27	10	73	<0.5	27	9	576	3.10	<5	<20	<4	7	124	1.2	<5	<5	77	2.52	0.070
REP EN-33	QC																				
Reference Materials																					
STD CSC	Standard																				
STD OREAS24P	Standard																				
STD OREAS24P	Standard	3	48	<5	113	<0.5	150	43	1084	7.35	<5	<20	<4	2	380	0.5	5	<5	164	5.29	0.132
STD OREAS45C	Standard																				
STD OREAS45C	Standard	3	616	14	85	<0.5	339	104	1137	17.82	10	<20	<4	9	36	<0.4	5	<5	266	0.48	0.047
STD OREAS76A	Standard																				
STD SO-18	Standard																				
STD SY-4(D)	Standard																				
STD CSC Expected																					
STD OREAS76A Expected																					
STD SY-4(D) Expected																					
STD SO-18 Expected																					
STD OREAS24P Expected		1.5	52	2.9	119	0.05	141	44	1100	7.53	1.2	0.75		2.85	403	0.15	0.09		158	5.83	0.136
STD OREAS45C Expected		2.26	620	24	83	0.28	333	104	1160	18.33	10.1	2.4	0.045	10.2	36.4	0.15	0.79	0.21	270	0.482	0.051
BLK	Blank																				
BLK	Blank																				
BLK	Blank																				
BLK	Blank	<2	<2	<5	<2	<0.5	<2	<2	<5	<0.01	<5	<20	<4	<2	<2	<0.4	<5	<5	<2	<0.01	<0.001
Prep Wash																					
G1	Prep Blank	3	3	12	52	<0.5	6	4	728	2.29	<5	<20	<4	6	691	1.9	<5	7	48	2.24	0.072

Acme Analytical Laboratories (Vancouver) Ltd.
1020 Cordova St. East Vancouver BC V6A 4A3 Canada
Phone (604) 253-3158 Fax (604) 253-1716
www.acmelab.com

Client: **Alberta Innovates Technology Futures**
250 Karl Clark Road
Edmonton AB T6N 1E4 Canada

Project: Enhance
Report Date: October 23, 2011

QUALITY CONTROL REPORT VAN11004088.1

	Method	1E	1E	1E	1E	1E	1E	1E	1E	1E	1E	1E	1E	1E	1E	1E	1T	1T	1T	1T
	Analyte	La	Cr	Mg	Ba	Ti	Al	Na	K	W	Zr	Sn	Y	Nb	Be	Sc	S	Mo	Cu	Pb	Zn
	Unit	ppm	ppm	%	ppm	%	%	%	%	ppm	ppm	ppm	ppm	ppm	ppm	ppm	%	ppm	ppm	ppm	ppm
	MDL	2	2	0.01	1	0.01	0.01	0.01	0.01	4	2	2	2	2	1	1	0.1	0.05	0.02	0.02	0.2
Pulp Duplicates																					
EN-33	Core Chip	26	40	1.80	605	0.24	5.23	0.93	1.96	<4	73	<2	18	9	2	6	0.2	2.11	25.31	16.31	70.2
REP EN-33	QC																				
Reference Materials																					
STD CSC	Standard																				
STD OREAS24P	Standard																	1.47	50.77	3.06	124.5
STD OREAS24P	Standard	16	206	3.97	265	1.02	7.42	2.37	0.69	<4	126	5	21	19	1	19	<0.1				
STD OREAS45C	Standard																	2.17	617.9	26.22	91.9
STD OREAS45C	Standard	25	967	0.24	264	1.12	7.10	0.11	0.34	<4	162	5	13	22	<1	60	<0.1				
STD OREAS76A	Standard																				
STD SO-18	Standard																				
STD SY-4(D)	Standard																				
STD CSC Expected																					
STD OREAS76A Expected																					
STD SY-4(D) Expected																					
STD SO-18 Expected																					
STD OREAS24P Expected		17.4	196	4.13	285	1.1	7.66	2.34	0.7	0.5	141	1.6	21.3	21		20		1.5	52	2.9	119
STD OREAS45C Expected		26.2	962	0.25	270	1.1313	7.59	0.097	0.36	1.06	169.7	2.9	12.9	23.05		59.03	0.021	2.28	620	24	83
BLK	Blank																				
BLK	Blank																				
BLK	Blank																	<0.05	<0.02	<0.02	<0.2
BLK	Blank	<2	<2	<0.01	<1	<0.01	<0.01	<0.01	<0.01	<4	<2	<2	<2	<2	<1	<1	<0.1				
Prep Wash																					
G1	Prep Blank	19	6	0.56	953	0.23	6.90	2.55	3.01	<4	11	<2	14	25	3	5	<0.1	0.82	4.21	18.93	48.4

Alberta Innovates Technology Futures

APPENDIX B

Acme Analytical Laboratories (Vancouver) Ltd.
1020 Cordova St. East Vancouver BC V6A 4A3 Canada
Phone (604) 253-3158 Fax (604) 253-1716
www.acmelab.com

Client: **Alberta Innovates Technology Futures**
250 Karl Clark Road
Edmonton AB T6N 1E4 Canada

Project: Enhance
Report Date: October 23, 2011

QUALITY CONTROL REPORT VAN11004088.1

	Method	1T	1T	1T	1T	1T	1T	1T	1T	1T	1T	1T	1T	1T	1T	1T	1T	1T	1T	1T
	Analyte	Ag	Ni	Co	Mn	Fe	As	U	Au	Th	Sr	Cd	Sb	Bi	V	Ca	P	La	Cr	Mg	Ba
	Unit	ppb	ppm	ppm	ppm	%	ppm	ppm	ppm	ppm	ppm	ppm	ppm	ppm	ppm	%	%	ppm	ppm	%	ppm
	MDL	20	0.1	0.2	2	0.02	0.2	0.1	0.1	0.1	1	0.02	0.02	0.04	1	0.02	0.001	0.1	1	0.02	1
Pulp Duplicates																					
EN-33	Core Chip	181	23.9	10.6	559	2.94	9.0	2.0	<0.1	7.3	110	1.02	0.94	0.27	72	2.49	0.071	23.7	40	1.76	564
REP EN-33	QC																				
Reference Materials																					
STD CSC	Standard																				
STD OREAS24P	Standard	85	137.4	44.7	1061	7.34	1.6	0.6	<0.1	3.0	377	0.20	0.09	<0.04	157	5.41	0.137	19.6	192	4.17	287
STD OREAS24P	Standard																				
STD OREAS45C	Standard	418	329.0	101.4	1105	18.27	13.9	2.3	<0.1	11.4	37	0.25	0.90	0.25	253	0.48	0.053	28.3	945	0.24	291
STD OREAS45C	Standard																				
STD OREAS76A	Standard																				
STD SO-18	Standard																				
STD SY-4(D)	Standard																				
STD CSC Expected																					
STD OREAS76A Expected																					
STD SY-4(D) Expected																					
STD SO-18 Expected																					
STD OREAS24P Expected		60	141	44	1100	7.53	1.2	0.75		2.85	403	0.15	0.09		158	5.83	0.136	17.4	196	4.13	285
STD OREAS45C Expected		280	333	104	1160	18.33	10.1	2.4	0.045	10.2	36.4	0.15	0.79	0.21	270	0.482	0.051	26.2	962	0.25	270
BLK	Blank																				
BLK	Blank																				
BLK	Blank	<20	<0.1	<0.2	<2	<0.02	<0.2	<0.1	<0.1	<0.1	<1	<0.02	<0.02	<0.04	<1	<0.02	<0.001	<0.1	<1	<0.02	<1
BLK	Blank																				
Prep Wash																					
G1	Prep Blank	22	4.8	4.4	741	2.30	1.9	2.5	<0.1	7.3	666	0.02	0.03	0.13	48	2.28	0.079	20.5	7	0.59	951

Acme Analytical Laboratories (Vancouver) Ltd.
1020 Cordova St. East Vancouver BC V6A 4A3 Canada
Phone (604) 253-3158 Fax (604) 253-1716
www.acmelab.com

Client: **Alberta Innovates Technology Futures**
250 Karl Clark Road
Edmonton AB T6N 1E4 Canada

Project: Enhance
Report Date: October 23, 2011

QUALITY CONTROL REPORT VAN11004088.1

	Method	1T	1T	1T	1T	1T	1T	1T	1T	1T	1T	1T	1T	1T	1T	1T	1T	1T	1T	1T	1T
	Analyte	Tl	Al	Na	K	W	Zr	Sn	Be	Sc	S	Y	Ce	Pr	Nd	Sm	Eu	Gd	Tb	Dy	Ho
	Unit	%	%	%	%	ppm	ppm	ppm	ppm	ppm	%	ppm	ppm	ppm	ppm	ppm	ppm	ppm	ppm	ppm	ppm
	MDL	0.001	0.02	0.002	0.02	0.1	0.2	0.1	1	0.1	0.04	0.1	0.02	0.1	0.1	0.1	0.1	0.1	0.1	0.1	0.1
Pulp Duplicates																					
EN-33	Core Chip	0.186	5.02	0.942	1.91	1.2	60.5	1.4	2	7.9	0.22	15.2	46.28	5.5	22.6	4.3	1.4	3.7	0.6	3.2	0.6
REP EN-33	QC																				
Reference Materials																					
STD CSC	Standard																				
STD OREAS24P	Standard	0.968	7.71	2.548	0.67	0.6	134.7	1.5	3	19.0	<0.04	21.3	37.95	4.8	21.0	5.0	2.0	5.5	0.9	5.1	0.9
STD OREAS24P	Standard																				
STD OREAS45C	Standard	1.027	7.02	0.092	0.36	1.1	159.7	2.9	1	58.5	<0.04	12.7	54.33	6.4	24.7	4.2	1.6	4.1	0.7	3.8	0.6
STD OREAS45C	Standard																				
STD OREAS76A	Standard																				
STD SO-18	Standard																				
STD SY-4(D)	Standard																				
STD CSC Expected																					
STD OREAS76A Expected																					
STD SY-4(D) Expected																					
STD SO-18 Expected																					
STD OREAS24P Expected		1.1	7.66	2.34	0.7	0.5	141	1.6		20		21.3	37.6	4.7	22	4.7	1.6	5.3	0.81	4.6	0.8
STD OREAS45C Expected		1.1313	7.59	0.097	0.36	1.06	169.7	2.9		59.03	0.021	12.9	54	6.31	24.49	4.3	1.13	3.64	0.6	3.41	0.64
BLK	Blank																				
BLK	Blank																				
BLK	Blank	<0.001	<0.02	<0.002	<0.02	<0.1	<0.2	<0.1	<1	<0.1	<0.04	<0.1	<0.02	<0.1	<0.1	<0.1	<0.1	<0.1	<0.1	<0.1	<0.1
BLK	Blank																				
Prep Wash																					
G1	Prep Blank	0.210	7.17	2.749	3.12	0.3	12.0	1.5	3	4.8	<0.04	13.9	45.91	5.3	19.6	3.4	1.8	3.4	0.5	2.9	0.5

AcmeLabs Acme Analytical Laboratories (Vancouver) Ltd.
1020 Cordova St. East Vancouver BC V6A 4A3 Canada
Phone (604) 253-3158 Fax (604) 253-1716
www.acmelab.com

Client: **Alberta Innovates Technology Futures**
250 Karl Clark Road
Edmonton AB T6N 1E4 Canada

Project: Enhance
Report Date: October 23, 2011

QUALITY CONTROL REPORT VAN11004088.1

	Method	1T	1T	1T	1T	1T	1T	1T	1T	1T	1T	1T	2A Leco	2A Leco	4X	4X	4X	4X	4X	4X	4X
	Analyte	Er	Tm	Yb	Lu	Hf	Li	Rb	Ta	Nb	Cs	Ga	TOT/C	TOT/S	SiO2	Al2O3	Fe2O3	CaO	MgO	Na2O	K2O
	Unit	ppm	ppm	ppm	ppm	ppm	ppm	ppm	ppm	ppm	ppm	ppm	%	%	%	%	%	%	%	%	%
	MDL	0.1	0.1	0.1	0.1	0.02	0.1	0.1	0.1	0.04	0.1	0.02	0.02	0.02	0.1	0.01	0.01	0.01	0.01	0.01	0.01
Pulp Duplicates																					
EN-33	Core Chip	1.7	0.2	1.5	0.3	1.71	30.4	62.9	0.5	7.25	4.9	14.28	2.99	0.20	63.3	10.47	4.60	3.87	3.27	1.35	2.53
REP EN-33	QC												2.99	0.20							
Reference Materials																					
STD CSC	Standard												3.23	4.22							
STD OREAS24P	Standard	2.3	0.4	1.9	0.3	3.71	8.4	19.5	1.1	19.60	0.8	20.77									
STD OREAS24P	Standard																				
STD OREAS45C	Standard	1.8	0.2	1.7	0.2	4.03	14.9	21.5	1.4	20.93	2.3	25.78									
STD OREAS45C	Standard																				
STD OREAS76A	Standard												0.15	17.84							
STD SO-18	Standard														58.7	14.14	7.69	6.46	3.44	3.85	2.17
STD SY-4(D)	Standard														50.1	20.81	6.28	8.08	0.54	7.30	1.62
STD CSC Expected													2.94	4.25							
STD OREAS76A Expected													0.16	18							
STD SY-4(D) Expected															49.9	20.69	6.21	8.05	0.54	7.1	1.66
STD SO-18 Expected															58.47		7.67	6.42	3.35	3.71	2.17
STD OREAS24P Expected		2.2	0.3	1.83	0.25	3.6	8.7	22.4	1.04	21	0.8	19.43									
STD OREAS45C Expected		1.52	0.21	1.51	0.23	4.27	15.69	24	1.43	23.05	2.3	24.8									
BLK	Blank												<0.02	<0.02							
BLK	Blank														<0.1	0.03	<0.01	<0.01	<0.01	<0.01	<0.01
BLK	Blank	<0.1	<0.1	<0.1	<0.1	<0.02	<0.1	<0.1	<0.1	<0.04	<0.1	0.19									
BLK	Blank																				
Prep Wash																					
G1	Prep Blank	1.7	0.3	1.7	0.2	0.82	30.5	93.2	1.5	23.89	3.9	18.18	<0.02	<0.02	68.1	15.68	3.45	3.45	1.10	3.78	3.73

Alberta Innovates Technology Futures

Acme Analytical Laboratories (Vancouver) Ltd.
1020 Cordova St. East Vancouver BC V6A 4A3 Canada
Phone (604) 253-3158 Fax (604) 253-1716
www.acmelab.com

Client: **Alberta Innovates Technology Futures**
250 Karl Clark Road
Edmonton AB T6N 1E4 Canada

Project: Enhance
Report Date: October 23, 2011

QUALITY CONTROL REPORT VAN11004088.1

	Method	4X	4X	4X	4X	4X	4X	4X
	Analyte	MnO	TiO2	P2O5	Cr2O3	Ba	LOI	SUM
	Unit	%	%	%	%	%	%	%
	MDL	0.01	0.01	0.01	0.001	0.01	-5.11	0.01
Pulp Duplicates								
EN-33	Core Chip	0.08	0.45	0.17	0.006	0.07	10.16	100.3
REP EN-33	QC							
Reference Materials								
STD CSC	Standard							
STD OREAS24P	Standard							
STD OREAS24P	Standard							
STD OREAS45C	Standard							
STD OREAS45C	Standard							
STD OREAS76A	Standard							
STD SO-18	Standard	0.41	0.71	0.82	0.587	0.05	1.90	101.1
STD SY-4(D)	Standard	0.12	0.27	0.13	0.001	0.05	4.56	100.1
STD CSC Expected								
STD OREAS76A Expected								
STD SY-4(D) Expected		0.108	0.287	0.131		0.034	4.56	
STD SO-18 Expected		0.39	0.69	0.83				
STD OREAS24P Expected								
STD OREAS45C Expected								
BLK	Blank							
BLK	Blank	<0.01	0.01	<0.01	<0.001	<0.01	0.00	<0.01
BLK	Blank							
BLK	Blank							
Prep Wash								
G1	Prep Blank	0.10	0.40	0.18	0.002	0.10	0.65	100.8

Alberta Innovates Technology Futures

11.18 Additional ICP-MS, & XRF of samples EN-10 and EN-11.

The following tables contain duplicate analytical results for samples EN-10 and EN-11. These analyses include XRF, and acid digestion followed by ICP-AES. The analyses were undertaken at Waterloo University, Ontario, Canada, and have been included for completeness.

Major Oxide Determinations by Fusion XRF analysis (in wt%)

Sample	SiO2	TiO2	Al2O3	Fe2O3	MnO	MgO	CaO	K2O
EN10	0.49	0.01	0.12	0.12	0.02	20.40	31.78	0.02
EN11	0.78	0.01	0.24	0.14	0.01	20.63	29.94	0.02
Standard	SiO2	TiO2	Al2O3	Fe2O3	MnO	MgO	CaO	K2O
JA-3	62.23	0.67	15.30	6.49	0.09	3.70	6.22	1.39
R.V.	62.26	0.68	15.57	6.39	0.11	3.65	6.28	1.41
MRG-1	39.08	3.76	8.52	17.88	0.15	13.53	14.58	0.17
R.V.	39.12	3.77	8.47	17.94	0.17	13.55	14.70	0.18

Major Oxide Determinations by Fusion XRF analysis (in wt%)

Sample	Na2O	P2O5	Cr2O3	L.O.I.	Total
EN10	< 0.01	0.01	0.02	44.93	97.92
EN11	< 0.01	0.01	0.00	47.10	98.88
Standard	Na2O	P2O5	Cr2O3	L.O.I.	Total
JA-3	3.07	0.12	0.01	0.88	100.17
R.V.	3.17	0.11	0.02		
MRG-1	0.70	0.06	0.07	1.86	100.36
R.V.	0.74	0.08	0.06		

Alberta Innovates Technology Futures

Aqua-regia Digestion ICP-AES metal analysis (mg/l).

Sample	Al	As	B	Ba	Be	Ca
EN-10	380	1.10	7.82	2.53	n.d.	157450
EN-11	443	0.86	10.55	2.97	n.d.	152087
Standard	**Al**	**As**	**B**	**Ba**	**Be**	**Ca**
BLANK	n.d.	n.d.	n.d.	n.d.	n.d.	n.d.
SPIKE	4.27	4.25	4.49	4.53	4.28	0.66
SPIKE DUP	4.34	4.33	4.34	4.34	4.20	0.54
AQR VHG-3 0.5 ppm	5.07	5.04	5.07	5.05	5.07	5.01
WAVECAL 0.5 ppm	n.d.	0.51	n.d.	n.d.	n.d.	n.d.
AQR QCS-26 1.0 ppm	0.97	0.88	0.90	0.91	0.90	1.13

Sample	Cd	Co	Cr	Cu	Fe	Hg
EN-10	0.43	0.31	0.48	0.45	532	n.d.
EN-11	0.41	0.49	2.35	0.62	578	n.d.
Standard	**Cd**	**Co**	**Cr**	**Cu**	**Fe**	**Hg**
BLANK	n.d.	n.d.	n.d.	n.d.	n.d.	n.d.
SPIKE	4.53	4.44	4.54	4.22	4.42	4.38
SPIKE DUP	4.47	4.38	4.50	4.19	4.32	4.33
AQR VHG-3 0.5 ppm	5.04	5.10	5.05	5.03	5.06	5.04
WAVECAL 0.5 ppm	n.d.	n.d.	n.d.	n.d.	0.01	0.01
AQR QCS-26 1.0 ppm	0.95	0.92	0.92	0.93	1.01	0.00

Alberta Innovates Technology Futures

Sample	K	Li	Mg	Mn	Mo	Na
EN-10	312	2.26	50661	62	n.d.	541
EN-11	326	2.36	53728	46	n.d.	634

Standard	K	Li	Mg	Mn	Mo	Na
BLANK	n.d.	n.d.	n.d.	n.d.	n.d.	n.d.
SPIKE	4.17	4.33	2.74	4.42	4.08	4.35
SPIKE DUP	4.28	4.15	2.67	4.35	4.07	3.81
AQR VHG-3 0.5 ppm	5.07	5.08	5.04	5.05	5.05	5.07
WAVECAL 0.5 ppm	2.52	0.51	n.d.	0.55	0.52	0.60
AQR QCS-26 1.0 ppm	9.61	n.d.	1.01	0.94	0.89	0.91

Sample	Ni	P	Pb	S	Sb	Se
EN-10	0.26	56.6	n.d.	1699	n.d.	n.d.
EN-11	0.83	73.1	1.45	105	n.d.	n.d.

Standard	Ni	P	Pb	S	Sb	Se
BLANK	n.d.	n.d.	n.d.	n.d.	n.d.	n.d.
SPIKE	4.35	3.94	4.24	n.d.	4.25	4.27
SPIKE DUP	4.32	3.71	4.23	n.d.	4.28	4.29
AQR VHG-3 0.5 ppm	5.04	5.10	5.08	0.03	5.06	1.89
WAVECAL 0.5 ppm	0.54	0.52	n.d.	0.49	n.d.	0.01
AQR QCS-26 1.0 ppm	0.95	n.d.	0.93	n.d.	0.92	0.92

Alberta Innovates Technology Futures

Sample	Si	Sn	Sr	Ti	Tl	V
EN-10	534	n.d.	164	n.d.	n.d.	5.40
EN-11	503	n.d.	91	n.d.	n.d.	11.35
Standard	**Si**	**Sn**	**Sr**	**Ti**	**Tl**	**V**
BLANK	n.d.	n.d.	n.d.	n.d.	n.d.	n.d.
SPIKE	3.83	4.55	4.28	4.42	4.42	4.46
SPIKE DUP	3.81	4.47	4.13	4.38	4.37	4.39
AQR VHG-3 0.5 ppm	5.08	5.10	5.06	5.05	5.08	5.05
WAVECAL 0.5 ppm	n.d.	0.01	n.d.	0.10	0.01	n.d.
AQR QCS-26 1.0 ppm	0.82	n.d.	n.d.	0.90	0.88	0.91

Sample	Zn
EN-10	5.05
EN-11	3.75
Standard	**Zn**
BLANK	n.d.
SPIKE	4.58
SPIKE DUP	4.51
AQR VHG-3 0.5 ppm	5.03
WAVECAL 0.5 ppm	n.d.
AQR QCS-26 1.0 ppm	0.98